THERMODYNAMIC AND STRUCTURAL DESIGN AND ANALYSIS OF A
NOVEL TURBO ROTARY ENGINE

A THESIS SUBMITTED TO
THE GRADUATE SCHOOL OF NATURAL AND APPLIED SCIENCES
OF
MIDDLE EAST TECHNICAL UNIVERSITY

BY

TAYLAN ERCAN

IN PARTIAL FULFILLMENT OF THE REQUIREMENTS
FOR
THE DEGREE OF MASTER OF SCIENCE
IN
AEROSPACE ENGINEERING

SEPTEMBER 2005

Approval of the Graduate School of Natural and Applied Sciences

_____

Prof. Dr. Canan ÖZGEN

I certify that this thesis satisfies all the requirements as a thesis for the degree of Master of Science.

_____

Prof. Dr. Nafiz ALEMDAROĞLU
Head of Department

This is to certify that we have read this thesis and that in our opinion it is fully adequate, in scope and quality, as a thesis for the degree of Master of Science.

_____   _____

Assoc. Prof. Dr. Altan KAYRAN   Prof. Dr. İ. Sinan AKMANDOR
Co-Supervisor   Supervisor

Examining Committee Members

Prof. Dr. Cevdet Çelenligil   (METU, AEE) ————————————————

Prof. Dr. İ. Sinan Akmandor   (METU, AEE) ————————————————

Prof. Dr. Mehmet Şerif Kavsaoğlu   (ITU, AEE) ————————————————

Assoc. Prof. Dr. Ozan Tekinalp   (METU, AEE) ————————————————

Assoc. Prof. Dr. Altan Kayran   (METU, AEE) ————————————————

I hereby declare that all information in this document has been obtained and presented in accordance with academic rules and ethical conduct. I also declare that, as required by these rules and conduct, I have fully cited and referenced all material and results that are not original to this work.

Name, Last name: Taylan ERCAN

Signature   :

ABSTRACT

THERMODYNAMIC AND STRUCTURAL DESIGN AND ANALYSIS OF A NOVEL TURBO ROTARY ENGINE

Ercan, Taylan

M.Sc., Department of Aerospace Engineering

Supervisor   : Prof. Dr. İ.Sinan Akmandor

Co-Supervisor: Assoc. Prof. Dr. Altan Kayran

September 2005, 227 pages

A novel turbo rotary engine, operating according to a novel thermodynamic cycle, having an efficient compression phase, a limited temperature combustion phase followed by a long power extraction phase is designed. Thermodynamic and structural design and analysis of this novel engine is carried out and two prototypes are manufactured according to these analysis. High performance figures such as torque, power and low specific fuel consumption are calculated. Also the component tests of the manufactured prototypes are completed and their results are demonstrated.

Keywords: Internal combustion engine, Rotary engine, Novel thermodynamic cycle, Structural design and analysis of an engine, Engine test.

ÖZ

YENİ BİR TURBO DÖNGÜSEL MOTORUN TERMODİNAMİK VE YAPISAL
TASARIMI VE ANALİZİ.

Ercan, Taylan

Y. Lisans, Havacılık ve Uzay Mühendisliği Bölümü

Tez Yöneticisi   : Prof. Dr. İ. Sinan Akmandor

Ortak Tez Yöneticisi: Doç. Dr. Altan Kayran

Eylül 2005, 227 sayfa

Verimli bir sıkıştırma evresi, limitli sıcaklıktaki yanma evresi ve bunu takip eden uzun bir güç alma evresinden oluşan yeni bir termodinamik çevrim ile çalışan yeni bir turbo döngüsel motor tasarlanmıştır. Motorun termodinamik ve yapısal tasarımı ve analizleri yapılmış ve bu analizler doğrultusunda iki tane prototip imal edilmiştir. Tork, güç ve düşük yakıt tüketimi gibi yüksek performans değerleri hesaplanmıştır. Ayrıca imal edilen prototiplerin komponent testleri tamamlanmış ve sonuçlar sunulmuştur.

Anahtar Kelimeler: İçten yanmalı motor, Döngüsel motor, Yeni termodinamik çevrim, Motor yapısal tasarımı ve analizi, Motor test.

To My Father

ACKNOWLEDGMENTS

TABLE OF CONTENTS

LIST OF TABLES

LIST OF FIGURES

NOMENCLATURE

η_{th}	=	Thermal Efficiency
T_L	=	Lowest Temperature
T_H	=	Highest Temperature
P	=	Pressure
V	=	Volume
r	=	Compression Ratio
k	=	Polytrophic Coefficient
C_p	=	Specific Heat Coefficient (Constant P)
C_v	=	Specific Heat Coefficient (Constant V)
r_c	=	Cut Off Ratio
r_p	=	Pressure Ratio
s	=	Entropy
θ_{ec}	=	External Combustion Angle
θ_{ic}	=	Internal Combustion Angle
θ_{cp}	=	Constant Pressure Combustion Angle
θ_{ce}	=	Compressor Exit Angle
θ_{ci}	=	Compressor Inlet Angle
θ_s	=	Stroke Angle
θ_{ti}	=	Turbine inlet Angle
θ_e	=	Exhaust Angle
θ_{eb}	=	External Burning Angle
θ_{ib}	=	Internal Burning Angle
θ_{vc}	=	Compressor Vane Open Angle
θ_{vti}	=	Turbine Vane Angle
θ_{phase}	=	Phase Angle Between Turbine and Compressor
θ_{vte}	=	Turbine Displacement Angle
θ_{pp}	=	Process Period Angle
Q_{in}	=	Energy Input

Q_{out}	=	Energy Output
P_1	=	Atmospheric Air Pressure
T_1	=	Atmospheric Air Temperature
ρ_1	=	Atmospheric Air Density
R	=	Universal Gas Coefficient
Far	=	Fuel/Air Ratio
hfu	=	Fuel Enthalpy
V_1	=	Compressor Inlet Volume
r_c	=	Radius of the Compressor
e_c	=	Eccentricity of the Compressor
α_c	=	Compressor Vane Front Angle for the Inlet Volume
δ_c	=	Compressor Vane Back Angle for the Inlet Volume
m	=	Mass of the Air
ρ_1	=	Density of Air at Inlet
h_c	=	Height of the Compressor
d_c	=	Diameter of Compressor
P_2	=	Air Pressure after Compression
T_2	=	Air Temperature after Compression
ρ_2	=	Air Density after Compression
W_2	=	Compression Work
V_2	=	Combustion Chamber Volume
T_3	=	Air Temperature after Constant Volume Combustion
f_{cv}	=	Constant Volume Combustion Fuel Ratio
P_3	=	Air Pressure after Constant Volume Combustion
V_3	=	Combustion Chamber Volume
ρ_3	=	Air Density after Constant Volume Combustion
T_4	=	Air Temperature after Constant Pressure Combustion
P_4	=	Air Pressure after Constant Pressure Combustion
V_4	=	Combustion Chamber Volume

ρ_4 = Air Density after Constant Pressure Combustion

V_5 = Turbine Inlet Volume

r_t = Radius of the Turbine

h_t = Estimated Height of the Turbine

e_t = Eccentricity of the Turbine

α_t = Turbine Vane Angle for the Exhaust Volume

ρ_5 = Density of the Air after Expansion

W_5 = Expansion Work

T_5 = Air Temperature after Expansion

P_5 = Air Pressure after Expansion

m_{fuel} = Fuel Mass Flow Rate

W_{net} = Net Work Done by the Engine

m_{dot} = Air Mass Flow Rate

θ = Swept Angle

S_w = Swept Volume

t_v = Vane Thickness

m_{air} = Air Mass Flow Rate

ϕ = Fuel/Air Equivalence Ratio

λ = Relative Air/Fuel Ratio

V_{eff} = Volumetric Efficiency

T_{CL} = Vane Tip Clearance

LIST OF ACRONYMS

BHP = Brake Horse Power

LPG = Liquid Petrol Gas

TVO = Tractor Vaporizing Oil

IC   = Internal Combustion

UAV = Unmanned Air Vehicle

SFC   = Specific Fuel Consumption

RPM = Revolution per Minute

CVO = Compressor Valve Open

CVC = Compressor Valve Close

TVO = Turbine Valve Open

TVC = Turbine Valve Close

WOT = Wide Open Throttle

PLC   = Programmable Logic Control

MAV = Micro Air Vehicle

ICE   = Internal Combustion Engine

CAD = Computer Aided Design

NC   = Numeric Control

TRCE = Turbo Rotary Compound Engine

TAI   = TUSAŞ Aerospace Industry

TEI   = TUSAŞ Engine Industry

CHAPTER 1

INTRODUCTION

Since the start of the industrial revolution, the reciprocating piston engine based on the Otto and Diesel cycles and, the gas turbine engine based on the Brayton cycle, have largely dominated the market [1]. Despite this fact, for many years, patents on rotary combustion engines [2,3,4,5,6] have claimed that rotary engines possess many advantages over reciprocating engines such as having high torque, fewer parts, lower weight and fewer reciprocating imbalance. Although heat engines have received little industrial attention, for over 5 decades, sliding vane rotary compressors have taken an important place in general engineering applications, especially in the capacity range of 10-1000 cc/sec and for delivery pressures in the range of 2-18 bars. Early rotary compressor designs had low volumetric efficiencies, undesirable high delivery air temperatures due to internal air leakage and considerable blade and cylinder wear due to lack of adequate lubrication [1]. These disadvantages have all been addressed in this thesis. In this thesis, an engine compressor with a volumetric efficiency of 85.6% is designed and the long expansion power stroke which lasts up to a wide rotation angle (270°), is amply sufficient to overtake any net shaft power production figure of a non-turbocharged piston engine of similar size and of higher compressor volumetric efficiency. Further, the longer compression stroke rotation angle (330°) enhances the fuel-air mixing as fuel is injected by a carburetor alongside the air intake phase. The fuel evaporates in the compression phase and helps lower the compression temperature which further decreases the required shaft power input to the rotary compressor. A good fuel-air mixing permits leaner combustion to occur in the external burner which is placed downstream of the compressor.

Contrary to expectations gained through the design of compression devices, a high compressor air delivery temperature positively contributes to the temperature rise requirement in the combustion chamber.

As less fuel input is needed to reach allowable turbine inlet temperature, the specific fuel consumption is favorably decreased.

Air and oil cooled sliding vane engine have additional very desirable features such as nearly steady air flow processing, small pressure fluctuations, low noise levels and smooth running characteristics.

Another objective of this thesis is to increase the overall thermal efficiency above levels reached by today's heat engines. This is achieved by adopting a novel thermodynamic cycle which allows a longer power extraction phase. The designed rotary vane engine also achieves high compression ratios with less shaft power input as air is processed through a smooth crescent shape constriction which progressively squeezes out the fluid to the combustion chamber. As maximum peak temperature is limited, the operational and maintenance costs are also minimized. All together, in the presented thesis, an efficient, powerful, compact, simple and reliable heat engine is designed, analyzed, manufactured and tested.

1.1 History of Internal Combustion Engines

The purpose of internal combustion engines is the production of mechanical power from chemical energy contained in the fuel. In internal combustion engines, as distinct from external combustion engines, this energy is released by burning or oxidizing the fuel inside the engine. The fuel – air mixture before the combustion, and the burned products after combustion are the actual working fluids. The work transfers which provide the desired power output occur directly between these working fluids and the mechanical components of the engine. The spark ignition engines (sometimes called Otto engines or gasoline engines), compression – ignition or diesel engines are the main internal combustion engines.

Because of their simplicity, ruggedness and high power/weight ratio, these two types of engine have found wide application in transportation (land, sea and air) and power generation. It is the fact that combustion takes place inside the work producing part of these engines that makes their design and operating characteristics fundamentally different from those of other types of engines.

Practical heat engines have served mankind for over two and a half centuries. For the first 150 years, water rose to steam, was interposed between the combustion gases produced by burning the fuel and the work producing piston in cylinder expander. It was not until the 1860s that the internal combustion engine became a practical reality [7,8]. The early engines developed for commercial use burned coal-gas air mixtures at atmospheric pressure- there was no compression before combustion. J.J.E. Lenoir (1822-1900) developed the first marketable engine of this type. Gas and air were drawn into the cylinder during the first half of the piston stroke. The charge was then ignited with a spark, the pressure increased, and the burned gases then delivered power to the piston for the second half of the stroke. The cycle was completed with an exhaust stroke. Some 5000 of these engines were built between 1860 and 1865 in sizes up to six horsepower. Efficiency was at best about 5 percent.

A more successful development – an atmospheric engine introduced in 1867 by Nicolaus A. Otto (1832-1891) and Eugen Langen (1833 – 1895) – used the pressure rise resulting from combustion of the fuel – air charge early in the outward stroke to accelerate a free piston and rack assembly so its momentum would generate a vacuum in the cylinder. Atmospheric pressure then pushed the piston inward, with the rack engaged through a roller clutch to the output shaft. Production engines, of which about 5000 were built, obtained thermal efficiencies of up to 11 percent. A slide valve controlled intake, ignition by a gas flame, and exhaust [8].

To overcome this engine's shortcomings of low thermal efficiency and excessive weight, Otto proposed an engine cycle with four piston strokes: an intake stroke, then a compression stroke before ignition, an expansion or power stroke where work was delivered to the crankshaft, and finally an exhaust stroke. His prototype four stroke engine first ran in 1876.

A comparison between the Otto engine and the atmospheric type predecessor indicates the reason for its success; the enormous reduction in engine weight and volume. By 1890, almost 50,000 of these engines had been sold in Europe and the United States [8].

In 1884, an unpublished French patent issued in 1862 to Alphonse Beau de Rochas (1815 – 1893) was found which described the principles of the four stroke cycle. This chance discovery cast doubt on the validity of Otto's own patent for this concept, and in Germany it was declared invalid. Beau de Rochas also outlined the conditions under which maximum efficiency in an external combustion engine could be achieved [9]. These were:

1. The largest possible cylinder volume with minimum boundary surface.
2. The greatest possible working speed.
3. The greatest possible expansion ratio.
4. The greatest possible pressure at the beginning of expansion.

The first two conditions hold heat losses from the charge to a minimum. The third condition recognizes that the greater the expansion of the post combustion gases, the greater the work extracted. The fourth condition recognizes that bigger initial pressures make greater expansion possible, and give higher pressures throughout the process, both resulting in greater work transfer.

Further developments followed fast once the full impact of what Otto had achieved became apparent. By the 1880s several engineers had successfully developed the two stroke internal combustion engines where the exhaust and intake processes occur during the end of the power stroke and the beginning of the compression stroke. James Atkinson (1846 – 1914) in England made an engine with longer expansion then compression stroke, which had a high efficiency for the times but mechanical weaknesses. It was recognized that efficiency was a direct function of expansion ratio, yet compression ratios were limited to less then four if serious knock problems were to be avoided with the available fuels. Substantial carburetor and ignition system were required, and occurred, before high speed gasoline engines suitable for automobiles became available in the late 1880s.

By the late 1890s, large single cylinder engines of 1.3 –m bore fueled by low energy blast furnace gas produced 600 bhp at 90rev/min [8].

In Britain, legal restrictions on volatile fuels turned their engine builders toward kerosene. Low compression ratio 'oil' engines with heated external fuel vaporizers and electric ignition were developed with efficiencies comparable to those of gas engines (14 to 18 percent). The Hornsby – Ackroyd engine became the most popular oil engine in Britain, and was also built in large numbers in the United States [8].

In 1892, the German engineer Rudolf Diesel (1853 – 1913) outlined his patent a new form of internal combustion engine. His concept of initiating combustion by injecting a liquid fuel into air heated solely by compression permitted a doubling of efficiency over other internal combustion engines. Much greater expansion ratios, without detonation or knock, were now possible. However, even with the efforts of Diesel and the resources of M.A.N in Augsburg combined, it took five years to develop a practical engine. [8]

Engine developments, perhaps less fundamental but nonetheless important to the steadily widening internal combustion engine markets have continued ever since [8, 9, 10]. One more recent major development has been the rotary internal combustion engine. Although, a wide variety of experimental rotary engines have been proposed over the years [11], the first practical rotary internal combustion engine, the Wankel, was not successfully tested until 1957. That engine, which evolved through many years of research and development, was based on the designs of the German inventor Felix Wankel [12, 13].

Fuels have also had a major impact on engine development. The earliest engines used for generating mechanical power burned gas. Gasoline and lighter fractions of crude oil, became available in the late 1800s and various types of carburetors were developed to vaporize the fuel and mix it with air Before 1905 there were few problems with gasoline; tough compression ratios were low (4 or less) to avoid knock, the highly volatile fuel made starting easy and gave good cold weather performance. However, a serious crude oil shortage developed, and to meet the fivefold increase in gasoline demand between 1907 and 1915, the yield from crude had to be raised.

Through the work of William Burton (1865-1954) and his associates of Standard Oil of Indiana, a thermal cracking process was developed whereby heavier oils were heated under pressure and decomposed into less complex more volatile compounds. These thermally cracked gasoline satisfied demand, but their higher boiling point range created cold weather starting problems. Fortunately, electrically driven starters, introduced in 1912, came along just in time.

On the farm, kerosene was the logical fuel for internal combustion engines since it was used for heat and light. Many early farm engines had heated carburetors or vaporizers to enable them to operate with such a fuel.

The period following World War I, saw a tremendous advance in our understanding of how fuels affect combustion, and especially the problem of knock. The antiknock effect of tetraethyl lead was discovered at General Motors [10] and it became commercially available as a gasoline additive in the United States in 1923. In the late 1930s, Eugene Houdry found that vaporized oils passed over an activated catalyst at 450 to 480 C were converted to high quality gasoline in much higher yields than was possible with thermal cracking. These advances, and others, permitted fuels with better and better antiknock properties to be produced in large quantities; thus engine compression ratios steadily increased, improving power and efficiency [10].

During the past three decades, new factors for change have become important and now significantly affect the engine design and operation. These factors are, first, the need to control the automotive contribution to urban air pollution and, second, the need to achieve significant improvements in automotive fuel consumption. The emission – control requirements and the fuel developments have produced significant changes in the way internal combustion engines are designed and operated.

Internal combustion engines are also important sources of noise. There are several sources of engine noise; the exhaust system, the intake system, the fan used for cooling, and the engine block surface. The noise may be generated by aerodynamic effects, may be due to forces that result from the combustion process, or may result from mechanical excitation by rotating or reciprocating engine components.

During the 1970s the price of crude petroleum rose rapidly. Pressures for substantial improvements in internal combustion efficiency have become very substantial indeed. Yet emission control requirements have made improving engine fuel consumption more difficult, and the removal and reduction of lead in gasoline has forced spark ignition engine compression ratios to be reduced. Much work is being done on the use of alternative fuels to gasoline and diesel.

It might be thought that after over a century of development, the internal combustion engine has reached its peak and little potential for further improvement remains. Such is not the case. Conventional spark ignition and diesel engines continue to show substantial improvements in efficiency, power and degree of emission control. New material now becoming available offer the possibilities of reduced engine weight, cost and heat losses and of different and more efficient internal combustion engine systems. The engine development opportunities of the future are substantial. While they present a formidable challenge to automotive engineers they will be made possible in large part by the enormous expansion of our knowledge of engine processes which the last twenty years has witnessed.

1.2 Main Types of Internal Combustion Engines

There are many different types of internal combustion engines [14, 15, 16]. They can be classified by:

- *Application.* Automobile, truck, locomotive, light aircraft, marine, portable power systems, power generation.

- *Basic Engine Design.* Reciprocating engines (in-line, V, radial, opposed), rotary engines (Wankel and other geometries)

Internal combustion engines can be classified by their configuration which affects their physical size and smoothness (with smoother engines producing less vibration). Common configurations include the straight or inline configuration, the more compact V configuration and the wider but smoother flat or boxer configuration. Aircraft engines can also adopt a radial configuration which allows more effective cooling. More unusual configurations, such as "H", "U", "X", or "W" have also been used.

Reciprocating Engine: The most common internal-combustion engine is the piston-type gasoline engine used in most automobiles. The confined space in which combustion occurs is called a cylinder. The cylinders are now usually arranged in one of four ways: a single row with the centerlines of the cylinders vertical (in-line engine); a double row with the centerlines of opposite cylinders converging in a V (V-engine); a double zigzag row somewhat similar to that of the V-engine but with alternate pairs of opposite cylinders converging in two Vs (W-engine); or two horizontal, opposed rows (opposed, pancake, flat, or boxer engine). In each cylinder a piston slides up and down. One end of a connecting rod is attached to the bottom of the piston by a joint; the other end of the rod clamps around a bearing on one of the throws, or convolutions, of a crankshaft; the reciprocating (up-and-down) motions of the piston rotate the crankshaft, which is connected by suitable gearing to the drive wheels of the automobile. (Figure 1-1)
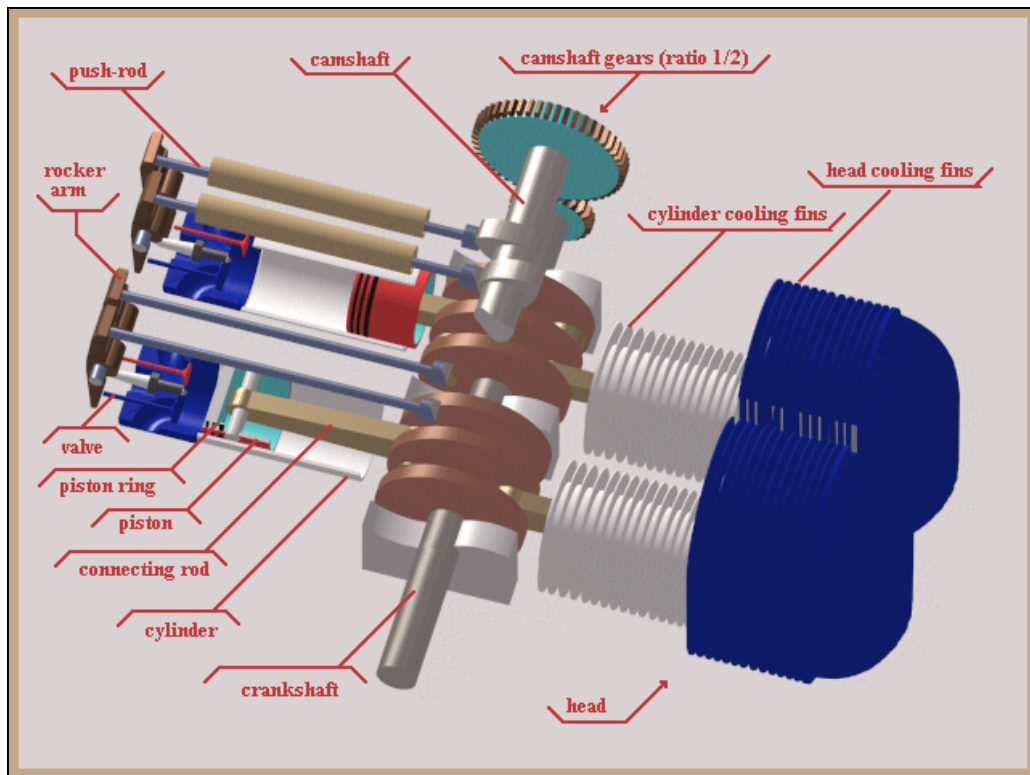
Figure 1-1   Reciprocating Engine

Rotary Engine: The most successful rotary engine is the Wankel engine. Developed by the German engineer Felix Wankel in 1956, it has a disk that looks like a triangle with bulging sides rotating inside a cylinder shaped like a figure eight with a thick waist. Intake and exhaust are through ports in the flat sides of the cylinder. The spaces between the sides of the disk and the walls of the cylinder form combustion pockets. During a single rotation of the disk each pocket alternately grows smaller, then larger, because of the contoured outline of the cylinder. This provides for compression and expansion (Fig 1-2). The engine runs on a four-stroke cycle.
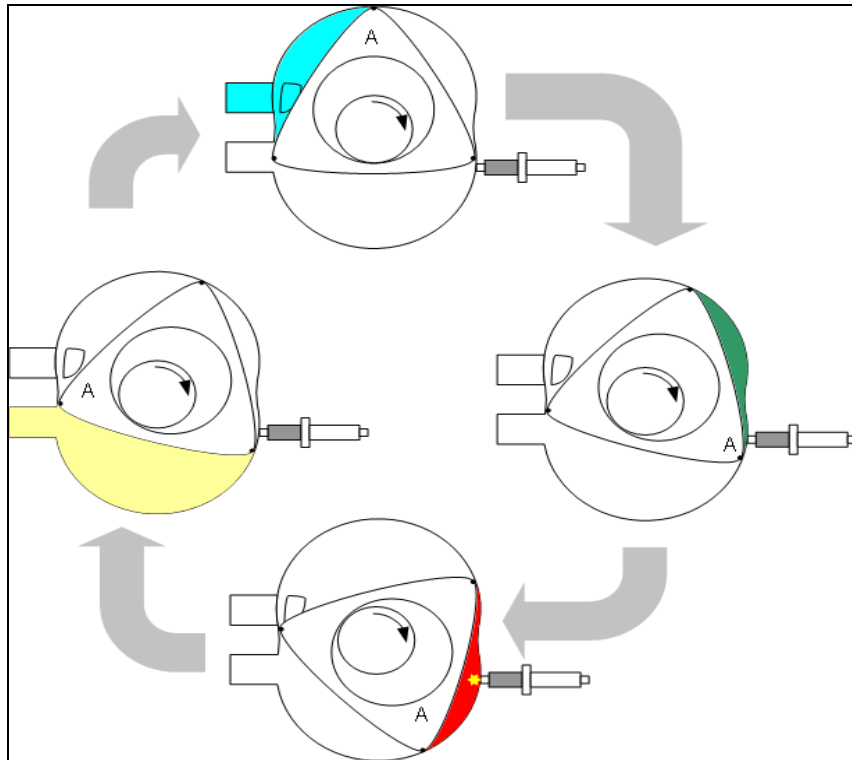
Figure 1-2   Wankel Engine

- ***Working Cycle***. Four stroke cycle: naturally aspirated, supercharged and turbo charged, two stroke cycle: crankcase scavenged, supercharged, turbocharged.

The two-stroke cycle: The two stroke cycle delivers one power stroke every two strokes instead of one every four; thus it develops more power with the same displacement, or can be lighter and yet deliver the same power (Figure 1-3). For this reason it is used in lawn mowers, chain saws, small automobiles, motorcycles, and outboard marine engines.

However, there are several disadvantages that restrict its use. Since there are twice as many power strokes during the operation of a two-stroke engine as there are during the operation of a four-stroke engine, the engine tends to heat up more, and thus is likely to have a shorter life. Also, in the two-stroke engine lubricating oil must be mixed with the fuel. This causes a very high level of hydrocarbons in its exhaust, unless the fuel-air mixture is computer calculated to maximize combustion.
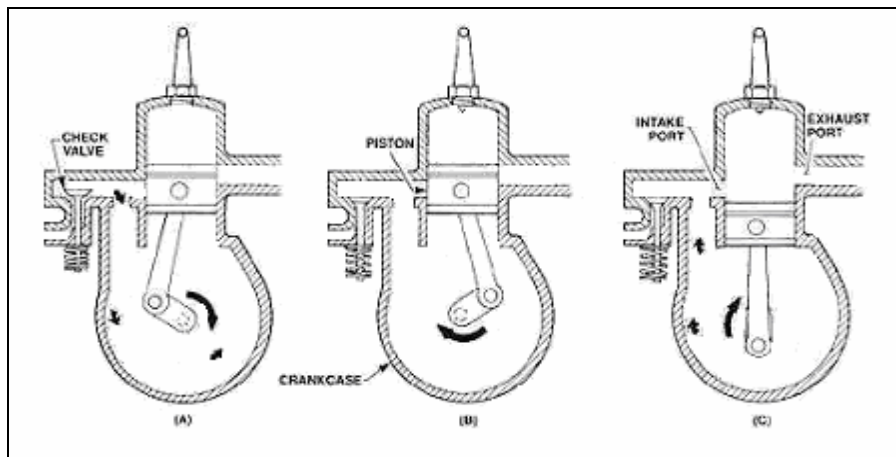
Figure 1-3   Two Stroke Cycle Engine

Four Stroke Engine: In most engines, a single cycle of operation (intake, compression, power, and exhaust) takes place over four strokes of a piston, made in two engine revolutions (Figure 1-4). When an engine has more than one cylinder the cycles are evenly staggered for smooth operation, but each cylinder will go through a full cycle in any two engine revolutions. When the piston is at the top of the cylinder at the beginning of the intake stroke, the intake valve opens and the descending piston draws in the air-fuel mixture.

At the bottom of the stroke the intake valve closes and the piston starts upward on the compression stroke, during which it squeezes the air-fuel mixture into a small space at the top of the cylinder. Just before the piston reaches the top again, the spark plug fires, igniting the air-fuel mixture (alternatively, the heat of compression ignites the mixture). The mixture on burning becomes a hot, expanding gas forcing the piston down on its power stroke. As the piston reaches the bottom, the exhaust valve opens, allowing the piston to force the combustion products—mainly carbon dioxide, carbon monoxide, nitrogen oxides, and unburned hydrocarbons—out of the cylinder during the upward exhaust stroke.
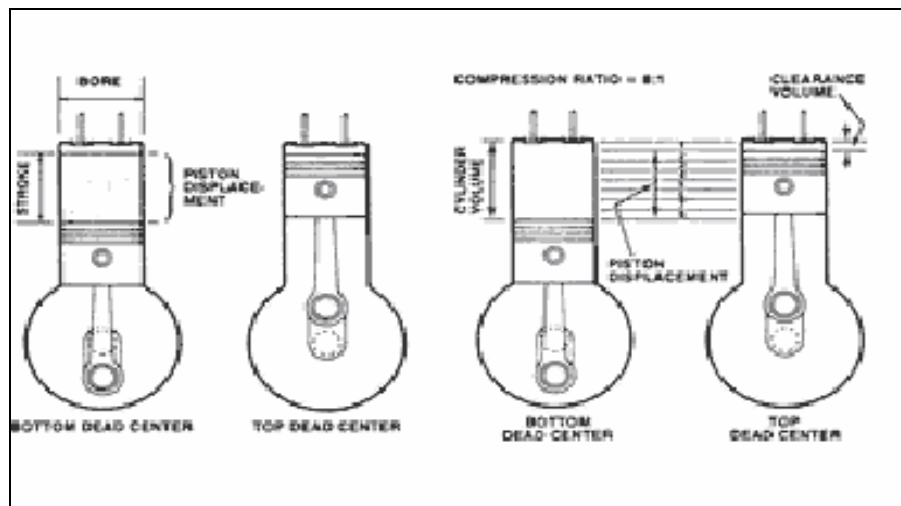
Figure 1-4   Four Stroke Cycle Engine

- *Valve or port design and location.* Overhead valves, under-head valves, rotary valves, cross scavenged porting, loop scavenged porting, through or uniflow scavenged.

- *Fuel.* Gasoline (or petrol), fuel oil (or diesel), natural gas, liquid petroleum gas, alcohols (methanol, ethanol), hydrogen, dual fuel.

The diesel engine: The diesel engine differs from the gasoline engine in that the ignition of fuel is caused by compression of air in its cylinders instead of by a spark: the high compression ratio allows the air in the cylinder to become hot enough to ignite the fuel. Because of the high temperatures of operation, a diesel engine must be water-cooled. The speed and power of the diesel are controlled by varying the amount of fuel injected into the cylinder, not the amount of air admitted as in the gasoline engine.

Diesel engines are generally heavier, noisier and more powerful at lower speeds than gasoline engines. They are also more fuel-efficient in some circumstances and are used in heavy road-vehicles, some automobiles, ships and some locomotives and light aircraft. Gasoline engines are used in most other road-vehicles including most cars, motorcycles and mopeds. Both gasoline and diesel engines produce significant emissions.

There are also engines that run on hydrogen, methanol, ethanol, liquefied petroleum gas (LPG) and bio-diesel. Paraffin and Tractor vaporizing oil (TVO) engines are no longer seen.

- *Method of mixture preparation.* Carburetion, fuel injection into the intake ports or intake manifold, fuel injection into the engine cylinder.

  Often for simpler reciprocating engines a carburetor is used to supply fuel into the cylinder. However, exact control of the correct amount of fuel supplied to the engine is difficult. Car engines have mostly moved to fuel injection systems, and Diesel engines essentially always use this technique. Other internal combustion engines like Jet engines use burners, and rocket engines use various different ideas including impinging jets, gas/liquid shear, pre-burners and many other ideas.

- *Method of ignition.* Spark ignition, compression ignition.

  Internal combustion engines can be classified by their ignition system. Today most engines use an electrical or compression heating system for ignition. However outside flame and hot-tube systems have been used historically.

- *Combustion chamber design.* Open chamber (disc, wedge, hemisphere, bowl in piston), divided chambers (swirl chambers, pre-chambers).

- *Method of load control.* Throttling of fuel and air flow together so mixture composition is essentially unchanged, control of fuel flow alone, a combination of these.

- *Method of cooling.* Water cooled, air cooled, un-cooled.

  Most small two-stroke engines are air-cooled. Air flows over cooling fins around the outside of the cylinder and head, either by the natural motion of the vehicle or from a fan. Many aircraft four-stroke engines are also air-cooled; larger engines have the cylinders arranged radially so that all cylinders are directly in the air stream. Most four-stroke engines, however, are water-cooled. A water jacket encloses the cylinders; a water pump forces water through the jacket, where it draws heat from the engine. Next, the water flows into a radiator where the heat is given off to the air; it then moves back into the jacket to repeat the cycle. During warm-up a thermostatic valve keeps water from passing to the radiator until optimum operating temperatures are attained.

1.3 Thermodynamic Cycles of Engines

The Carnot Cycle

The Carnot Cycle is composed of four totally reversible processes: isothermal heat addition, isentropic expansion, isothermal heat rejection, and isentropic compression. The Carnot Cycle is the most efficient cycle that can be executed between a thermal energy source at temperature T_H and a sink at temperature T_L and the thermal efficiency is expressed as;

$$\eta_{th, Carnot} \equiv 1 - \frac{T_L}{T_H} \tag{1.1}$$

Reversible isothermal heat transfer is very difficult to achieve in reality because it would require very large heat exchangers and it would take a very long time Therefore, it is not practical to build an engine that would operate on a cycle which closely approximates the Carnot cycle.
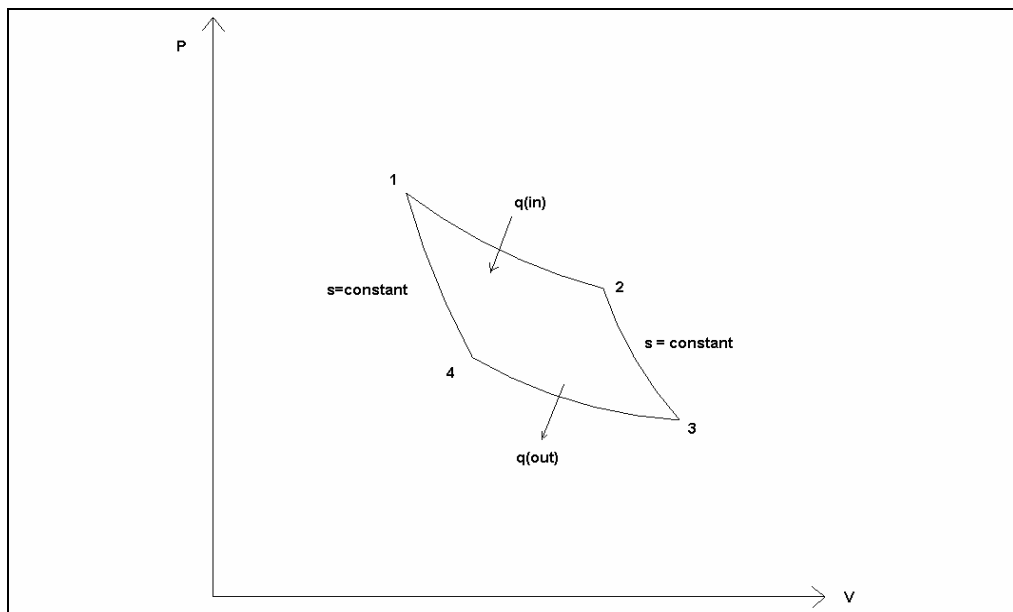
Figure 1-5   P – V Diagram of Carnot Cycle

The Otto Cycle

The Otto Cycle is the ideal cycle for spark ignition reciprocating engines. It consists of four internally reversible processes; isentropic compression, constant volume heat addition, isentropic expansion and constant volume heat rejection. In most spark ignition engines, the piston executes four complete strokes within the cylinder, and the crankshaft completes 2 revolutions for each thermodynamic cycle. These engines are called four-stroke internal combustion engines. The thermal efficiency of the cycle is expressed as;

$$\eta_{th, Otto} \equiv 1 - \frac{1}{r^{k-1}} \tag{1.2}$$

where,

$$r \equiv \frac{V_{max}}{V_{min}} \; ; \; k \equiv \frac{C_p}{C_v} \tag{1.3}$$
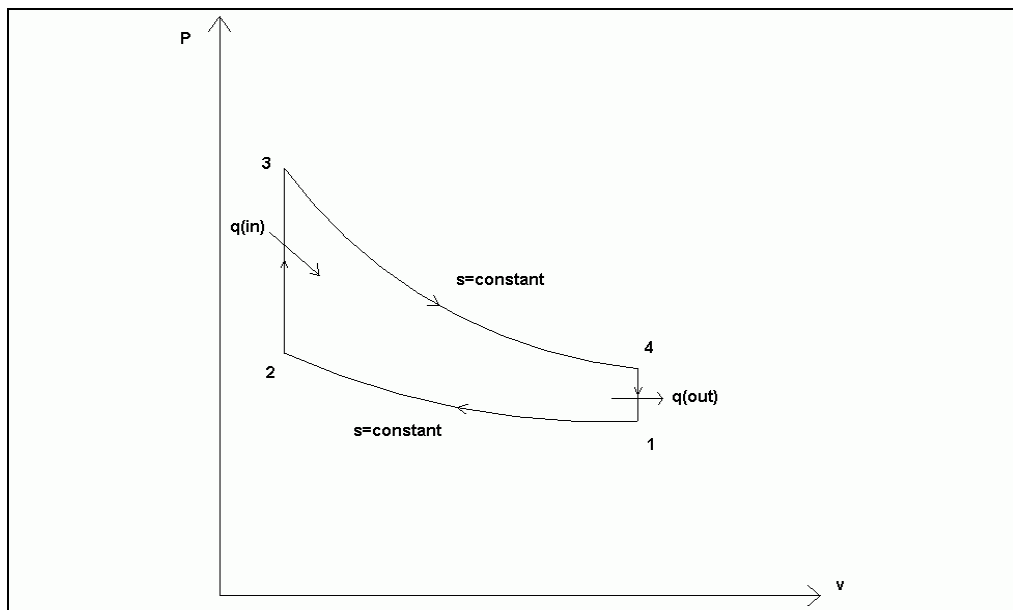
Figure 1-6 P – V Diagram of Otto Cycle

The Diesel Cycle

The Diesel Cycle is the ideal cycle for compression ignition reciprocating engines. It consists of four internally reversible processes; isentropic compression, constant pressure heat addition, isentropic expansion and constant volume heat rejection. The thermal efficiency of the cycle is expressed as;

$$\eta_{th,\,Diesel} \equiv 1 - \frac{1}{r^{k-1}}\left(\frac{r_c^{\,k} - 1}{k\,(r_c - 1)}\right) \tag{1.4}$$

where,

$$r \equiv \frac{V_{max}}{V_{min}} \;;\; k \equiv \frac{C_p}{C_v} \;;\; r_c \equiv \frac{V_3}{V_2} \tag{1.5}$$
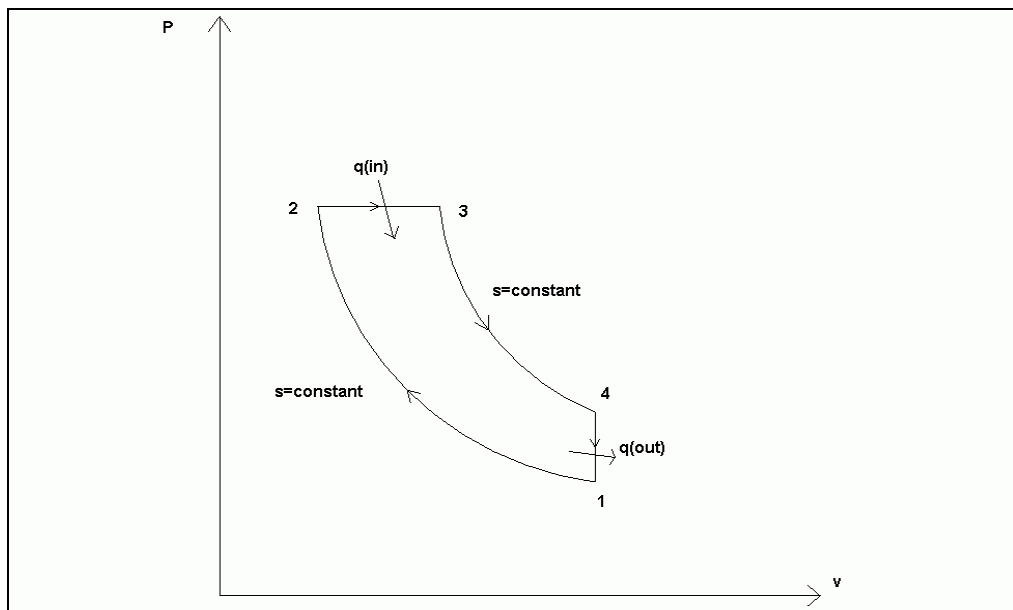
Figure 1-7   P – V Diagram of Diesel Cycle

17

The Brayton Cycle

The Brayton Cycle is the ideal cycle for gas turbine engines. It consists of four internally reversible processes; isentropic compression, constant pressure heat addition, isentropic expansion and constant pressure heat rejection. The thermal efficiency of the cycle is expressed as;

$$\eta_{th, Brayton} \equiv 1 - \frac{1}{r_p^{(k-1)/k}} \qquad (1.6)$$

where,

$$r_p \equiv \frac{P_2}{P_1}; \quad k \equiv \frac{C_p}{C_v} \qquad (1.7)$$
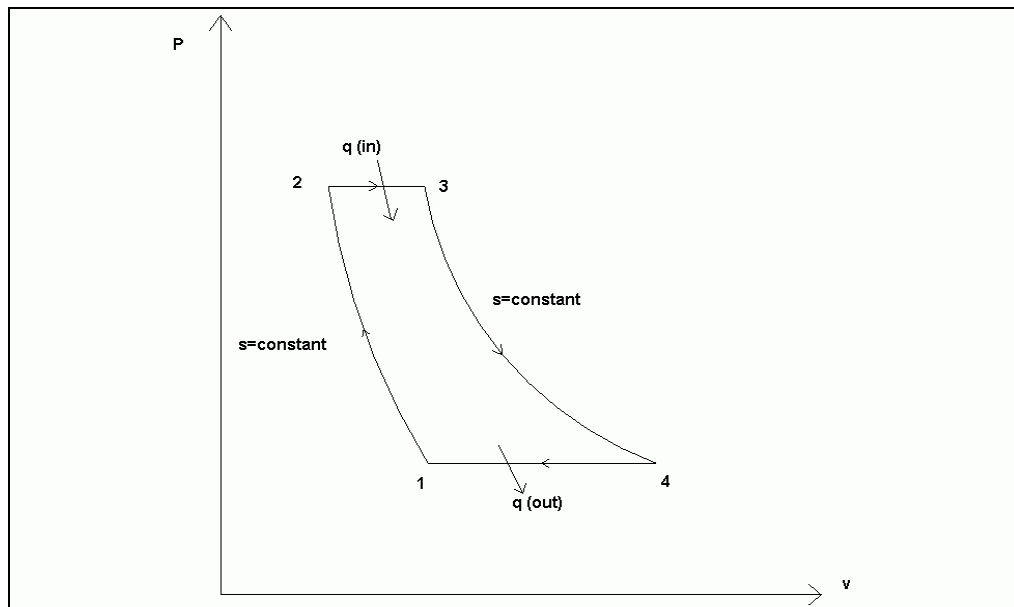
Figure 1-8   P – V Diagram of Brayton Cycle

18

1.4   Rotary Engine Development

The rotary combustion engine must not be confused with "rotary" aircraft engines which are piston cylinders arranged in a circle. The whole engine rotates. They came into vogue in the First World War.

There are three main types of true rotary engines:

1. Wankel types based on eccentric rotors,
2. Scissor action types using vanes or pistons, and
3. Revolving block types ('cat and mouse' type).

Engines are closely related to pumps and compressors: the former drives and the latter are driven.

Designs for rotary engines were proposed as early as 1588 by Ramelli, though it took the development of the Otto cycle engine in 1876 and the advent of the automobile in 1896 to set the stage for a proper rotary combustion engine. Furthermore, it took Felix Wankel to catalogue and organizes 862 configuration pairs, of which 278 are impractical. Wankel investigated 149. Prior to 1910, more than 2000 patents for rotary pistons were filed [11].

Other early designs were made by Huygens in 1673 and Kepler. James Watt made a rotary piston steam engine in 1759, as did Ericsson. The American John Cooley made an invention of a sort of reverse Wankel in 1903, which Umpleby applied to internal combustion in 1908, but never developed successfully. Some people report that Elwood Haynes invented one in 1893, but I think they are confusing it with his invention of a "rotary valve gas engine" in 1903. Frenchman Sensaud de Lavaud obtained a patent for a four phase rotary piston engine in 1938, two years after Felix Wankel. There were also designs by Pappenheim, Hornblower, Murdoch, Bramah, Flint, Poole, Wright, Marriott, Trotter, Galloway, Parsons, Roots, Wallinder, Skoog, Baylin, Larsen, Ljungström, Behrens, Maillard, and Jernaes. Marsh has made a good summary with diagrams [13].

1.5   Reciprocating Versus Rotary Engines

The advantages and the disadvantages of the reciprocating and rotary engines are summarized as follows;

Disadvantages of Reciprocating Engines

- Reciprocating motion of piston engine require inertial change of rotating mass of pistons, rods, assembly. (*Power Loss*)
- Together with inertial changes of valves, springs, lifters, rocker arms, push rods. (*Additional Loss*)
- Mechanical complexity.
- Include many moving parts lead to fatigue or wear.
- Large number of parts thus, large inertia mass change. (*Power loss*)
- Frictional loss between those parts. (*Power loss*)
- Expensive to manufacture and maintain equipment for large number of moving parts.
- Low torque, high rpm machine. (Highest internal pressure at lowest torsional moment in piston).
- Transmissions are needed to amplify the low torque which is weight, complexity, additional power requirement.
- Expansion volume is not equal to compression volume. (combustion heat the gas, thus increasing the expansion volume beyond initial volume) Relatively high-pressure combustion gasses are exhausted without performing any useful work.
- Leakage of pressurized gas between high and low pressure sides around pistons and inlet and exhaust parts.
- Lack of design diversity in engine industry. Internal combustion engine itself is incapable of functioning as an air compressor, a vacuum pump, external combustion engine, water pump, and a drive turbine for expandable gas.

Advantages of Rotary Engines

- The main advantage is the high power to weight ratio.
- Light weight and compact.
- Smooth: no reciprocating motion.
- All the parts in a rotary engine spin continuously in one direction, rather than violently changing directions like the pistons in a conventional engine do. Rotary engines are internally balanced with spinning counterweights that are phased to cancel out any vibrations.
- Extended power "stroke" rotation of the output shaft: 270 degrees vs. the 180 degrees of a piston.
- Fewer moving parts: no valves, connecting rods, cams, timing chains. Intake and exhaust timing are accomplished directly by the motion of the rotor.
- Separation of combustion region from intake region is good for hydrogen fuel.
- Lower oxides of nitrogen (NOx) emissions.

Disadvantages of Rotary Engines

- High surface to volume ratio in combustion chamber is less thermodynamically efficient. The Wankel's long and narrow chamber makes for long flame travel, but this is countered by the Mazda's two spark plugs (three on some racing engines).
- Higher fuel consumption in naive designs. This is relative to the application because the high power of the engine must be considered. Thus Mazda has been successful with the RX-7 sports car, where its fuel economy is comparable to other cars in its class. Only 16 years after the first engine ran, the 1973 oil crisis devastated the RCE before it had sufficiently developed to become more economical. Thus the engine has a more negative reputation regarding fuel consumption than is actually deserved.
- The manufacturing costs can be higher, mostly because the number of these engines produced is not as high as the number of piston engines.

1.6   Characteristics of the Novel Rotary Engine

1.6.1   Improved Thermodynamic Cycle

One of the main characteristic of the designed engine is the increased the thermal efficiency above the reciprocating engines. This is achieved by implementing a new thermodynamic cycle and by realizing high compression ratios with less shaft power input within the working crescent shape cavity. This is achieved by the gradual and smooth work of the rotor and the sliding vane against the harmonious shape of the cycloid housing inner peripheral and the rotor side wall.

The designed novel rotary engine combines the advantages of Otto and Diesel cycles at intake, compression and combustion phases of the thermodynamic cycle, the engine also achieves an expanded power stroke that improves power extraction and efficiency. With a proper thermodynamic and geometrical match of the compressor and turbine working chambers, the expansion process can be improved and lower exhaust pressure and temperature levels can be achieved.

1.6.2   Separate Compression and Expansion Chambers

Actually, almost all rotary vane type engines produce very high torque because the combusted gas expands right against the hot section vane which also constitutes the arm length of the generated power torque. Therefore, not only is the crankshaft unnecessary for rotary engines, but when comparing engines of equal volumes, the power leverage on the drive shaft of a rotary engine is greater than that of a corresponding reciprocating engine.

1.6.3 Limited Peak and Extended Expansion Thermodynamic Cycle

The designed novel rotary engine combines the advantages of Otto and Diesel cycles at intake, compression and combustion phases of the thermodynamic cycle. It is well known that for a given compression ratio, the ideal Otto cycle currently provides the most efficient combustion / expansion process since it combines high peak temperature during the isochoric (constant volume) heat addition, while still keeping an acceptable mean chamber temperature. However, high peak combustion temperatures can cause auto-ignition of a portion of fuel-air mixture, resulting in engine knocks. Diesel is an improvement of the Otto cycle as it provides higher useful compression ratios and isobaric (constant pressure) heat addition and do not have knock problem as air alone is present during the compression process. The high compression ratios make Diesel engines more fuel efficient but for this same reason, they also become much heavier.

Compared to the Otto cycle, Diesel cycle also delivers less power for the same displacement. For the compression and combustion phases of the cycle, the ideal would be to follow a limited combustion pressure cycle that would first use a combined isochoric heat addition followed by isobaric and / or isothermal heat additions. Such hybrid engine process has been developed but they have proven impractical.

The designed novel rotary engine naturally follows the above-described limited peak cycle during the intake, compression and the two-step (isochoric, isobaric and / or isothermal) combustion phases.

Besides limiting the peak combustion pressures and temperatures within the rotary engine, the engine also achieves an expanded power stroke that improves power extraction by at least 10% and efficiency by more than 15%.

The designed novel engine configuration can be rearranged to form other thermodynamic cycles for a variety of power generation, ventilation, fluid pump, pressurization, heating and cooling applications.

1.6.4   Improved Sealing and Avoiding Wear.

Another characteristic of the designed engine is the decreased wear. The wear is minimized through the incorporation of the pivot axle vane retention mechanism and by providing efficient oil lubrication. The operational and maintenance costs are also minimized as the engine is an intermittent combustion engine with allows two combustion cycle per rotor revolution, thus allowing the hot section material to remain within an acceptable temperature levels. The new thermodynamic cycle has a shaved top pressure level that also limits the maximum operational temperature that is reached. Finally effective oil and water jacket cooling system is also implemented so as to provide a longer operational schedule between consecutive maintenance stops.

In the designed novel rotary engine, the intermediary cylindrical slides are eliminated all together as the vane tips are always in a natural contact with the housing inner peripheral. The basic reason for this natural contact is that the housing inner peripheral is non-circular and has a cycloid shape that accommodates well an eccentrically placed sliding vane of fixed length.

The cycloid peripheral is a unique shape, mainly depending on 4 parameters: the radial offset distance between the rotor center and the center of the chamber and, the sliding vane length, the seal height and the seal spring properties.

The dynamic and thermal loading behavior of the seal spring under rotation and the peripheral temperature differences, dictate a cycloid shape different than those given by exact equations of previous arts

The geometry has a good sealing capability as the rotating vane fits well the chamber cavity at all rotational angles.

Another characteristic of the designed engine is the decreased leakage. This has been achieved by the use of multi channel seals and by avoiding any use of complex mechanism. Therefore a compact, simple and reliable system was achieved.

1.7   Outline of the Thesis

In chapter two, the novel thermodynamic cycle of the novel rotary engine is being introduced. The P-V and T-S diagrams, basic equations and the efficiency calculations are given. Also in chapter two, the thermodynamic design code written to dimension the engine is explained and the dimension calculations of the novel engine are given.

The third chapter consists of the structural and mechanical design of the novel rotary engine with the dimensions taken from the thermodynamic design code. The structural analysis of the critical components and the material selection are explained and the results are presented. This chapter also includes brief explanation of the auxiliary systems (fuel, lubrication, ignition and cooling) of the engine.

The fourth chapter includes information on the test study of the prototype of the engine. Compressor, turbine and combustion chamber component tests and their results are presented.

In chapter five, all the work done in this thesis is summarized, the future work for this study is given and the application of this thesis in the industry is explained. A discussion of the results and the conclusion are also presented in this chapter.

CHAPTER 2

THERMODYNAMIC DESIGN OF THE NOVEL ROTARY ENGINE

2.1 Novel Thermodynamic Cycle

It is well known that for a given compression ratio, the ideal Otto cycle currently provides the most efficient combustion / expansion process as it combines high peak temperature during the isochoric (constant volume) heat addition, while still keeping an acceptable mean chamber temperature. However, high peak combustion temperatures can cause auto-ignition of a portion of fuel-air mixture, resulting in engine knocks. Diesel is an improvement of the Otto cycle as it provides higher useful compression ratios and isobaric (constant pressure) heat addition and do not have knock problem as air alone is present during the compression process. The high compression ratio makes Diesel engines more fuel-efficient but for this same reason, they also become much heavier. Compared to the Otto cycle, Diesel cycle also delivers less power for the same displacement. For the compression and combustion phases of the cycle, the ideal would be to follow a limited combustion pressure cycle that would first use a combined isochoric heat addition followed by isobaric and/or isothermal heat additions. As mentioned in a prior patent, such hybrid engine process has been developed (Texaco TCCS, Ford PROCO, Ricardo, MAN-FM and KHD-AD) but they have been proven impractical. This is probably because the piston engine was forced unsuccessfully to follow the hybrid Otto-Diesel thermodynamic cycle.

It is important to understand that, not only the thermodynamics but also the kinematics and the fluid mechanics are involved when adapting a thermodynamic cycle to an engine.

The rotary vane engine designed in this thesis naturally follows the new limited peak thermodynamic cycle (Figure 2-1 and 2-2).

This novel cycle [17], combines the advantages of Otto and Diesel cycles at intake, compression and combustion phases by limiting the peak combustion temperature. The present cycle also has an expanded power stroke. With a proper thermodynamic and geometrical match of the compressor and turbine working chambers volumes, ambient exhaust pressure levels can be achieved. These features explained below, fundamentally differ from previous thermodynamic cycles.

2.1.1   P – V, T – S Diagrams
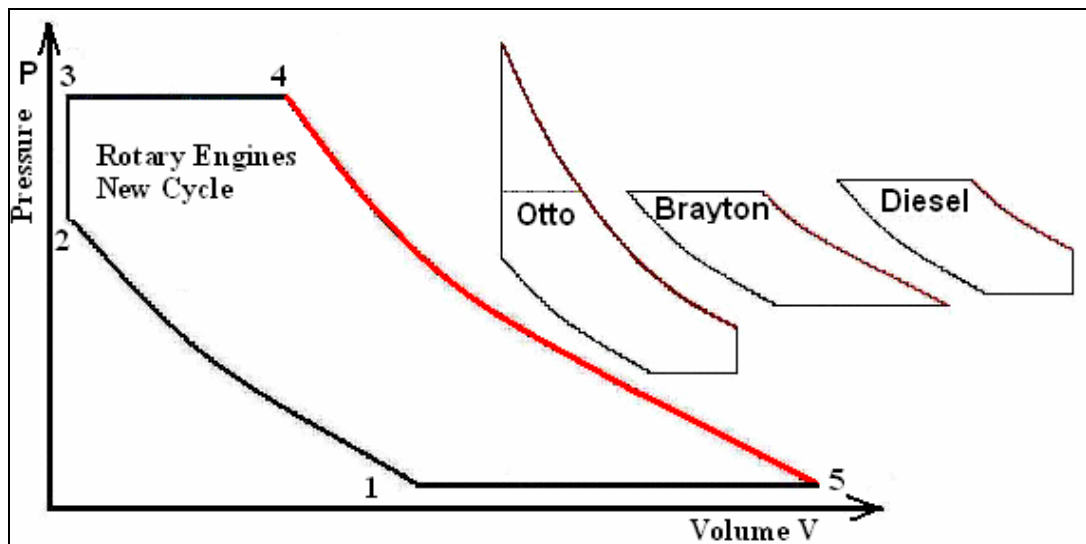
Figure 2-1   Novel Thermodynamic Cycle (P – V) for Rotary Vane Engine

27
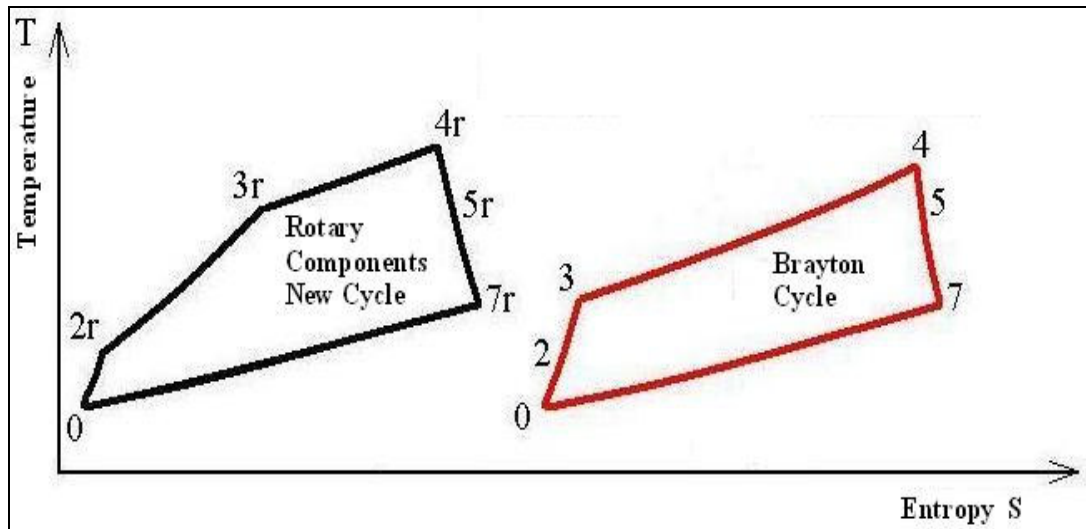
Figure 2-2   Novel Thermodynamic Cycle (T – S) for Rotary Vane Engine

Firstly, the combustion phase is divided into two parts; θ_{ec}, the external combustion phase occurring in a burner placed midway between the compressor and turbine chambers, and θ_{ic}, the internal combustion phase which occurs within the turbine.(Figure 2-3) In the designed novel engine, θ_{ec} can arbitrarily take very large angle bracket values up to 180°. This angle bracket by far exceeds those allowed in a piston engine where the combustion process is generally squeezed down to a narrow angle bracket (θ_{cp}-90°, given in Figure 2-4) not exceeding 30°. This shows that the designed novel engine operating thermodynamic cycle allows ample time for enhanced fuel-air mixing and also allows wave compression within the burner prior to let the gas expands through a Laval nozzle like crescent shape rotary turbine area.

The ample time given for the combustion chamber is the key to a successful lean combustion, further improving the thermal efficiency and protecting the turbine vane and the rotor from high temperatures spots. Secondly, the rotary engine allows 2 firings per revolution. Therefore, at every time within the engine two overlapping power stroke exists forming a powerful torque couple that acts on both sides of the turbine vane. The strong torque couple is driven by gas that expands up to ambient pressures within the turbine chamber.

28
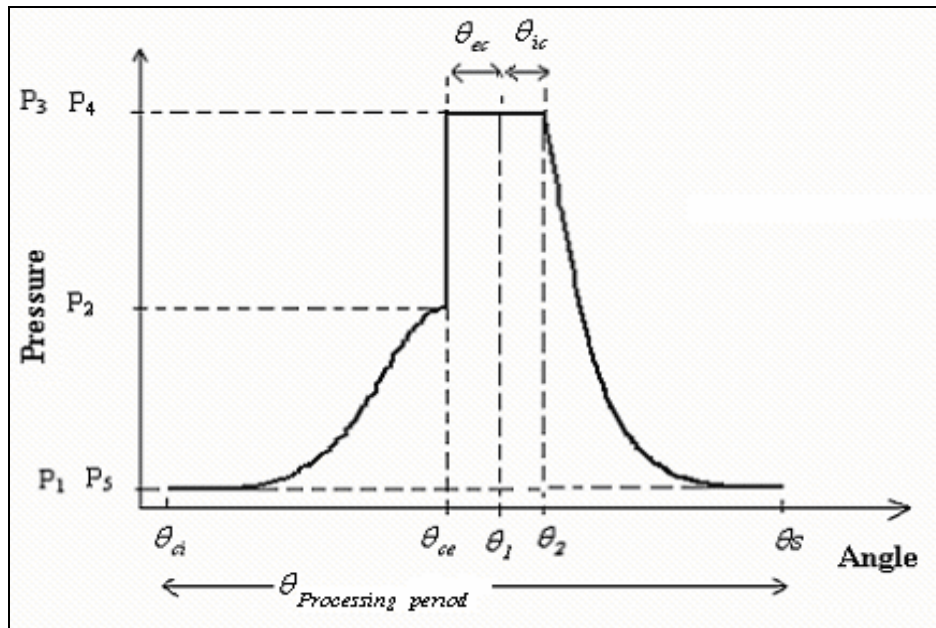
Figure 2-3   P-θ chart for the novel thermodynamic cycle
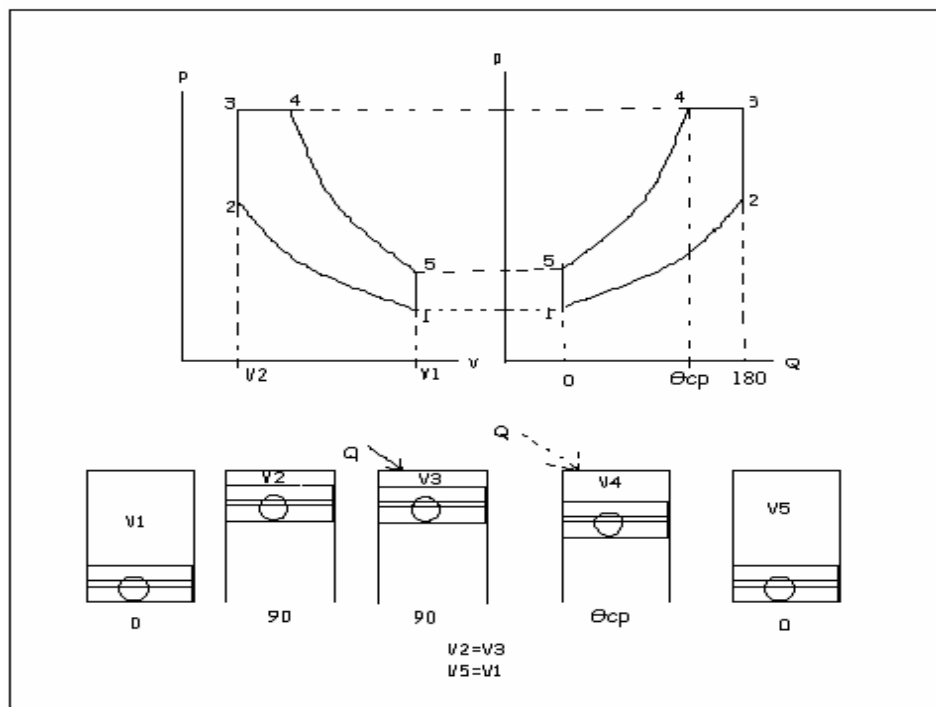
Figure 2-4   Thermodynamic cycle of the duel (Otto-Diesel) cycle

29

2.1.2 Efficiency of the Cycle

By limiting the peak combustion pressures, the present design of the novel engine also provides an expanded power stroke that improves power extraction. It is possible to derive the new cycle ideal thermal efficiency by writing the proper temperature, pressure and specific volume relations within the thermal efficiency definition (Equation 2.1 and 2.2) given below.

$$\eta_{th} = \frac{Qin - Qout}{Qin} = 1 - \frac{Qout}{Qin} \tag{2.1}$$

$$\eta_{th} = \frac{mC_p(T_5 - T_1)}{mC_v(T_3 - T_2) + mC_p(T_4 - T_3)} \tag{2.2}$$

$$\eta_{th} = \frac{k(T_5 - T_1)}{(T_3 - T_2) + k(T_4 - T_3)} \tag{2.3}$$

Writing all of the temperatures in terms of T_1 to simplify the efficiency equation;

$$T_2 = T_1\left(\frac{V_1}{V_2}\right)^{k-1} = T_1 r_1^{k-1} \tag{2.4}$$

$$T_3 = T_2\left(\frac{P_3}{P_2}\right) = T_1 r_p r_1^{k-1} \tag{2.5}$$

$$T_4 = T_3\left(\frac{V_4}{V_3}\right) = T_3 r_c = T_1 r_c r_p r_1^{k-1} \tag{2.6}$$

30

$$T_5 = T_4 \left(\frac{V_4}{V_5} \right)^{k-1} \tag{2.7}$$

$$\frac{V_4}{V_5} = \frac{1}{r_2} = \left(\frac{P_5}{P_4} \right)^{\frac{1}{k}} = \left(\frac{P_1}{P_4} \right)^{\frac{1}{k}} = \left(\frac{P_1}{P_2} \frac{P_2}{P_3} \right)^{\frac{1}{k}} = \frac{1}{r_1} \left(\frac{1}{r_p} \right)^{\frac{1}{k}} \tag{2.8}$$

Inserting the equation. 2.8 into the equation. 2.7;

$$T_5 = T_1 r_c r_p (r_1 / r_2)^{k-1} = T_1 r_c r_p^{1/k} \tag{2.9}$$

Therefore;

$$\eta_{th} = 1 - \frac{kT_1 \left(r_c r_p \left(\frac{r_1}{r_2} \right)^{k-1} - 1 \right)}{T_1 \left(r_p r_1^{k-1} - r_1^{k-1} \right) + kT_1 \left(r_c r_p r_1^{k-1} - r_p r_1^{k-1} \right)} \tag{2.10}$$

$$\eta_{th} = 1 - \frac{k}{r_1^{k-1}} \left(\frac{r_c r_p^{1/k} - 1}{(r_p - 1) + (r_p k)(r_c - 1)} \right) \tag{2.11}$$

where;

$$r_c = \frac{V_4}{V_3} \qquad r_p = \frac{P_3}{P_2} \qquad r_1 = \frac{V_1}{V_2} \tag{2.12}$$

Comparing with the Otto cycle thermal efficiency given below (Equation 2.13), it is seen that the new thermodynamic cycle thermal efficiency has a much higher degree of freedom as Equation 2.11 is defined in terms of 3 variables (namely r_L, r_p, r_c)all defined above, compared to only one variable $r = V_1 / V_2$ for the Otto cycle. As temperature upper limit restricts the increase of Otto cycle volume ratio r, the Otto thermal efficiency reaches a modest peak value. As for the diesel cycle thermal efficiency given below (Equation 2.14), it is even lower because the term A is bigger than 1.

$$\eta_{th\,Otto} = 1 - \frac{1}{r^{k-1}} \tag{2.13}$$

$$\eta_{th\,Diesel} = 1 - \frac{1}{r^{k-1}} A \tag{2.14}$$

As the bracketed term in Equation 2.11 is always less than 1, the new thermodynamic cycle thermal efficiency is guaranteed to be always bigger than those pertaining to Otto and Diesel cycles.

2.2 Dimensioning the Engine

2.2.1   Thermodynamic Design Code

This thermodynamic design code is written to calculate the necessary geometry of the novel rotary engine for the desired performance values and to determine the thermodynamic properties during compression, combustion and expansion phases which will be used in the structural analysis of the engine parts.

Firstly, performance parameters (power output, rpm) of the novel rotary engine that will be designed are made certain. After describing the performance of the engine, the critical parameters of the engine such as maximum temperature during combustion, fuel to air ratio, compression ratio are specified. By processing the basic inputs (atmospheric properties, thermodynamic constants and desired engine properties) and the geometric inputs (basic dimensions of the engine), the code calculates the properties for the compression phase, constant volume and constant pressure combustion phases and the expansion and exhaust phases, and matches the compressor and turbine geometry. After finalizing the engine geometry, the code makes the necessary performance calculations to determine the power output, and thermal efficiency. If the required power output is not managed, then the compressor geometry is revised and the compressor – turbine matching is remade. After finalizing the engine geometry, the thermal efficiency and the thermal properties during compression, combustion and expansion phases which will be used in the structural analysis of the engine parts are calculated.

The flowchart of the thermodynamic code is given in Figure 2-5.

CODE FLOWCHART START

Basic Inputs:

- Atmospheric properties
- Thermodynamic constants
- Desired properties
  - Rotational speed
  - Compression Ratio
  - Fuel/Air Ratio

Geometry Inputs:

Determine basic dimensions of engine:
- Compressor vane length & thickness, rotor diameter
- Compressor & turbine chamber height
- Turbine vane length & thickness, rotor diameter

Inlet:

- Atmospheric air conditions
- Calculate inlet volume.

0

Compression:

- Polytrophic compression of inlet air.

1

Constant Volume Combustion:

- Combustion in combustion chamber with valves closed.

2

Constant Pressure Combustion:

- Combustion through combustion chamber and turbine chamber.

3

Expansion:

- Polytrophic expansion of gas inside turbine.
- Polytrophic expansion of gas to the atmospheric pressure.
- Exhaust

4

Under-expansion

No   Increase turbine height.

Atmospheric expansion succeeded?

Over-expansion

Yes   Decrease turbine height

Performance Calculation:

- Calculate shaft power and thermal efficiency.

Output:
- Geometry
- Thermodynamic properties at each state.
- Performance

END

Figure 2-5   Flowchart of the Thermodynamic Code

34

DESCRIPTION OF THE THERMODYNAMIC CODE:

INPUTS

Table 2.1   Thermodynamic Code Basic Inputs

C_p	Specific heat constant (constant pressure)
C_v	Specific heat constant (constant volume)
P_1	Atmospheric air pressure
T_1	Atmospheric air temperature
ρ_1	Atmospheric air density
R	Universal gas coefficient
k	Polytrophic expansion and compression constants
C_r	Compression ratio
rpm	Revolution per minute
far	Fuel/Air ratio
hfu	Fuel properties (Fuel enthalpy)
	Geometrical properties

CALCULATIONS

- ***Compressor Inlet Volume and Inlet Air Properties Calculation***
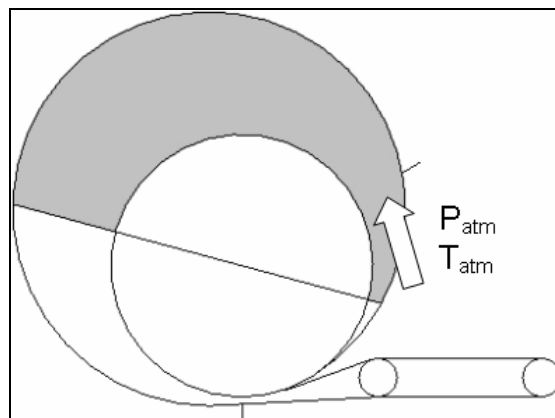
Figure 2-6   Compressor Air Intake Phase

Table 2.2 Thermodynamic Code Air Intake Variables

V_1	Compressor inlet volume
r_c	Radius of the compressor
e_c	Eccentricity of the compressor
α_c	Compressor vane front angle for the inlet volume
δ_c	Compressor vane back angle for the inlet volume
m	Mass of the air
ρ_1	Atmospheric air density
h_c	Height of the compressor
d_c	Diameter of compressor

$$r_c = d_c / 2 \tag{2.15}$$

$$e_c = (l - 2 \times r_c)/4 \tag{2.16}$$

$$\delta_c = \alpha_c + 180 \tag{2.17}$$

$$V_1 = \begin{bmatrix} (0.5 \times e_c^2 \times \sin 2\alpha_c - 2 \times (e_c \times r_c + 2 \times e_c^2) \times \sin \alpha_c \\ + (3 \times e_c^2 + 2 \times e_c \times r_c) \times \alpha_c) - (0.5 \times e_c^2 \times \sin 2\delta_c - 2 \times (e_c \times r_c + 2 \times e_c^2) \\ \times \sin \delta_c + (3 \times e_c^2 + 2 \times e_c \times r_c) \times \alpha_c) - 2 \times e_c \times t_c \end{bmatrix} \times h_c \tag{2.18}$$

$$m = V1 \times \rho_1 \tag{2.19}$$

- *Compression and Combustion Chamber Volume Calculation*
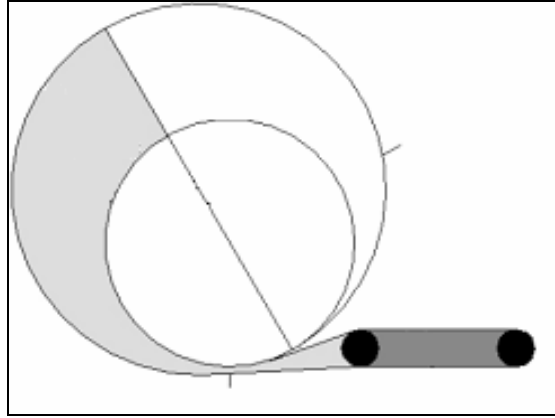
Figure 2-7   Compression Phase

Table 2.3   Thermodynamic Code Compression Variables

P_2	Air pressure after compression
T_2	Air temperature after compression
ρ_2	Air density after compression
W_2	Compression work
C_r	Compression ratio
V_2	Combustion chamber volume

$$V_2 = V_1 / C_r \tag{2.20}$$

$$P_2 = C_r^{\,k} \times P_1 \tag{2.21}$$

$$T_2 = T_1 \times C_r^{\,k-1} \tag{2.22}$$

$$\rho_2 = P_2 / (R \times T_2) \tag{2.23}$$

$$W_2 = C_v \times (T_1 - T_2) * m \times rpm / 60 \times 2 \tag{2.24}$$

- *Combustion*

  o *Constant Volume Combustion*
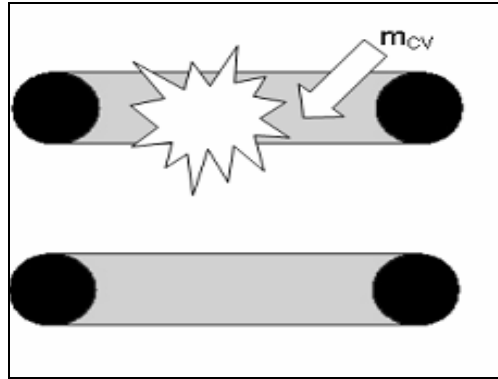
Figure 2-8   Constant Volume Combustion Phase

Table 2.4   Thermodynamic Code Constant Volume Combustion Variables

T_3	Air temperature after constant volume combustion
f_{cv}	Constant volume combustion fuel ratio
far	Fuel/Air ratio
hfu	Fuel enthalpy
P_3	Air pressure after constant volume combustion
V_3	Combustion volume
ρ_3	Air density after constant volume combustion

$$T_3 = T_2 + ((m \times f_{cv} \times far \times hfu)/(m \times C_v) \tag{2.25}$$

$$P_3 = P_2 \times T_3 / T_2 \tag{2.26}$$

$$\rho_3 = P_3 /(R \times T_3) \tag{2.27}$$

$$V_3 = V_2 \tag{2.28}$$

o *Constant Pressure Combustion*
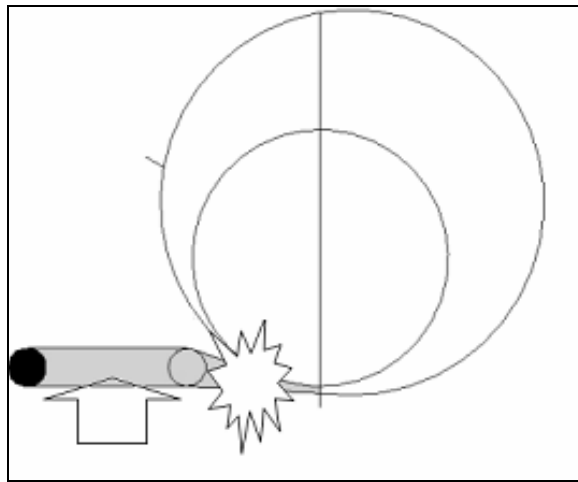
Figure 2-9   Constant Pressure Combustion Phase

Table 2.5   Thermodynamic Code Constant Pressure Combustion Variables

T$_4$	Air temperature after constant pressure combustion
P$_4$	Air pressure after constant pressure combustion
V$_4$	Combustion volume
ρ_4	Air density after constant pressure combustion

$$T_4 = T_3 + ((m \times (1 - f_{cv}) \times far \times hfu)/(m \times C_p) \tag{2.29}$$

$$P_4 = P_3 \tag{2.30}$$

$$\rho_4 = P_4 /(R \times T_4) \tag{2.31}$$

$$V_4 = V_3 \times T_4 / T_3 \tag{2.32}$$

- *Turbine Expansion Volume and Air Properties After Expansion in the Turbine Calculation*
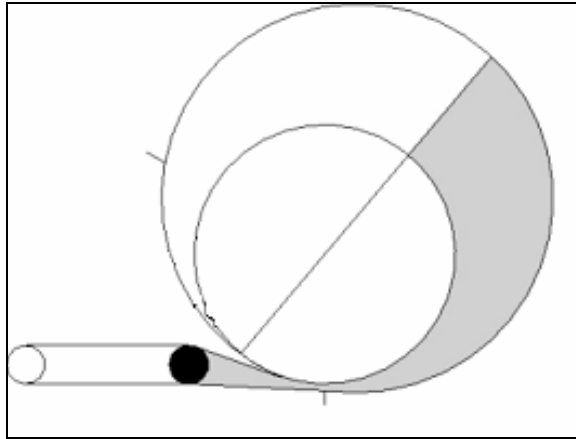
Figure 2-10   Turbine Expansion Phase

Table 2.6   Thermodynamic Code Expansion Variables

V_5	Turbine inlet volume
r_t	Radius of the turbine
h_t	Estimated height of the turbine
e_t	Eccentricity of the turbine
α_t	Turbine vane angle for the exhaust volume
ρ_5	Density of the air after expansion
W_5	Expansion work
T_5	Air temperature after expansion
P_5	Air pressure after expansion

$$r_t = d_t / 2 \tag{2.33}$$

$$e_t = (l - 2 \times r_t)/4 \tag{2.34}$$

$$V_5 = \begin{bmatrix} (0.5 \times e_t^2 \times \sin 2\alpha_t - 2 \times (e_t \times r_t + 2 \times e_t^2) \times \sin \alpha_t + (3 \times e_t^2 + 2 \times e_t \times r_t) \times \alpha_t) \\ -(0.5 \times e_t^2 \times \sin 2(\alpha_t - 180) - 2 \times (e_t \times r_t + 2 \times e_t^2) \times \sin(\alpha_t - 180) \\ +(3 \times e_t^2 + 2 \times e_t \times r_t) \times (\alpha_t - 180)) - 2 \times e_t \times t_t \end{bmatrix} \times h_t \tag{2.35}$$

$$P_5 = (V_4 / V_5)^k \times P_4 \tag{2.36}$$

Checking P$_5$ for 1 atm or not

If not increase or decrease the turbine height
If 1 atm then

$$T_5 = T_4 \times (V_4 / V_5)^{k-1} \tag{2.37}$$

$$\rho_2 = P_5 /(R \times T_5) \tag{2.38}$$

$$W_5 = C_v \times (T_4 - T_5) * m \times rpm / 60 \times 2 \tag{2-39}$$

- **Performance Calculations**

Table 2.7   Thermodynamic Code Performance Variables

m_{fuel}	Fuel mass
Q_{in}	Energy going into the engine
Q_{out}	Energy going out from the engine
η_{th}	Thermal efficiency
W_{net}	Net work done by the engine
m_{dot}	Air mass flow rate

$$m_{fuel} = m \times far \times 2 \times rpm / 60 \qquad (2.40)$$

$$Q_{in} = m_{fuel} \times hfu \qquad (2.41)$$

$$Q_{ex} = m \times C_p \times (T_5 - T_1) \times 2 \times rpm / 60 \qquad (2.42)$$

$$\eta_{th} = 1 - Q_{ex} / q_{in} \qquad (2.43)$$

$$W_{net} = Q_{in} - Q_{ex} \qquad (2.44)$$

$$m_{dot} = m \times rpm / 60 \times 2 \qquad (2.45)$$

The calculated pressure, volume and temperature values are given in Figures 2-11 and 2-12 respectively.
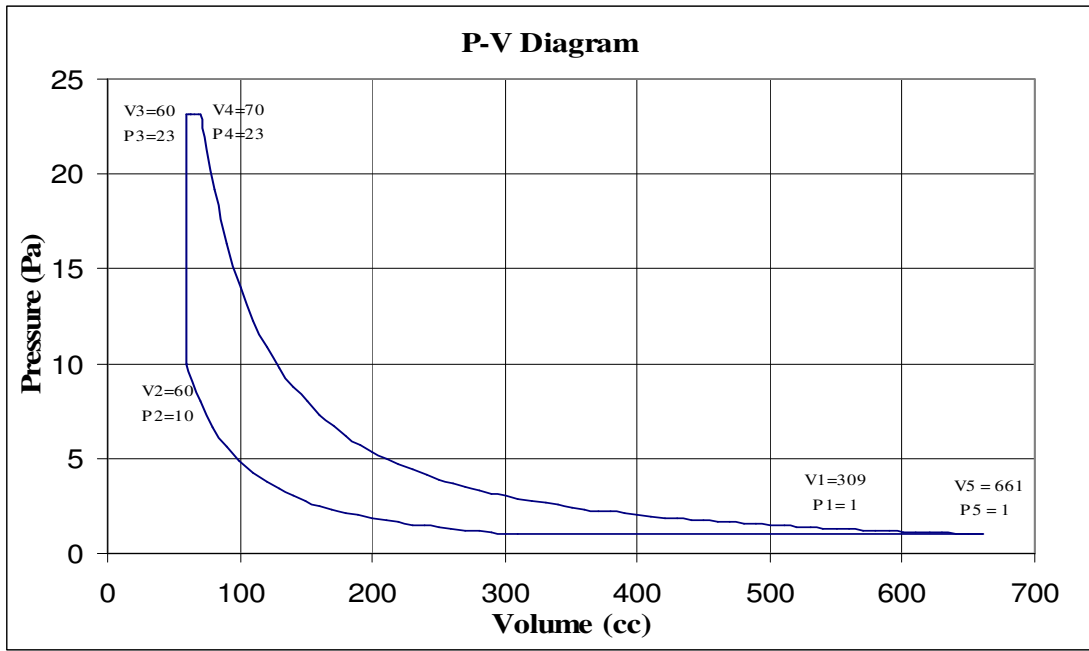
Figure 2-11   P – V Diagram of Novel Thermodynamic Cycle
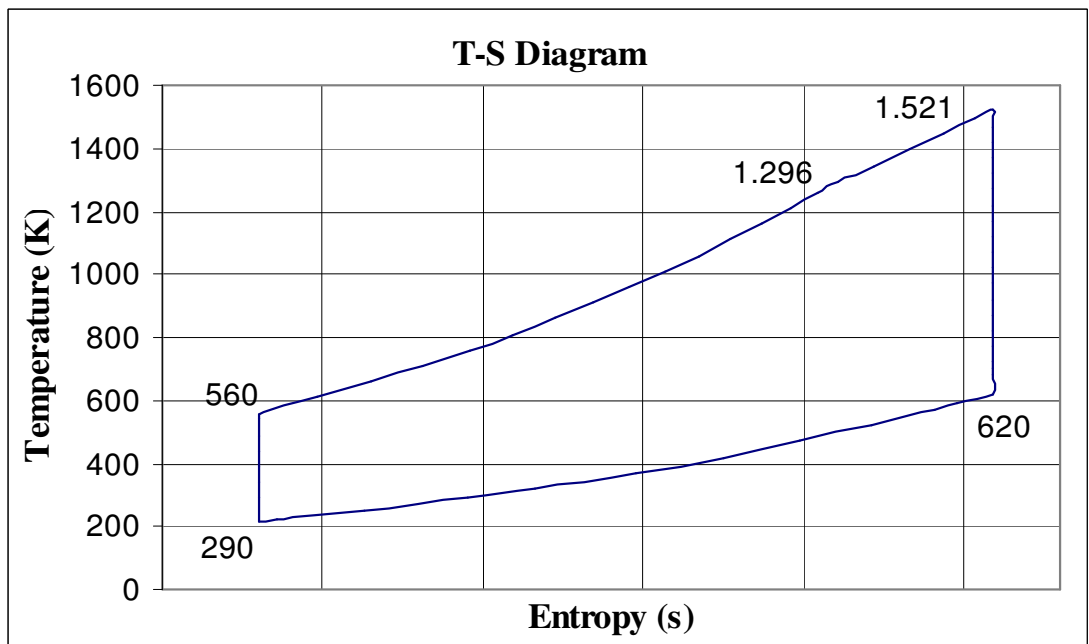
Figure 2-12   T - S Diagram of Novel Thermodynamic Cycle

2.2.2 Requirements of the Engine

As a high speed, low cost aerial target system solution, Turna (Fig.2-13) is an unmanned air vehicle (UAV), designed and developed by Tusas Aerospace Industries as a firing target drone. It is a low-wing monoplane with delta wings and detachable sweptback V-tail. Turna has a composite body structure, an improved aerodynamics and a highly performing avionics. The characteristics of the unmanned air vehicle are given below. [23]

Power plant	: WANKEL engine
Power Output	: 38 hp @ SL
Fuel Consumption	: 0.236 kg/h/hp
Propeller	: 66x60cm, 2-Blades
Endurance	: 1.5 hrs
Launch	: Bungee catapult
Recovery	: Parachute recovery
	: Skid landing
Mission Radius	: 3 km, visible command range
	: 15 km, with optical aids

Figure 2-13   Turna, TAI's Unmanned Air Vehicle

2.2.3 Dimensions of the Engine

By using the thermodynamic design code, the novel rotary engine is dimensioned to give the required power. The dimensions of the compressor and turbine of the rotary engine were given in tables 2.8 and 2.9 respectively.

Table 2.8   Compressor Dimensions

Compressor Dimensions		
Compressor Vane Length	[m]	0,14
Compressor Rotor Diameter	[m]	0,11
Compressor Eccentricity	[m]	0,0075
Compressor Vane Thickness	[m]	0,012
Compressor Height	[m]	0,0593
Compressor Inlet Volume	[cm^3]	299,18
Compressor Inlet Close Angle	[deg]	90
Compressor Valve Open Angle	[deg]	180
Compressor Valve Close Angle	[deg]	330

Table 2.9   Turbine Dimensions

Turbine Dimensions		
Turbine Vane Length	[m]	0,2
Turbine Rotor Diameter	[m]	0,15
Turbine Eccentricity	[m]	0,0125
Turbine Vane Thickness	[m]	0,012
Turbine Height	[m]	0,0548
Turbine Max Expansion Vol. Volume	[cm^3]	661,05
Turbine Exhaust Angle	[deg]	270
Turbine Valve Open Angle	[deg]	30
Turbine Valve Close Angle	[deg]	180

External burner volume and fuel to air ratios for the external burner and turbine are given in table 2.10.

Table 2.10   External Burner and F/A Ratios

External Burner and F/A Ratios		
External Burner Volume	[cm^3]	59,82
Lower Heating Value of the Fuel	[J/kg]	48000000
Total Fuel to Air Ratio		0,01572
Fuel to Air Ratio in External Burner		0,011
Fuel to Air Ratio in Turbine		0,00471

2.2.4   Calculated Performance of the Engine

The non-ideal aerothermodynamics performance calculations of the rotary vane engine are given below.

Table 2.11   Performance Parameters

Calculated Performance Parameters		
RPM		6000
Total Energy Input	[kW]	56,928
Total Energy Output	[kW]	25,041
Shaft Power	[kW]	31,887
Shaft Power	[hp]	42,744
Thermal Efficiency	[%]	56,012

Table 2.12   Rotary Vane Engine Pressure and Temperature Distribution

Rotary Vane Engine Pressure and Temperature Distribution							
	Compressor		External Burner		Turbine		
	Inlet	Exit	Inlet	Exit	Inlet	Internal combustion	Exit
P (Pa)	101325	1013229	1013229	2344497	2344497	2344497	101582.3
T (K)	290	559	559	1295	1295	1520	620

46

The temperature and pressure levels based on these calculations are given in table 2.12 A non-ideal thermal efficiency of 56,012% has been calculated. Calculated performances of the rotary vane engine are compared with a UAV Engines Ltd. AR-741 Wankel engine producing 38 kW shaft power at sea level. Figure 2-14 shows 67 % surplus in rotary power at low speeds and 48 % excess in rotary power at high speeds. Best of all, the high improvement in the power performance is also accompanied by a drop in specific fuel consumption (Figure 2-15). If the rotary vane engine is used, a drop of 68% is expected at relatively low speeds and a drop of 66% is expected at high speeds. A similar performance improvement is expected for torque production (Figure 2-16). At low rpm, rotary vane engine torque production is greater by 62% where as at high rpm values, torque is increased by 47%.
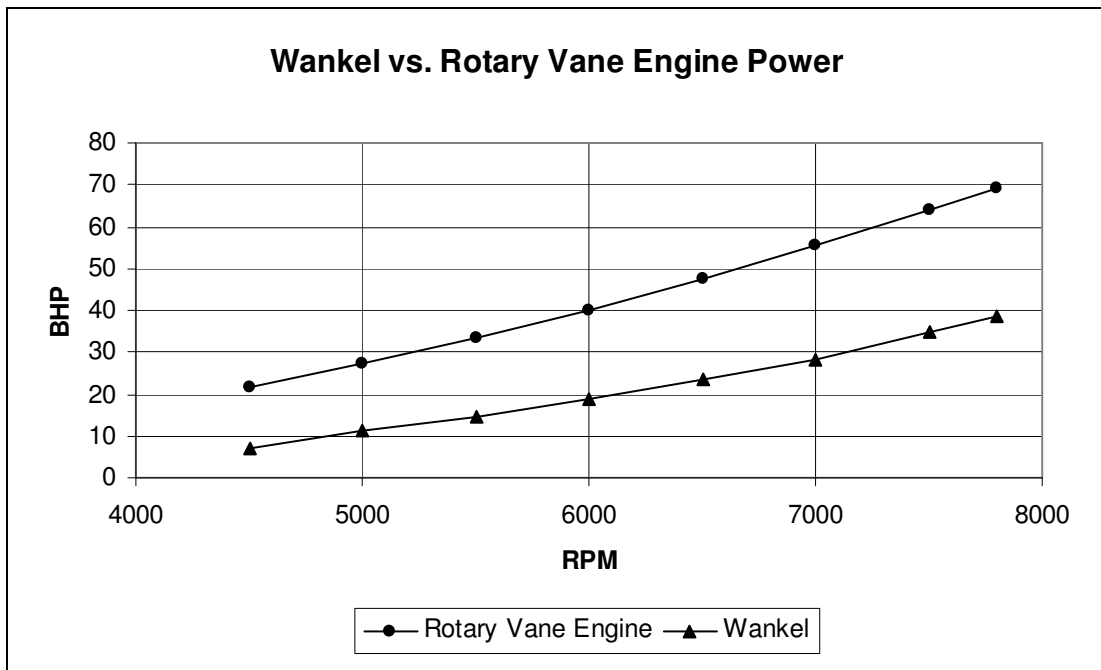
Figure 2-14   Rotary Vane Engine Shaft Power vs. RPM
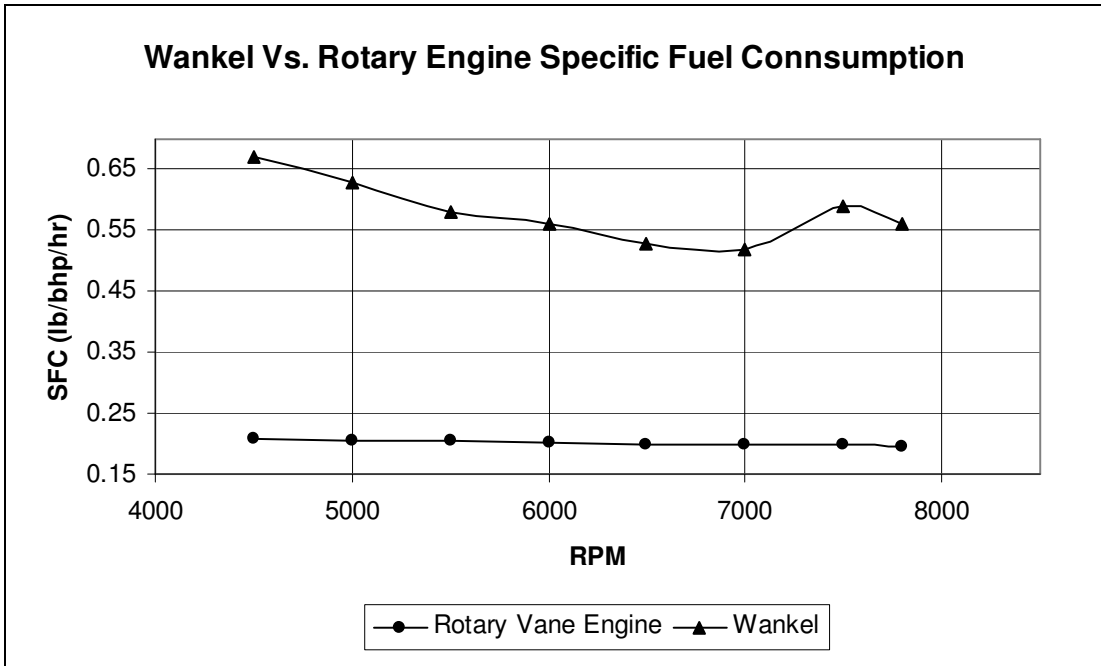
Figure 2-15   Rotary Vane Engine Specific Fuel Consumption vs. RPM
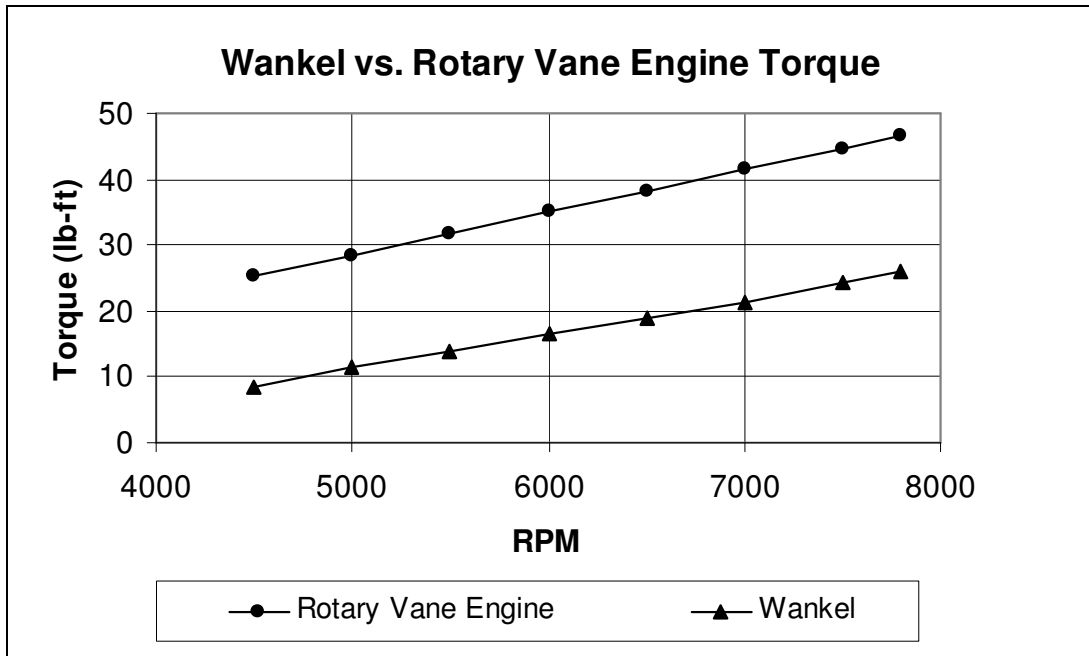
Figure 2-16   Rotary Vane Engine Net Torque vs. RPM

Table 2.13   Comparison of Engines

Comparison of Engines Characteristics and Related Thermodynamic Cycles					
Engine Type and Thermodynamic cycle	**Wankel Otto**	**Rotary Vane New cycle**	**Piston Otto**	**Piston Diesel**	**Small Gas turbine (0-500 kW) Brayton**
Power production	1 time per 1 revolution	2 times per 1 revolution	1 time per 2 revolutions	1 time per 2 revolutions	Continuous
Thermal efficiency	Low	Very high	Average	High	Low
Expansion up to ambient pressure?	No	Yes	No	No	Yes
Maximum engine temperature	Very high but intermittent: internal combustion engine	Limited and intermittent: External-internal combustion engine	High but intermittent	Limited and intermittent: internal combustion engine	Very high and continuous: external combustion engine
Torque production at low RPM	Average	Very high	Low	High	Very low
Torque production at high RPM	Average	Very high	High	High	Very high
Number of moving parts	Low	Low	High	High	Very low
Can inlet, compressor, combustor, turbine be optimized separately	No	Yes	No	No	Yes
Rotor dynamics	Off-center rotation, cyclic acceleration	Quasi steady rotation and acceleration	Reciprocating motion, high unsteady acceleration	Reciprocating motion, high unsteady acceleration	Steady rotation and acceleration

CHAPTER 3

STRUCTURAL AND MECHANICAL DESIGN OF THE NOVEL TURBO ROTARY ENGINE

3.1 Compressor Design

- The designed compressor of the novel turbo rotary engine is a sliding vane compressor which is a positive displacement type rotary compressor. This compressor uses a rotor equipped with a radially movable single sliding vane, mounted eccentrically in a crescent shape cavity. The single vane is free to slide in and out of the slot cut into the rotor. As the rotor rotates, both ends of the sliding vane are extending radially outward and are in contact with the cycloid inner surface of the housing peripheral at all rotational angles by the centrifugal force. Apex seals at the tips of the vane are used to achieve proper sealing. Air enters through the suction port. As the eccentrically mounted rotor turns, space between the rotor and the housing decreases and the trapped air between the vane, the rotor and the inner housing surface is compressed until the discharge valve opens.

- Also cooling oil is sprayed into the housing to absorb heat of compression; keeping air temperature relatively low, improving efficiency and sealing and lubricating the vane tips. For oil free applications, oil separators and effective special air filters can be used to remove oil and oil vapor from the compressed air. The designed sliding vane compressor does not need a valve at the suction port because of continuous suction occurring in the inlet port. Once the suction of first cell ends, the suction of the second cell begins. If the valve at the discharge port is taken off, the compressor can work as a blower.

The designed compressor diagram can be seen in figure 3-1.
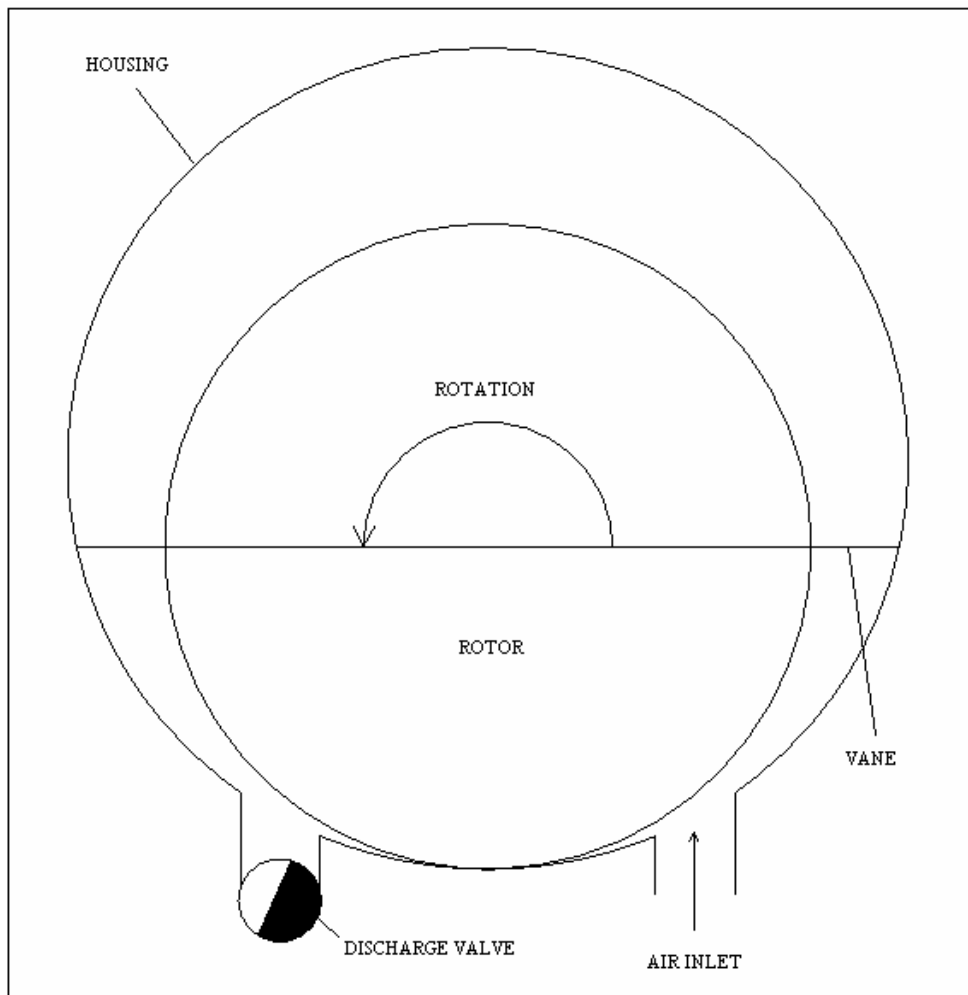
Figure 3-1   Rotary Compressor Diagram

Swept Volume of the Rotary Compressor

The swept volume by a vane can be calculated as a function of swept angle θ from figure 3-2.
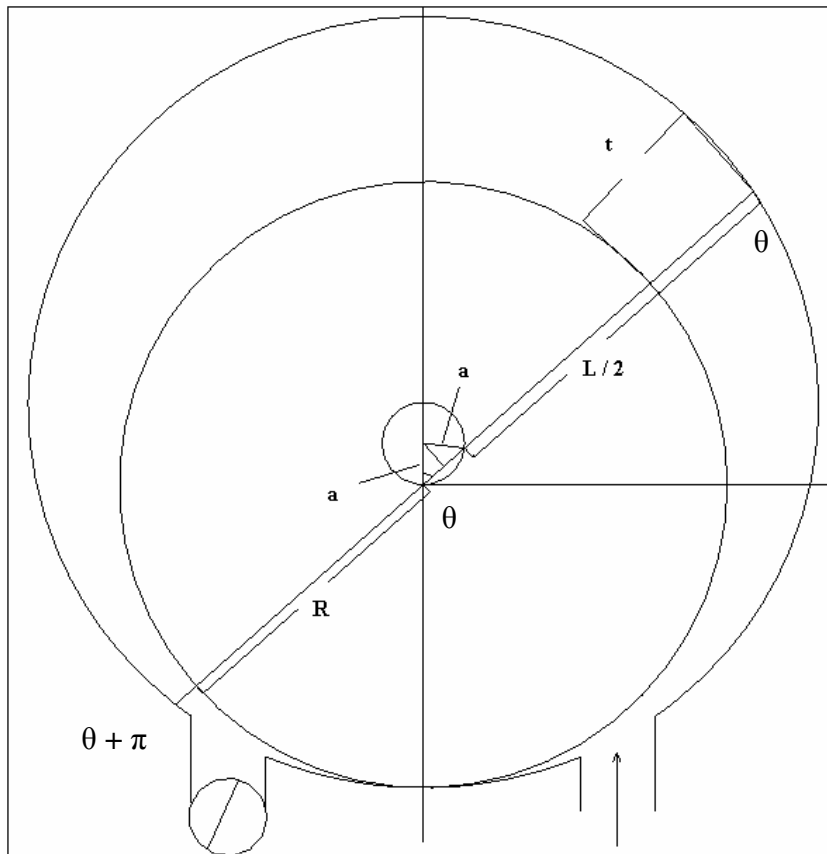
Figure 3-2   Rotary Compressor Kinematics

Table 3.1   Rotary Compressor Parameters

R	Rotor Radius
L	Vane Length
a	Eccentricity / 2
t	Vane Length Between Rotor and Housing
θ	Swept Angle
h_c	Compressor Height

Swept Volume (S_w) can be calculated as follows;

$$S_w = \left[\int_{\theta}^{\theta+\pi} t.d\theta \right] \times h_c \qquad (3.1)$$

From geometry t can be found as;

$$t = (L/2 - (2.a.\cos\theta) - (R)) \qquad (3.2)$$

Substituting t into equation 3.1;

$$S_w = \left[\int_{\theta}^{\theta+\pi} [L/2 - (2 \times a \times \cos\theta) - (R)]d\theta \right] \times h_c \qquad (3.3)$$

Inlet Volume

Inlet volume is the maximum swept volume.
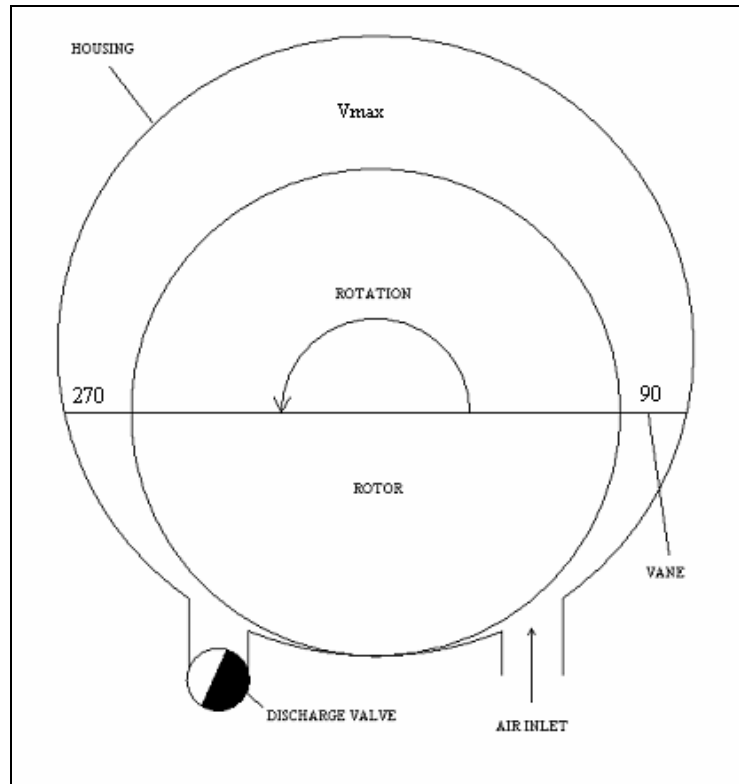
Figure 3-3   Rotary Compressor Inlet Volume

$$S_w = \left[\int_{90}^{270} [L / 2 - (2 \times a \times \cos \theta) - (R)]d\theta \right] \times h_c \qquad (3.4)$$

Design Parameters

Using the thermodynamic design code explained in Chapter 2, the geometry of the compressor is calculated. The geometric parameters of the rotary compressor are given below;

R	110 mm
L	140 mm
a	7.5 mm
h_c	596 mm
t_v	12 mm

Using the geometric data taken from the thermodynamic design code the rotary compressor was designed in CAD environment.

The rotary compressor is composed of a housing, upper and lower taps, upper and lower bearing housings, a rotor and its top seals, a vane and its apex seals and springs, a discharge valve and its bearing housing, two timing pulleys and one timing belt and two discharge ports.

As the compressor vane divides the compressor housing into two parts, for one complete revolution, compressor discharges two units of compressed air. The compressor valve is so designed that it discharges this two units of compressed air to the discharge ports respectively.

The discharge valve is coupled with the rotary compressor rotor with the help of two timing pulleys and one timing belt and revolves at the same rpm with the rotor. The position of the discharge valve relative to the compressor rotor is adjusted with the timing pulleys by the help of set screws, such that it discharges the compressed air to both discharge ports at correct times.

An oil pump is used to lubricate the compressor inner surface and the three bearings. (Two main rotor bearings and one discharge valve bearing)
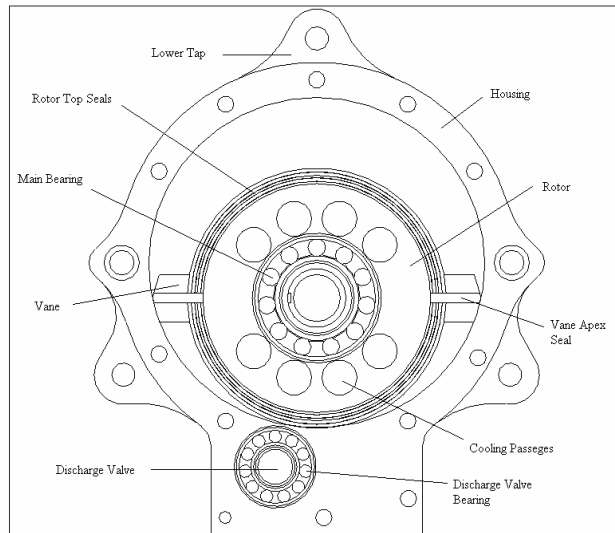
Figure 3-4   2-D Drawing Of Rotary Compressor
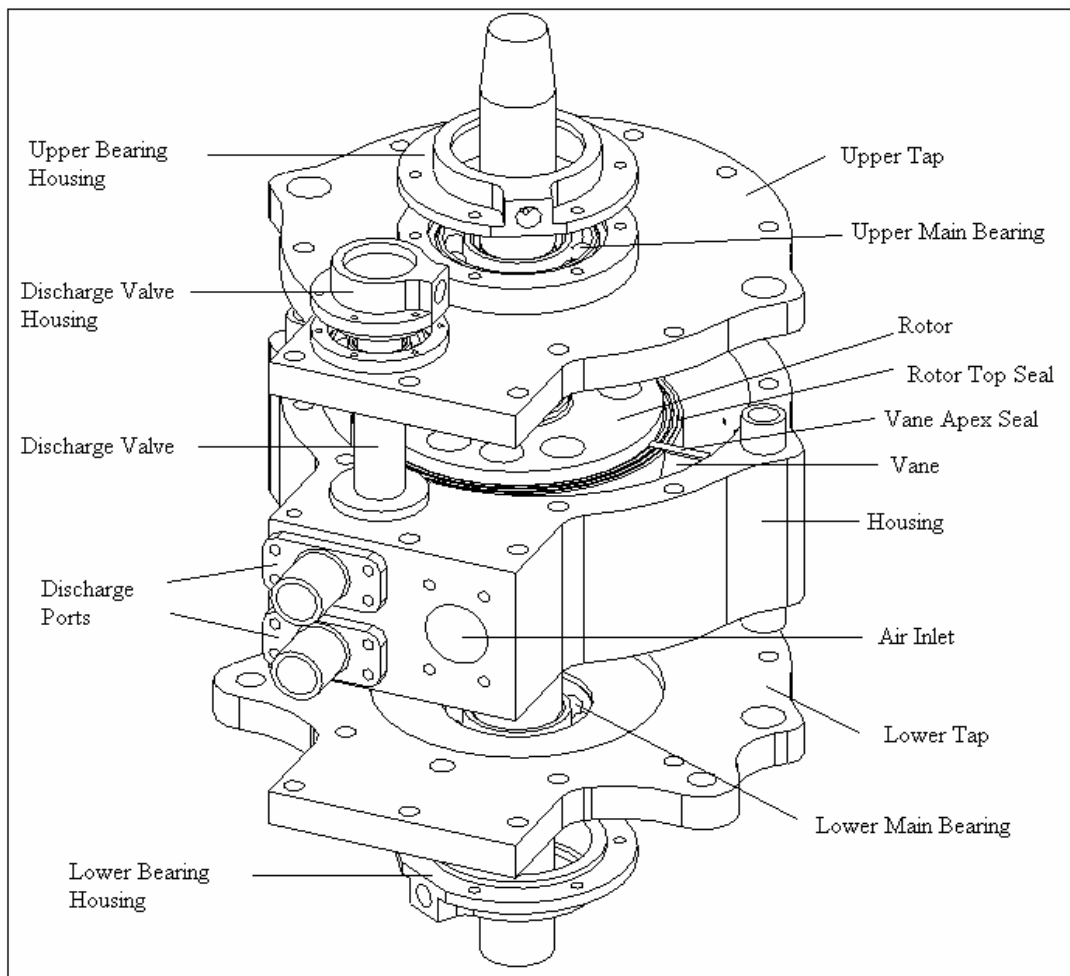
Figure 3-5   3-D Wire-Frame Drawing of Rotary Compressor

56
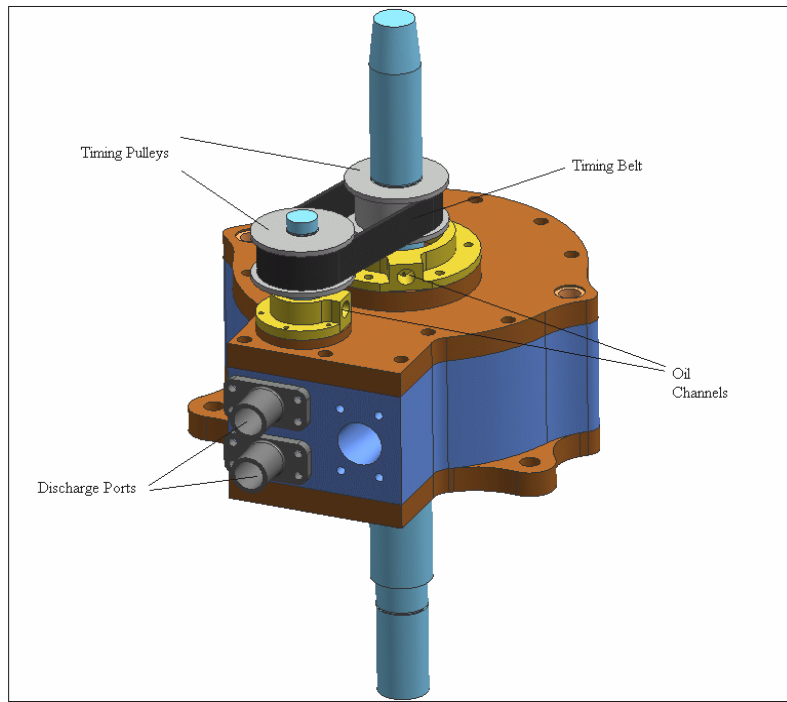
Figure 3-6   3-D CAD Model of the Rotary Compressor
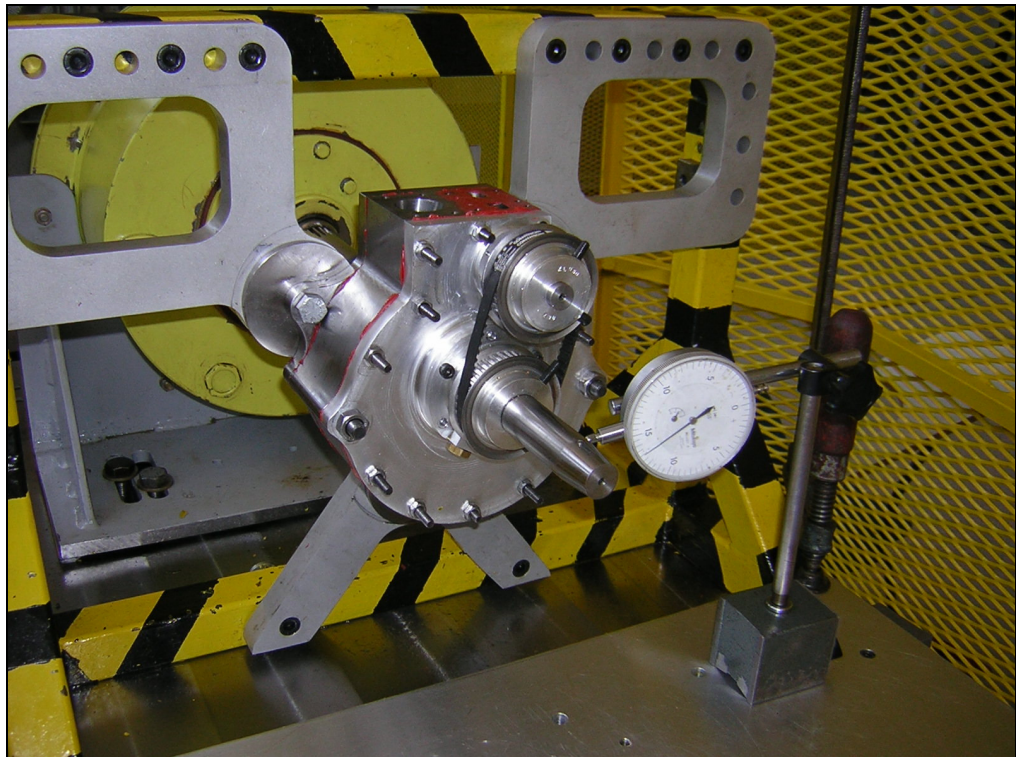
Figure 3-7   Photograph of the Manufactured Rotary Compressor

3.1.1 Compressor Parts

Compressor Housing

- Compressor housing is the main body of the compressor in which a rotor is mounted eccentrically.
- Compressor housing is closed by two taps which are positioned by the help of two bushings and tightened with 13 (Metric 6) bolts and 2 (Metric 10) bolts.
- Inside the housing is machined with a 3-Axis NC Machining Lathe due to its cycloid shape.
- Two discharge ports are mounted on the housing.
- Discharge valve seal and spring are placed in their channel on the top of the housing to avoid air leakage.
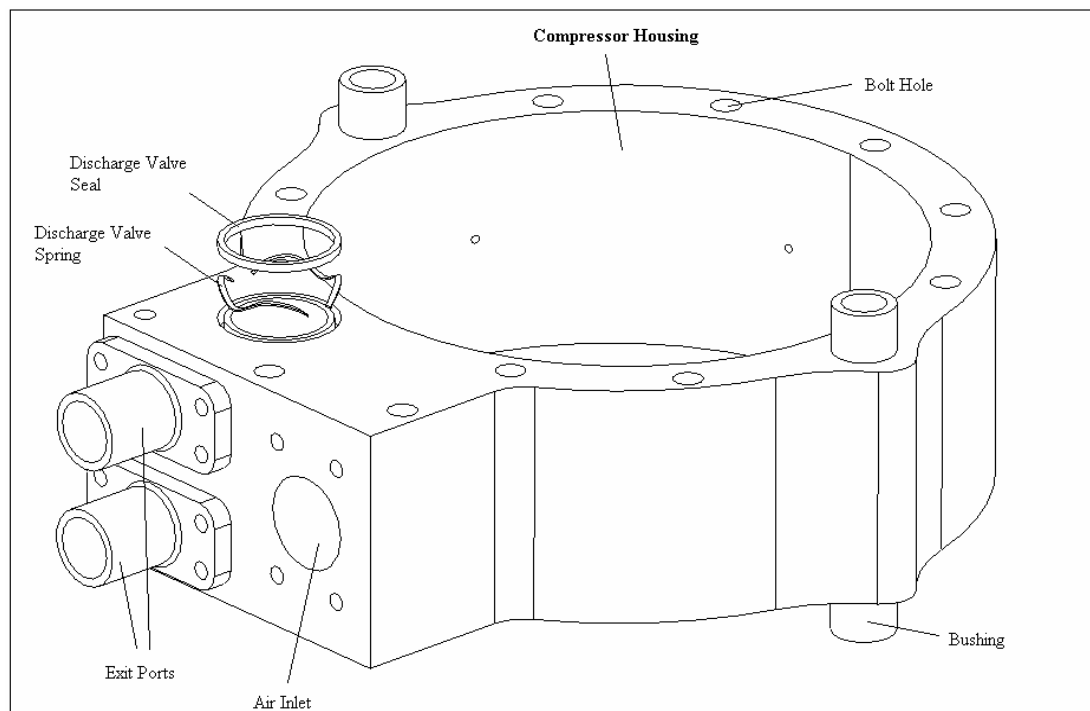
Figure 3-8   Compressor Housing Model

Compressor Upper Tap

- Compressor upper tap has two housings (mean bearing housing and discharge valve housing)

- The eccentricity of the compressor is defined by the place of the main bearing housing and the two bushings.

- Main bearing and discharge valve housing taps are mounted on the top of the upper tap.

- 17 x 35 x 9 ball bearing is tight fitted in the main bearing housing.

- 10 x 17 x 6 ball bearing is tight fitted in the discharge valve housing.
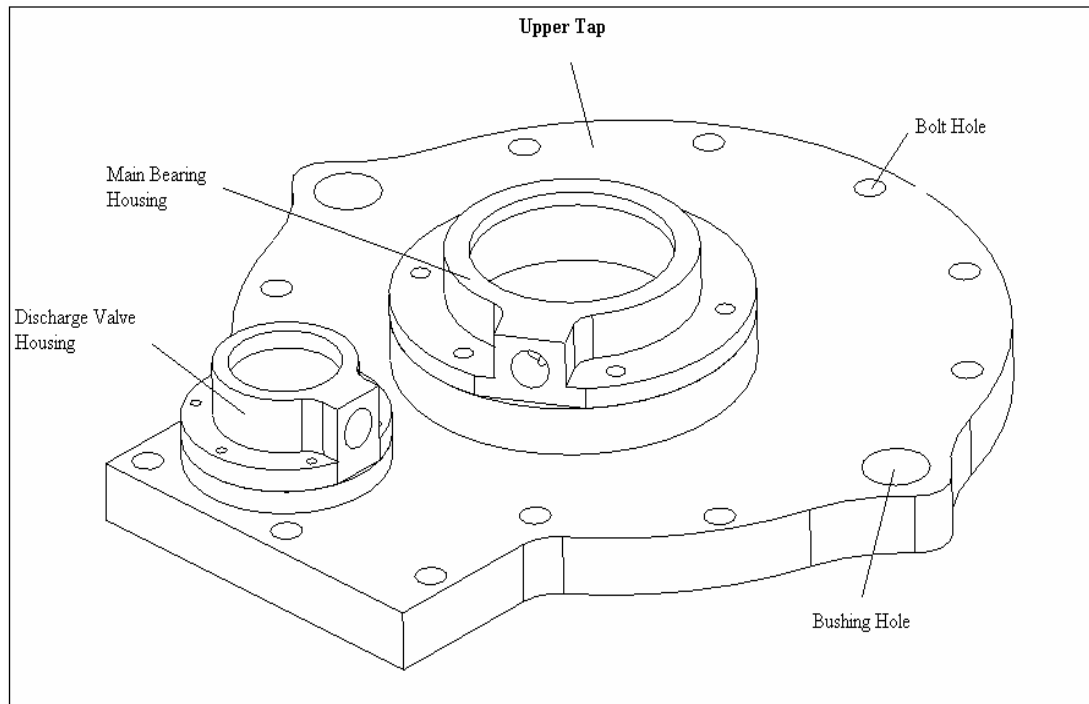
Figure 3-9   Compressor Upper Tap Model

Compressor Lower Tap

- Compressor lower tap has one bearing housing.
- The compressor is mounted to the ground with three (Metric 10) bolts from the three mounting holes on the lower tap.
- Main bearing housing tap is mounted on the top of the upper tap.
- 17 x 35 x 9 ball bearing is tight fitted in the main bearing housing.
- An oil seal is also placed with in the bearing housing tap.
- Main bearing is lubricated from the oil hole on the bearing housing tap.
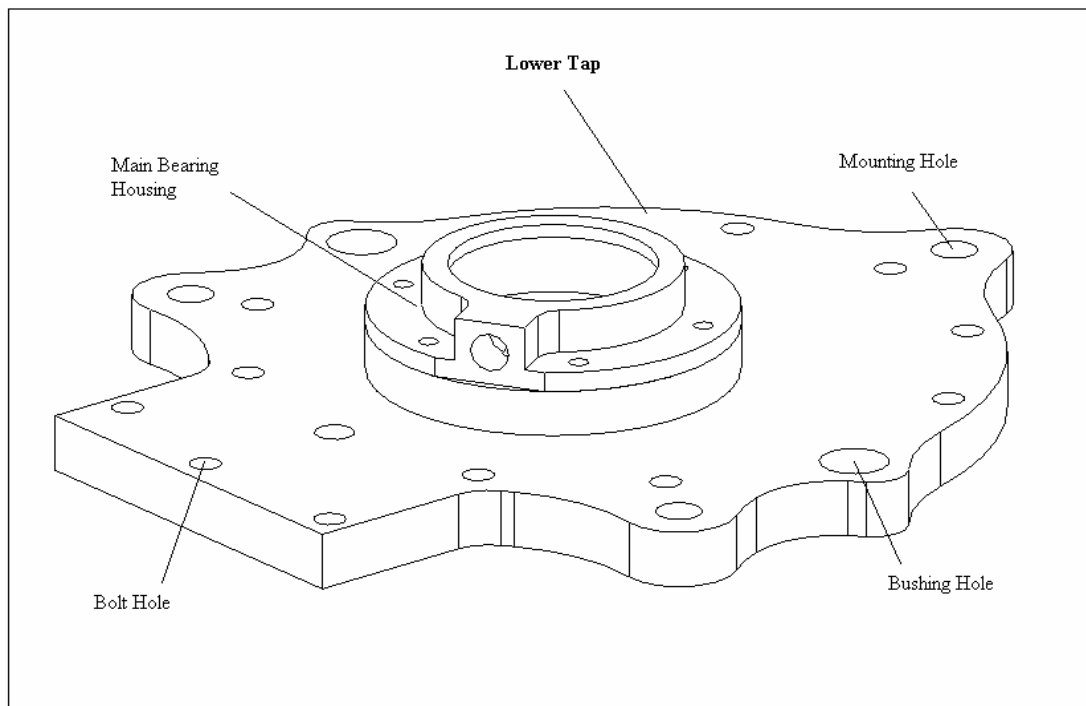
Figure 3-10   Compressor Lower Tap

Compressor Rotor

- Rotor upper and lower seals and springs are placed with in their channels on both sides of the rotor body.
- Rotor inner seals and springs are placed with in their channel in the vane channel.
- Rotor is placed in the housing by two main bearings fitted in the housing taps.
- Cooling holes are opened on the top sides of the rotor.
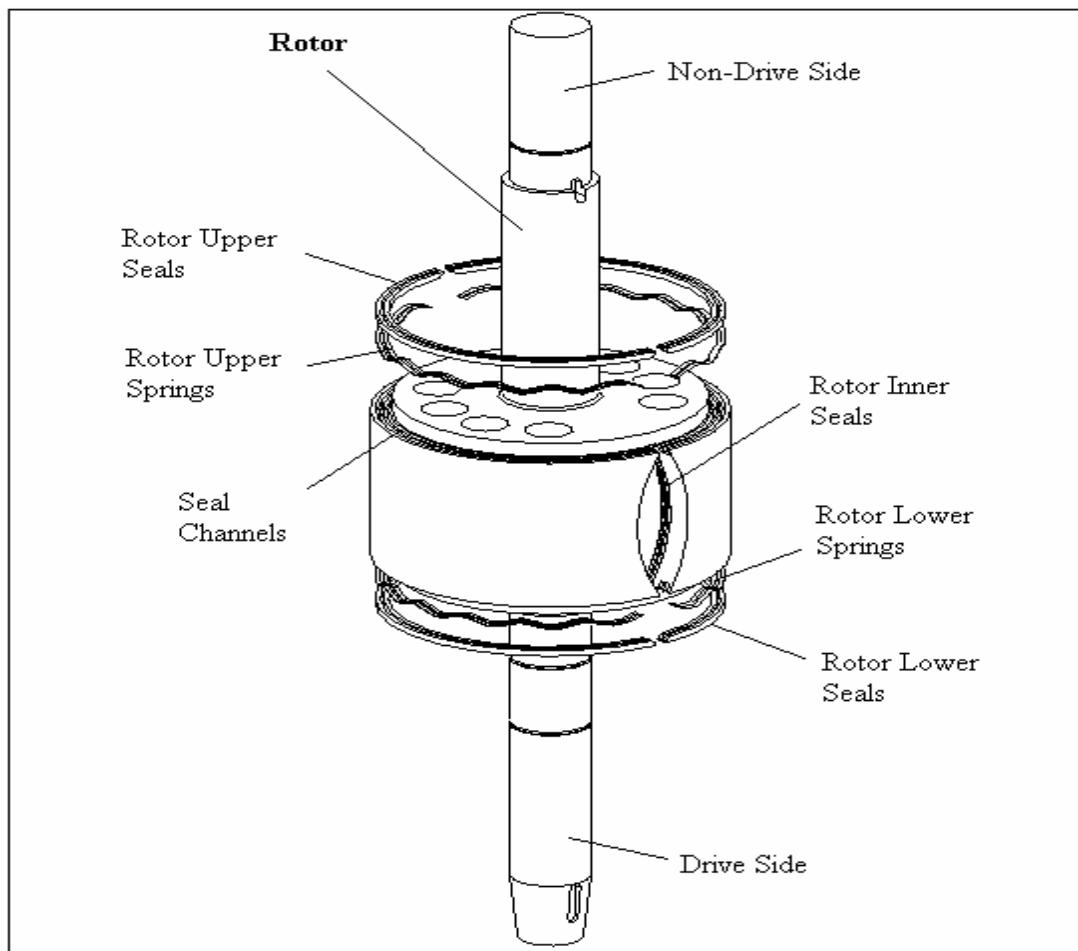
Figure 3-11   Compressor Rotor

Compressor Vane

- Vane is placed with in its channel inside the rotor and can freely slide in and out of the channel by the centrifugal forces formed due to rotation.
- Vane apex seals and springs are placed within their channels at the two ends of the vane.
- Vane apex seals avoid leakage between the vane tip and the inner surface of the housing.
- Vane apex seals also avoid leakage between the vane and the upper and lower taps.
- Vane tip geometry is determined by a kinematical analysis. (Appendix B)
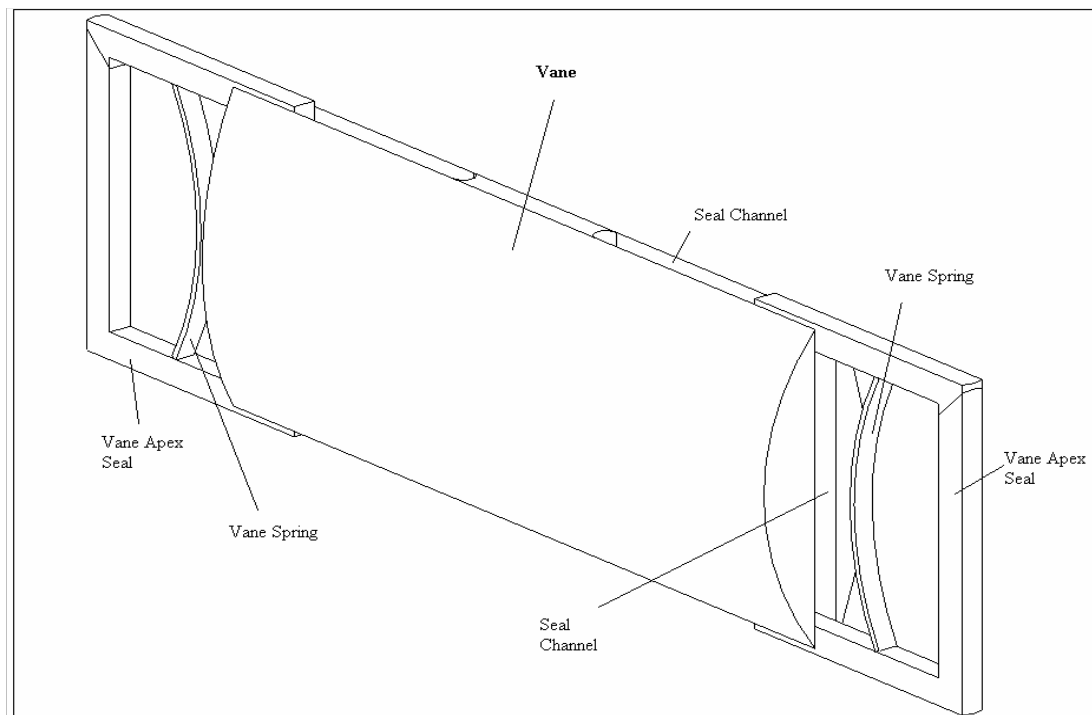
Figure 3-12   Compressor Vane

Compressor Discharge Valve

- Discharge valve is placed with in its housing inside the housing.
- Discharge valve is directly coupled with the rotor by the help of timing pulleys and timing belt and rotates at the same rpm with the rotor.
- Discharge valve delivers compressed air to the two combustion chambers from the upper and lower discharge channels opened on it.
- Discharge timing is adjusted by the timing pulleys and timing belt.
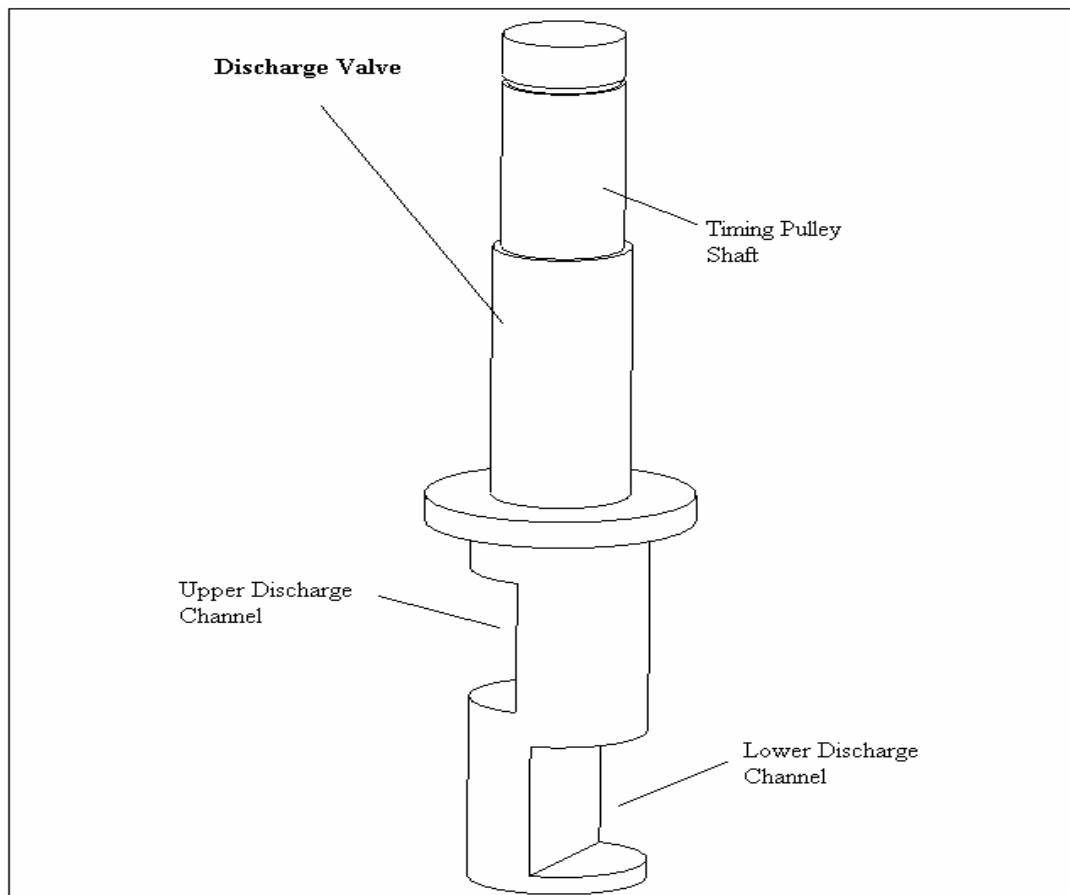
Figure 3-13   Compressor Discharge Valve

3.1.2 Structural Analysis and Material Selection

Structural analysis of the rotary compressor of the novel engine is done in ANSYS 9.0 Environment (Finite Element Program). The aim of this work is to define the manufacturing tolerances and to select the material of the compressor parts. To do the structural analysis, firstly the critical parts are defined as follows;

For material selection;

• Stress distribution on the housing and the taps of the compressor due to pressure and temperature exerted by the compressed air onto the inner surfaces.

• Stress distribution on the rotor due to pressure and temperature exerted by the compressed air, together with the centrifugal force caused by rotation.

• Stress distribution on the vane due to pressure and temperature exerted by the compressed air, together with the centrifugal force caused by rotation.

• Stress distribution on the discharge valve due to pressure and temperature exerted by the compressed air, together with the centrifugal force caused by rotation.

For defining the manufacturing tolerance;

• Deformation of the discharge valve and its housing in the compressor housing, due to thermal and pressure loads.

• Deformation of the vane and its housing in the rotor, due to thermal, pressure and inertia loads.

• Deformation of the rotor seals and their housings in the rotor, due to thermal, pressure and inertia loads.

• Deformation of the vane apex seals and their housings in the vane, due to thermal, pressure and inertia loads.

To make the structural analysis of the rotary compressor, the necessary temperature and pressure data is taken from the thermodynamic design code where the temperature and pressure data is given with respect to compressor vane angle θ. The pressure and temperature data wrt compressor vane angle θ are given in figures 3-14 and 3-15 respectively.
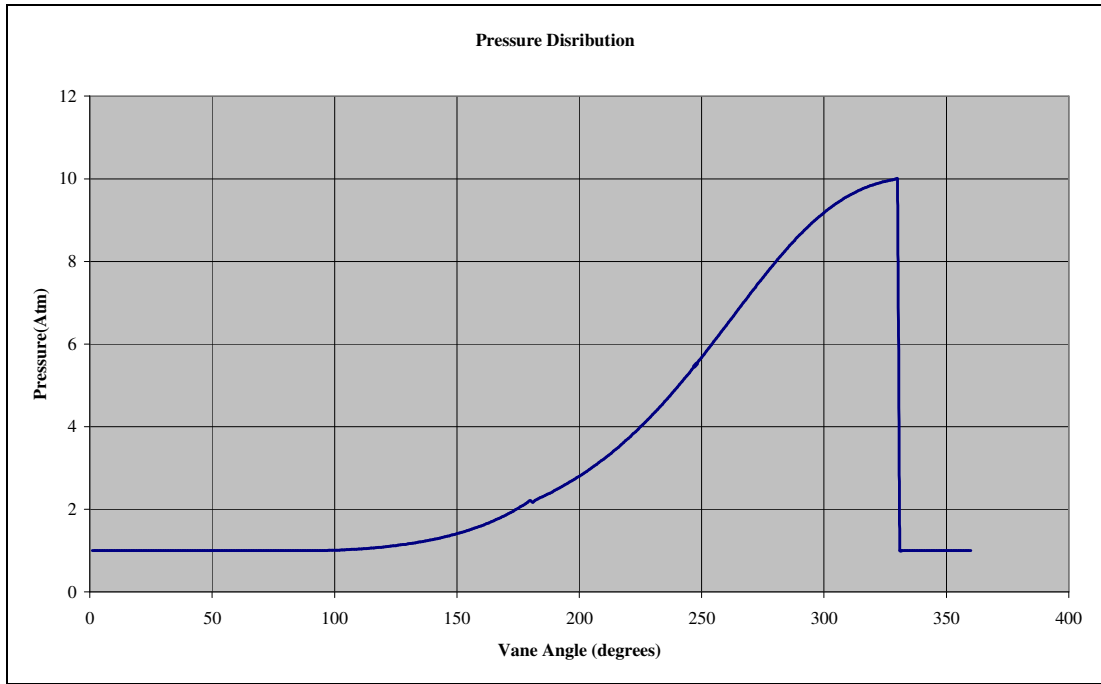
Figure 3-14   Pressure Distribution in the Rotary Compressor
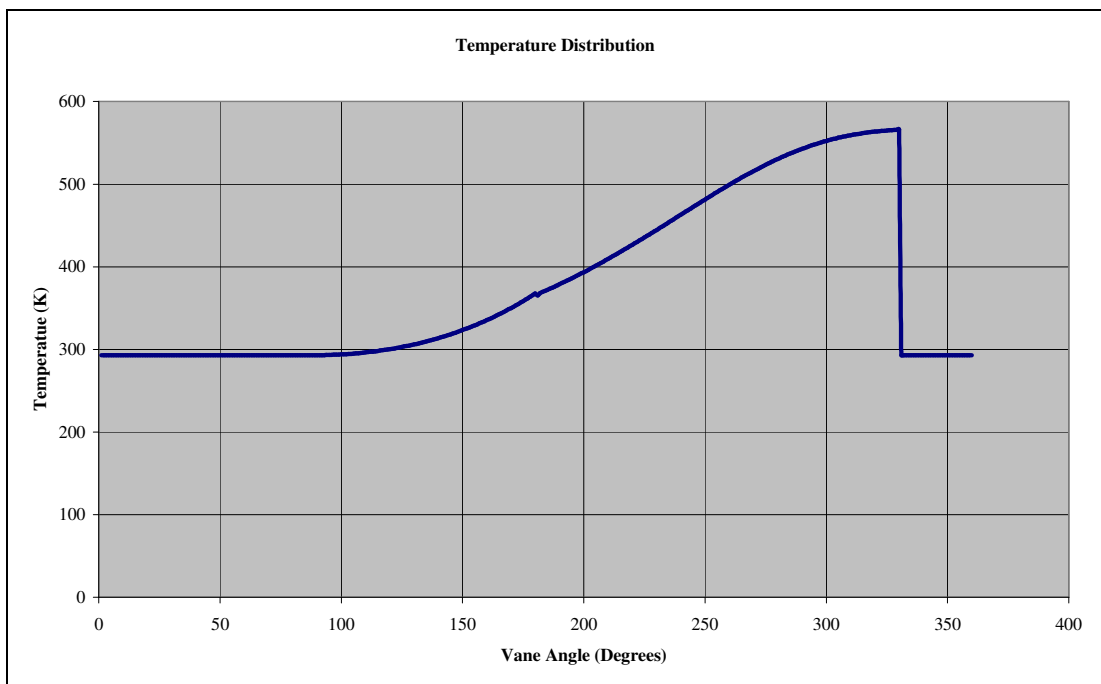
Figure 3-15   Temperature Distribution in the Rotary Compressor

65

Stress Distribution on the Compressor Housing

The stress distribution and deformations on the compressor housing due to thermal and pressure loads is analyzed in ANSYS environment. A linear analysis with the following specifications is done.

Material:	H13 Hot Work Tool Steel
Element Type:	Solid 20 Node 95 (Structure)
	Solid 20 Node 90 (Thermal)
Mesh:	Structured (Hex Sweep)
B.C's:	All DOF on bushing areas
Loads:	Convection on divided surfaces
	Pressure load on divided surfaces
Assumptions:	Temperature and pressure values calculated by the thermodynamic code are approximated on the divided inner surfaces.
	Convection Heat Transfer Coefficient for compressed air is approximated as 40 W/m^2 .K
	Convection Heat Transfer Coefficient for cooling air is approximated as 100 W/m^2 .K

Firstly, a thermal analysis of the housing is done to determine the temperatures on each node due to convection between the compressed air and the inner surfaces and between the cooling air and the outer surfaces of the housing.

Secondly, a structural analysis of the housing is done to determine the stress distribution and the deformation on the housing. The temperatures calculated in the thermal analysis are applied to the nodes as thermal load and the compressed air pressure is applied to the inner surfaces of the housing as pressure load.

The results of the analysis showed that the stress values on the compressor housing are in the elastic region and are much below the yield tensile strength of the material and can be safely used. Also the deformations on the discharge valve housing are later used to determine the manufacturing tolerances between the valve and the housing.

Figure 3-16   Structural Analysis Model of the Compressor Housing
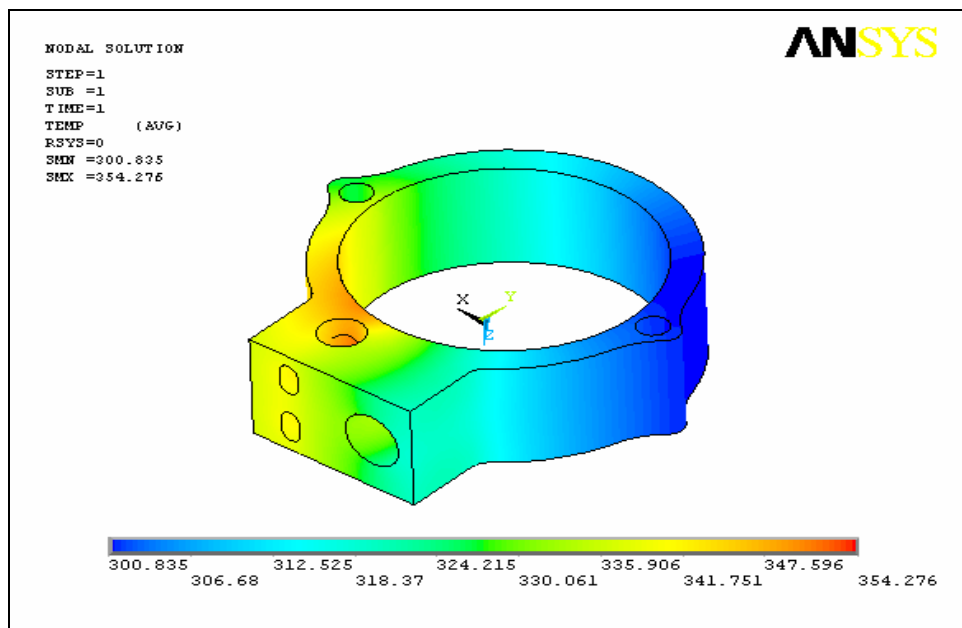
Figure 3-17   Temperature Distribution on Compressor Housing

Max Temperature on the housing: 354$^{\mathrm{o}}$ K
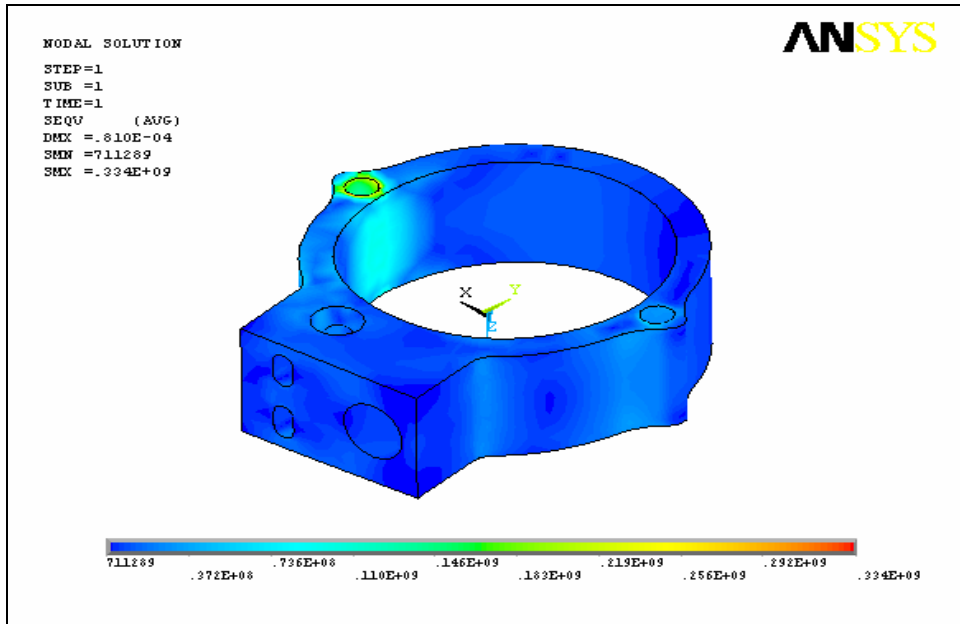
Figure 3-18   Stress Distribution on the Compressor Housing

Max Stress: 334 MPa   Yield Tensile Strength: 1650 MPa
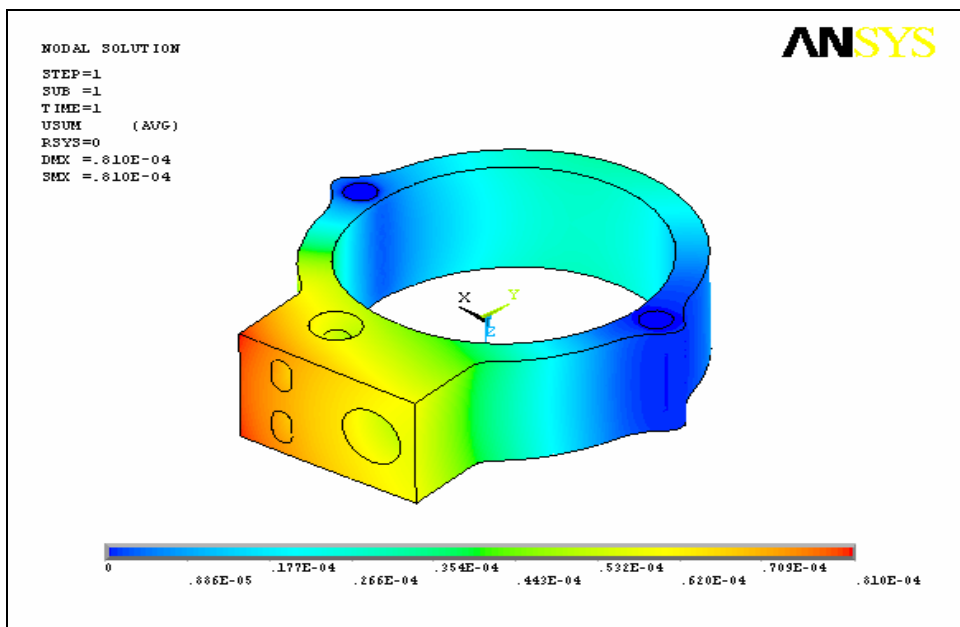
Figure 3-19   Deformation on the Compressor Housing

Stress Distribution on the Compressor Upper Tap

The stress distribution and deformations on the compressor upper tap due to thermal and pressure loads is analyzed in ANSYS environment. A linear analysis with the following specifications is done.

Material:	H13 Hot Work Tool Steel
Element Type:	Solid 20 Node 95 (Structure)
	Solid 20 Node 90 (Thermal)
Mesh:	Structured (Hex Sweep)
B.C's:	Fixed all DOF on bushing areas
Loads:	Convection on divided surfaces
	Pressure load on divided surfaces
Assumptions:	Temperature and pressure values calculated by the thermodynamic code are approximated on the divided inner surfaces.
	Convection Heat Transfer Coefficient for compressed air is approximated as 40 W/m^2 .K
	Convection Heat Transfer Coefficient for cooling air is approximated as 100 W/m^2 .K

Firstly, a thermal analysis of the compressor upper tap is done to determine the temperatures on each node due to convection between the compressed air and the inner surfaces and between the cooling air and the outer surfaces of the upper tap.

Secondly, a structural analysis of the compressor upper tap is done to determine the stress distribution and the deformation on the upper tap. The temperatures calculated in the thermal analysis are applied to the nodes as thermal load and the compressed air pressure is applied to the inner surfaces of the upper tap as pressure load.

The results of the analysis showed that the stress values on the compressor upper tap are in the elastic region and are much below the yield tensile strength of the material and can be safely used.
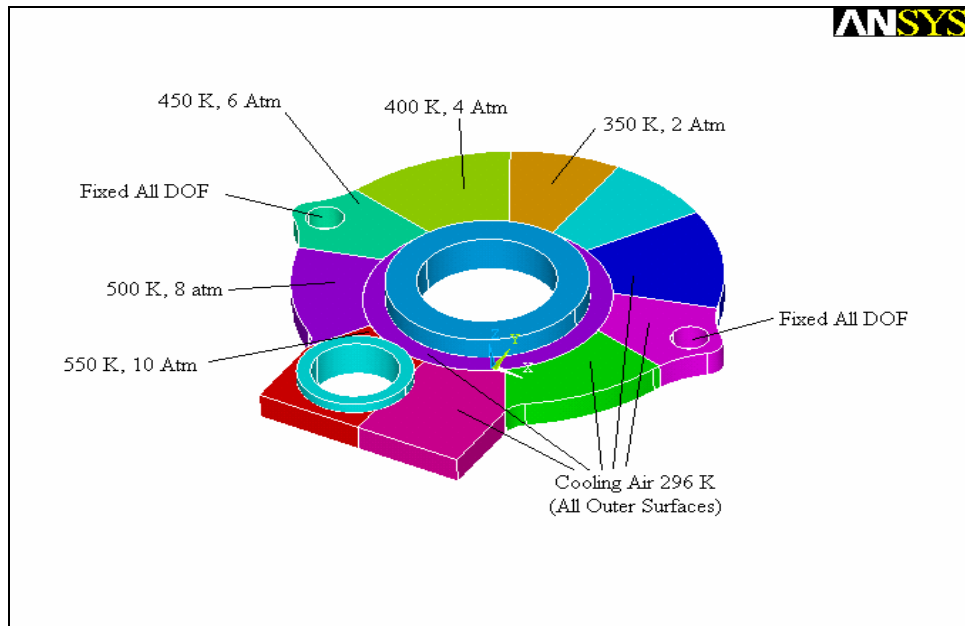
Figure 3-20   Structural Analysis Model of the Compressor Upper Tap

Figure 3-21   Temperature Distribution on Compressor Upper Tap

Max Temperature on the upper tap: 348° K

70

Figure 3-22   Stress Distribution on the Compressor Upper Tap

Max Stress: 332 MPa   Yield Tensile Strength: 1650 MPa
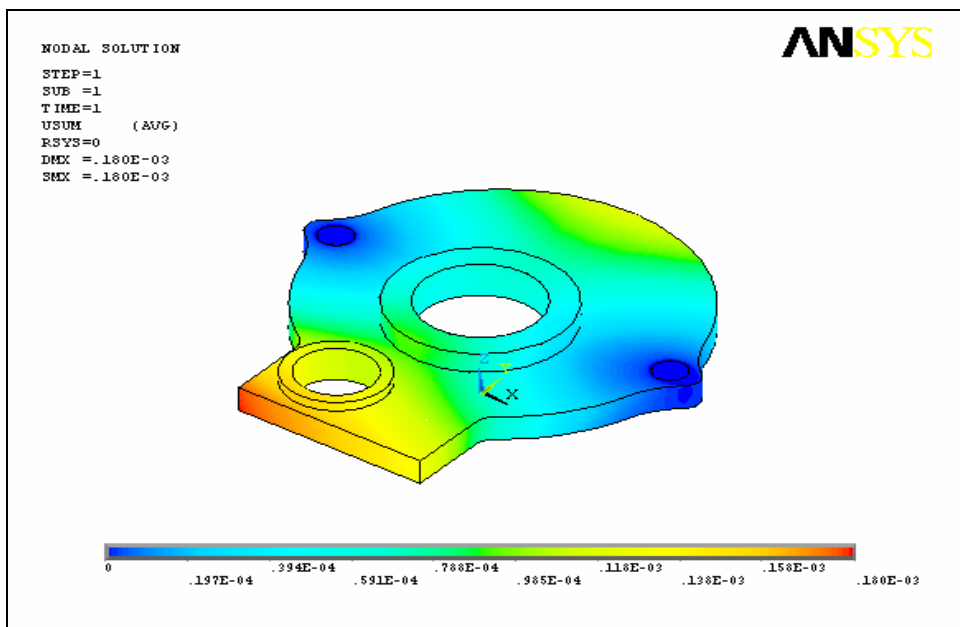
Figure 3-23   Deformation on the Compressor Upper Tap

Stress Distribution on the Compressor Lower Tap

The stress distribution and deformations on the compressor lower tap due to thermal and pressure loads is analyzed in ANSYS environment. A linear analysis with the following specifications is done.

Material:	H13 Hot Work Tool Steel
Element Type:	Solid 20 Node 95 (Structure)
	Solid 20 Node 90 (Thermal)
Mesh:	Structured (Hex Sweep)
B.C's:	Fixed all DOF on mounting holes
Loads:	Convection on divided surfaces
	Pressure load on divided surfaces
Assumptions:	Temperature and pressure values calculated by the thermodynamic code are approximated on the divided inner surfaces.
	Convection Heat Transfer Coefficient for compressed air is approximated as 40 W/m^2 .K
	Convection Heat Transfer Coefficient for cooling air is approximated as 100 W/m^2 .K

Firstly, a thermal analysis of the compressor lower tap is done to determine the temperatures on each node due to convection between the compressed air and the inner surfaces and between the cooling air and the outer surfaces of the lower tap.

Secondly, a structural analysis of the compressor lower tap is done to determine the stress distribution and the deformation on the lower tap. The temperatures calculated in the thermal analysis are applied to the nodes as thermal load and the compressed air pressure is applied to the inner surfaces of the lower tap as pressure load.

The results of the analysis showed that the stress values on the compressor lower tap are in the elastic region and are much below the yield tensile strength of the material and can be safely used.
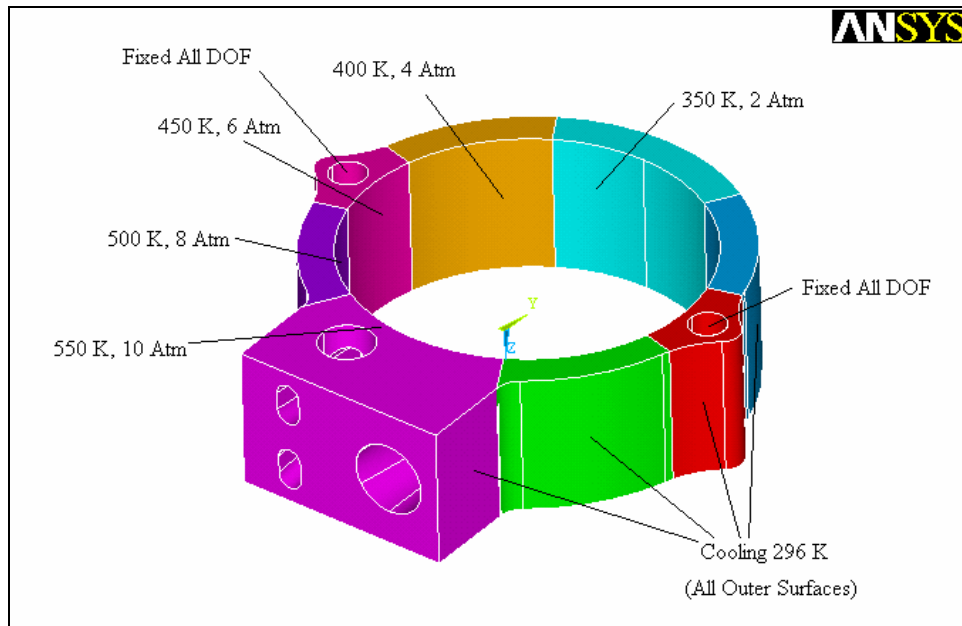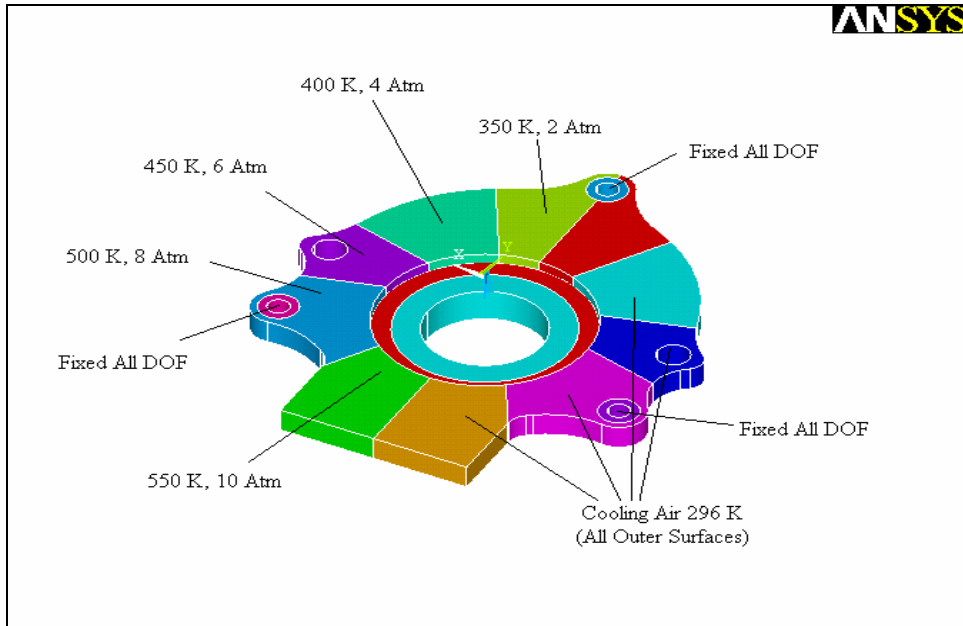
Figure 3-24   Structural Analysis Model of the Compressor Lower Tap
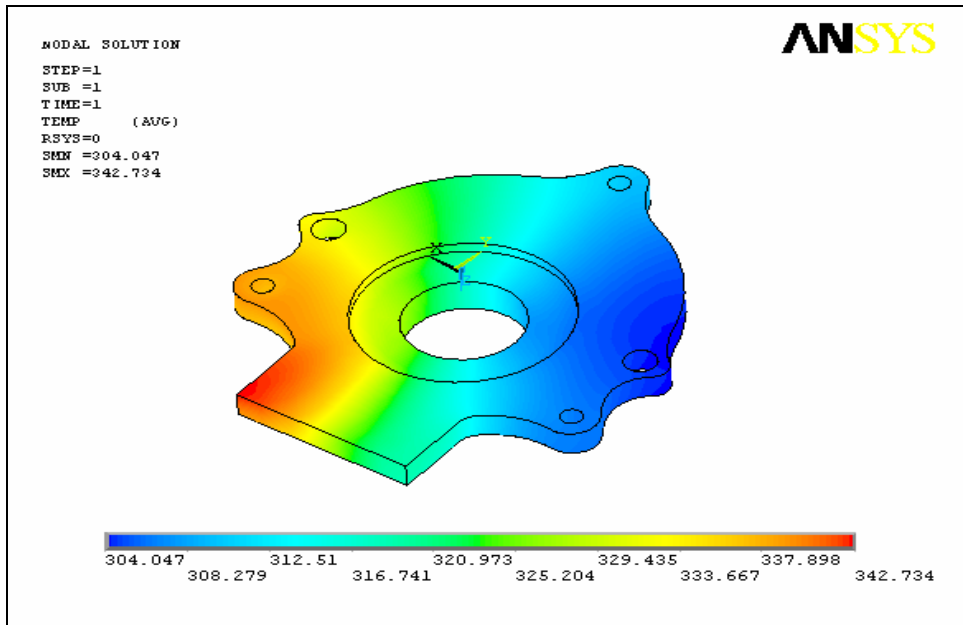
Figure 3-25   Temperature Distribution on Compressor Lower Tap

Max Temperature on the lower tap: 343° K

73
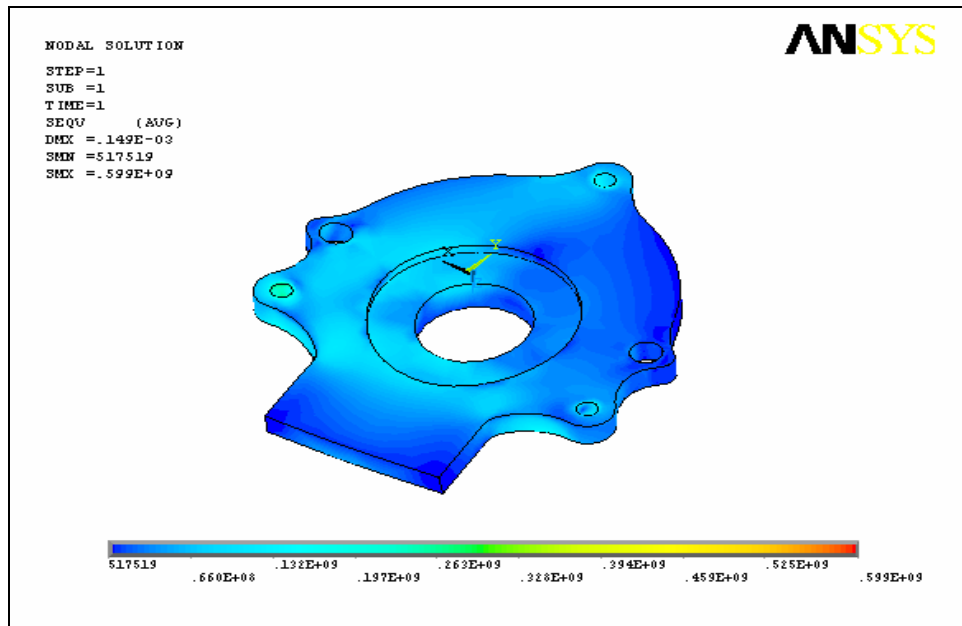
Figure 3-26   Stress Distribution on the Compressor Lower Tap

Max Stress: 599MPa   Yield Tensile Strength: 1650 MPa
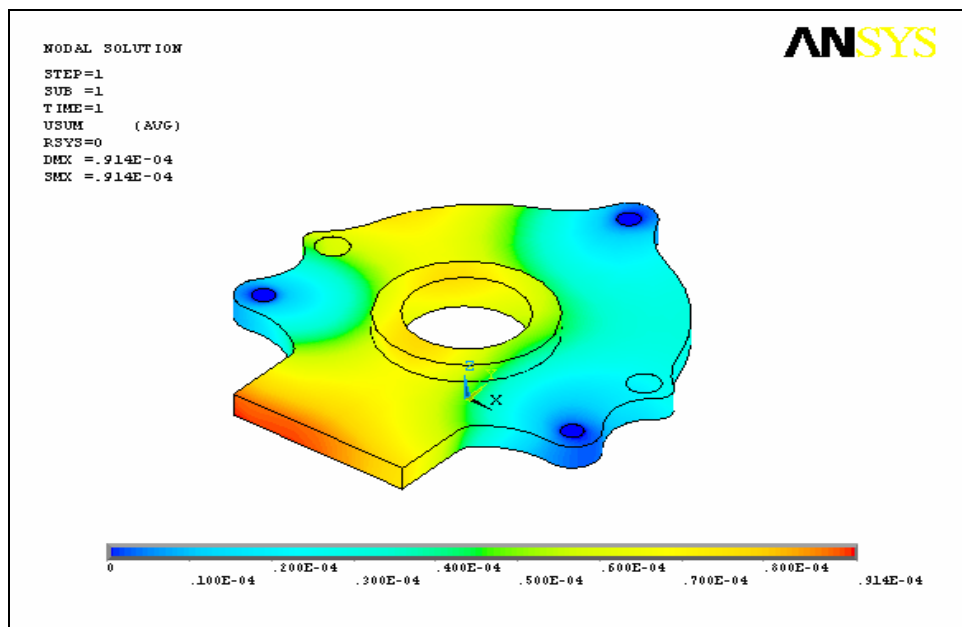
Figure 3-27   Deformation on the Compressor Lower Tap

Stress Distribution on the Compressor Vane

The stress distribution and deformations on the compressor vane due to thermal and pressure loads is analyzed in ANSYS environment. A linear analysis with the following specifications is done.

Material: H13 Hot Work Tool Steel

Element Type: Solid 20 Node 95 (Structure)

                       Solid 20 Node 90 (Thermal)

Mesh: Structured (Hex Sweep)

B.C's: Fixed X_Axis on vane tip surface

                       Fixed Y_Axis on one vane side surface

                       Fixed Z_Axis on vane top surface

Loads: Approximate temperature load

                       Pressure load on divided surfaces

Assumptions: Average temperature is applied to the vane.

                       Max pressure of the compressed air is applied to the vane inner surface.

Structural analysis of the compressor vane is done to determine the stress distribution and the deformation on the vane. Average temperature is applied to the nodes as thermal load and the max compressed air pressure (10 atm) is applied to the inner surfaces of the vane as pressure load.

The results of the analysis showed that the stress values on the compressor vane are in elastic region and much below the yield tensile strength of the material and can be safely used. Also the deformations of the vane are later used to define the manufacturing tolerances between the vane and the rotor.

Figure 3-28   Structural Analysis Model of the Compressor Vane
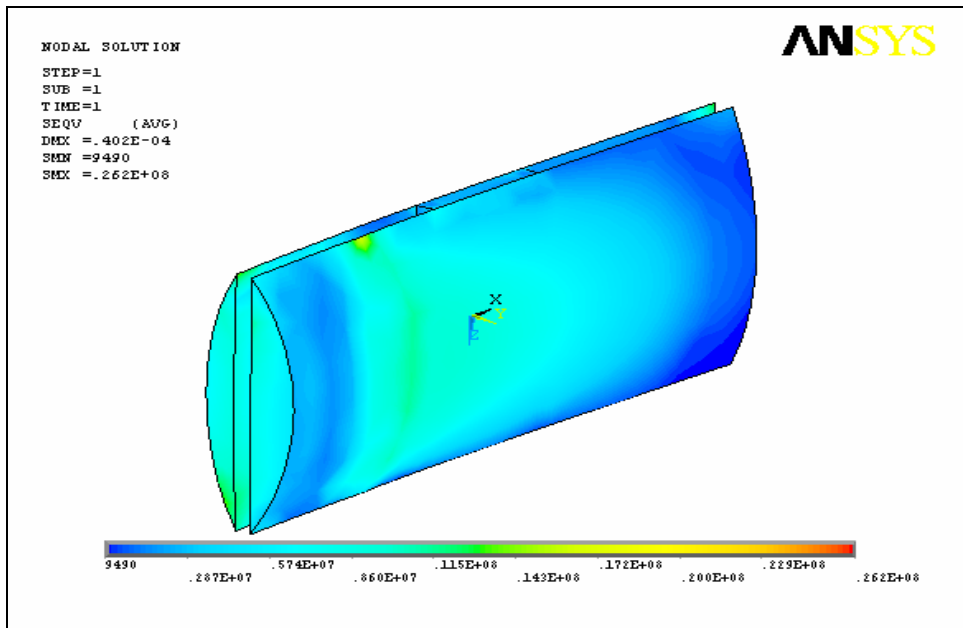
Figure 3-29   Stress Distribution on Compressor Vane

Max Stress: 262MPa	Yield Tensile Strength: 1650 MPa
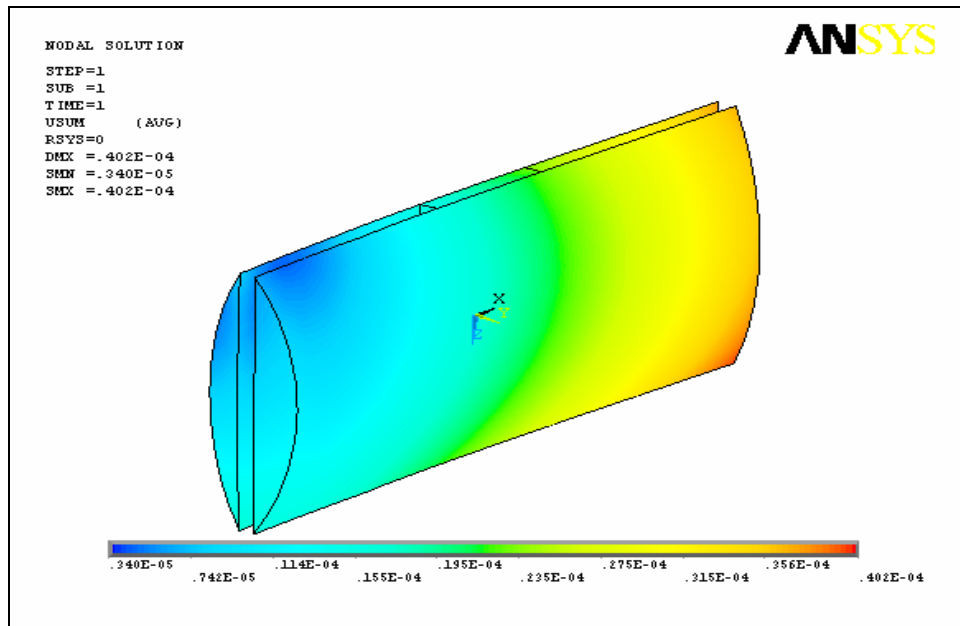
Figure 3-30   Deformation on the Compressor Vane

Stress Distribution on the Compressor Rotor

The stress distribution and deformations on the compressor rotor due to thermal and pressure and inertia loads is analyzed in ANSYS environment. A linear analysis with the following specifications is done.

Material:	H13 Hot Work Tool Steel
Element Type:	Tet 10 Node 92 (Structure)
	Tet 10 Node 87 (Thermal)
Mesh:	Unstructured (Tet)
B.C's:	Fixed in radial and Z_Axis on bearing surfaces
Loads:	Convection on divided surfaces
	Max. Pressure load on divided surfaces
	Angular Velocity of 6000 rpm
Assumptions:	Convection Heat Transfer Coefficient for compressed air is approximated as 40 W/m^2 .K
	Convection Heat Transfer Coefficient for cooling air is approximated as 100 W/m^2 .K
	Convection Heat Transfer Coefficient for cooling oil is approximated as 150 W/m^2 .K

Firstly, a thermal analysis of the compressor rotor is done to determine the temperatures on each node due to convection between the compressed air and the inner surfaces and between the cooling air and oil and the outer surfaces of the rotor.

Secondly, a structural analysis of the compressor rotor is done to determine the stress distribution and the deformation on the rotor. The temperatures calculated in the thermal analysis are applied to the nodes as thermal load and the max compressed air pressure is applied to the inner surfaces of the rotor as pressure load. Also angular velocity of 6000 rpm is applied.

The results of the analysis showed that the stress values on the compressor rotor are in the elastic region and are much below the yield tensile strength of the material and can be safely used. Also the deformations on the vane housing are later used to determine the manufacturing tolerances between the rotor and the vane.

Figure 3-31   Structural Analysis Model of the Compressor Rotor
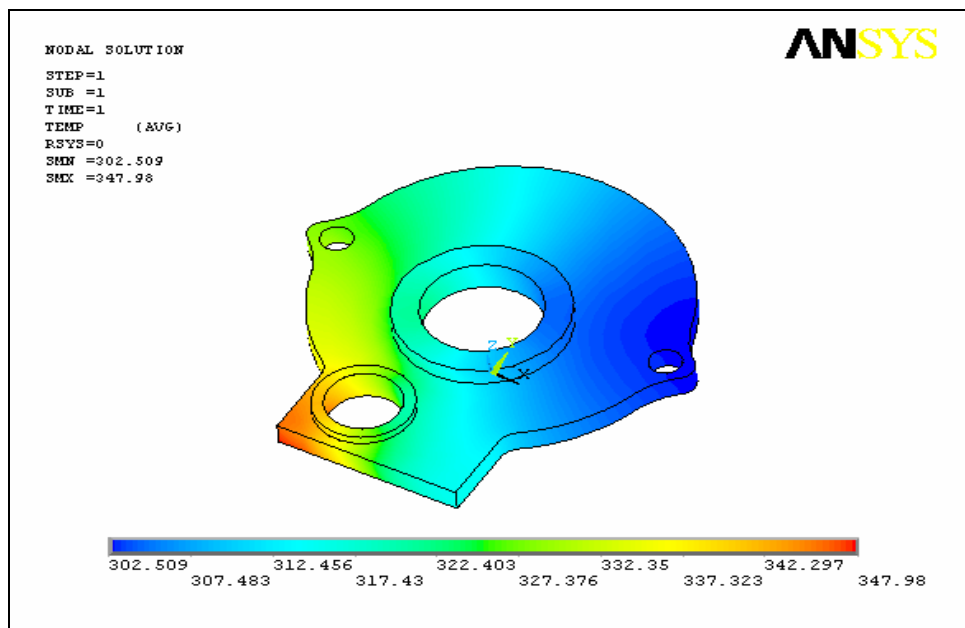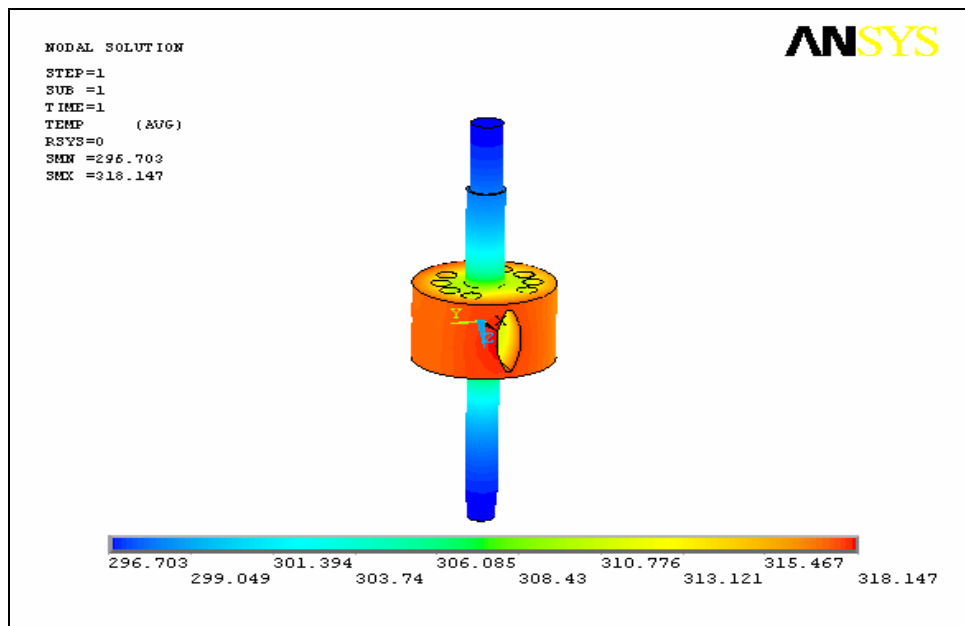

Figure 3-32   Temperature Distribution on Compressor Rotor

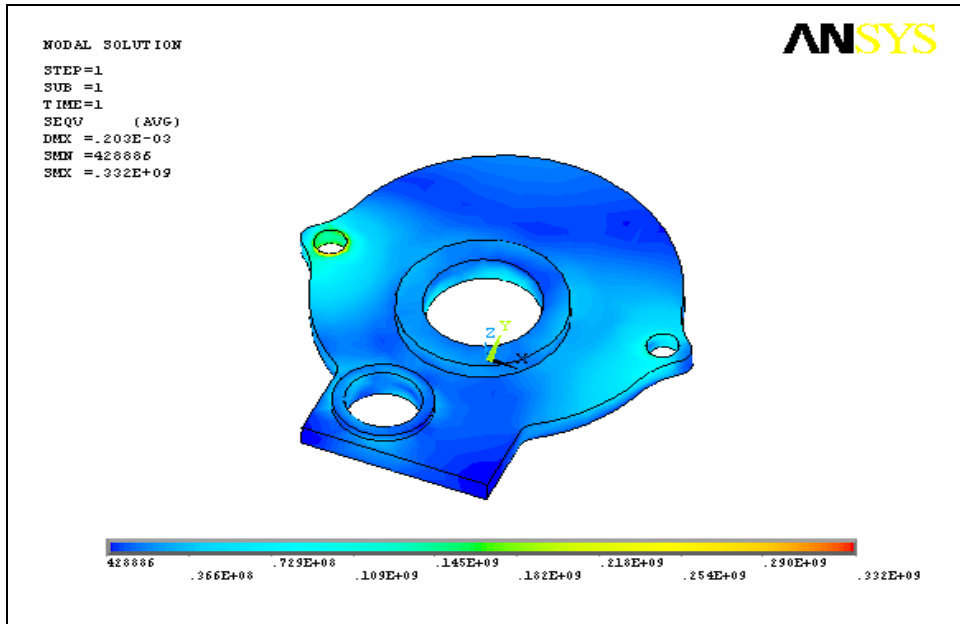Max Temperature on the rotor: 318° K

Figure 3-33   Stress Distribution on the Compressor Rotor

Max Stress: 259 MPa   Yield Tensile Strength: 1650 MPa
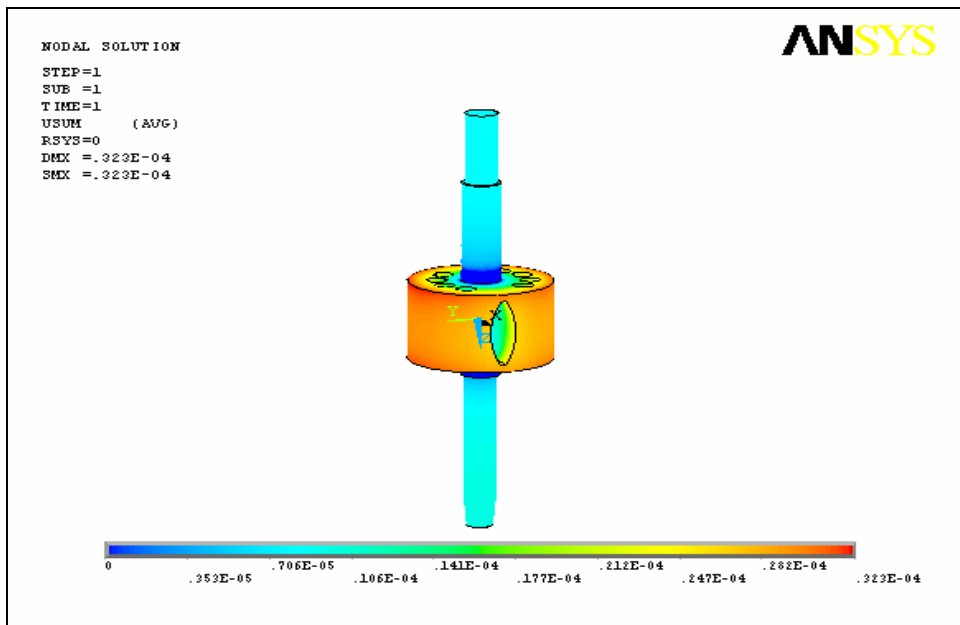
Figure 3-34   Deformation on the Compressor Rotor

Stress Distribution on the Compressor Discharge Valve

The stress distribution and deformations on the compressor discharge valve due to thermal and pressure loads is analyzed in ANSYS environment. A linear analysis with the following specifications is done.

Material:	H13 Hot Work Tool Steel
Element Type:	Solid 20 Node 95 (Structure)
	Solid 20 Node 90 (Thermal)
Mesh:	Structured (Hex Sweep)
B.C's:	Fixed in radial and Z_Axis on bearing surfaces
Loads:	Convection on divided surfaces
	Pressure load on divided surfaces
	Angular velocity of 6000 rpm
Assumptions:	Convection Heat Transfer Coefficient for compressed air is approximated as 40 W/m^2 .K
	Convection Heat Transfer Coefficient for cooling air is approximated as 100 W/m^2 .K

Firstly, a thermal analysis of the compressor discharge valve is done to determine the temperatures on each node due to convection between the compressed air and the discharge surfaces and between the cooling air and the outer surfaces of the discharge valve.

Secondly, a structural analysis of the compressor discharge valve is done to determine the stress distribution and the deformation on the discharge valve. The temperatures calculated in the thermal analysis are applied to the nodes as thermal load and the max compressed air pressure is applied to the discharge surfaces of the discharge valve as pressure load. Also angular velocity of 6000 rpm is applied.

The results of the analysis showed that the stress values on the compressor discharge valve are in the elastic region and are much below the yield tensile strength of the material and can be safely used. Also the deformations of the valve are later used to define manufacturing tolerance between the discharge valve and the housing.
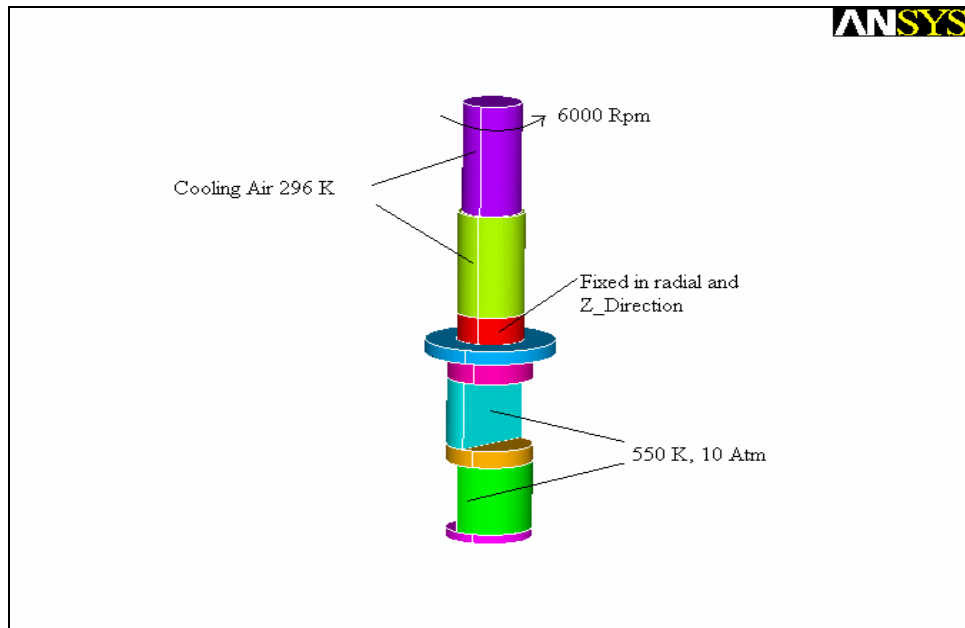
Figure 3-35   Structural Analysis Model of the Compressor Discharge Valve
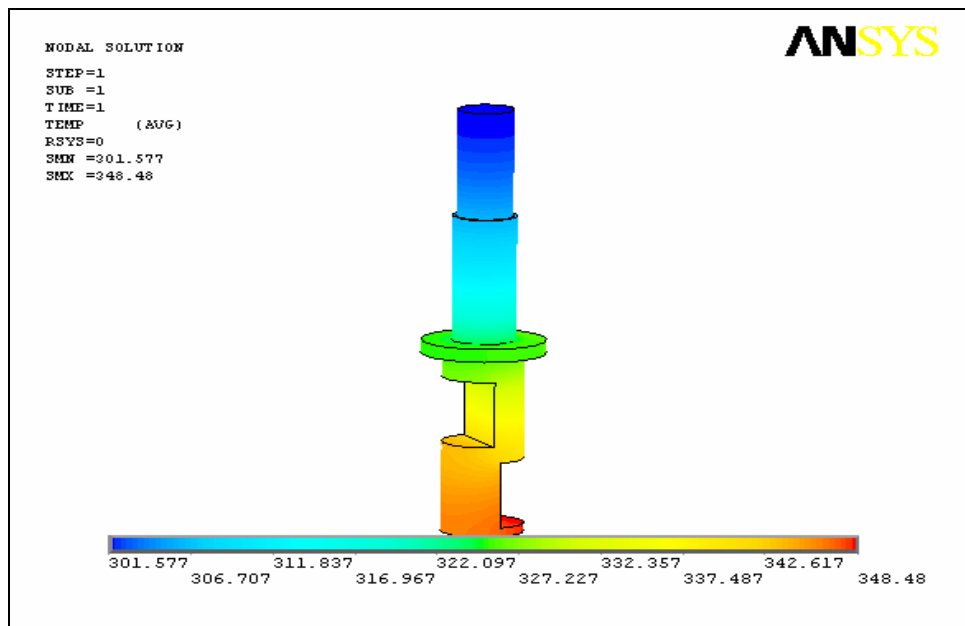
Figure 3-36   Temperature Distribution on Compressor Discharge Valve

Max Temperature on the discharge valve: 348° K
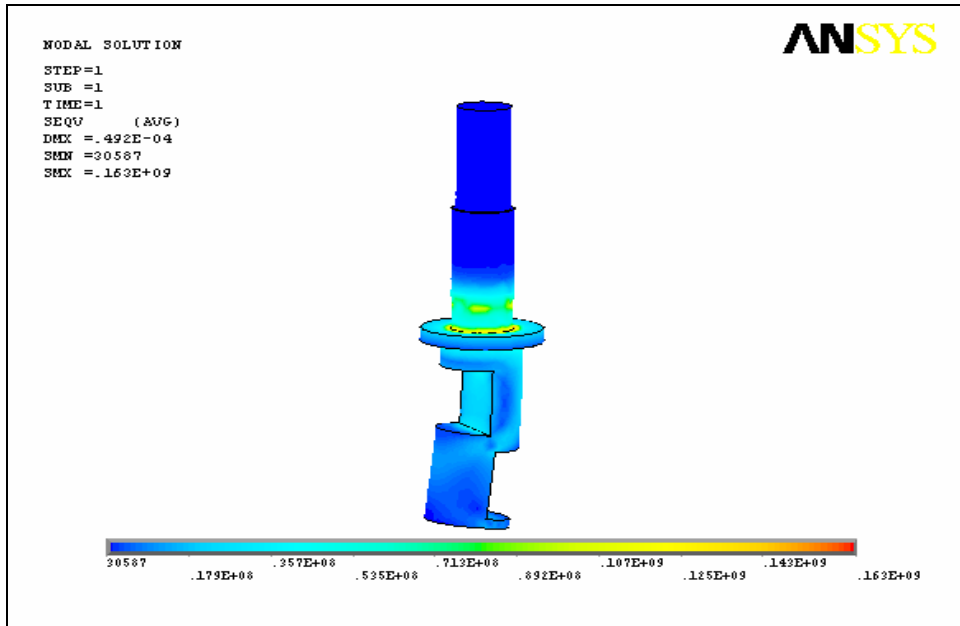
Figure 3-37   Stress Distribution on the Compressor Discharge Valve

Max Stress: 163MPa	Yield Tensile Strength: 1650 MPa
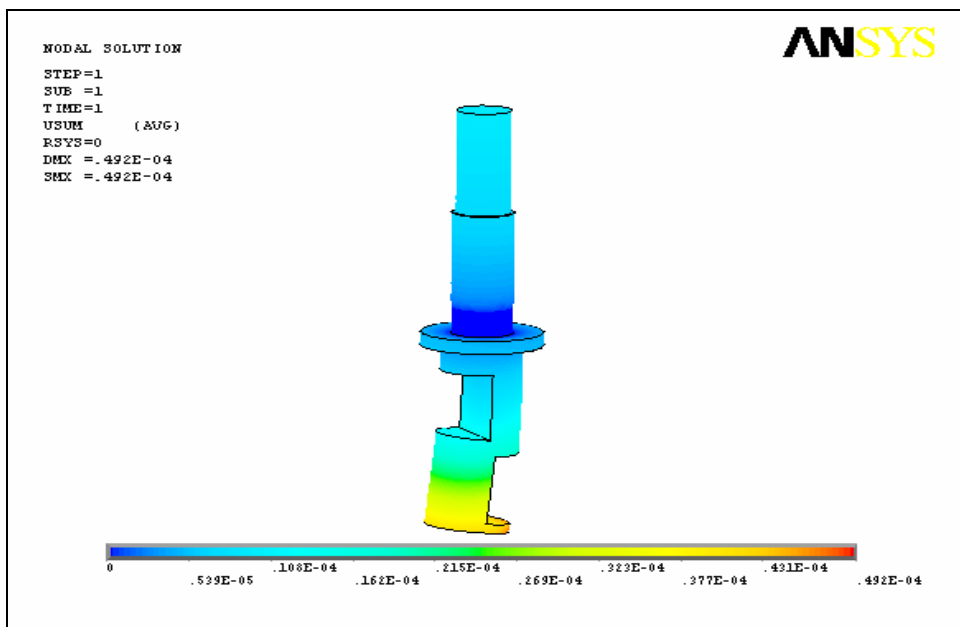
Figure 3-38   Deformation on the Compressor Discharge Valve

Stress Distribution on the Compressor Vane Apex Seal

The stress distribution and deformations on the compressor vane apex seal due to thermal loads is analyzed in ANSYS environment. A linear analysis with the following specifications is done.

Material:	H13 Hot Work Tool Steel
Element Type:	Solid 20 Node 95 (Structure)
	Solid 20 Node 90 (Thermal)
Mesh:	Structured (Hex Sweep)
B.C's:	Fixed X_Axis on vane apex seal tip surface
	Fixed Y_Axis on vane apex seal top surface
	Fixed Z_Axis on one vane apex seal side surface
Loads:	Approximate temperature load
Assumptions:	Average temperature is applied to the vane apex seal.

Structural analysis of the compressor vane apex seal is done to determine the stress distribution and the deformation on the vane apex seal. Average temperature (400 K) is applied to the nodes as thermal load.

The results of the analysis showed that the stress values on the compressor vane apex seal are in elastic region and much below the yield tensile strength of the material and can be safely used. Also the deformations of the vane apex seal are later used to define the manufacturing tolerances between the vane and vane apex seal.
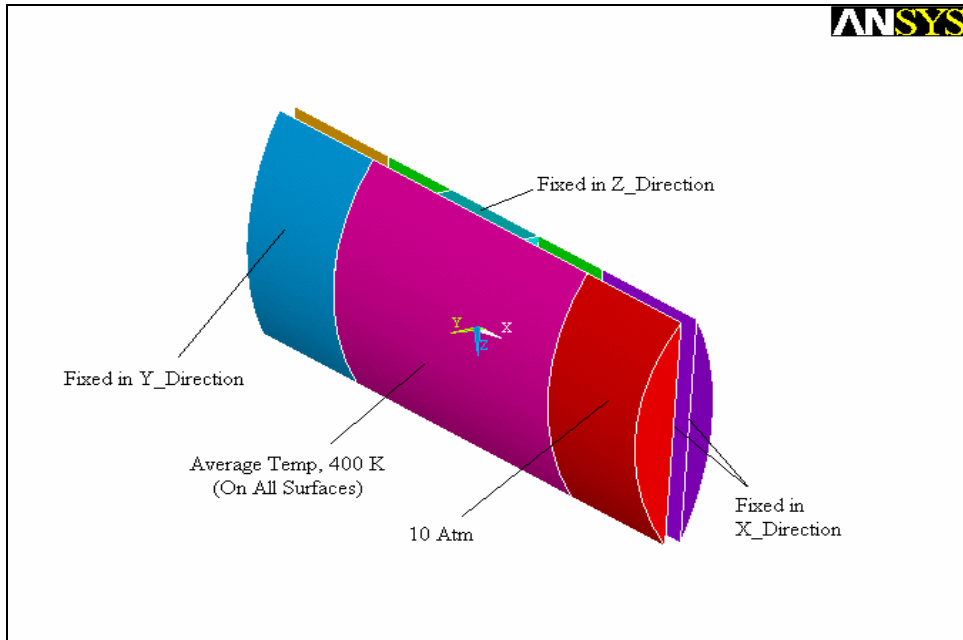
Figure 3-39   Structural Analysis Model of the Compressor Vane Apex Seal
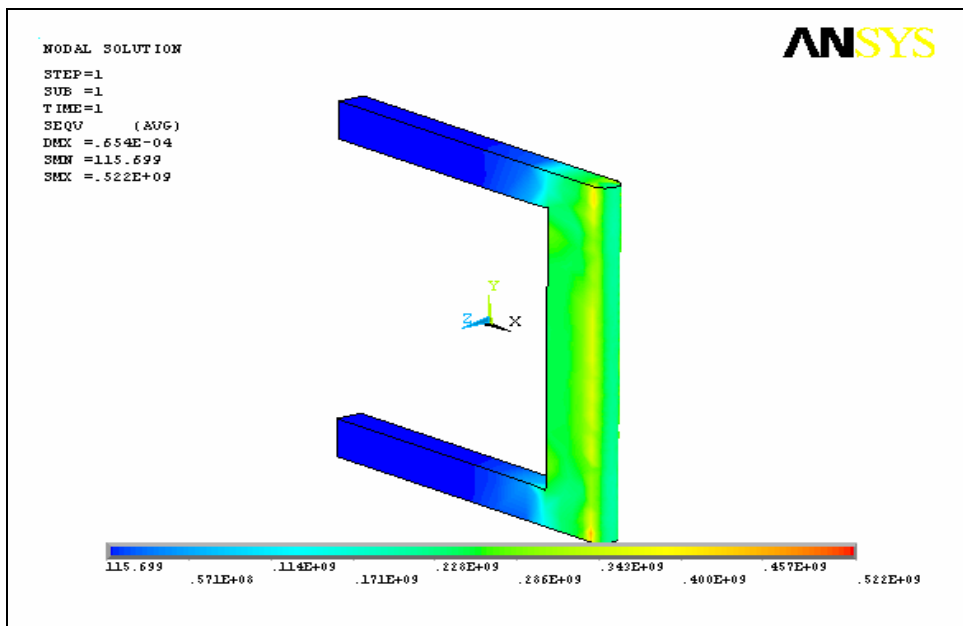
Figure 3-40   Stress Distribution on Compressor Vane Apex Seal

Max Stress: 522 MPa	Yield Tensile Strength: 1650 MPa
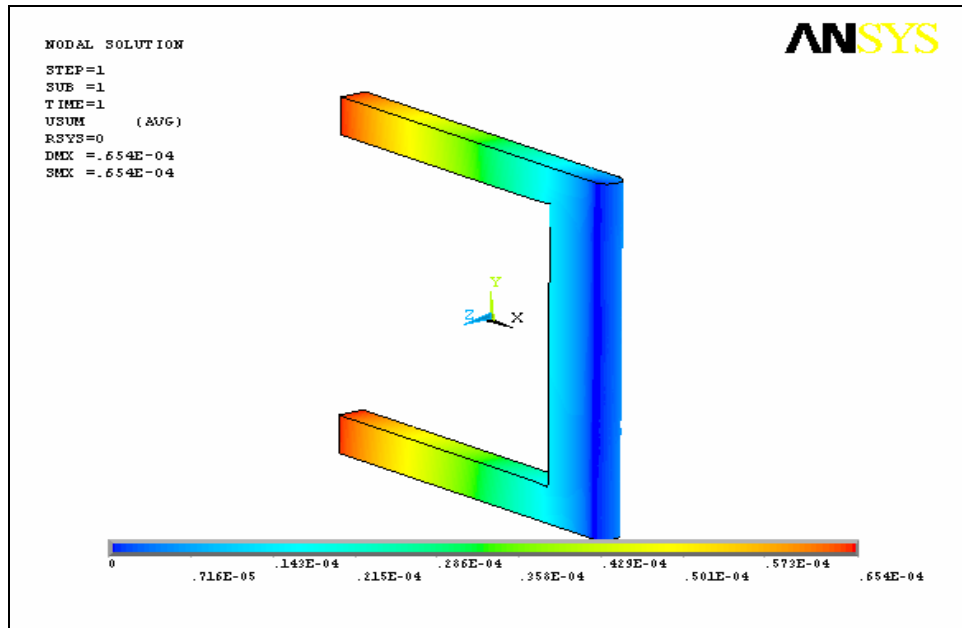
Figure 3-41   Deformation of Compressor Vane Apex Seal

Stress Distribution on the Compressor Rotor Top Seal

The stress distribution and deformations on the compressor rotor top seal due to thermal loads is analyzed in ANSYS environment. A linear analysis with the following specifications is done.

Material:	Gray Cast Iron
Element Type:	Solid 20 Node 95 (Structure)
	Solid 20 Node 90 (Thermal)
Mesh:	Structured (Hex Sweep)
B.C's:	Fixed X_Axis on rotor top seal tip surface
	Fixed Y_Axis on rotor top seal tip surface
	Fixed Z_Axis on one rotor top seal top surface
Loads:	Approximate temperature load
Assumptions:	Average temperature is applied to the rotor top seal.

Structural analysis of the compressor rotor top seal is done to determine the stress distribution and the deformation on the rotor top seal. Average temperature (400 K) is applied to the nodes as thermal load.

The results of the analysis showed that the stress values on the compressor rotor top seal are in elastic region and much below the yield tensile strength of the material and can be safely used. Also the deformations of the rotor top seal are later used to define the manufacturing tolerances between the rotor and rotor top seal.
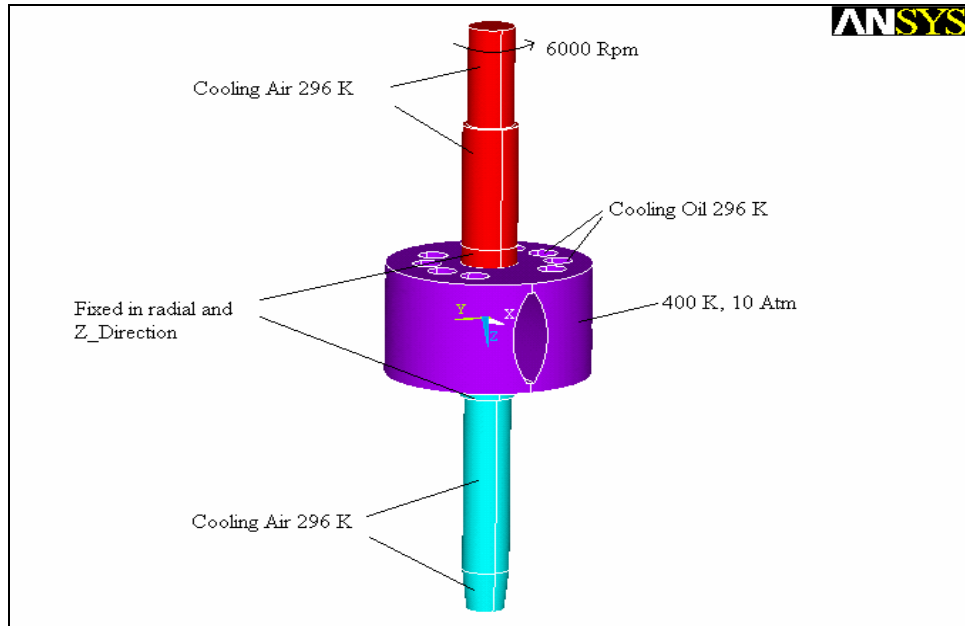
Figure 3-42   Structural Analysis Model of the Compressor Rotor Top Seal
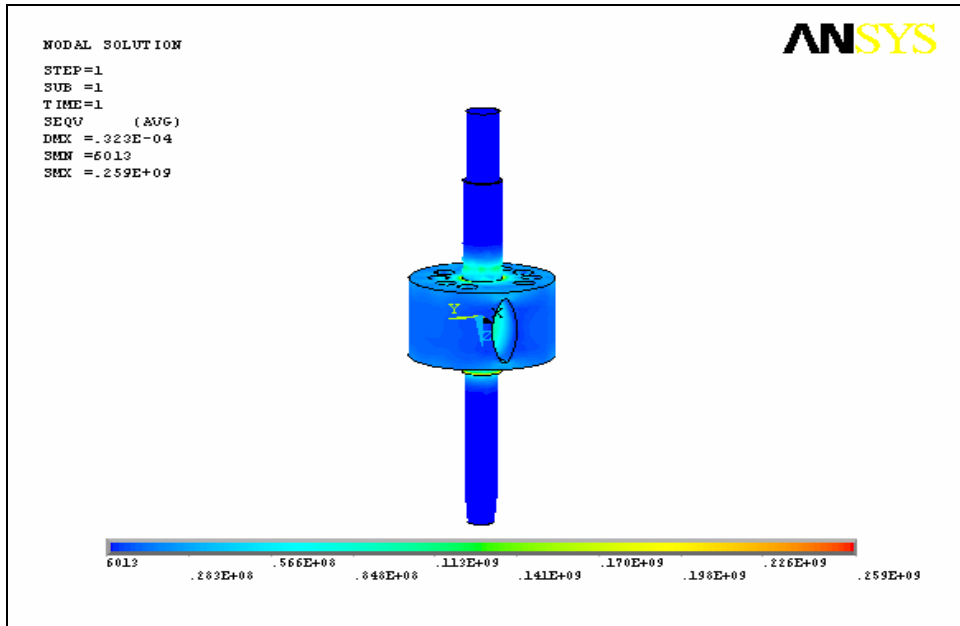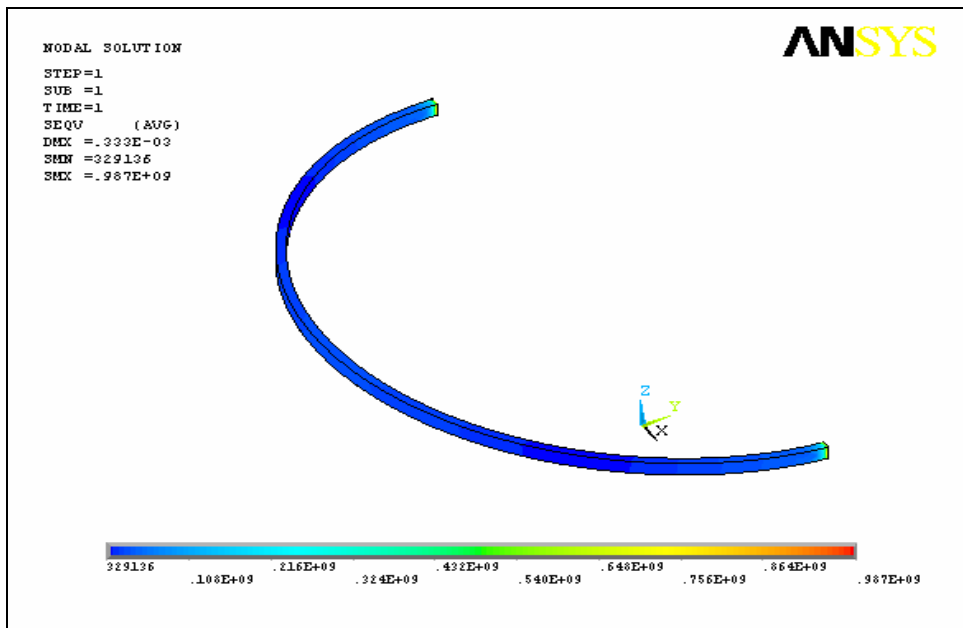

Figure 3-43   Stress Distribution on Compressor Rotor Top Seal

| Max Stress: 987 MPa | Yield Tensile Strength: 1650 MPa |
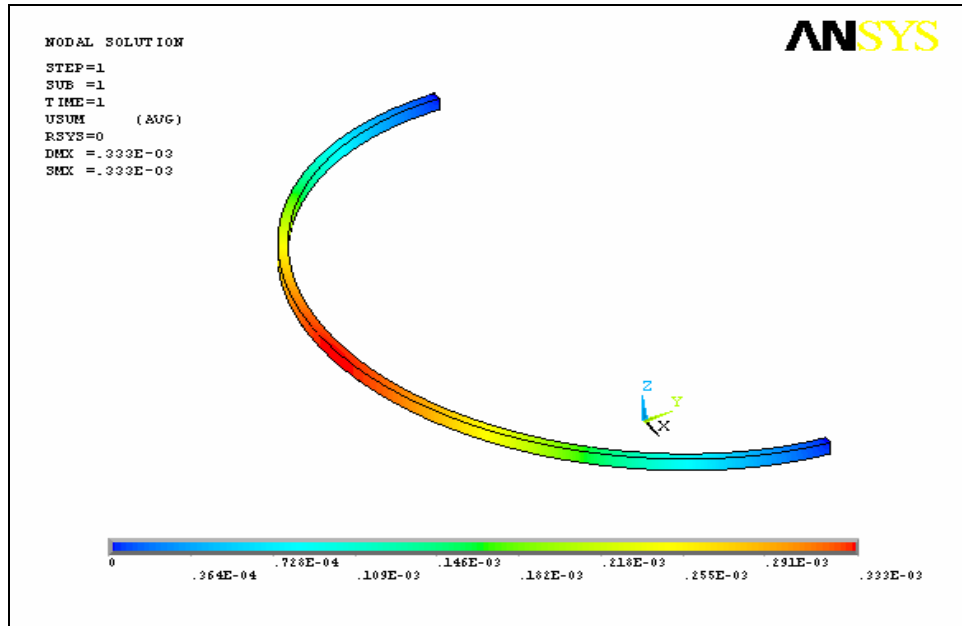
Figure 3-44   Deformation of Compressor Rotor Top Seal

Manufacturing Tolerance between Discharge Valve and Housing

Due to thermal and pressure loads on the discharge valve and housing surfaces, deformations on the materials occur. These deformations are examined to determine the manufacturing tolerances of both parts so that the discharge valve can revolve within its housing without stacking while still assuring good sealing capacity.

By examining the compressor discharge valve deformation, it is seen that the discharge valve deforms 0.0308 mm max radially.

By examining the compressor housing, it is seen that the discharge valve housing deforms 0.0409 mm max radially.

As a result, 0.08 mm gap tolerance between the discharge valve and the housing will assure discharge valve to revolve within the housing without stacking. This gap tolerance can be guaranteed by manufacturing the discharge valve 0.04 mm smaller in diameter and by opening the valve housing hole 0.04 mm larger in diameter.

Manufacturing Tolerance between Vane and Rotor

Due to thermal and pressure and inertia loads on the vane and rotor surfaces, deformations on the materials occur. These deformations are examined to determine the manufacturing tolerances of both parts so that the vane can move within the rotor without stacking while still assuring good sealing characteristics.

By examining the compressor vane deformation, it is seen that the vane deforms 0.04 mm max.

By examining the compressor rotor, it is seen that the vane channel deforms 0.3 mm max.

As a result, 0.35 mm gap tolerance between the vane and the rotor will assure compressor vane to revolve within the rotor without stacking. This gap tolerance can be guaranteed by manufacturing the compressor vane 0.05 mm smaller in thickness and by opening the vane channel 0.3 mm larger in thickness.

Manufacturing Tolerance between Vane Apex Seal and Vane

Due to thermal and pressure loads on the vane and vane apex seal surfaces, deformations on the materials occur. These deformations are examined to determine the manufacturing tolerances of both parts so that the vane apex seal can move within the vane without stacking, while still assuring good sealing characteristics.

By examining the compressor vane apex seal deformation, it is seen that the seal deforms 0.06 mm max in thickness.

By examining the compressor vane, it is seen that the apex seal channel deforms 0.04 mm max in thickness.

As a result, 0.1 mm gap tolerance between the vane apex seal and the vane will assure apex seal to move within the channel without stacking. This gap tolerance can be guaranteed by manufacturing the vane apex seal 0.06 mm smaller in thickness and by opening the vane seal channel 0.04 mm larger in thickness.

Manufacturing Tolerance between Rotor Top Seal and Rotor

Due to thermal and pressure loads on the rotor and rotor top seal surfaces, deformations on the materials occur. These deformations are examined to determine the manufacturing tolerances of both parts so that the rotor top seal can move within the rotor seal channel without stacking, while still assuring good sealing characteristics.

By examining the compressor rotor top seal deformation, it is seen that the seal deforms 0.3 mm max in diameter.

By examining the compressor rotor, it is seen that the rotor top seal channel deforms 0.05 mm max in thickness.

As a result, 0.35 mm gap tolerance between the rotor top seal and the rotor seal channel will assure top seal to move within the channel without stacking. This gap tolerance can be guaranteed by manufacturing the rotor top seal 0.3 mm smaller in thickness and by opening the rotor top seal channel 0.05 mm larger in diameter.

Compressor Material

With respect to the structural analysis results, *H13 Hot Work Tool Steel* is selected as the material of the rotary compressor prototype that will be manufactured.

The selection criteria of the material are given below;

- Excellent wear resistance and hot toughness.
- High thermal shock resistance.
- Good thermal conductivity and tolerate some water cooling in service.
- High temperature tensile strength.
- Good machinability.

Regarding these properties of the material, it is one of the best alternatives that can be used for the manufacturing of the rotary compressor prototype. Beside these properties, the structural analysis of the compressor parts is done using this material and the analysis results showed that the selected material is suitable for the prototype. Therefore the material of the rotary compressor housing, taps, bearing housings, rotor, vane, valve, valve housing is selected to be H13 Hot Work Tool Steel. (Properties of H13 Hot Work Tool Steel is given in Appendix D)

Compressor Vane Apex Seal Material

Two alternatives for the vane apex seal have been considered.

First alternative for the rotary compressor vane apex seal is H13 hot work tool steel because of its good mechanical and thermal properties.

However, as the material of the compressor housing is also H13, there would be great wear deformation on both surfaces of the housing and seal due to friction. By arranging the hardness of both parts (housing being harder) could decrease the wear but still it would be over the desired limits of deformation. (Properties of H13 Hot Work Tool Steel is given in Appendix D)

The second alternative for the rotary compressor vane apex seal is the fiber material which is mostly used for the vanes of the rotary vane compressors in the market. As the temperatures in the rotary compressor are quite low, fiber could display enough mechanical properties while decreasing wear deformation on the housing surface to nearly zero.

Compressor Rotor Top Seals

The best alternative for the rotary compressor rotor top seal is the *gray cast iron* which is also used in the piston engines' piston head seals. Also seal is plated with chromium to give excellent wear and scuff resistance under very marginal lubrication conditions. Because of its good wear properties, the deformation on the tap inner surfaces, where the rotor top seals are in contact with, will be minimum while good sealing will be achieved. (Properties of Gray Cast Iron is given in Appendix D)

Compressor Vane Apex and Rotor Top Seal Springs

Two alternatives for the springs have been considered.

The first alternative for the rotary compressor springs is a cobalt based super-alloy called *Elgiloy Co-Cr-Ni Alloy*. It has high strength, fatigue life and good mechanical properties. This material is also used in other rotary engine applications in the market as seal springs. (Properties of Elgiloy is given in Appendix D)

The second alternative for the rotary compressor springs is a nickel based super-alloy called *Inconel 718*. It has high strength, ductility, fatigue life and good mechanical properties. Its excellent relaxation resistance is useful for high-temperature springs and bolts. The alloy has good resistance to corrosion and oxidation along with high tensile and creep-rupture properties at temperatures to about 1300°F (700°C). (Properties of Inconel 718 is given in Appendix D)

3.2 Turbine Design

- The designed turbine of the novel turbo rotary engine is a sliding vane turbine which is a positive displacement type rotary turbine. This turbine uses a rotor equipped with a radially movable single sliding vane, mounted eccentrically in a crescent shape cavity. The single vane is free to slide in and out of the slot cut into the rotor. As the rotor rotates, both ends of the sliding vane are extending radially outward and are in contact with the cycloid inner surface of the housing peripheral at all rotational angles by the centrifugal force. Apex seals at the tips of the vane are used to achieve proper sealing. Combustion gases enter through the two inlet ports. As the combustion gases entering the turbine hit the vane and turn the eccentrically mounted rotor. As the space between the rotor, vane and the housing increases, combustion gases expand, until the vane reaches to the exhaust.

- Also cooling oil is sprayed into the housing to absorb heat; keeping air temperature relatively low, improving sealing and lubricating the vane tips before it is burned.

- The designed sliding vane turbine needs a valve at the inlet port to take the combustion gases from the two combustion chambers at the right time. The valve must open one port to expand the combustion gases while keeping the other port closed, enabling the compressor to compress the air to the desired pressure. After exhaust is completed it will close the port and wait for the next combustion to occur before opening the other port.

The designed turbine diagram can be seen in figure 3-45.
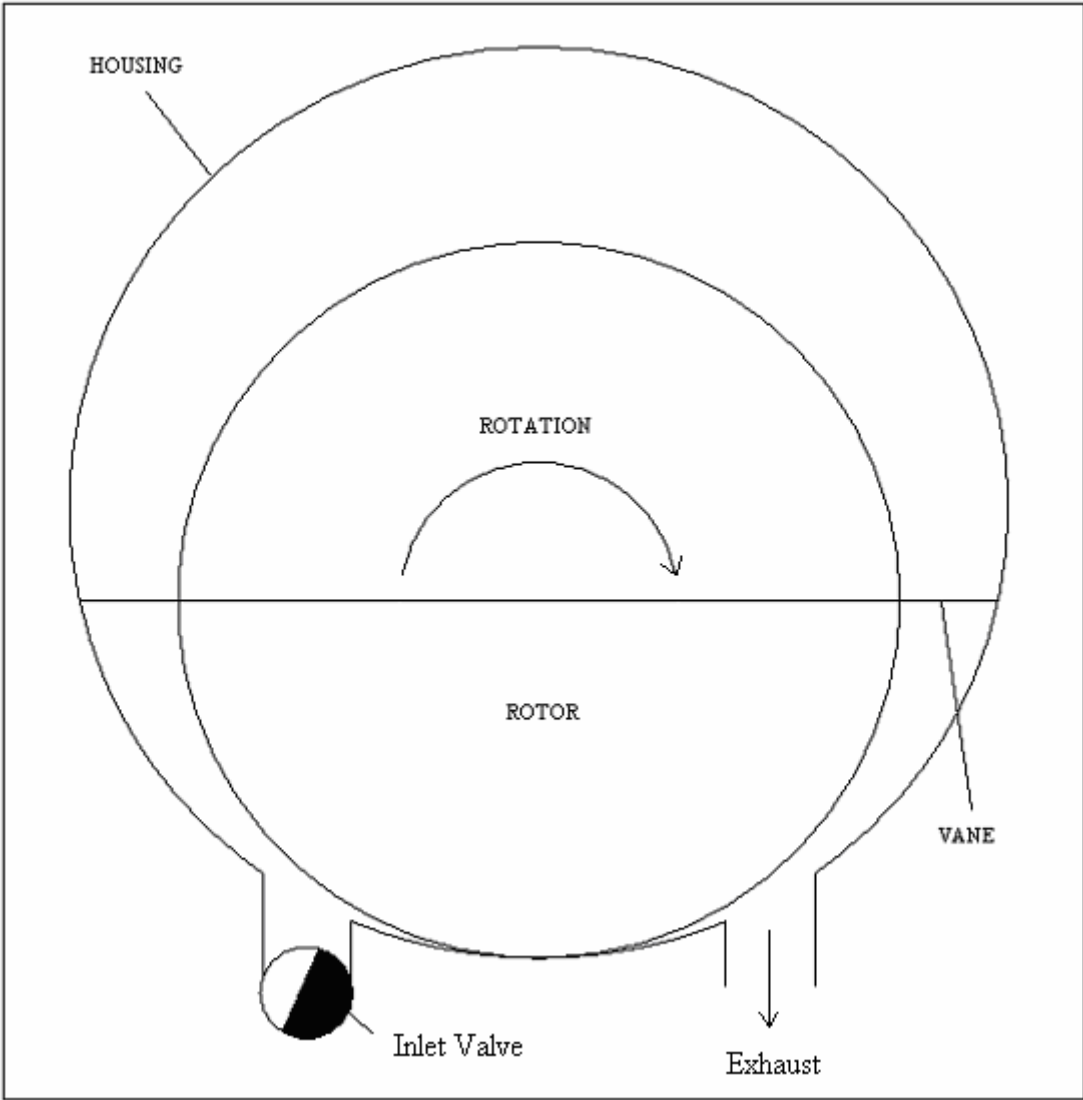
Figure 3-45   Rotary Turbine Diagram

Swept Volume of the Rotary Turbine

The swept volume by a vane can be calculated as a function of swept angle θ from figure 3.46.
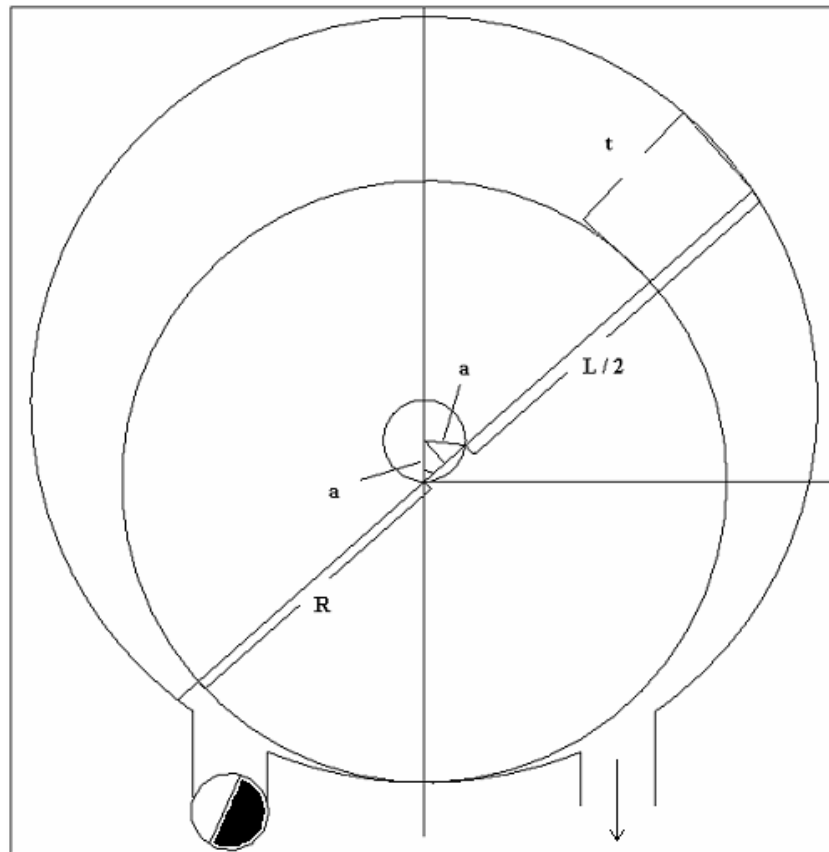
Figure 3-46   Rotary Turbine Kinematics

Table3.2   Rotary Turbine Parameters

R	Rotor Radius
L	Vane Length
a	Eccentricity / 2
t	Vane Length Between Rotor and Housing
θ	Swept Angle
h_t	Turbine Height

Swept Volume (S_w) can be calculated as follows;

$$S_w = \left[\int_{\theta}^{\theta+\pi} t.d\theta \right] \times h_t \qquad (3.5)$$

From geometry can be found as;

$$t = (L/2 - (2.a.\cos\theta) - (R)) \qquad (3.6)$$

Substituting t into equation 3.5;

$$S_w = \left[\int_{\theta}^{\theta+\pi} [L/2 - (2 \times a \times \cos\theta) - (R)]d\theta \right] \times h_t \qquad (3.7)$$

Expansion Volume

Expansion volume is the maximum swept volume.
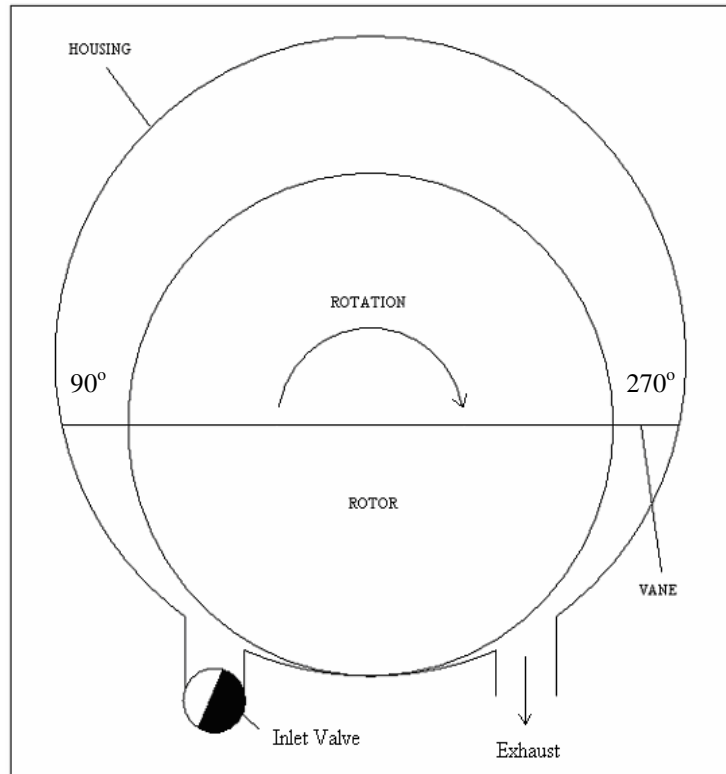
Figure 3-47   Turbine Expansion Volume

$$S_w = \left[\int_{90}^{270} [L / 2 - (2 \times a \times \cos \theta) - (R)] d\theta \right] \times h_t \qquad (3\text{-}8)$$

Design Parameters

Using the thermodynamic design code explained in Chapter 2, the geometry of the turbine is calculated. The geometric parameters of the rotary turbine are given below;

R	150 mm
L	200 mm
a	12.5 mm
h_t	672 mm
t_v	12 mm

Using the geometric data taken from the thermodynamic design code the rotary turbine was designed in CAD environment.

The rotary turbine is composed of a housing, upper and lower taps, upper and lower bearing housings, a rotor and its top seals, a vane and its apex seals and springs, an inlet valve and its bearing housing, two timing pulleys an done timing belt.

As the turbine vane divides the turbine housing into two parts, for one complete revolution, turbine expands two units of combustion gases. The turbine inlet valve is so designed that it discharges this two units of combustion gases to the turbine respectively.

The inlet valve is coupled with the rotary turbine rotor with the help of two timing pulleys and one timing belt and revolves at the same rpm with the rotor. The position of the inlet valve relative to the turbine rotor is adjusted with the timing pulleys by the help of set screws, such that it discharges the combustion gases to turbine at correct times.

An oil pump is used to lubricate the turbine inner surface and the three bearings. (Two main rotor bearings and one discharge valve bearing).
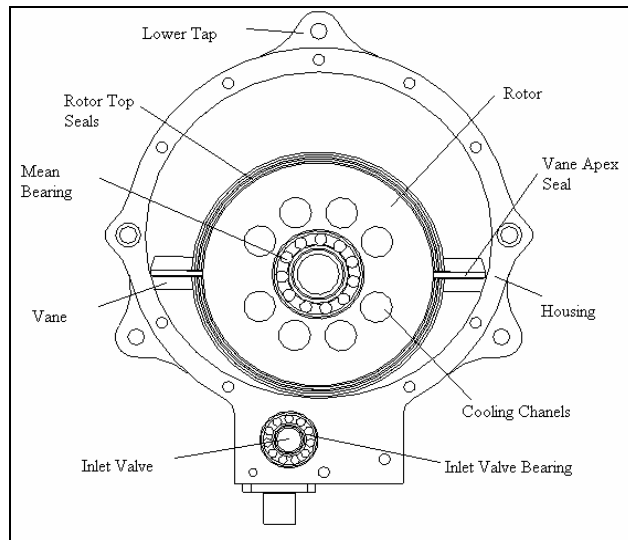
Figure 3-48   2-D Drawing of Rotary Turbine
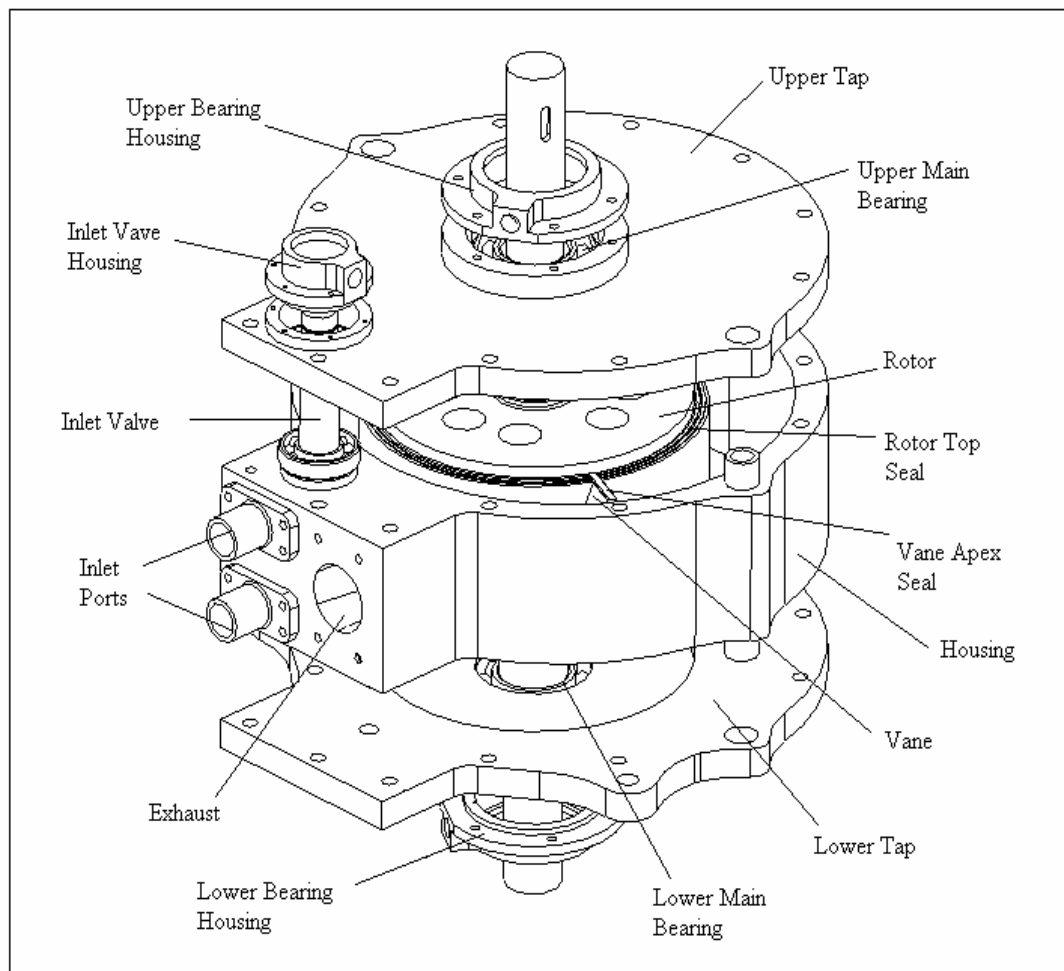
Figure 3-49   3-D Wire-Frame Drawing of Rotary Turbine
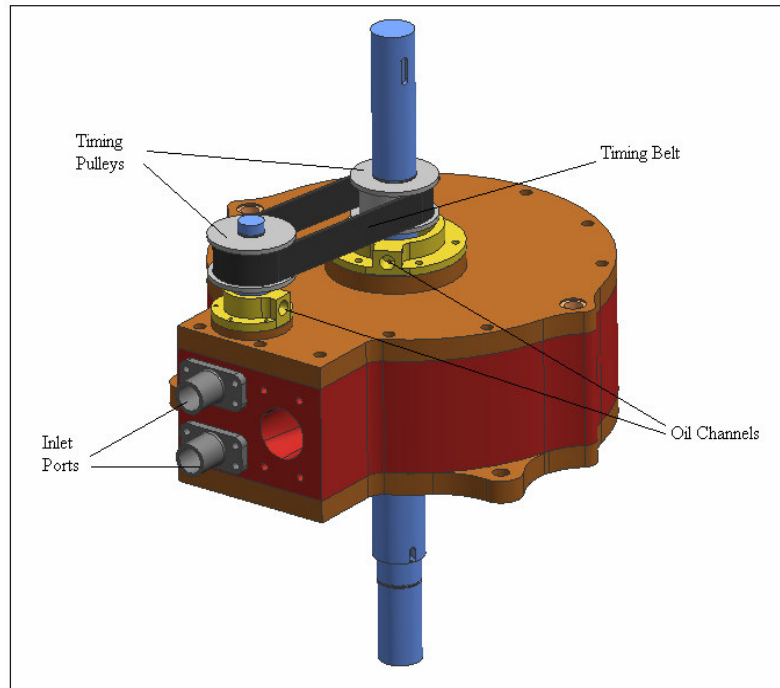
Figure 3-50   3-D CAD Model of the Rotary Turbine
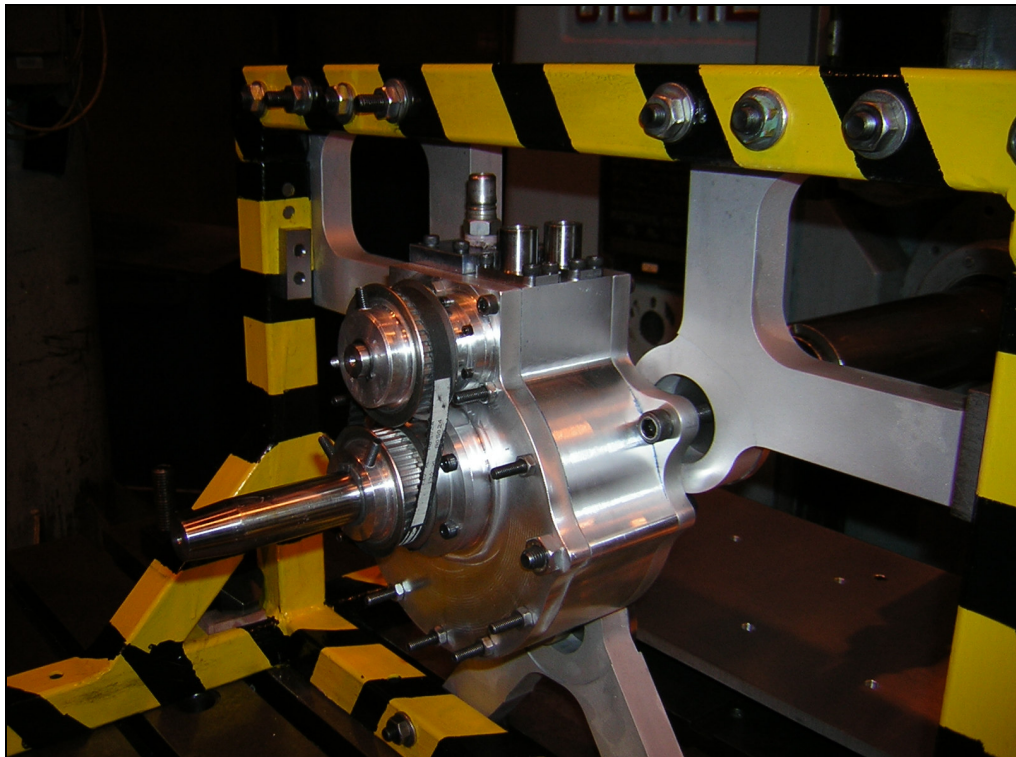
Figure 3-51   Photograph of the Manufactured Turbine

3.2.1 Turbine Parts

Turbine Housing

- Turbine housing is the main body of the turbine in which a rotor is mounted eccentrically.
- Turbine housing is closed by two taps which are positioned by the help of two bushings and tightened with 13 (Metric 6) bolts and 2 (Metric 10) bolts.
- Inside the housing is machined with a 3-Axis NC Machining Lathe due to its cycloid shape.
- Two inlet ports are mounted on the housing.
- Inlet valve seal and spring are placed in their channel on the top of the housing to avoid combustion gas leakage.
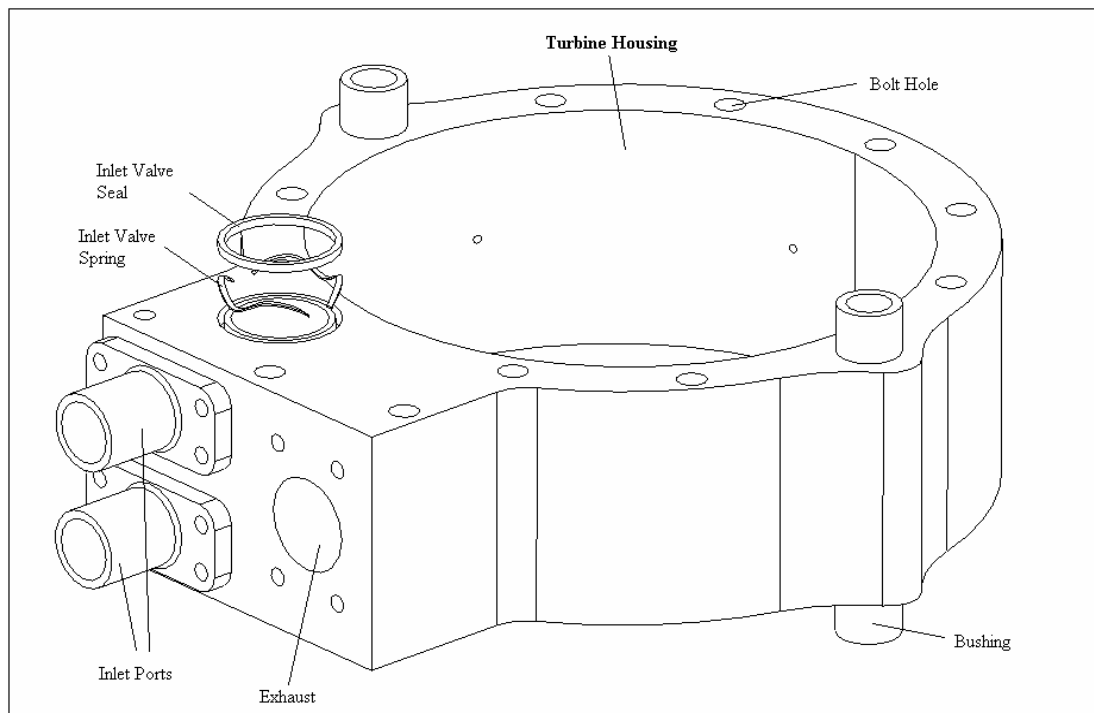
Figure 3-52   Turbine Housing Model

Turbine Upper Tap

- Turbine upper tap has two housings (mean bearing housing and inlet valve housing)
- The eccentricity of the turbine is defined by the place of the main bearing housing and the two bushings.
- Main bearing and inlet valve housing taps are mounted on the top of the upper tap.
- 17 x 35 x 9 ball bearing is tight fitted in the main bearing housing.
- 10 x 17 x 6 ball bearing is tight fitted in the inlet valve housing.
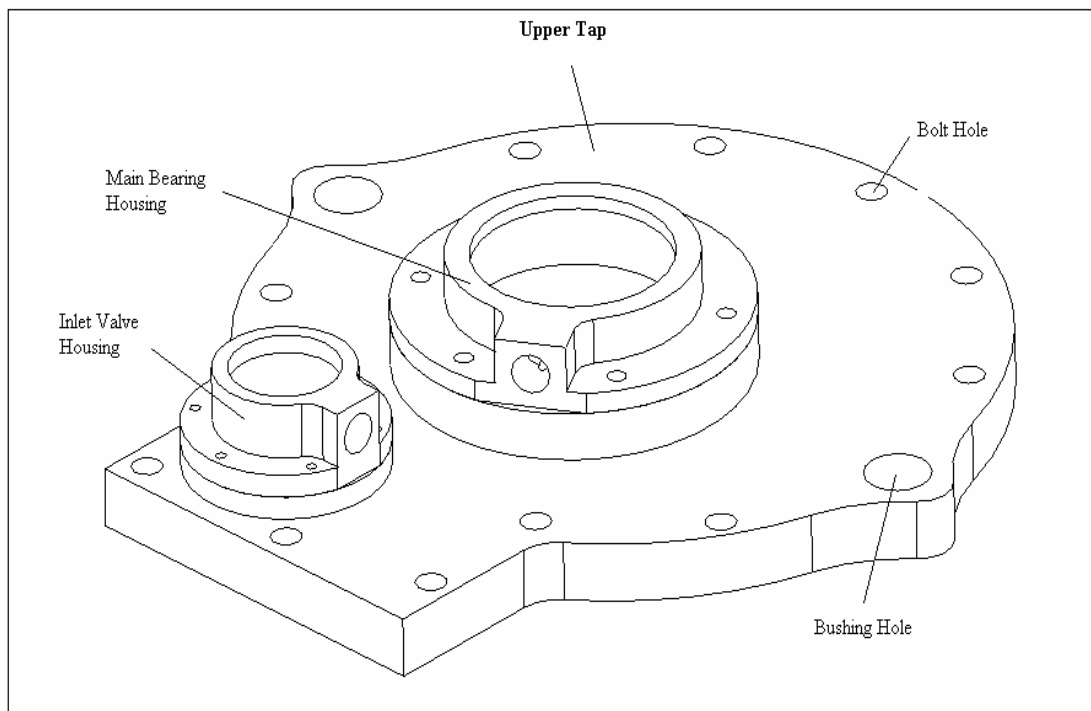
Figure 3-53   Turbine Upper Tap Model

Turbine Lower Tap

- Turbine lower tap has one bearing housing.
- The turbine is mounted to the ground with three (Metric 10) bolts from the three mounting holes on the lower tap.
- Main bearing housing tap is mounted on the top of the upper tap.
- 17 x 35 x 9 ball bearing is tight fitted in the main bearing housing.
- An oil seal is also placed with in the bearing housing tap.
- Main bearing is lubricated from the oil hole on the bearing housing tap.
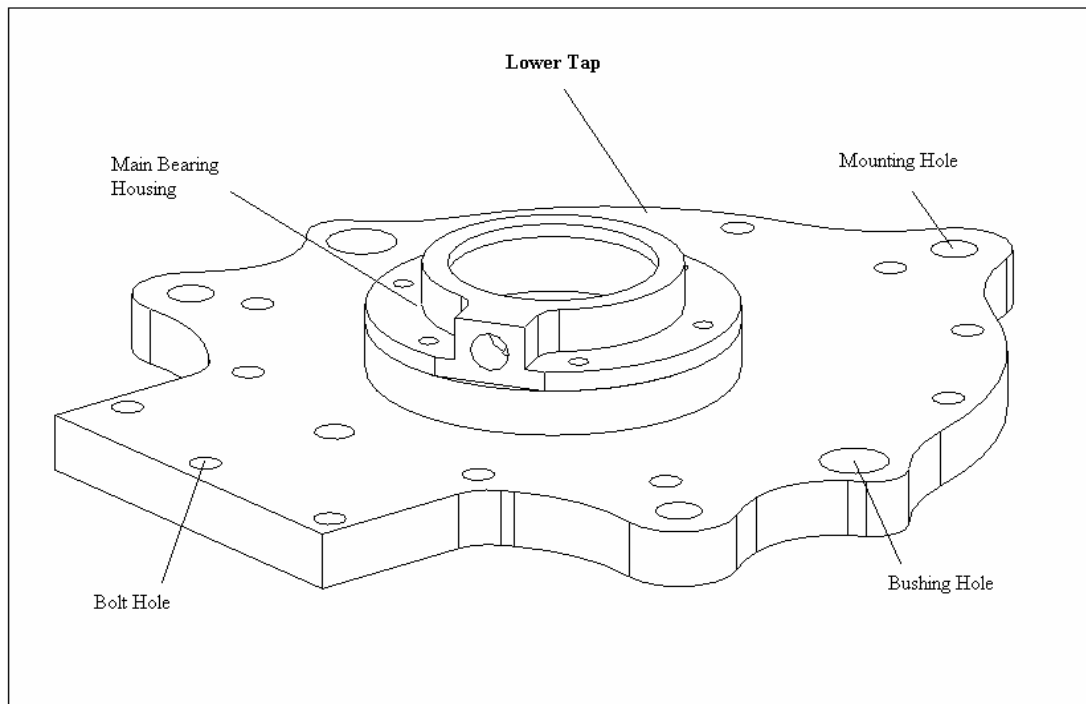
Figure 3-54   Turbine Lower Tap

Turbine Rotor

- Rotor upper and lower seals and springs are placed with in their channels on both sides of the rotor body.
- Rotor inner seals and springs are placed with in their channel in the vane channel.
- Rotor is placed in the housing by two main bearings fitted in the housing taps.
- Cooling holes are opened on the top sides of the rotor.
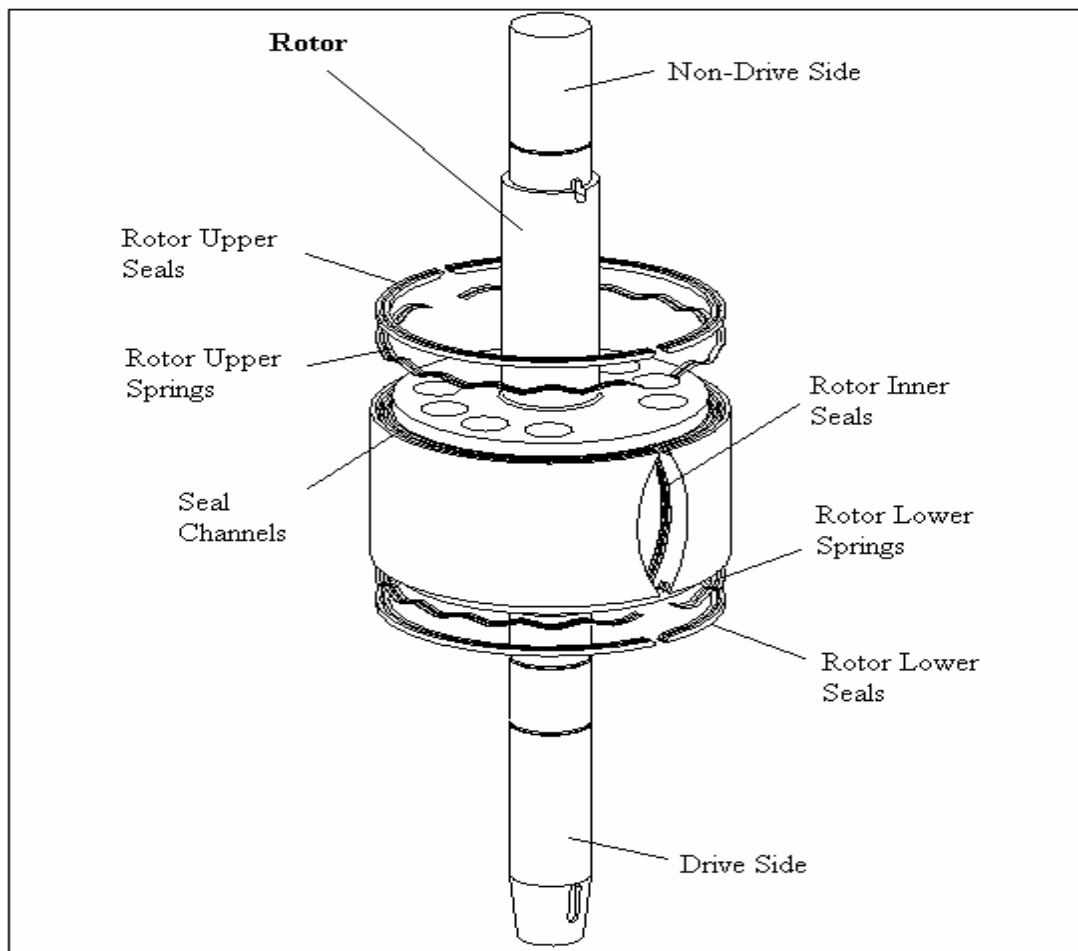
Figure 3-55   Turbine Rotor

Turbine Vane

- Vane is placed with in its channel inside the rotor and can freely slide in and out of the channel by the centrifugal forces formed due to rotation.
- Vane apex seals and springs are placed within their channels at the two ends of the vane.
- Vane apex seals avoid leakage between the vane tip and the inner surface of the housing.
- Vane apex seals also avoid leakage between the vane and the upper and lower taps.
- Vane tip geometry is determined by a kinematical analysis.
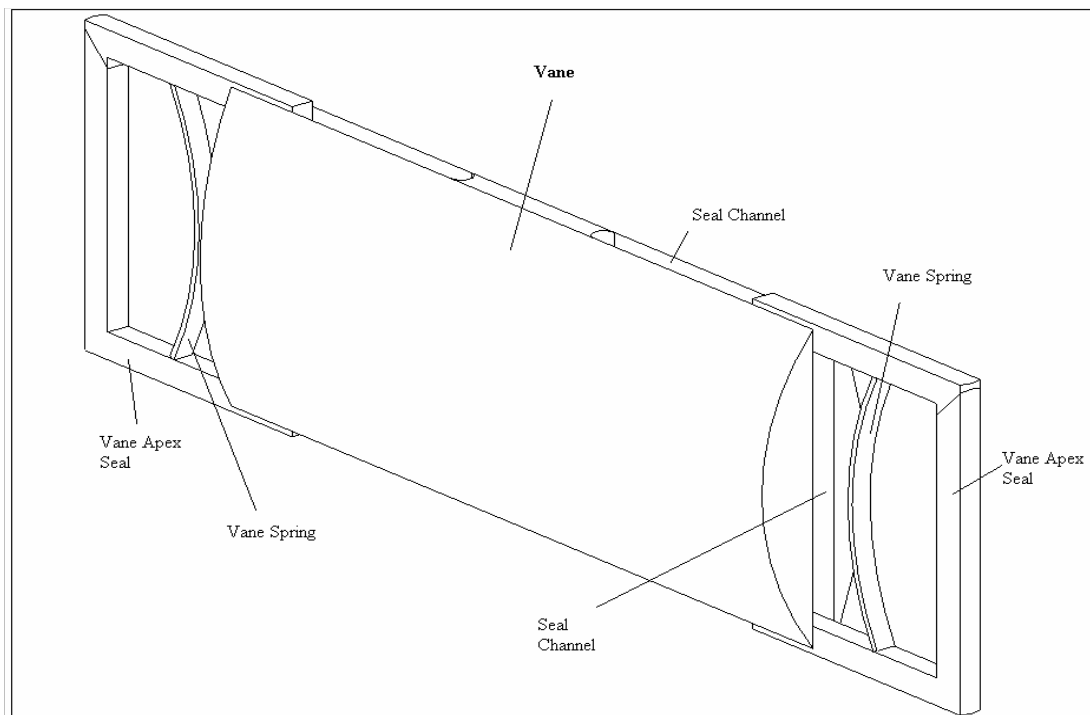
Figure 3-56   Turbine Vane

Turbine Inlet Valve

- Turbine inlet valve is placed with in its housing inside the housing.
- Turbine inlet valve is directly coupled with the rotor by the help of timing pulleys and timing belt and rotates at the same rpm with the rotor.
- Turbine inlet valve delivers combustion gases from the two combustion chambers by the upper and lower discharge channels opened on it.
- Deliver timing is adjusted by the timing pulleys and timing belt.
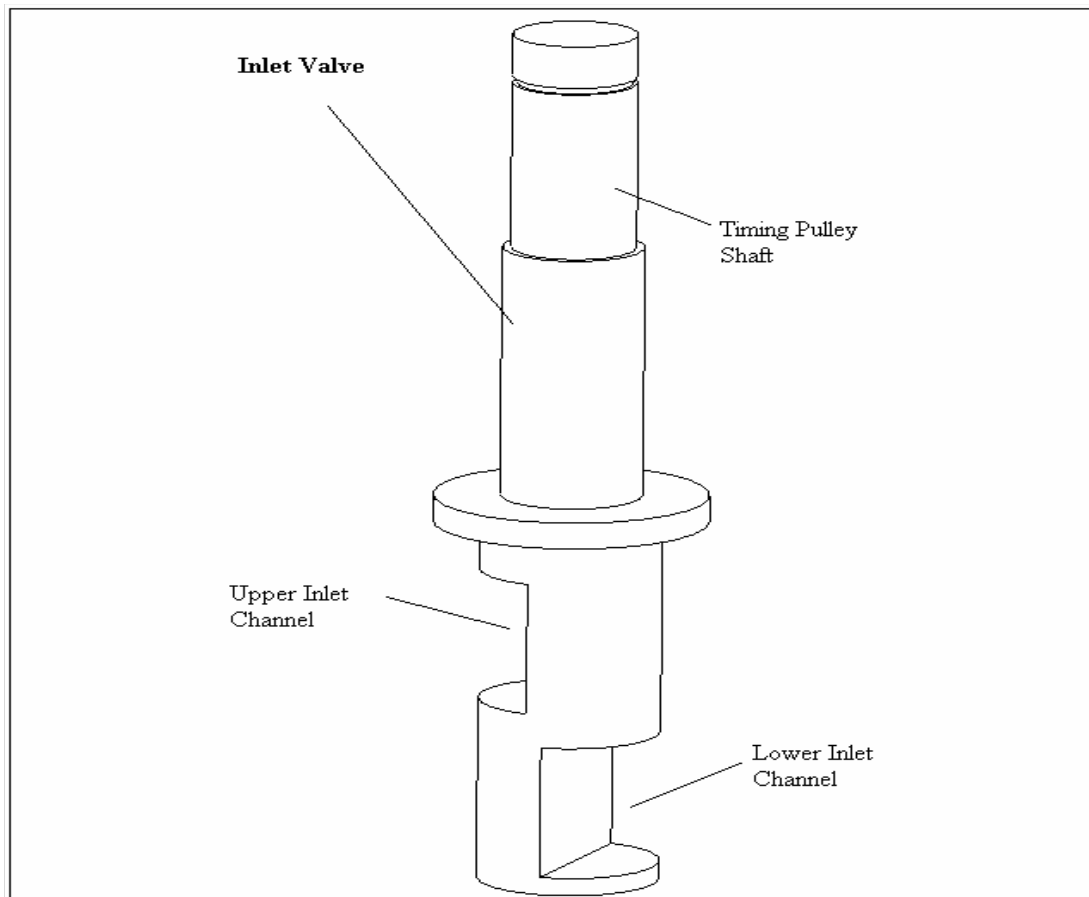
Figure 3-57   Turbine Inlet Valve

3.2.2 Structural Analysis and Material Selection

Structural analysis of the rotary turbine of the novel engine is done in ANSYS 9.0 Environment (Finite Element Program). The aim of this work is to define the manufacturing tolerances and to select the material of the turbine parts. To do the structural analysis, firstly the critical parts are defined as follows;

For material selection;
- Stress distribution on the housing and the taps of the turbine due to pressure and temperature exerted by the combustion gases onto the inner surfaces.
- Stress distribution on the rotor due to pressure and temperature exerted by the combustion gases, together with the centrifugal force caused by rotation.
- Stress distribution on the vane due to pressure and temperature exerted by the combustion gases, together with the centrifugal force caused by rotation.
- Stress distribution on the inlet valve due to pressure and temperature exerted by the combustion gases, together with the centrifugal force caused by rotation.

For defining the manufacturing tolerance;
- Deformation of the inlet valve and its housing in the turbine housing, due to thermal and pressure loads.
- Deformation of the vane and its housing in the rotor, due to thermal and pressure loads.
- Deformation of the rotor top seals and their housings in the rotor, due to thermal and pressure loads.
- Deformation of the vane apex seals and their housings in the vane, due to thermal and pressure loads.

To make the structural analysis of the rotary turbine, the necessary temperature and pressure data is taken from the thermodynamic design code where the temperature and pressure data is given with respect to turbine vane angle θ. The pressure and temperature data wrt turbine vane angle θ are given in figures 3-58 and 3-59 respectively.
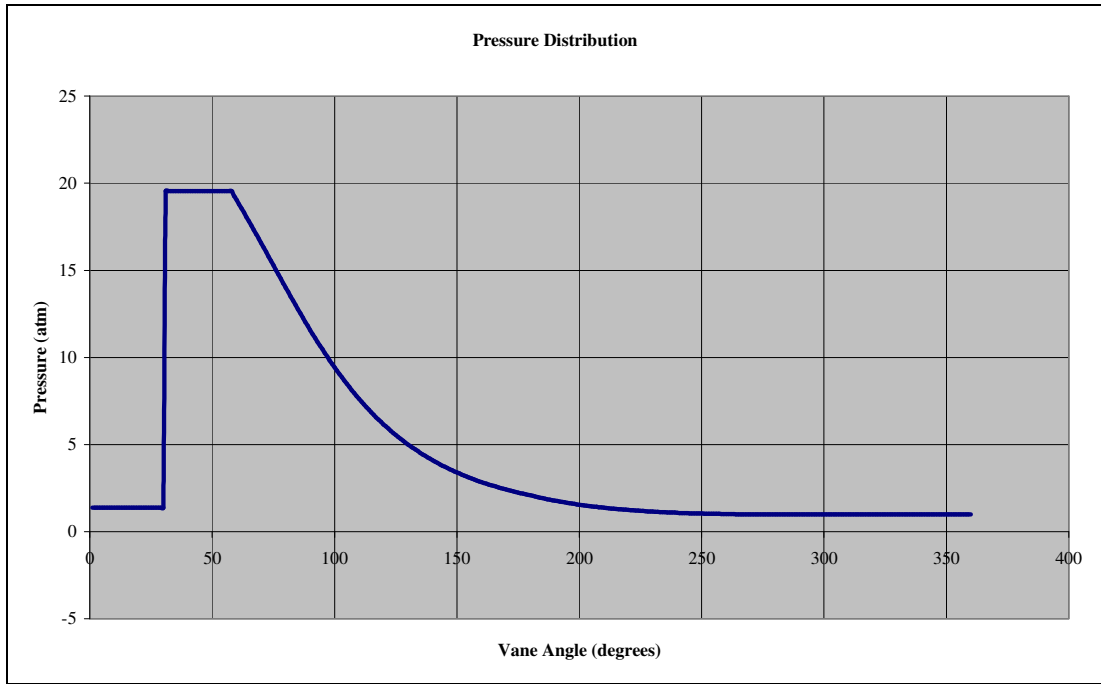
Figure 3-58   Pressure Distribution in the Rotary Turbine
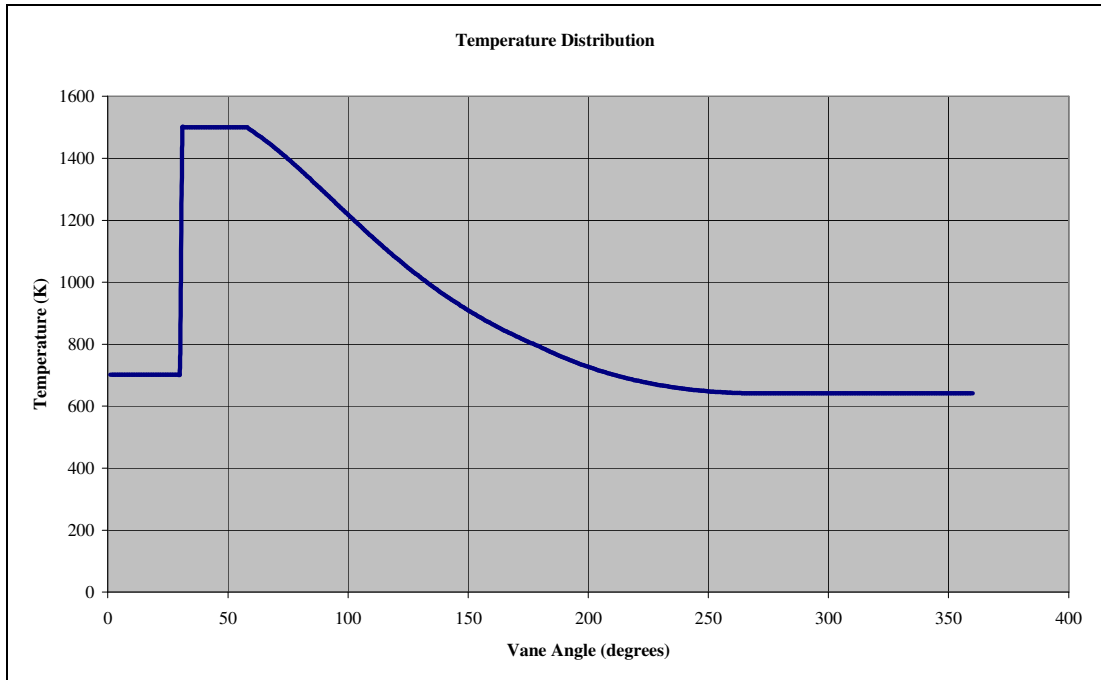
Figure 3-59   Temperature Distribution in the Turbine

109

Stress Distribution on the Turbine Housing

The stress distribution and deformations on the turbine housing due to thermal and pressure loads is analyzed in ANSYS environment. A linear analysis with the following specifications is done.

Material:	H13 Hot Work Tool Steel
Element Type:	Solid 20 Node 95 (Structure)
	Solid 20 Node 90 (Thermal)
Mesh:	Structured (Hex Sweep)
B.C's:	All DOF on bushing areas
Loads:	Convection on divided surfaces
	Pressure load on divided surfaces
Assumptions:	Temperature and pressure values calculated by the thermodynamic code are approximated on the divided inner surfaces.
	Convection Heat Transfer Coefficient for combustion gases is approximated as 50 W/m^2 .K
	Convection Heat Transfer Coefficient for cooling air is approximated as 100 W/m^2 .K

Firstly, a thermal analysis of the housing is done to determine the temperatures on each node due to convection between the combustion gases and the inner surfaces and between the cooling air and the outer surfaces of the housing.

Secondly, a structural analysis of the housing is done to determine the stress distribution and the deformation on the housing. The temperatures calculated in the thermal analysis are applied to the nodes as thermal load and the combustion gas pressure is applied to the inner surfaces of the housing as pressure load.

The results of the analysis showed that the stress values on the turbine housing are in the elastic region and are below the yield tensile strength of the material and can be safely used. Also the deformations on the inlet valve housing are later used to determine the manufacturing tolerances between the valve and the housing.

Figure 3-60   Structural Analysis Model of the Turbine Housing
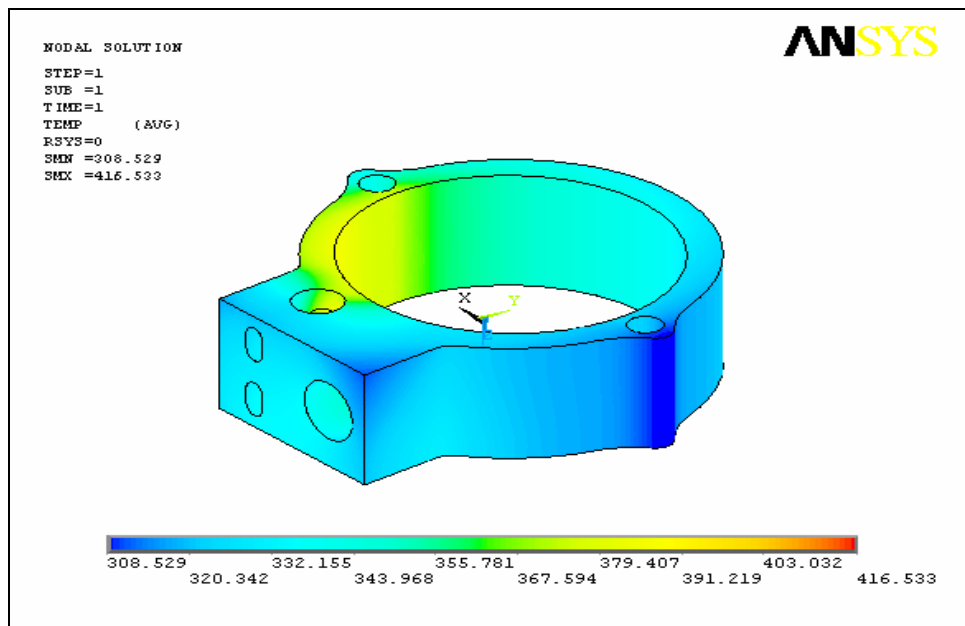
Figure 3-61   Temperature Distribution on Turbine Housing

Max Temperature on the housing: 417° K

111
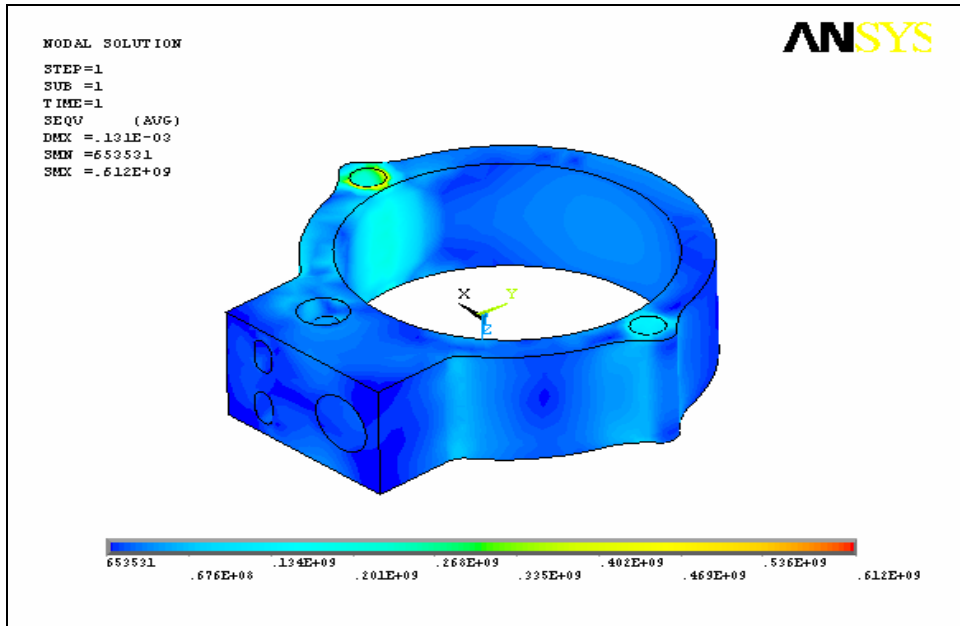
Figure 3-62   Stress Distribution on the Turbine Housing

Max Stress: 612 MPa   Yield Tensile Strength: 1650 MPa
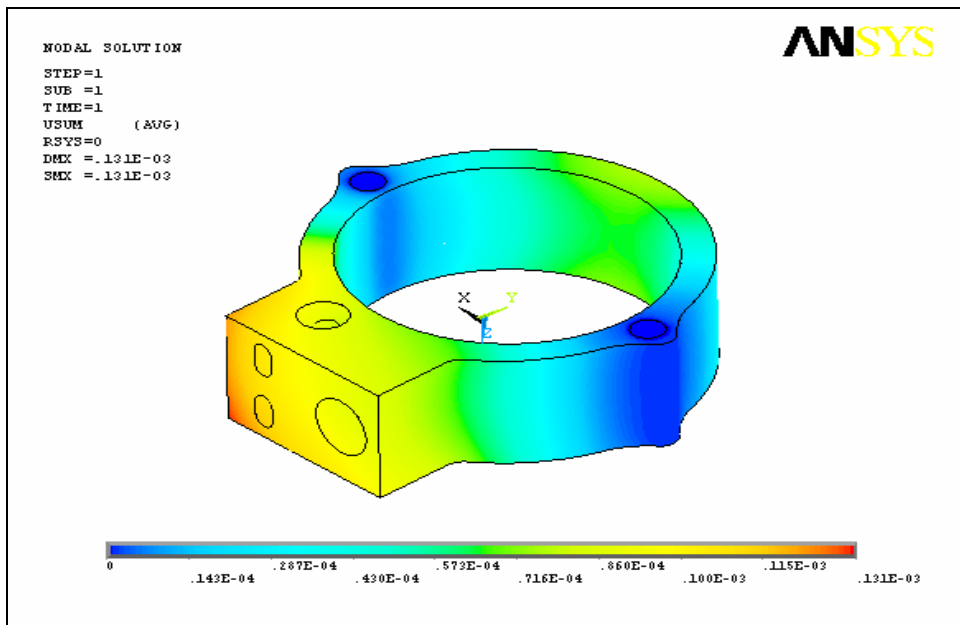
Figure 3-63   Deformation on the Turbine Housing

Stress Distribution on the Turbine Upper Tap

The stress distribution and deformations on the turbine upper tap due to thermal and pressure loads is analyzed in ANSYS environment. A linear analysis with the following specifications is done.

Material:	H13 Hot Work Tool Steel
Element Type:	Solid 20 Node 95 (Structure)
	Solid 20 Node 90 (Thermal)
Mesh:	Structured (Hex Sweep)
B.C's:	Fixed all DOF on bushing areas
Loads:	Convection on divided surfaces
	Pressure load on divided surfaces
Assumptions:	Temperature and pressure values calculated by the thermodynamic code are approximated on the divided inner surfaces.
	Convection Heat Transfer Coefficient for combustion gases is approximated as 50 W/m^2 .K
	Convection Heat Transfer Coefficient for cooling air is approximated as 100 W/m^2 .K

Firstly, a thermal analysis of the turbine upper tap is done to determine the temperatures on each node due to convection between the combustion gases and the inner surfaces and between the cooling air and the outer surfaces of the upper tap.

Secondly, a structural analysis of the turbine upper tap is done to determine the stress distribution and the deformation on the upper tap. The temperatures calculated in the thermal analysis are applied to the nodes as thermal load and the combustion gases pressure is applied to the inner surfaces of the upper tap as pressure load.

The results of the analysis showed that the stress values on the turbine upper tap are in the elastic region and are below the yield tensile strength of the material and can be safely used.
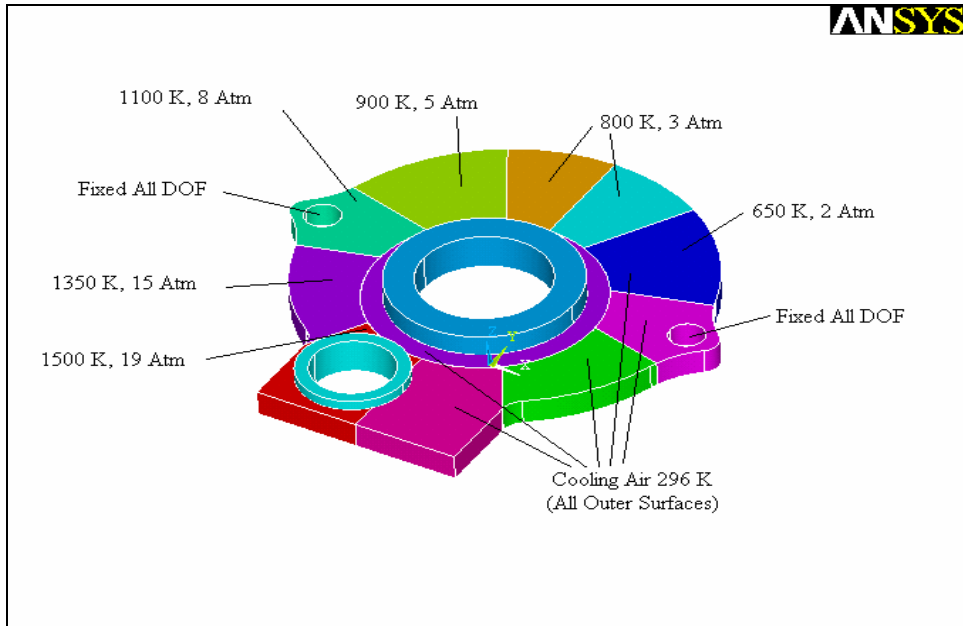
Figure 3-64   Structural Analysis Model of the Turbine Upper Tap
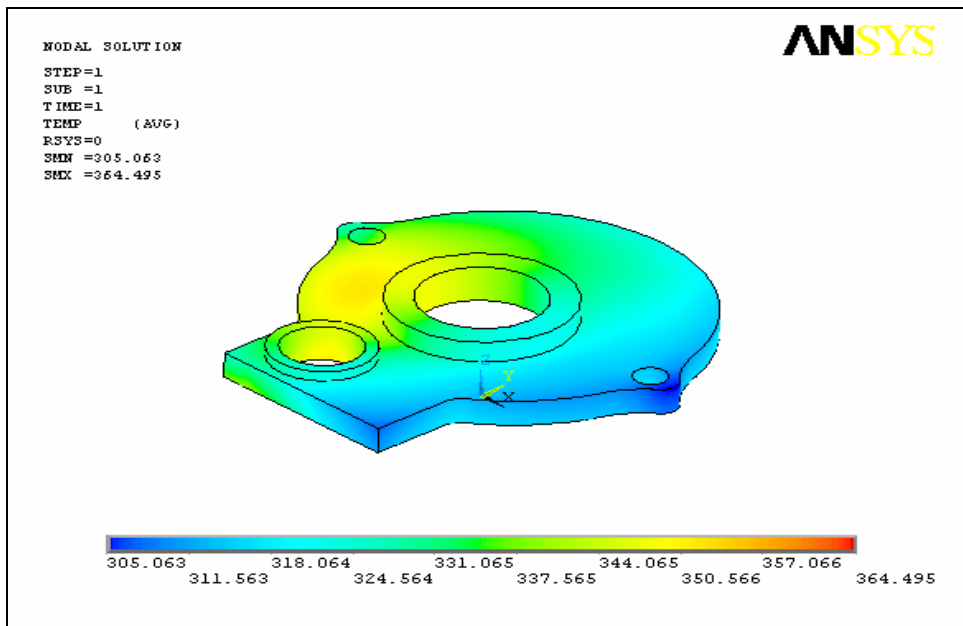
Figure 3-65   Temperature Distribution on Turbine Upper Tap

Max Temperature on the upper tap: 365° K
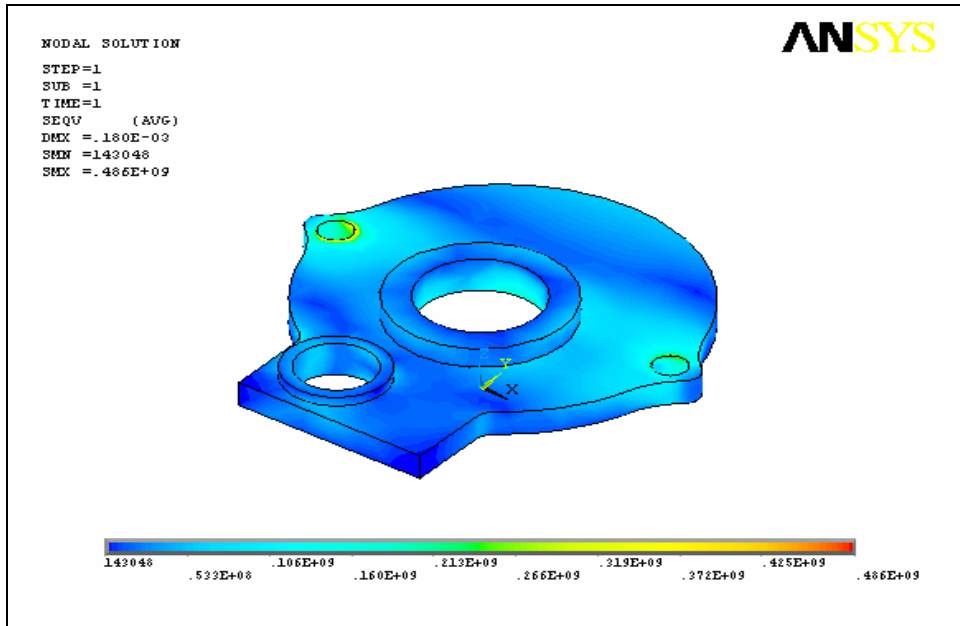
Figure 3-66   Stress Distribution on the Turbine Upper Tap

Max Stress: 486 MPa   Yield Tensile Strength: 1650 MPa
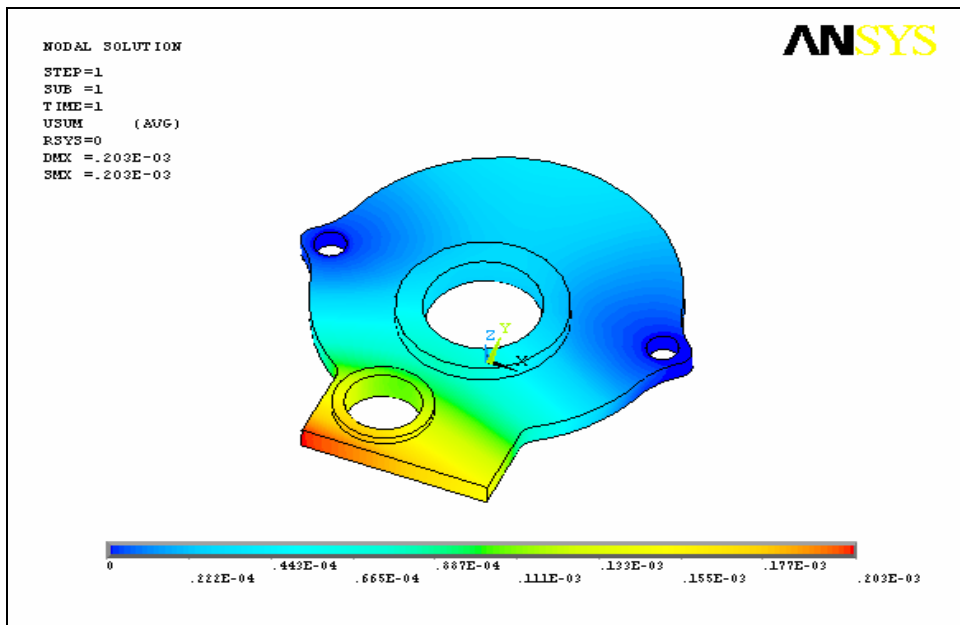
Figure 3-67   Deformation on the Turbine Upper Tap

Stress Distribution on the Turbine Lower Tap

The stress distribution and deformations on the turbine lower tap due to thermal and pressure loads is analyzed in ANSYS environment. A linear analysis with the following specifications is done.

Material:	H13 Hot Work Tool Steel
Element Type:	Solid 20 Node 95 (Structure)
	Solid 20 Node 90 (Thermal)
Mesh:	Structured (Hex Sweep)
B.C's:	Fixed all DOF on mounting areas
Loads:	Convection on divided surfaces
	Pressure load on divided surfaces
Assumptions:	Temperature and pressure values calculated by the thermodynamic code are approximated on the divided inner surfaces.
	Convection Heat Transfer Coefficient for combustion gases is approximated as 50 W/m^2 .K
	Convection Heat Transfer Coefficient for cooling air is approximated as 100 W/m^2 .K

Firstly, a thermal analysis of the turbine lower tap is done to determine the temperatures on each node due to convection between the combustion gases and the inner surfaces and between the cooling air and the outer surfaces of the lower tap.

Secondly, a structural analysis of the turbine lower tap is done to determine the stress distribution and the deformation on the lower tap. The temperatures calculated in the thermal analysis are applied to the nodes as thermal load and the combustion gases pressure is applied to the inner surfaces of the lower tap as pressure load.

The results of the analysis showed that the stress values on the turbine lower tap are in the elastic region and are below the yield tensile strength of the material and can be safely used.
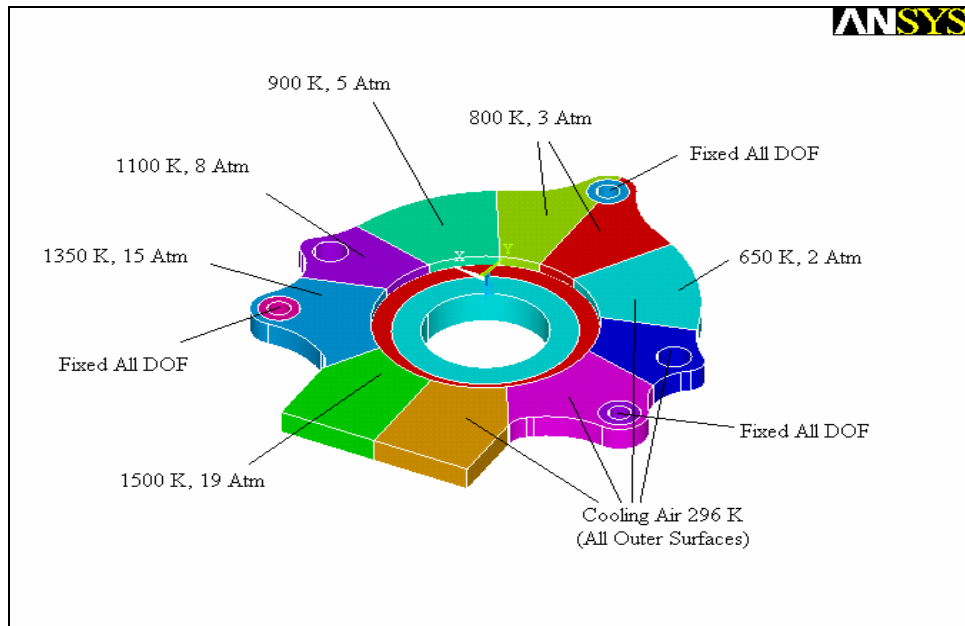
Figure 3-68   Structural Analysis Model of the Turbine Lower Tap
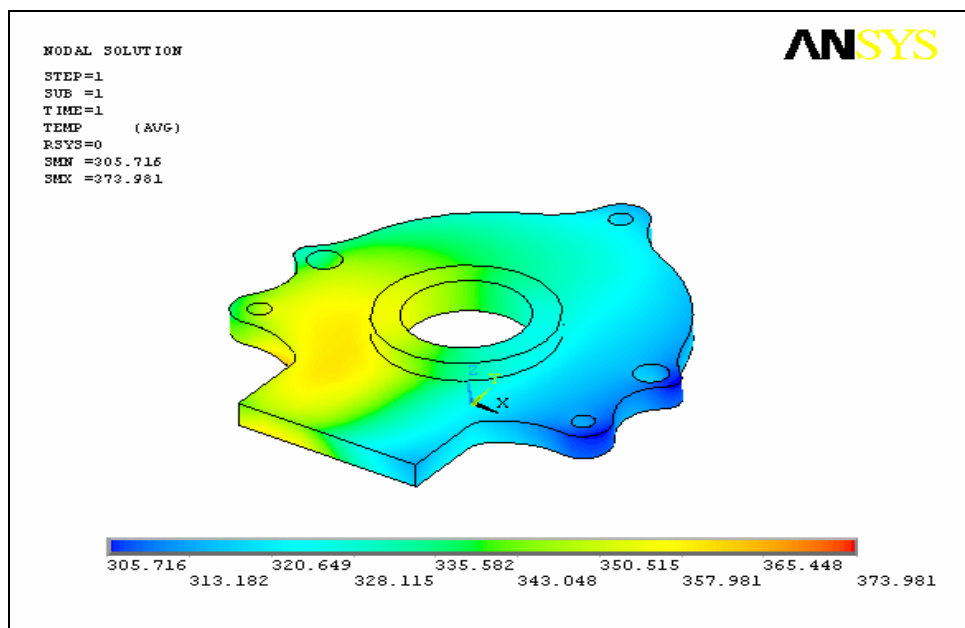
Figure 3-69   Temperature Distribution on Turbine Lower Tap

Max Temperature on the lower tap: 374° K
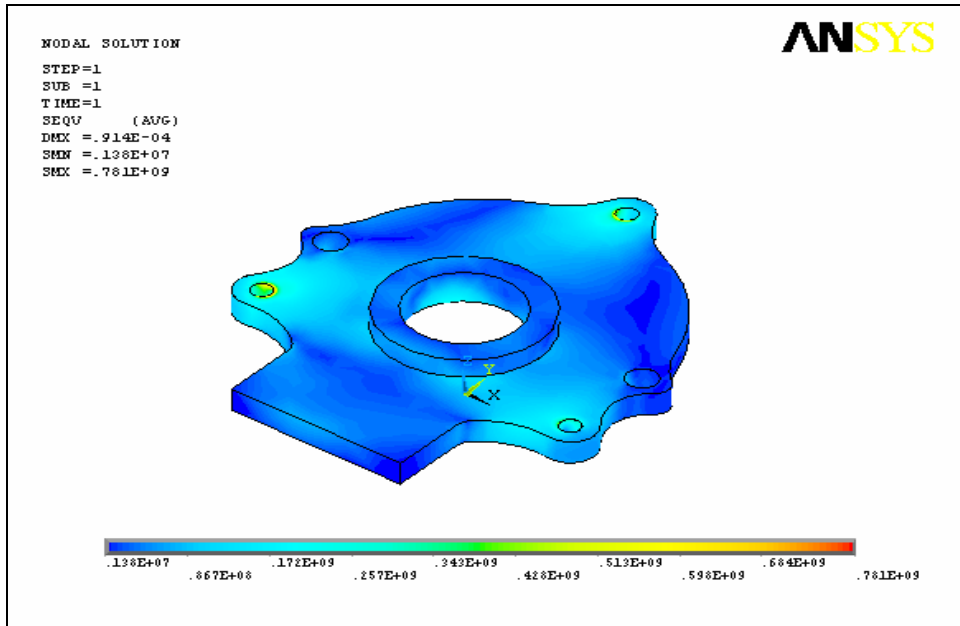
Figure 3-70   Stress Distribution on the Turbine Lower Tap

Max Stress: 781 MPa   Yield Tensile Strength: 1650 MPa
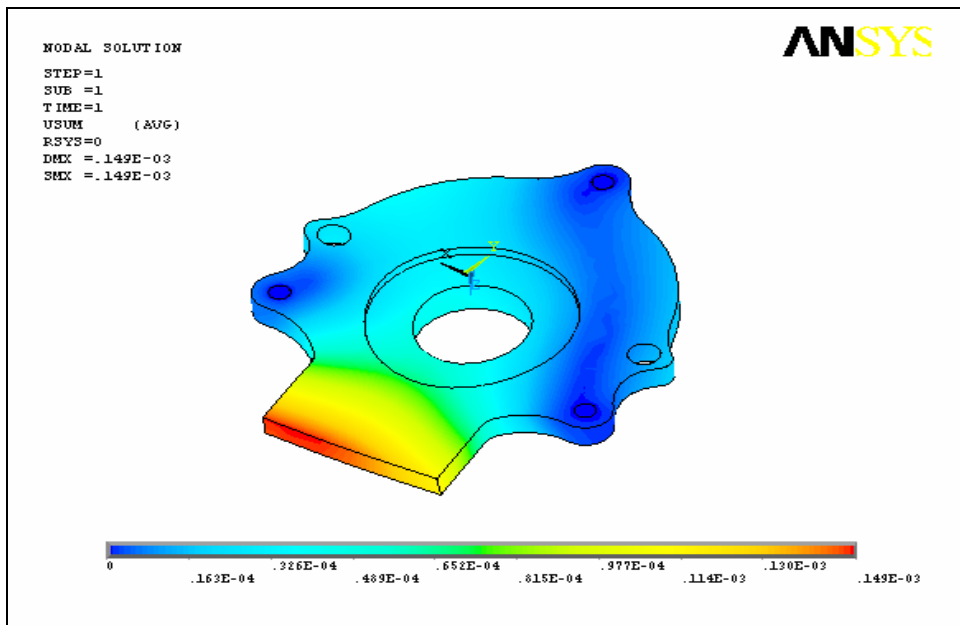
Figure 3-71   Deformation on the Turbine Lower Tap

Stress Distribution on the Turbine Vane

The stress distribution and deformations on the turbine vane due to thermal and pressure loads is analyzed in ANSYS environment. A linear analysis with the following specifications is done.

Material:	H13 Hot Work Tool Steel
Element Type:	Solid 20 Node 95 (Structure)
	Solid 20 Node 90 (Thermal)
Mesh:	Structured (Hex Sweep)
B.C's:	Fixed X_Axis on vane tip surface
	Fixed Y_Axis on one vane side surface
	Fixed Z_Axis on vane top surface
Loads:	Approximate temperature load
	Pressure load on divided surfaces
Assumptions:	Average temperature is applied to the vane.
	Max pressure of the combustion gases is applied to the vane inner surface.

Structural analysis of the turbine vane is done to determine the stress distribution and the deformation on the vane. Average temperature is applied to the nodes as thermal load and the max combustion gases pressure (19 atm) is applied to the inner surfaces of the vane as pressure load.

The results of the analysis showed that the stress values on the turbine vane are in elastic region and below the yield tensile strength of the material and can be safely used. Also the deformations of the vane are later used to define the manufacturing tolerances between the vane and the rotor.

Figure 3-72   Structural Analysis Model of the Turbine Vane
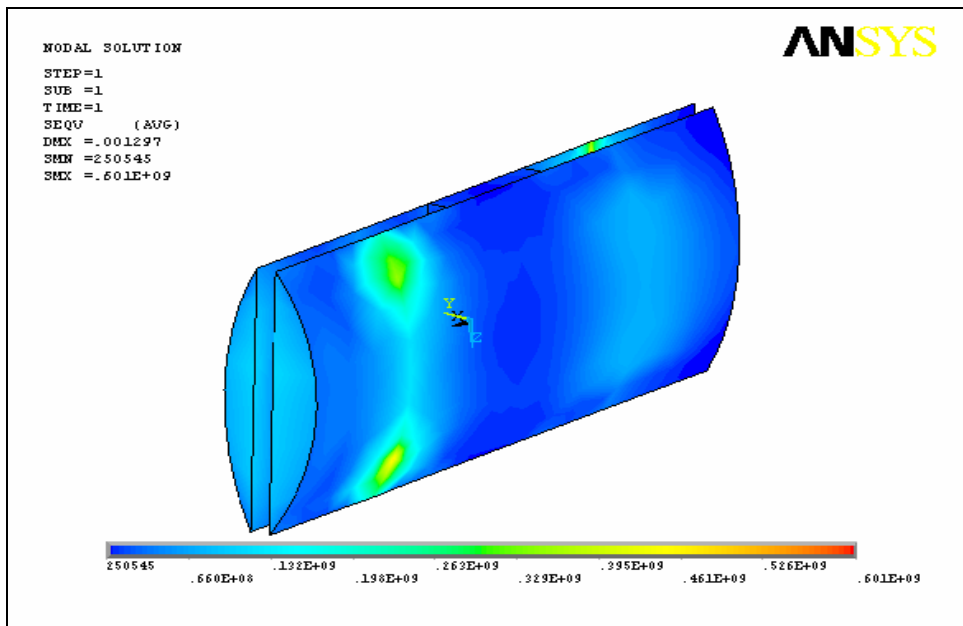
Figure 3-73   Stress Distribution on Turbine Vane

Max Stress: 601 MPa   Yield Tensile Strength: 1650 MPa
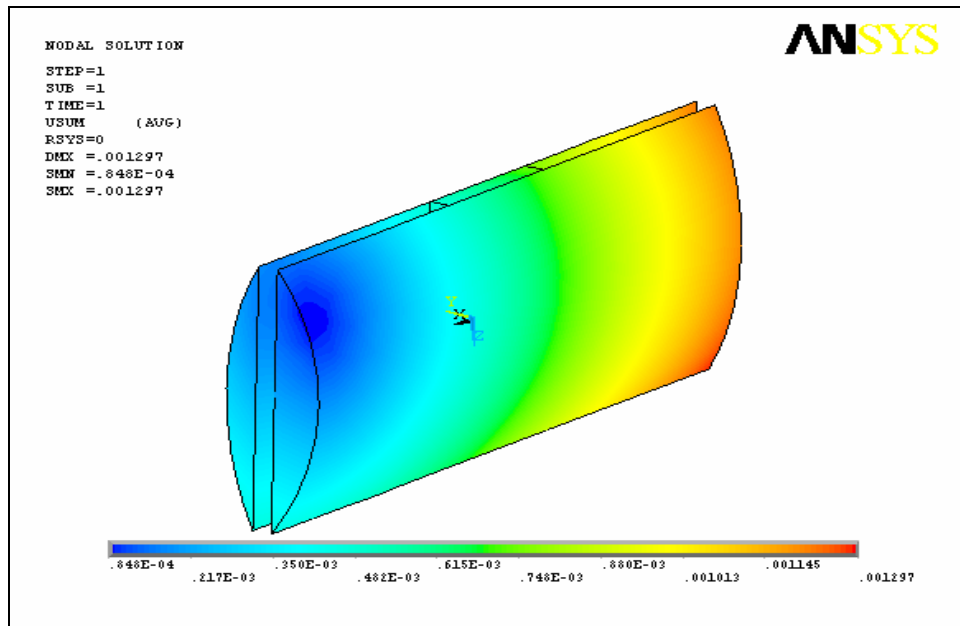
Figure 3-74   Deformation on the Turbine Vane

Stress Distribution on the Turbine Rotor

The stress distribution and deformations on the turbine rotor due to thermal and pressure and inertia loads is analyzed in ANSYS environment. A linear analysis with the following specifications is done.

Material:	H13 Hot Work Tool Steel
Element Type:	Tet 10 Node 92 (Structure)
	Tet 10 Node 87 (Thermal)
Mesh:	Unstructured (Tet)
B.C's:	Fixed in radial and Z_Axis on bearing surfaces
Loads:	Convection on divided surfaces
	Max. Pressure load on divided surfaces
	Angular Velocity of 6000 rpm
Assumptions:	Convection Heat Transfer Coefficient for combustion gases is approximated as 50 W/m^2 .K
	Convection Heat Transfer Coefficient for cooling air is approximated as 100 W/m^2 .K
	Convection Heat Transfer Coefficient for cooling oil is approximated as 150 W/m^2 .K

Firstly, a thermal analysis of the turbine rotor is done to determine the temperatures on each node due to convection between the combustion gases and the inner surfaces and between the cooling air and oil and the outer surfaces of the rotor.

Secondly, a structural analysis of the turbine rotor is done to determine the stress distribution and the deformation on the rotor. The temperatures calculated in the thermal analysis are applied to the nodes as thermal load and the max combustion gases pressure is applied to the inner surfaces of the rotor as pressure load. Also angular velocity of 6000 rpm is applied.

The results of the analysis showed that the stress values on the turbine rotor are in the elastic region and are below the yield tensile strength of the material and can be safely used. Also the deformations on the vane housing are later used to determine the manufacturing tolerances between the rotor and the vane.
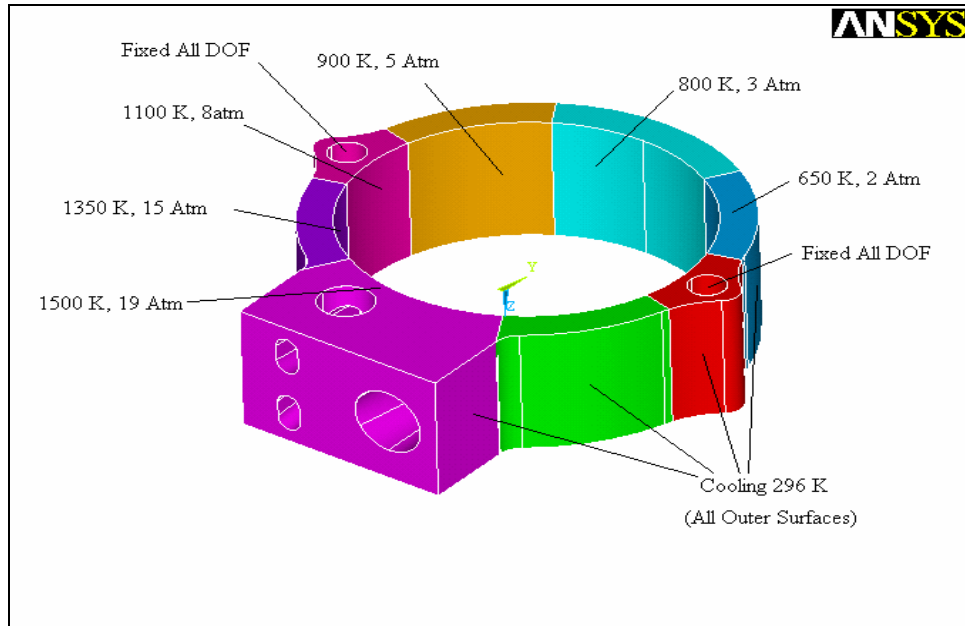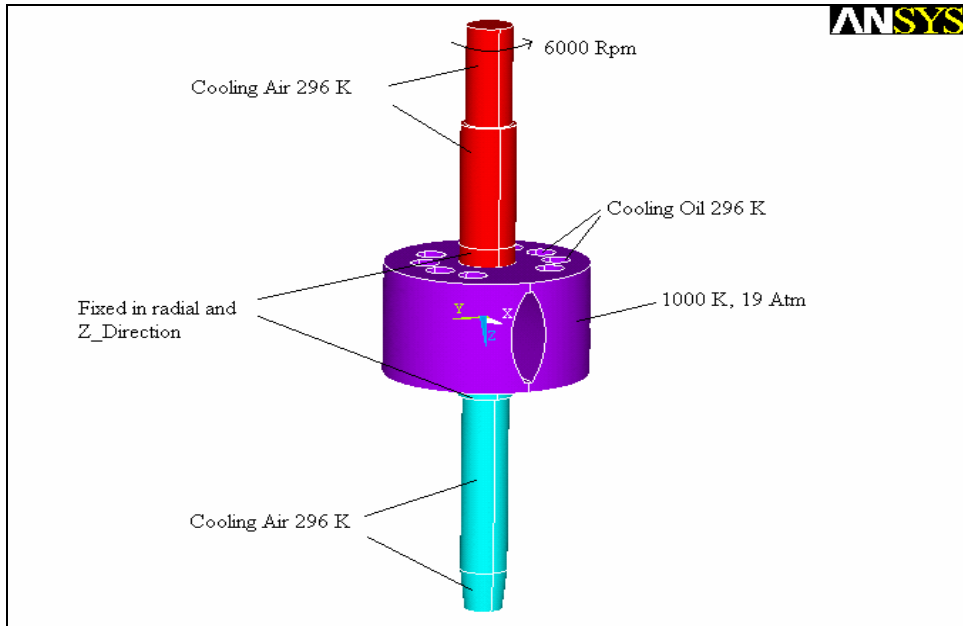
Figure 3-75   Structural Analysis Model of the Turbine Rotor
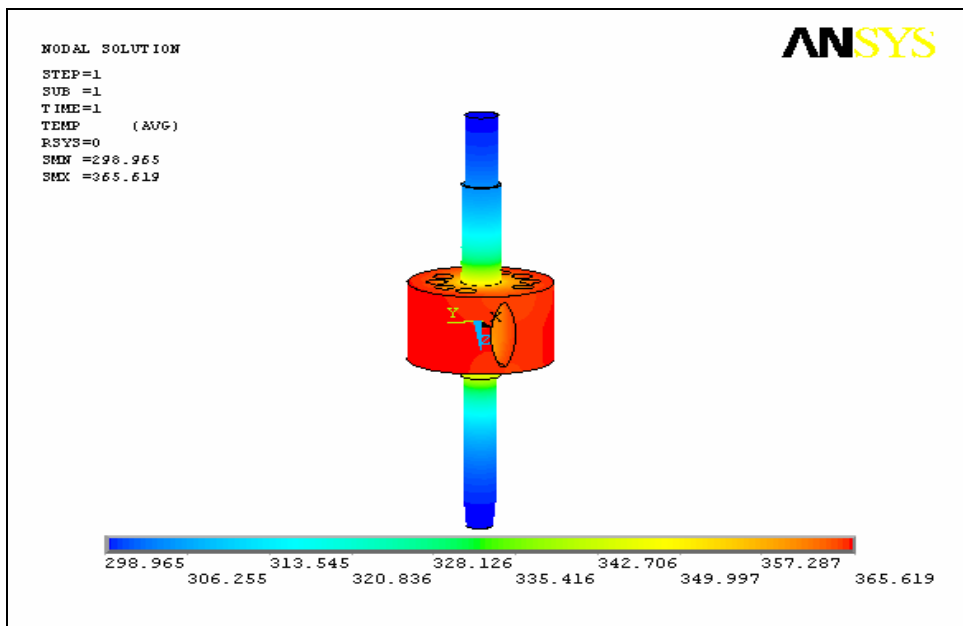
Figure 3-76   Temperature Distribution on Turbine Rotor

Max Temperature on the rotor: 366° K

123
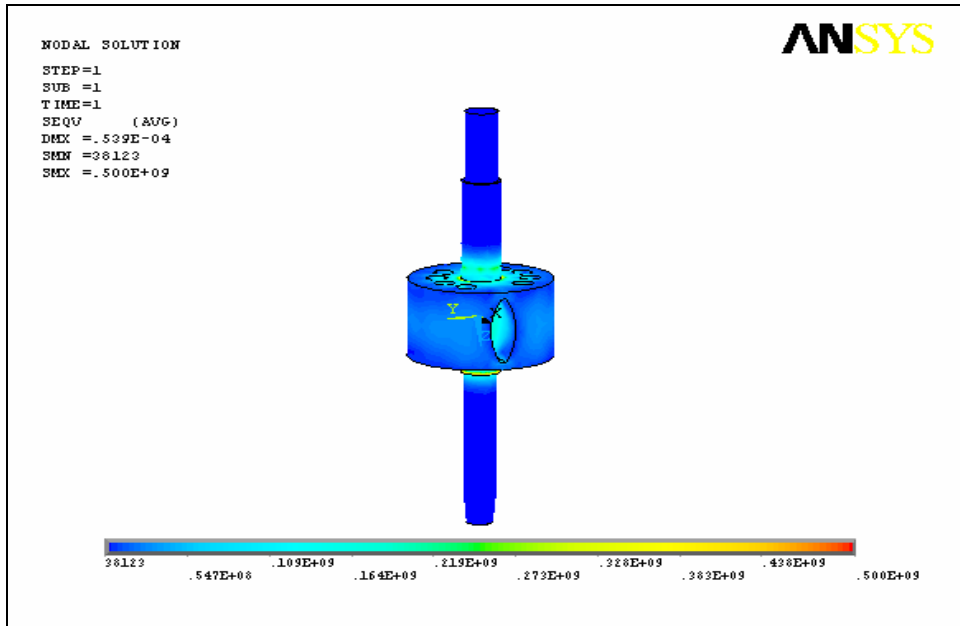
Figure 3-77   Stress Distribution on the Turbine Rotor

Max Stress: 500 MPa	Yield Tensile Strength: 1650 MPa
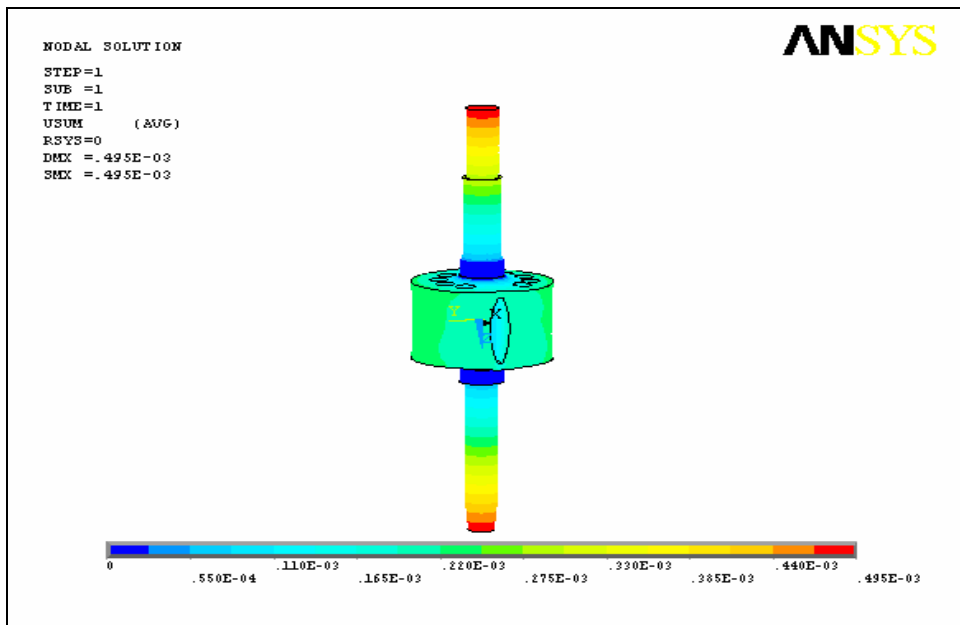
Figure 3-78   Deformation on the Turbine Rotor

Stress Distribution on the Turbine Inlet Valve

The stress distribution and deformations on the turbine inlet valve due to thermal and pressure loads is analyzed in ANSYS environment. A linear analysis with the following specifications is done.

Material:	H13 Hot Work Tool Steel
Element Type:	Solid 20 Node 95 (Structure)
	Solid 20 Node 90 (Thermal)
Mesh:	Structured (Hex Sweep)
B.C's:	Fixed in radial and Z_Axis on bearing surfaces
Loads:	Convection on divided surfaces
	Pressure load on divided surfaces
	Angular velocity of 6000 rpm
Assumptions:	Convection Heat Transfer Coefficient for combustion gases is approximated as 50 W/m^2 .K
	Convection Heat Transfer Coefficient for cooling air is approximated as 100 W/m^2 .K

Firstly, a thermal analysis of the turbine inlet valve is done to determine the temperatures on each node due to convection between the combustion gases and the inlet surfaces and between the cooling air and the outer surfaces of the inlet valve.

Secondly, a structural analysis of the turbine inlet valve is done to determine the stress distribution and the deformation on the inlet valve. The temperatures calculated in the thermal analysis are applied to the nodes as thermal load and the max combustion gases pressure is applied to the inlet surfaces of the inlet valve as pressure load. Also angular velocity of 6000 rpm is applied.

The results of the analysis showed that the stress values on the turbine inlet valve are in the elastic region and are below the yield tensile strength of the material and can be safely used. Also the deformations of the valve are later used to define manufacturing tolerance between the inlet valve and the housing.
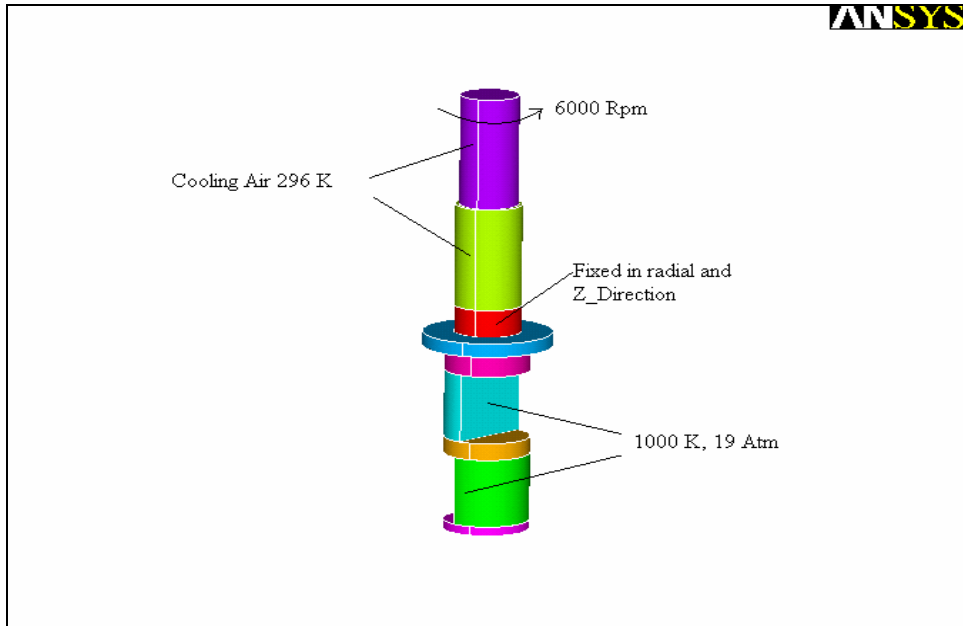
Figure 3-79   Structural Analysis Model of the Turbine Inlet Valve
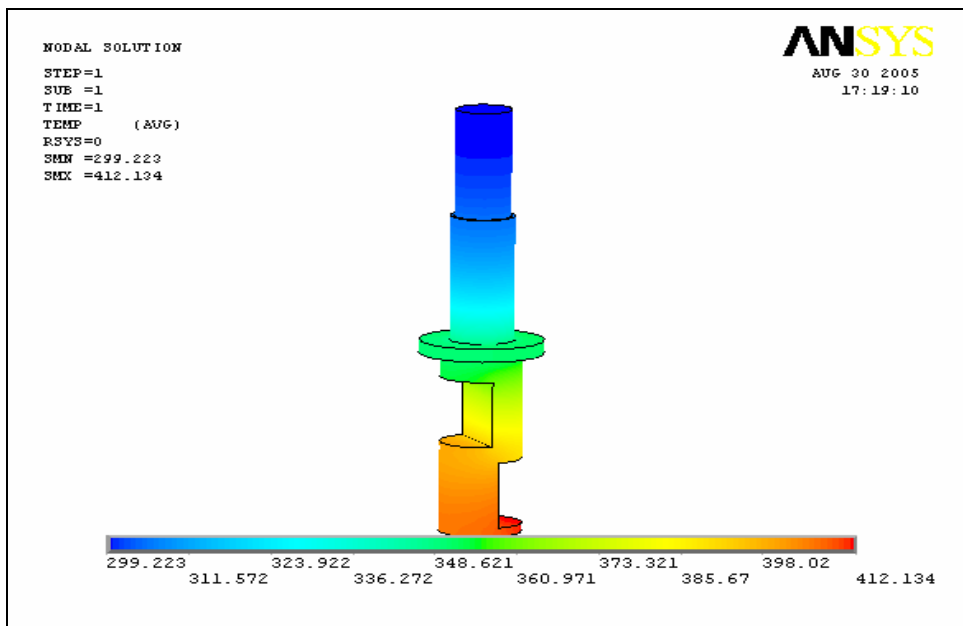
Figure 3-80   Temperature Distribution on Turbine Inlet Valve

Max Temperature on the inlet valve: 412$^{\text{o}}$ K
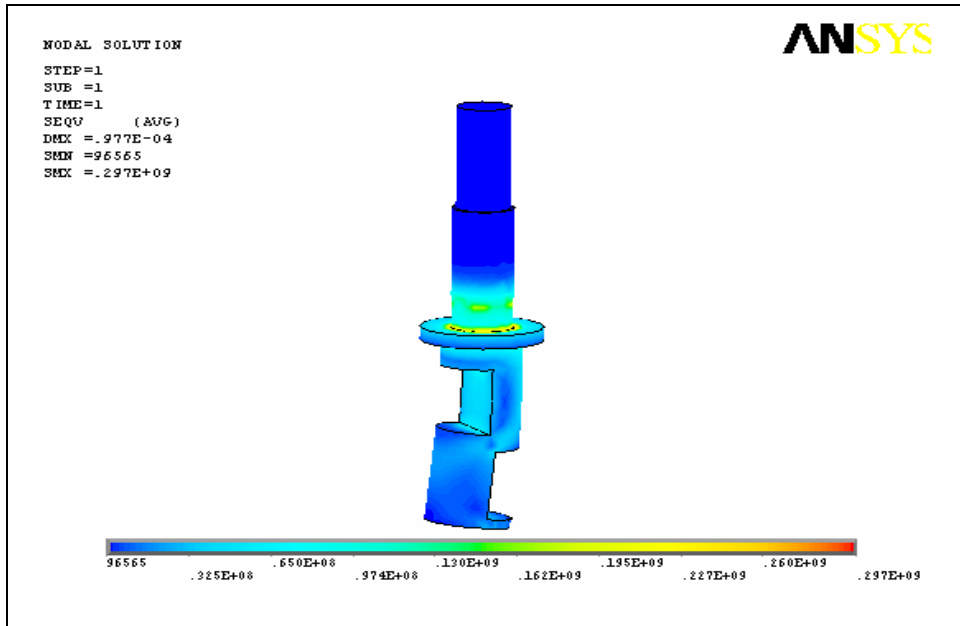
Figure 3-81   Stress Distribution on the Turbine Inlet Valve

Max Stress: 297 MPa	Yield Tensile Strength: 1650 MPa
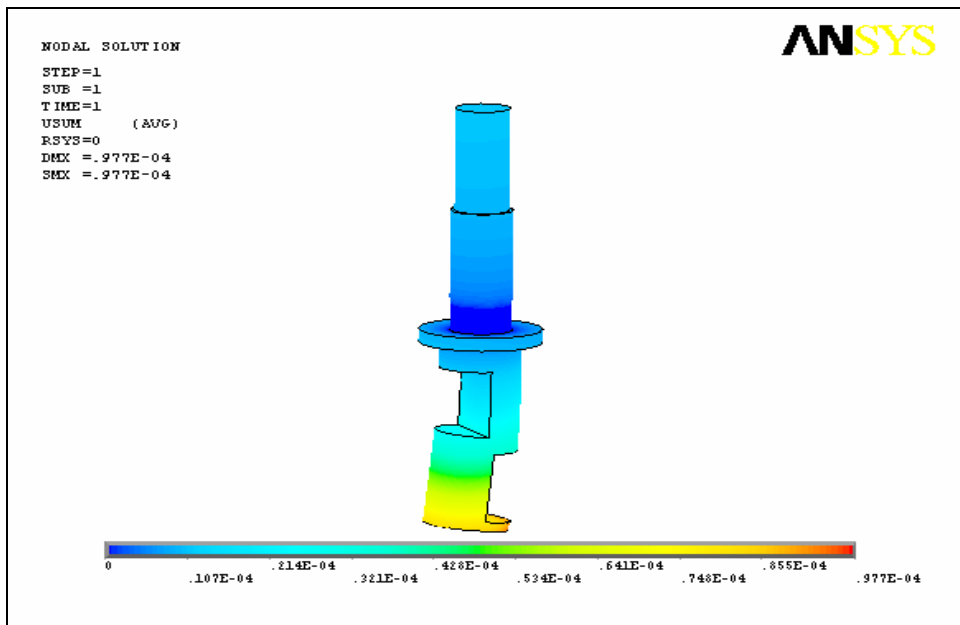
Figure 3-82   Deformation on the Turbine Inlet Valve

Stress Distribution on the Turbine Vane Apex Seal

The stress distribution and deformations on the turbine vane apex seal due to thermal loads is analyzed in ANSYS environment. A linear analysis with the following specifications is done.

Material:	H13 Hot Work Tool Steel
Element Type:	Solid 20 Node 95 (Structure)
	Solid 20 Node 90 (Thermal)
Mesh:	Structured (Hex Sweep)
B.C's:	Fixed X_Axis on vane apex seal tip surface
	Fixed Y_Axis on vane apex seal top surface
	Fixed Z_Axis on one vane apex seal side surface
Loads:	Approximate temperature load
Assumptions:	Average temperature is applied to the vane apex seal.

Structural analysis of the turbine vane apex seal is done to determine the stress distribution and the deformation on the vane apex seal. Average temperature (1000 K) is applied to the nodes as thermal load.

The results of the analysis showed that the stress values on the turbine vane apex seal are in elastic region and much below the yield tensile strength of the material and can be safely used. Also the deformations of the vane apex seal are later used to define the manufacturing tolerances between the vane and vane apex seal.

Figure 3-83   Structural Analysis Model of the Turbine Vane Apex Seal
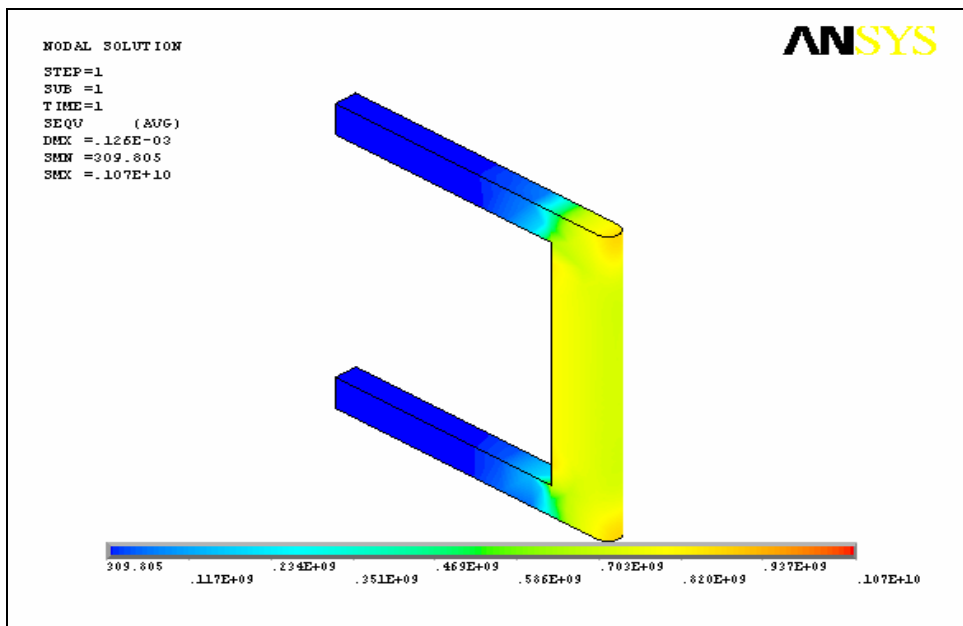
Figure 3-84   Stress Distribution on Turbine Vane Apex Seal

Max Stress: 1070 MPa	Yield Tensile Strength: 1650 MPa
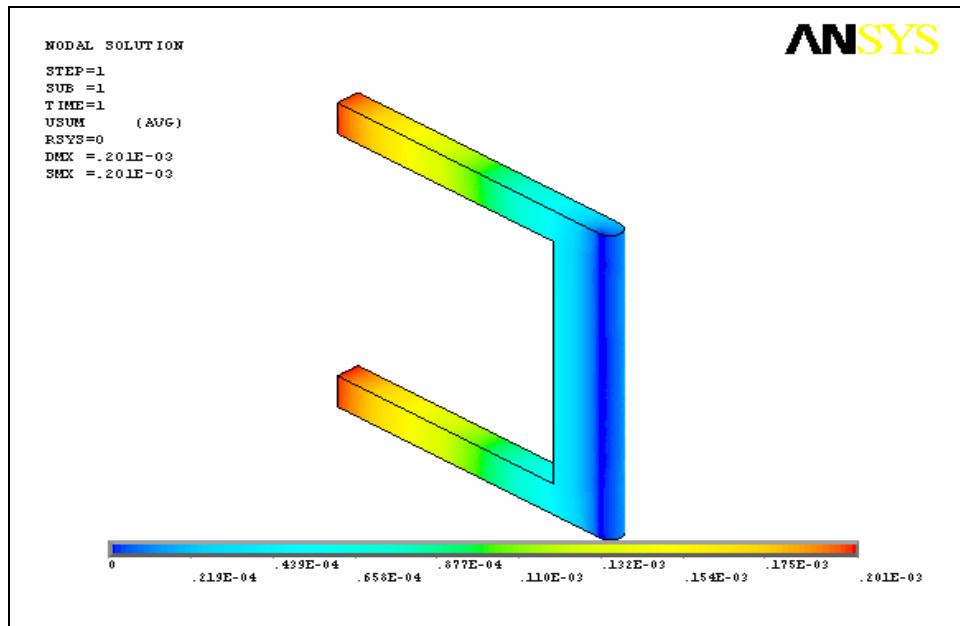
Figure 3-85   Deformation of Turbine Vane Apex Seal

Stress Distribution on the Turbine Rotor Top Seal

The stress distribution and deformations on the turbine rotor top seal due to thermal loads is analyzed in ANSYS environment. A linear analysis with the following specifications is done.

Material:	Gray Cast Iron
Element Type:	Solid 20 Node 95 (Structure)
	Solid 20 Node 90 (Thermal)
Mesh:	Structured (Hex Sweep)
B.C's:	Fixed X_Axis on rotor top seal tip surface
	Fixed Y_Axis on rotor top seal tip surface
	Fixed Z_Axis on one rotor top seal top surface
Loads:	Approximate temperature load
Assumptions:	Average temperature is applied to the rotor top seal.

Structural analysis of the turbine rotor top seal is done to determine the stress distribution and the deformation on the rotor top seal. Average temperature (1000 K) is applied to the nodes as thermal load.

The results of the analysis showed that the stress values on the turbine rotor top seal are in elastic region and below the yield tensile strength of the material and can be safely used. Also the deformations of the rotor top seal are later used to define the manufacturing tolerances between the rotor and rotor top seal.
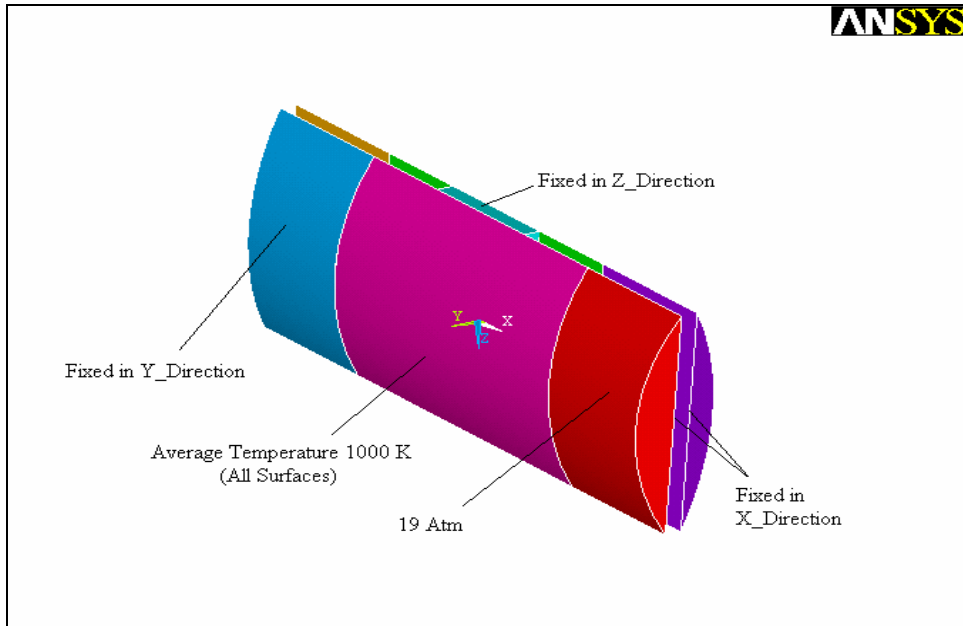
Figure 3-86   Structural Analysis Model of the Turbine Rotor Top Seal
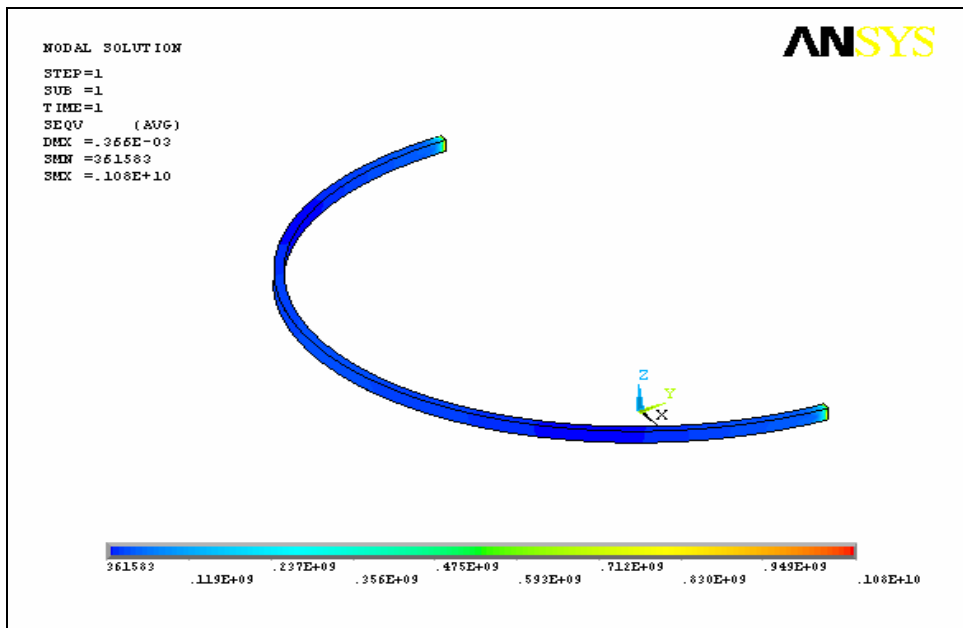
Figure 3-87   Stress Distribution on Turbine Rotor Top Seal

Max Stress: 1080 MPa   Yield Tensile Strength: 1650 MPa
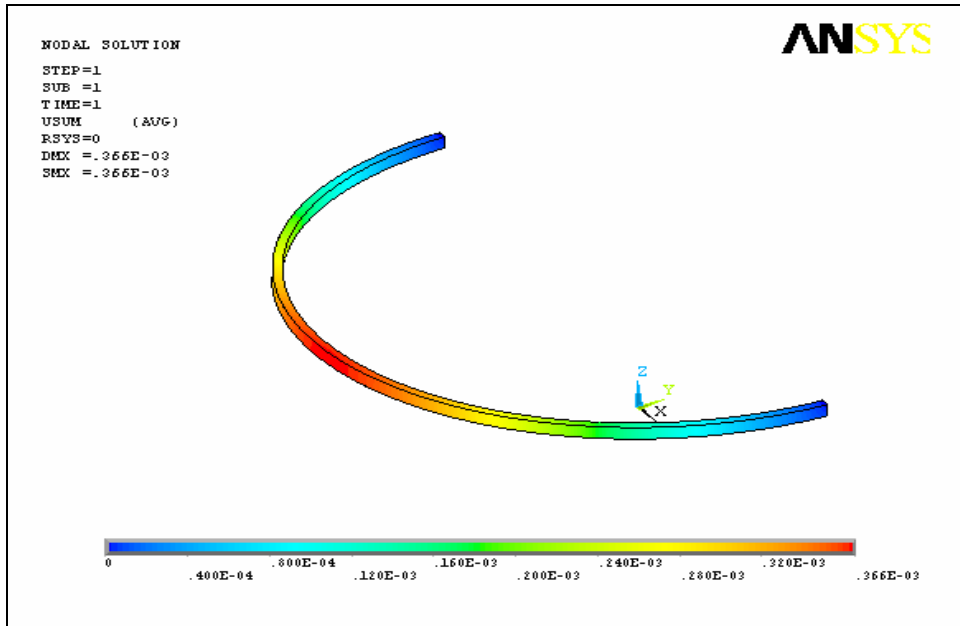
Figure 3-88   Deformation of Turbine Rotor Top Seal

Manufacturing Tolerance between Inlet Valve and Housing

Due to thermal and pressure loads on the inlet valve and housing surfaces, deformations on the materials occur. These deformations are examined to determine the manufacturing tolerances of both parts so that the inlet valve can revolve within its housing without stacking while still assuring good sealing capacity.

By examining the turbine inlet valve deformation, it is seen that the inlet valve deforms 0.1 mm max radially.

By examining the turbine housing, it is seen that the inlet valve housing deforms 0.085 mm max radially.

As a result, 0.185 mm gap tolerance between the inlet valve and the housing will assure inlet valve to revolve within the housing without stacking. This gap tolerance can be guaranteed by manufacturing the inlet valve 0.1 mm smaller in diameter and by opening the valve housing hole 0.085 mm larger in diameter.

Manufacturing Tolerance between Vane and Rotor

Due to thermal and pressure and inertia loads on the vane and rotor surfaces, deformations on the materials occur. These deformations are examined to determine the manufacturing tolerances of both parts so that the vane can move within the rotor without stacking while still assuring good sealing characteristics.

By examining the turbine vane deformation, it is seen that the vane deforms 1 mm max.

By examining the turbine rotor, it is seen that the vane channel deforms 0.2 mm max.

As a result, 1.2 mm gap tolerance between the vane and the rotor will assure turbine vane to revolve within the rotor without stacking. This gap tolerance can be guaranteed by manufacturing the turbine vane 1 mm smaller in thickness and by opening the vane channel 0.2 mm larger in thickness.

Manufacturing Tolerance between Vane Apex Seal and Vane

Due to thermal and pressure loads on the vane and vane apex seal surfaces, deformations on the materials occur. These deformations are examined to determine the manufacturing tolerances of both parts so that the vane apex seal can move within the vane without stacking, while still assuring good sealing characteristics.

By examining the turbine vane apex seal deformation, it is seen that the seal deforms 0.2 mm max in thickness.

By examining the turbine vane, it is seen that the apex seal channel deforms 0.8 mm max in thickness.

As a result, 1 mm gap tolerance between the vane apex seal and the vane will assure apex seal to move within the channel without stacking. This gap tolerance can be guaranteed by manufacturing the turbine vane apex seal 0.2 mm smaller in thickness and by opening the turbine vane seal channel 0.8 mm larger in thickness.

Manufacturing Tolerance between Rotor Top Seal and Rotor

Due to thermal and pressure loads on the rotor and rotor top seal surfaces, deformations on the materials occur. These deformations are examined to determine the manufacturing tolerances of both parts so that the rotor top seal can move within the rotor seal channel without stacking, while still assuring good sealing characteristics.

By examining the turbine rotor top seal deformation, it is seen that the seal deforms 0.35 mm max in diameter.

By examining the turbine rotor, it is seen that the rotor top seal channel deforms 0.1 mm max in thickness.

As a result, 0.135 mm gap tolerance between the rotor top seal and the rotor seal channel will assure top seal to move within the channel without stacking. This gap tolerance can be guaranteed by manufacturing the turbine rotor top seal 0.35 mm smaller in thickness and by opening the turbine rotor top seal channel 0.1 mm larger in diameter.

Turbine Material [24]

With respect to the structural analysis results, H13 Hot Work Tool Steel is selected as the material of the rotary turbine prototype that will be manufactured. The selection criteria of the material are given below;

- Excellent wear resistance and hot toughness.

- High thermal shock resistance.

- Good thermal conductivity and tolerate some water cooling in service.

- High temperature tensile strength.

- Good machinability.

Regarding these properties of the material, it is one of the best alternatives that can be used for the manufacturing of the rotary turbine prototype. Beside these properties, the structural analysis of the turbine parts is done using this material and the analysis results showed that the selected material is suitable for the prototype. (Properties of H13 Hot Work Tool Steel is given in Appendix D)

Turbine Vane Apex Seal Material

Two alternatives for the turbine vane apex seal have been considered.

First alternative for the rotary turbine vane apex seal is H13 hot work tool steel because of its good mechanical and thermal properties.

However, as the material of the turbine housing is also H13, there would be great wear deformation on both surfaces of the housing and seal due to friction. By arranging the hardness of both parts (housing being harder) could decrease the wear but still it would be over the desired limits of deformation.

The second alternative for the rotary turbine vane apex seal is a tool steel called _Carpenter Pyrowear Alloy 53 Tool Steel_. As the temperatures in the rotary turbine are very high, this material with its good temper resistance, high core impact strength and fracture toughness together with its excellent temperature resistance would be a good choice. (Properties of Carpenter Pyrowear is given in Appendix D)

Turbine Rotor Top Seals

The best alternative for the rotary turbine rotor top seal is the *gray cast iron* which is also used in the piston engines' piston head seals. Also seal is plated with chromium to give excellent wear and scuff resistance under very marginal lubrication conditions. Because of its good wear properties, the deformation on the tap inner surfaces where the rotor top seals are in contact with, will be minimum while good sealing will be achieved. (Properties of Gray Cast Iron is given in Appendix D)

Turbine Vane Apex and Rotor Top Seal Springs

Two alternatives for the springs have been considered.

The first alternative for the rotary turbine springs is a cobalt based super-alloy called *Elgiloy Co-Cr-Ni Alloy*. It has high strength, ductility, fatigue life and good mechanical properties. This material is also used in other rotary engine applications in the market as seal springs. (Properties of Elgiloy is given in Appendix D)

The second alternative for the rotary turbine springs is a nickel based super-alloy called *Inconel 718*. It has high strength, ductility, fatigue life and good mechanical properties. Its excellent relaxation resistance is useful for high-temperature springs and bolts. The alloy has good resistance to corrosion and oxidation along with high tensile and creep-rupture properties at temperatures to about 1300°F (700°C). (Properties of Inconel 718 is given in Appendix D)

3.3 Combustion Chamber Design

Combustion takes place in the external combustion chamber of the novel rotary engine which is designed using the geometric data calculated with the thermodynamic design code explained in chapter 2. By design the rotary compressor inlet volume is calculated as 299 cc. As the compression ratio is determined to be 10, the required combustion chamber volume, calculated by the code is 59 cc.

Combustion takes place with respect to the following ideal combustion equation;

Stoichiometric iso-octane air mixture:

$$C_8H_{18} + 12.5 \times (O_2 + 3.773N_2) \rightarrow 8CO_2 + 9H_2O + 47.16N_2 \qquad (3.9)$$
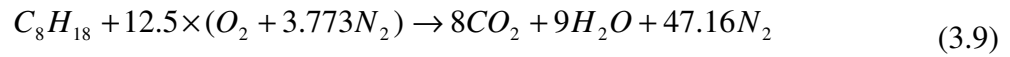
Table 3.3   Combustion Chamber Parameters

m_{fuel}	(8 x 12) + (18 x 1) = 114kg/kmol
m_{air}	12.5 x (32 + 3.773 x 28.16) = 1727.8 kg/kJ
$(A / F)_s$	15.14
$(F / A)_s$	0.0661
$(F / A)_{actual}$	0.01572

$$\phi = \frac{(F / A)_{actual}}{(F / A)_s} = \frac{0.01572}{0.0661} = 0.237 \qquad (3.10)$$

$$\lambda = \phi^{-1} = 4.20 \qquad (3.11)$$

where ϕ is fuel/air equivalence ratio and λ is the relative air/fuel ratio.

For $\lambda \, \phi \, 1, \phi \, \pi \, 1$ mixture is fuel-lean mixture.

3.3.1 Combustion Chamber Parts

- Combustion chamber is composed of upper and lower parts bolted together with 4 (Metric 8) bolts.
- A spark is placed on top of lower part to ignite the fuel air mixture.
- An injector is placed on the top of the upper part to inject fuel on the compressed air.
- A swirl motion step is placed at the inlet of the chamber to achieve good mixing of fuel and air.
- Two seal channels are placed at both sides of the chamber to avoid leakage from the contact surfaces of the parts.
- Four cooling passages are drilled on both parts in which cooling water is circulated.
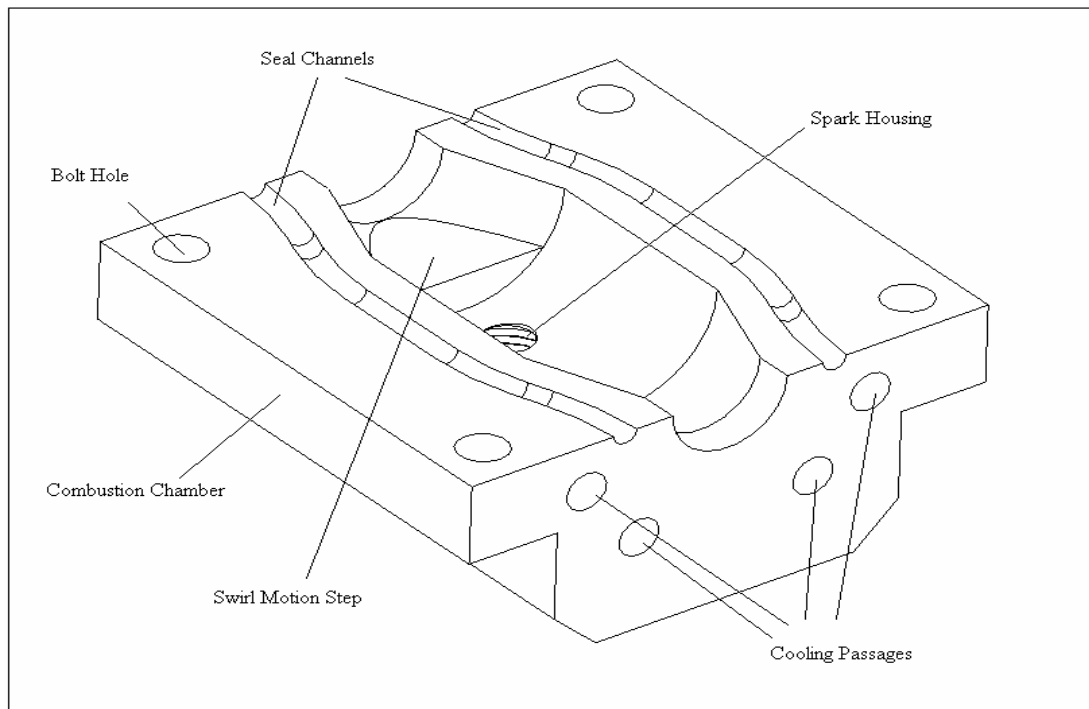
Figure 3-89   3-D Wire-Frame Drawing of Combustion Chamber
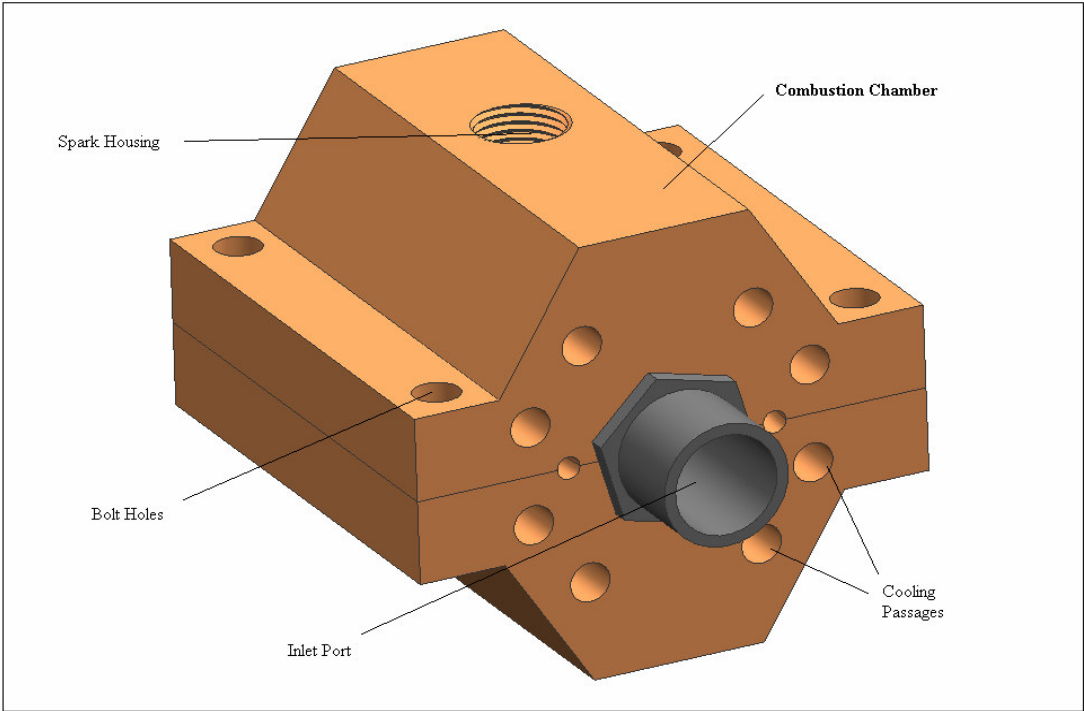
Figure 3-90   3-D CAD Model of the Combustion Chamber
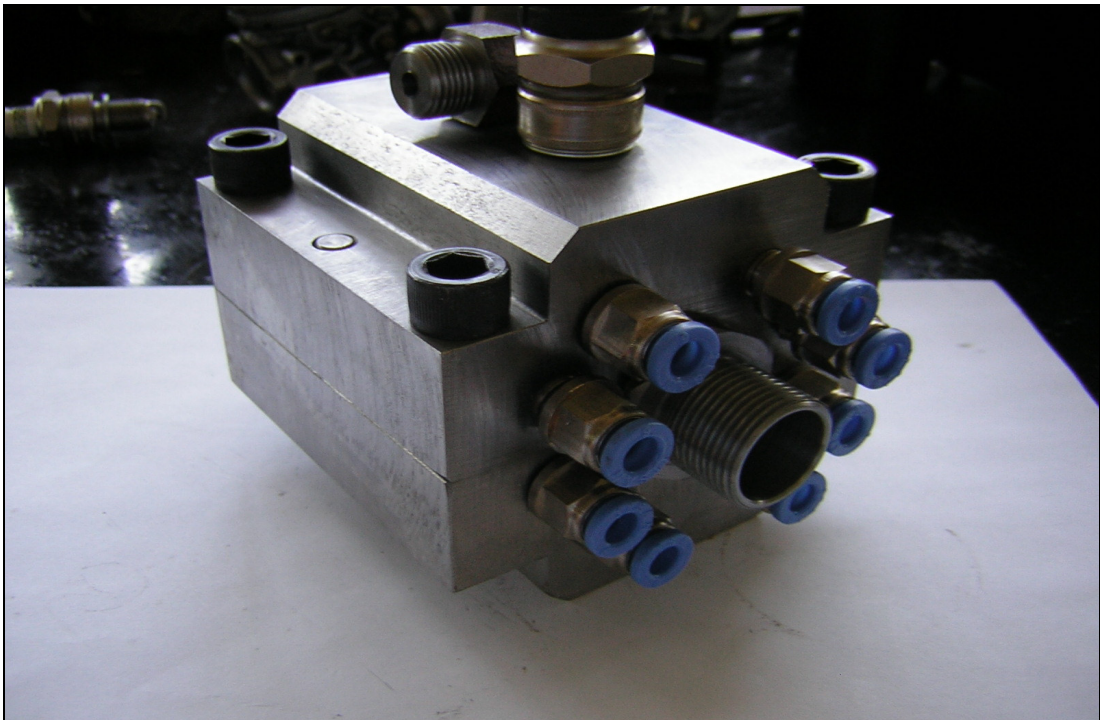
Figure 3-91   Photograph of the Combustion Chamber

3.3.2 Structural Analysis and Material Selection

Structural analysis of the combustion of the novel engine is done in ANSYS 9.0 Environment (Finite Element Program). The aim of this work is to select the material of the chamber and to determine the required cooling. To do the structural analysis, firstly the critical parts are defined as follows;

For material selection;
- Stress distribution on the chamber due to pressure and temperature exerted by the combustion gases onto the inner surfaces.

For determining the required cooling;
- Stress distribution on the chamber due to pressure and temperature exerted by the combustion gases onto the inner surfaces while cooling the chamber with cooling water injected from the cooling passages.

To make the structural analysis of the combustion chamber, the necessary temperature and pressure data is taken from the thermodynamic design code. Maximum combustion temperature and pressure is applied to the inner surfaces of the chamber for safety considerations.

P_{max} = 19 atm
T_{max} = 1500 K

Stress Distribution on the Combustion Chamber

The stress distribution and deformations on the combustion chamber due to thermal and pressure is analyzed in ANSYS environment. A linear analysis with the following specifications is done.

Material:	H13 Hot Work Tool Steel
Element Type:	Solid 20 Node 95 (Structure)
	Solid 20 Node 90 (Thermal)
Mesh:	Structured (Hex Sweep)
B.C's:	Fixed all DOF on inlet and outlet surfaces
Loads:	Convection on divided surfaces
	Max. Pressure load on divided surfaces
Assumptions:	Convection Heat Transfer Coefficient for combustion gases is approximated as 50 W/m^2 .K
	Convection Heat Transfer Coefficient for cooling air is approximated as 100 W/m^2 .K
	Convection Heat Transfer Coefficient for cooling water is approximated as 150 W/m^2 .K

Firstly, a thermal analysis of the combustion chamber is done to determine the temperatures on each node due to convection between the combustion gases and the inner surfaces and between the cooling air and water and the outer surfaces of the chamber.

Secondly, a structural analysis of the combustion chamber is done to determine the stress distribution and the deformation on the chamber. The temperatures calculated in the thermal analysis are applied to the nodes as thermal load and the max combustion gases pressure is applied to the inner surfaces of the chamber as pressure load.

The results of the analysis showed that the stress values on the combustion chamber are in the elastic region and are below the yield tensile strength of the material and can be safely used with adequate cooling.
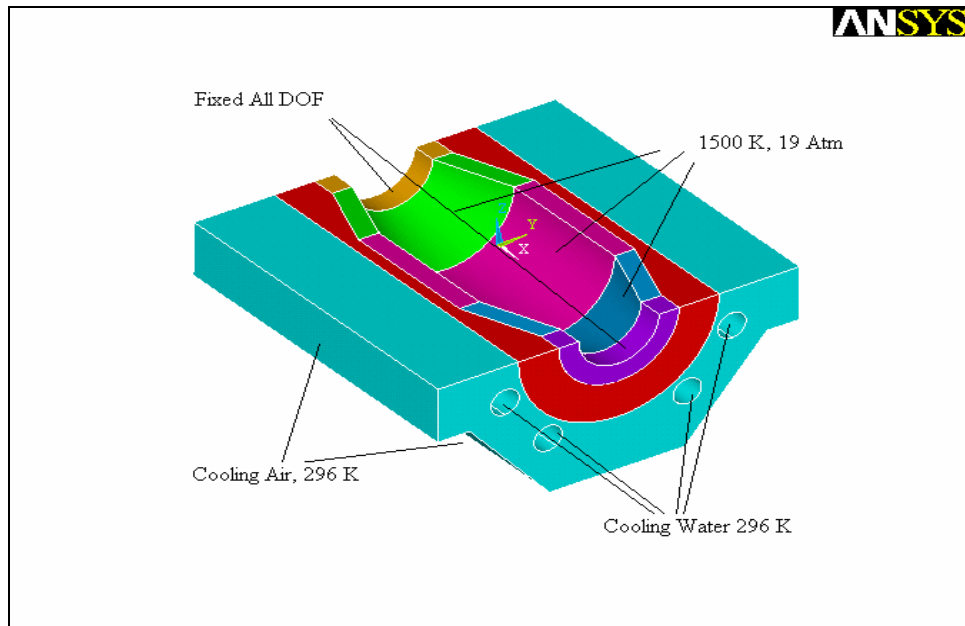
Figure 3-92 Structural Analysis Model of the Combustion Chamber
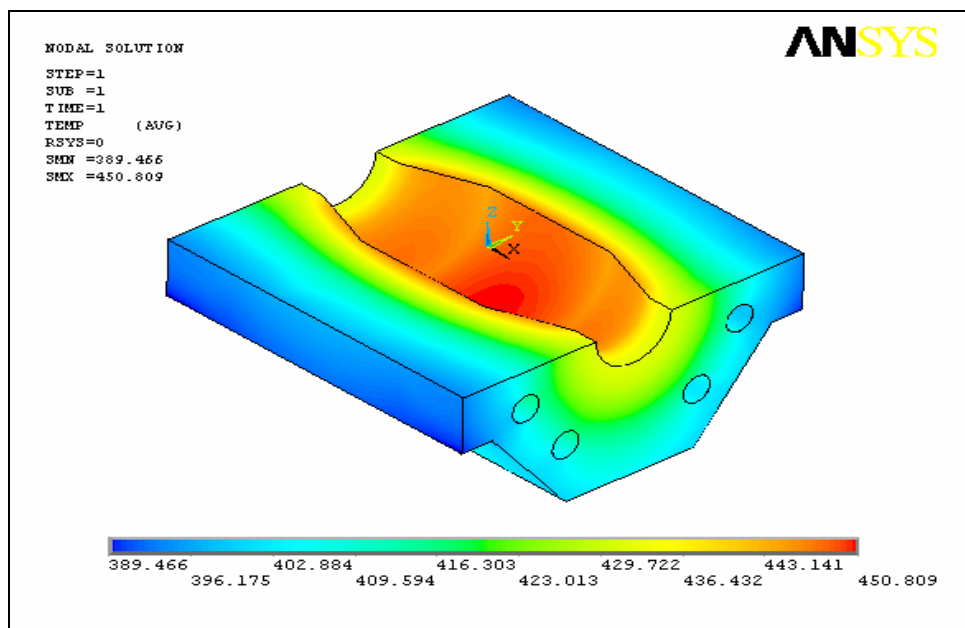
Figure 3-93 Temperature Distribution on the Combustion Chamber

Max Temperature on the chamber: 451° K

143
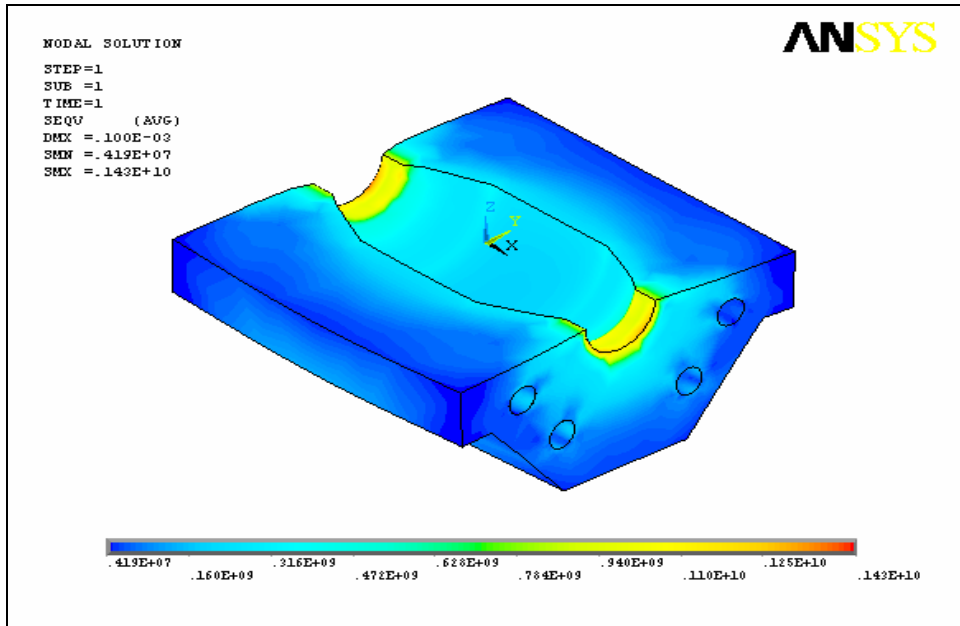
Figure 3-94 Stress Distribution on the Combustion Chamber

| Max Stress: 1430 MPa | Yield Tensile Strength: 1650 MPa |

Combustion Chamber Material

With respect to the structural analysis results, H13 Hot Work Tool Steel is selected as the material of the combustion chamber prototype that will be manufactured. The selection criteria of the material are given below;

- High thermal shock resistance.
- Good thermal conductivity and tolerate some water cooling in service.
- High temperature tensile strength.
- Good machinability.

Regarding these properties of the material, it is one of the best alternatives that can be used for the manufacturing of the combustion chamber prototype. Beside these properties, the structural analysis of the combustion chamber is done using this material and the analysis results showed that the selected material is suitable for the prototype. (Properties of H13 Hot Work Tool Steel is given in appendix D)

3.4 Rotary Engine Timing Design

3.4.1 Valve Timing Design

Timing Constants:

Timing constants are chosen at the design stage of the compressor and turbine. These angular constants don't change with engine operating parameters such as combustion process. There are four timing constants in rotary vane engine which are for compressor, turbine, external burner, combustion in turbine.

In Compressor: (Fig. 3-95)

Inlet Angle:

$$\theta_{ci} = 30^{\circ}$$

Compression Angle:

$$\theta_{ce} = 330^{\circ}$$
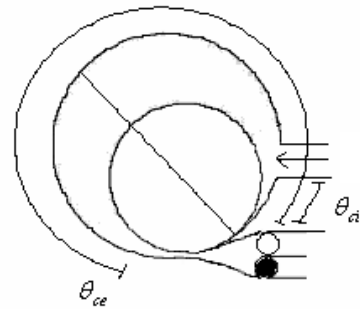
Figure 3-95

In Turbine: (Fig 3-96)

Inlet Angle:

$$\theta_{ti} = 30^{\circ}$$

Exhaust Angle:

$$\theta_{e} = 270^{\circ}$$
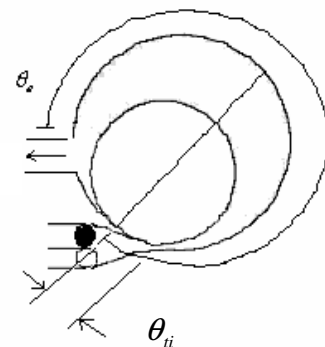
Figure 3-96

146

In Combustion Chamber: (Fig. 3-97)

External Burning Angle:

$$\theta_{eb} = 30°$$

Combustion Angle in Turbine:

$$\theta_{ib} = 12°$$

θ_{eb}
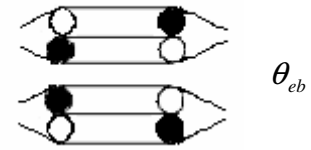
Figure 3-97

Valve and Vane Angles: (Fig. 3-98)

Valve and vane angles depend on timing constants and they can change the timing of the engine.

Maximum Compressor Valve Open Angle:

$$\theta_{vc} = 180° - \theta_{eb} = 150° \qquad (3.12)$$

θ_{vc}

Figure 3-98

Turbine Vane Angular Position:

$$\theta_{vti} = \theta_{eb} = 30° \qquad (3.13)$$

Phase Angle between Turbine and Compressor Vanes:

$$\theta_{phase} = \theta_{eb} = 30° \qquad (3.14)$$
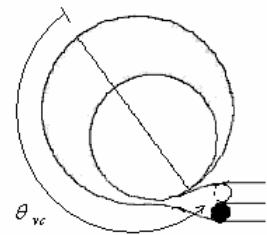
Angular Displacement of Turbine Vane through Out the Exhaust Process:

(Fig 3-99)

$$\theta_{vte} = \theta_e - \theta_{vti} = 240^{\circ} \qquad (3.15)$$
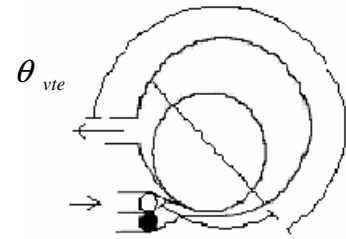
Process Period Angle:

$$\theta_{processperiod} = \theta_{ce} + \theta_e - \theta_{ci} = 600^{\circ} \qquad (3.16)$$
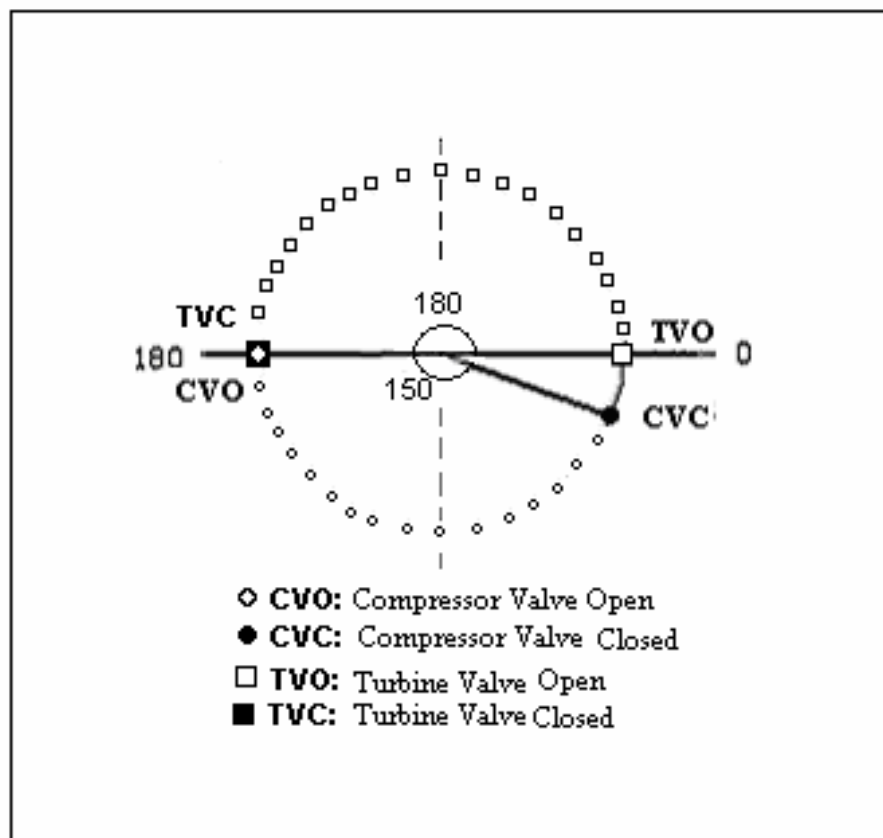
<u>*Valve Angles:*</u>

Figure 3-100   Valve Angles

TIMING IN ROTARY VANE ENGINE

Figure 3-101   Valve Timing
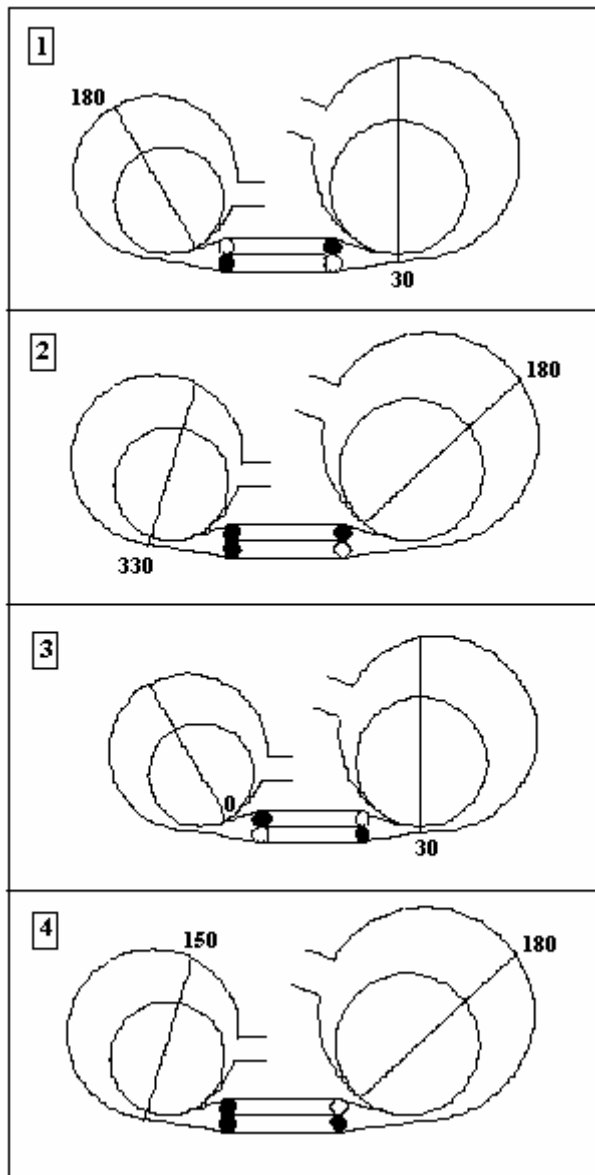
1) When compressor vane angle is 180 degrees compressor valve opens and air is compressed to the first external burner until the vane angle becomes 330 degree.

2) After 150 degrees from the opening of the first compressor valve (compressor vane reaches 330 degrees), the valve closes.

3) Combustion in the first external burner begins after the compressor valve is closed and the turbine valve is opened after 30 degrees from the closing of the compressor valve.

4) After the opening of the turbine valve the combustion gases begin to expand in the turbine until the turbine vane reaches 270 degrees at which exhaust begins.

3.4.2 Injection Timing

Fuel injection can start just after the turbine valve closes and can last until the compressor valve closes (just before ignition). Between these two times, injection start time and injection finish time can be adjusted depending on the air / fuel ratio. This timing adjustment is done by a timing disk shown in figure 3-102 which is mounted concentrically on the compressor rotor.

The working principle of the direct fuel system is that the fuel pump continuously pumps fuel from the fuel tank to the injector. A 12 Volt signal is used to open and close the injector. When the electronic valve on the injector senses 12 volts, it opens the injector and when 12 volts is cut off the injector is closed. A conducting part which can be positioned freely on the timing disk is used to open and close the current between the 12 volt power supply and the injector. By changing the position and the length of the conducting part on the disk, air to fuel ratio and the injection start and stop times can be adjusted.
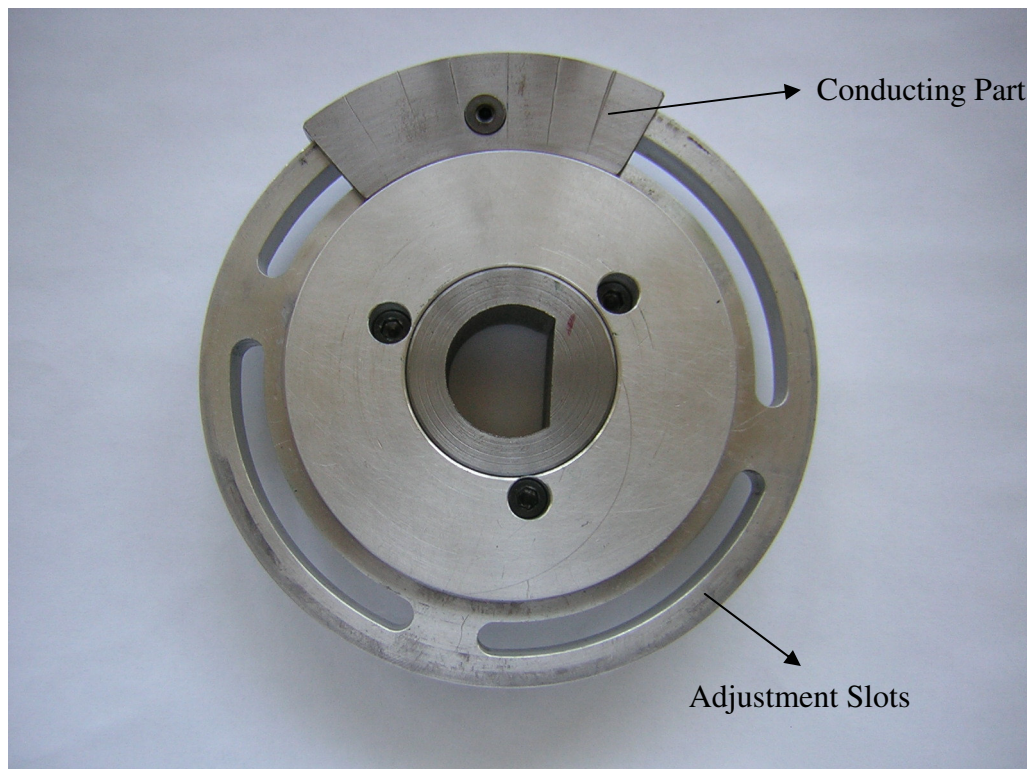
Figure 3-102   Timing Disk

3.4.3   Ignition Timing

As a switching device, a Hall Effect switch and its electronic unit is mounted on a timing disk (shown in figure 3-104) which is placed on the compressor rotor of the engine. The switch is activated by a magnetic field which is created with a ferrous material placed on the timing disk. In the absence of the magnetic field the switch is designed to be off. It will turn on and close the ignition system, producing the spark at the correct ignition time, when it is subjected to a magnetic field created by the ferrous material which is placed correctly on the timing disk. The Hall Effect switch system is given in figure 3-103.

Branded Face of Sensor
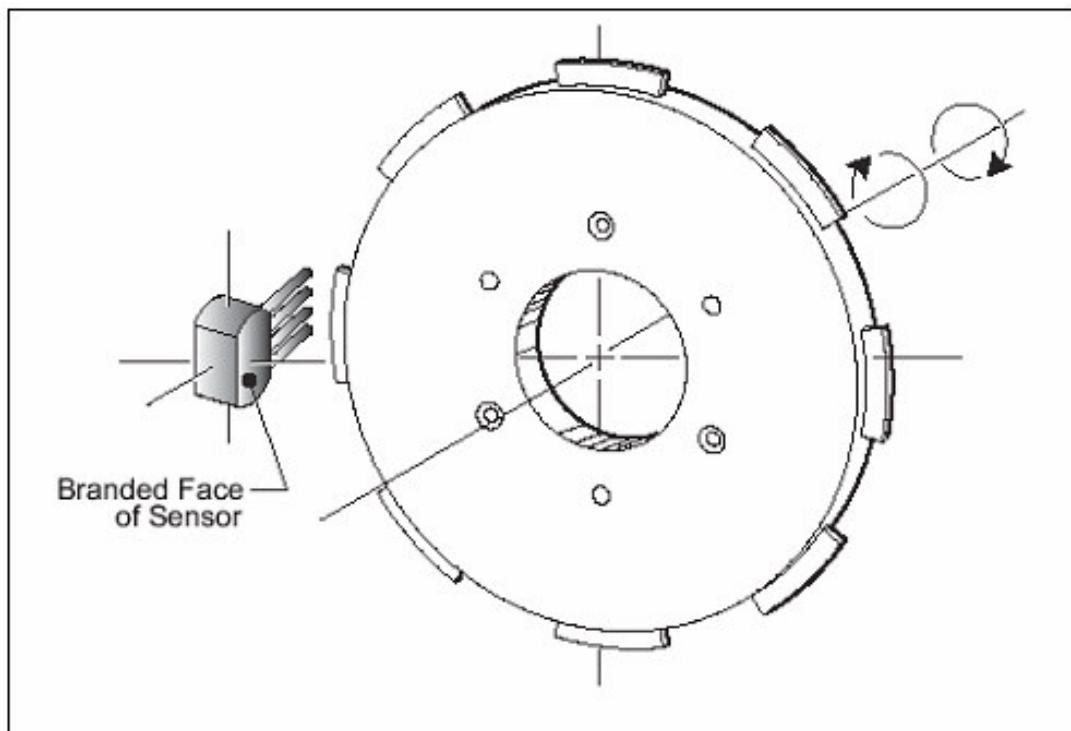
Figure 3-103   Hall Effect Switch System
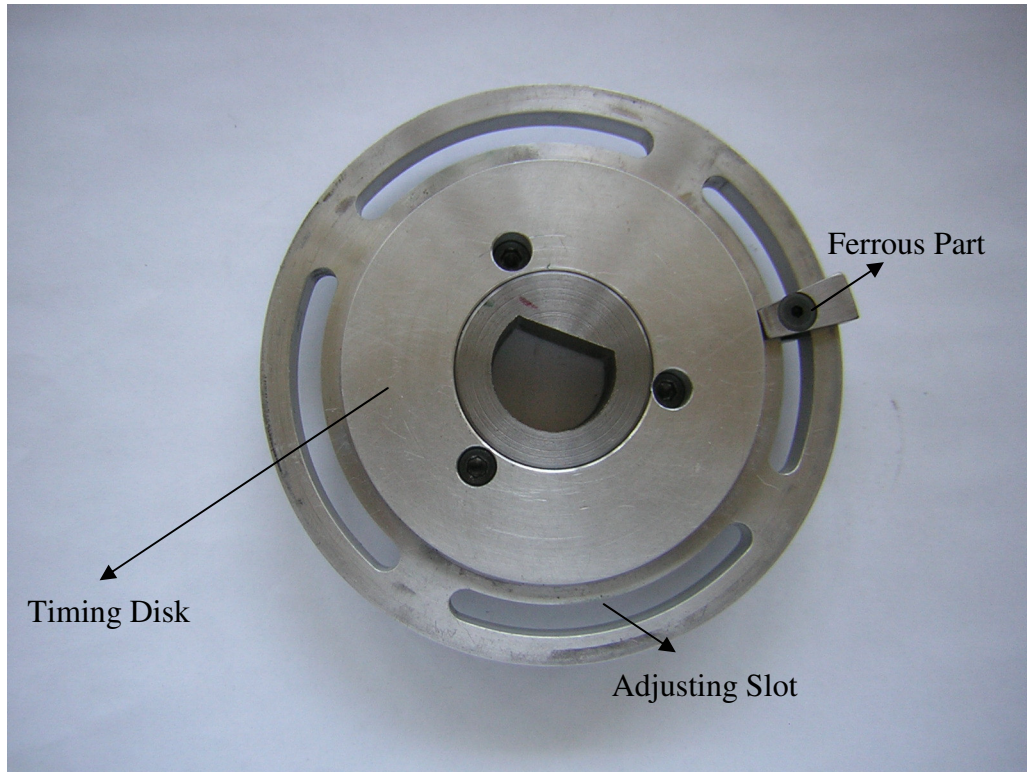
Figure 3-104   Timing Disk

The position of the ferrous part can be adjusted on the timing disk by the help of the adjustment slots so that the correct ignition timing can be achieved. By design, the correct ignition time is when the compressor valve closes.

3.4.4 Overall Engine Timing

The timing of the novel rotary engine is given below;

- *Air Intake:*

Atmospheric air is taken from the inlet port of the rotary compressor.
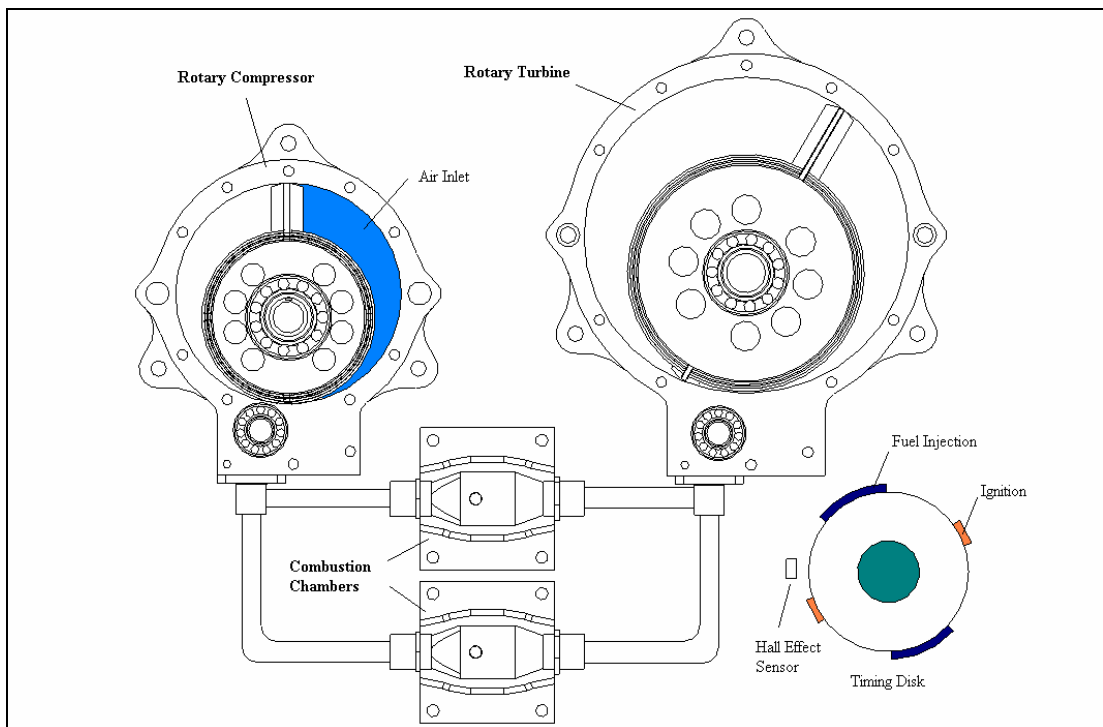
Figure 3-105   Air Intake of the Novel Rotary Engine

- *Max Air Taken:*

When rotary compressor vane reaches 270 degrees the vane passes the inlet port and the air taken in the compressor for the first stroke is trapped between the rotor, vane and the housing.
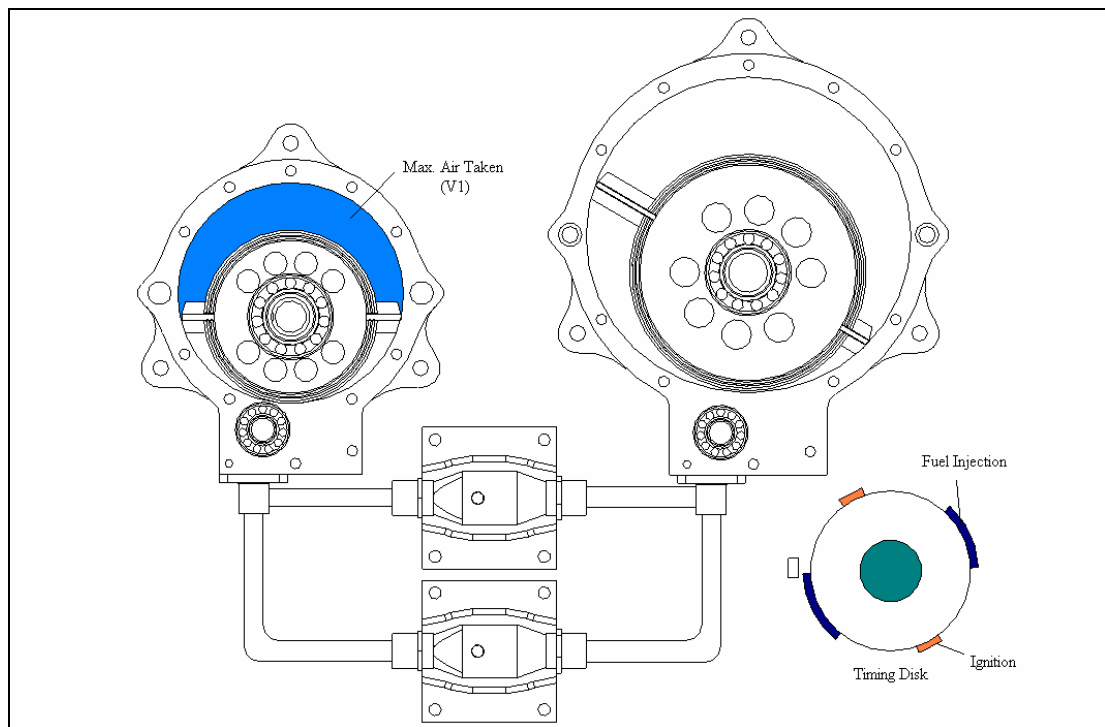
Figure 3-106   Max Air Taken of the Novel Rotary Engine

- *Air Discharge to First Combustion Chamber:*

     The trapped intake air is moved through and when rotary compressor vane reaches 360 degrees the discharge port of the first combustion chamber is opened and the compressed air (at 2.5 atm) is discharged to the first combustion chamber for further compression. Air is also being taken in for the second stroke.
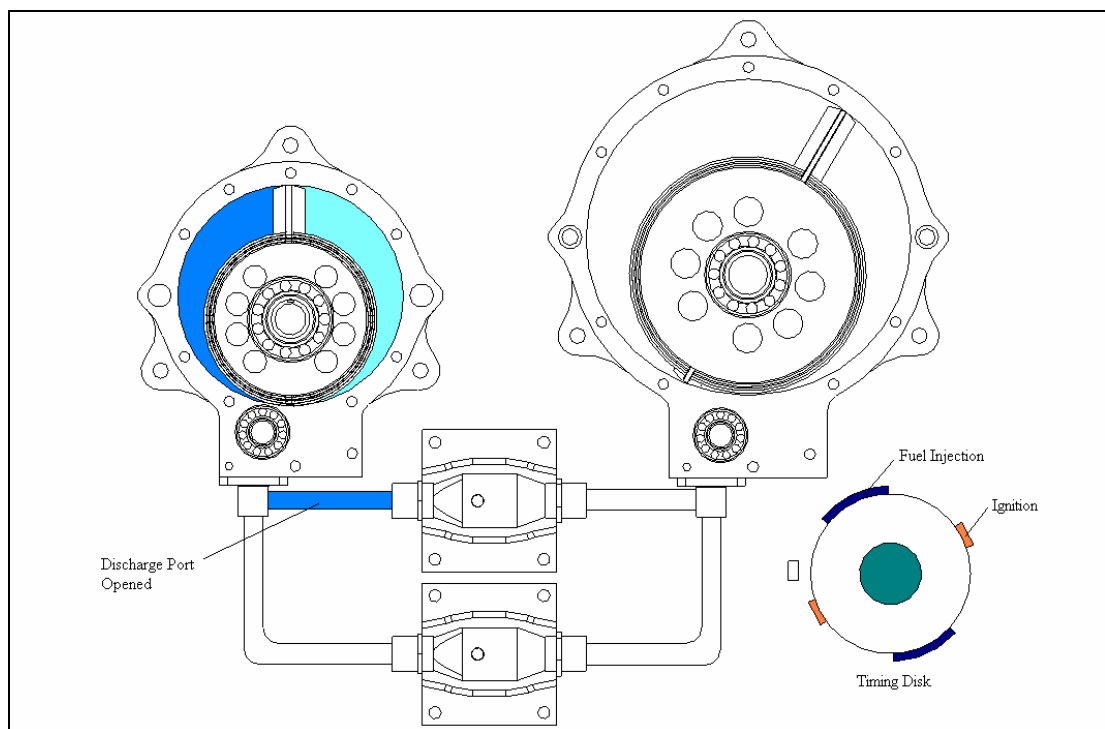
Figure 3-107   Air Discharge of the Novel Rotary Engine

- *Fuel Injection to First Combustion Chamber:*

       While the air is being discharged to the first combustion chamber, when the rotary compressor vane reaches 390 degrees, fuel injection to the first combustion chamber starts. The Hall Effect sensor mounted on the timing disk senses the fuel injection ferrous part and sends a signal to the injector to start injection. The changing the ferrous parts length, the fuel to air ratio can be adjusted.
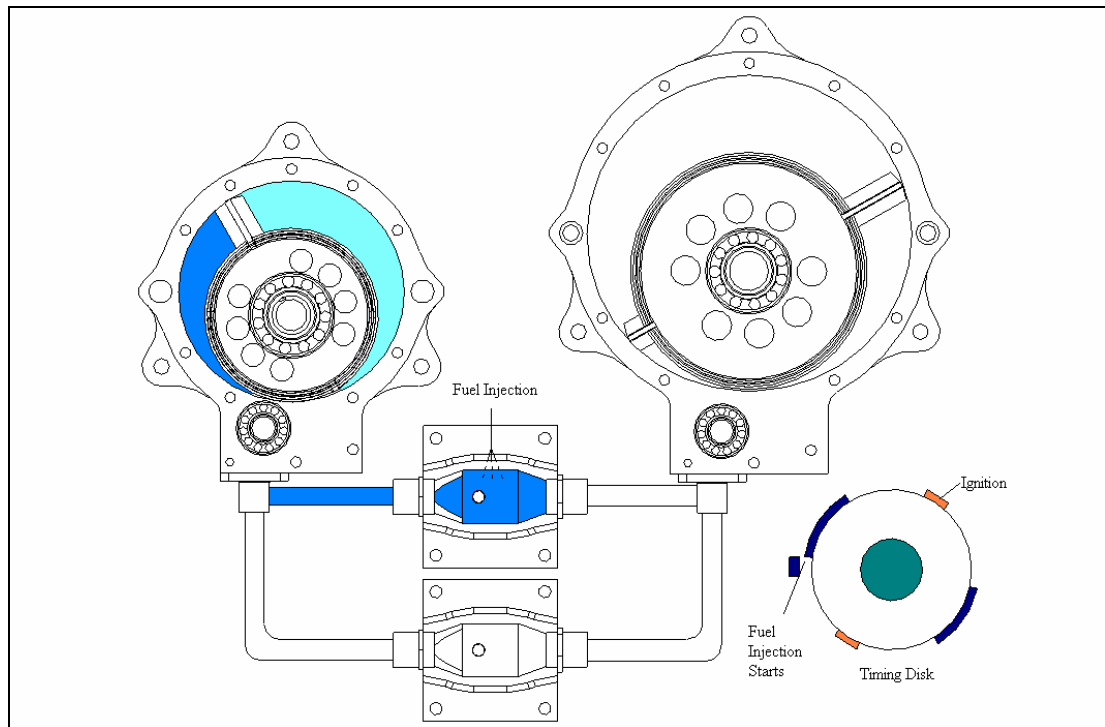
Figure 3-108   Fuel Injection to the First Combustion Chamber

- *Ignition in First Combustion Chamber:*

      When rotary compressor reaches 510 degrees, the discharge port of the first combustion chamber is closed. All the air taken in the first stroke is mixed with fuel and compressed in the first combustion chamber. (The volume of the combustion chamber determines the pressure of the compressed air) At that instance the Hall Effect sensor senses the ignition ferrous part and sends a signal to the first spark to create ignition.
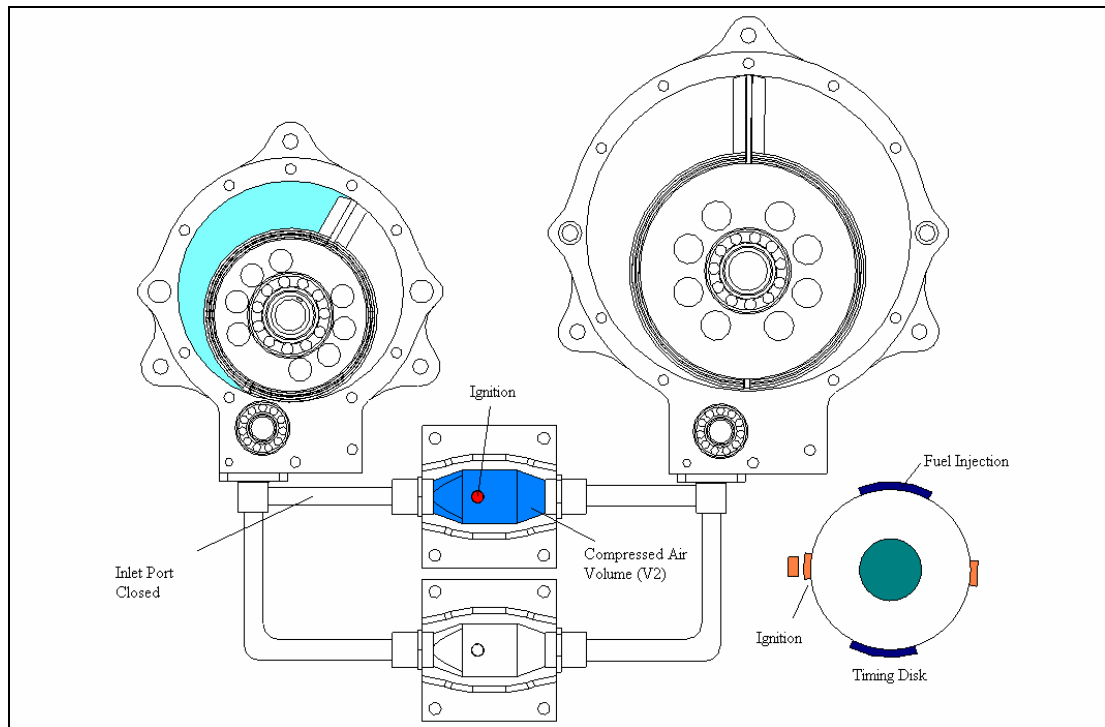
Figure 3-109   Ignition in the First Combustion Chamber

- *First Combustion Gas Discharge to Rotary Turbine:*

        Constant volume combustion takes place for 30 degrees of vane movement and when the vane reaches 540 degrees the first inlet port of the rotary turbine opens and the constant pressure combustion takes place. Also the second discharge port of the rotary compressor is opened and the air taken in the second stroke is being discharged to the second combustion chamber.
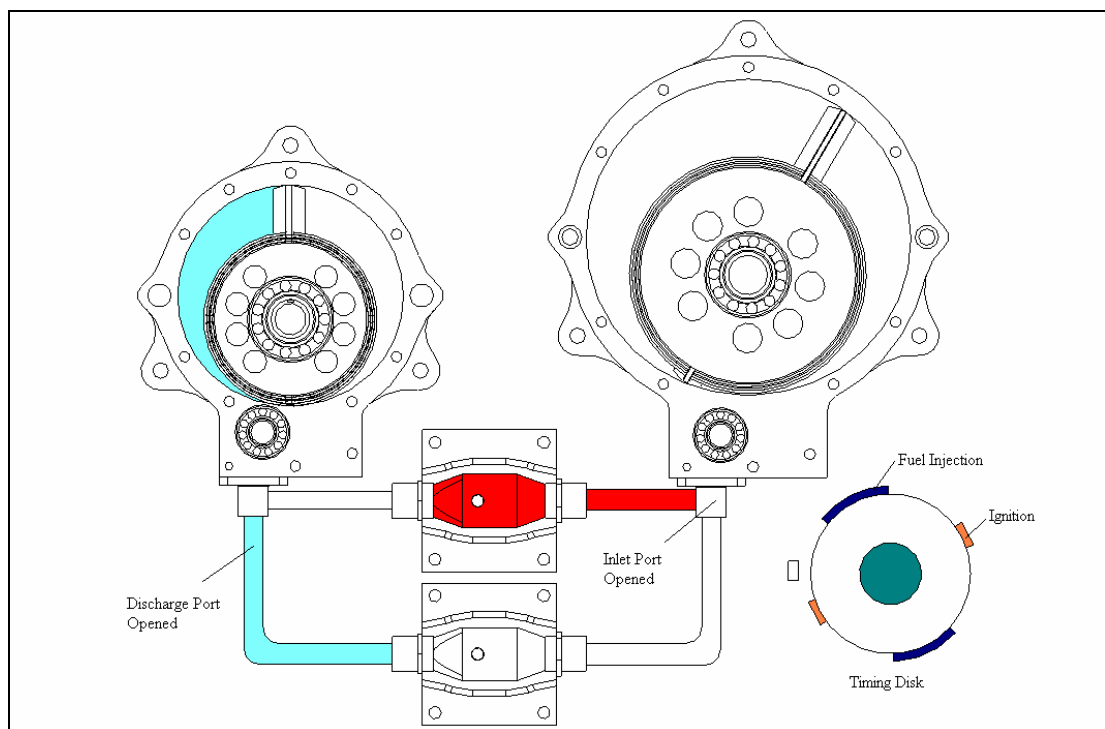
Figure 3-110   First Combustion Gas Discharge to the Rotary Turbine

- *Expansion in the Rotary Turbine:*

    After the constant pressure combustion is completed, the combustion gases start to expand in the rotary turbine. When rotary compressor vane reaches 570 degrees, fuel injection in the second combustion chamber begins.
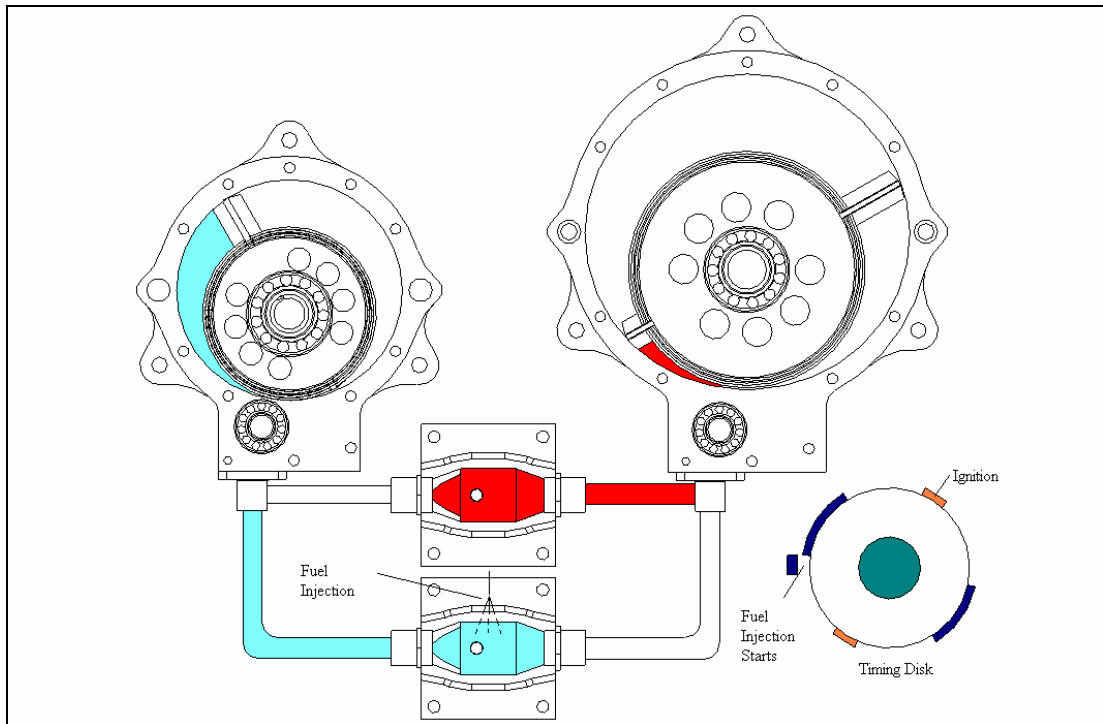
Figure 3-111   Expansion in the Rotary Turbine

- *Ignition in the Second Combustion Chamber:*

    While the first combustion gases expand in the rotary turbine, when the rotary compressor vane reaches 690 degrees the first inlet port of the rotary turbine closes and the first combustion gases passed the rotary turbine completely. At the same time, the second discharge port of the rotary compressor closes and all of the air taken in the second stroke is mixed with fuel and compressed in the second combustion chamber. At that instance the Hall Effect sensor senses the ignition ferrous part and sends a signal to the second spark to create ignition.
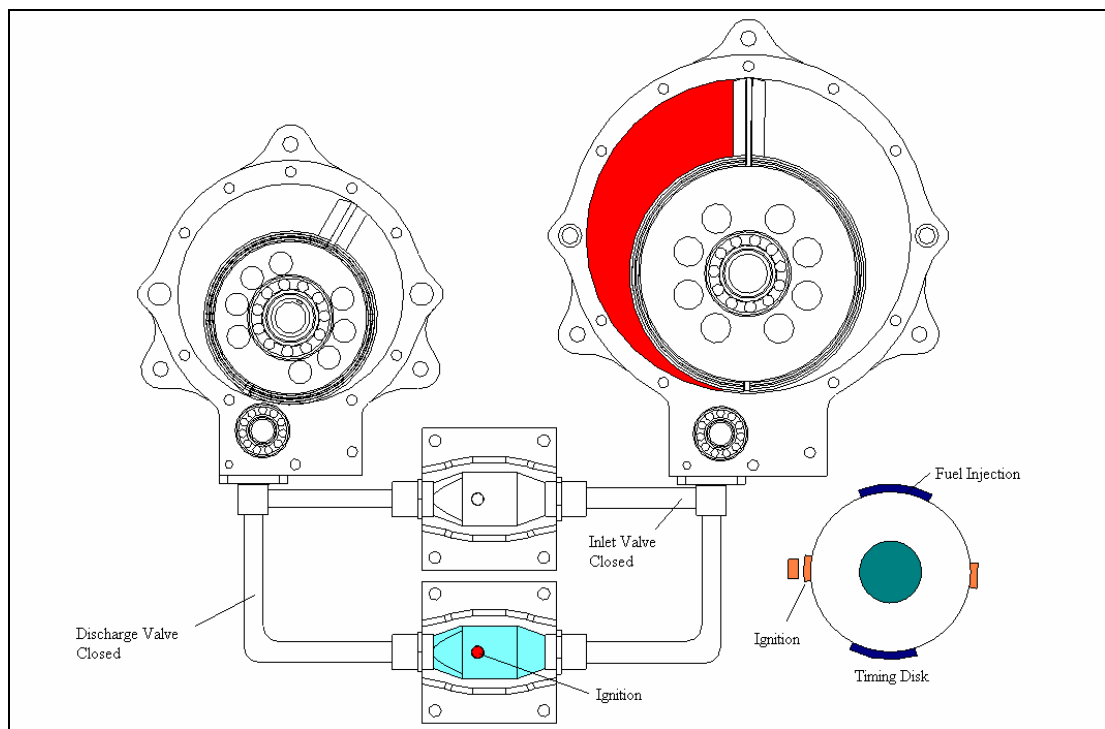
Figure 3-112   Ignition in the Second Combustion Chamber

- *Second Combustion Gas Discharge to the Rotary Turbine:*

    While first combustion gases expand in the rotary turbine, when the rotary compressor vane reaches 720 degrees, the constant volume combustion in the second combustion chamber end and the second inlet port of the rotary turbine opens and constant pressure combustion takes place.
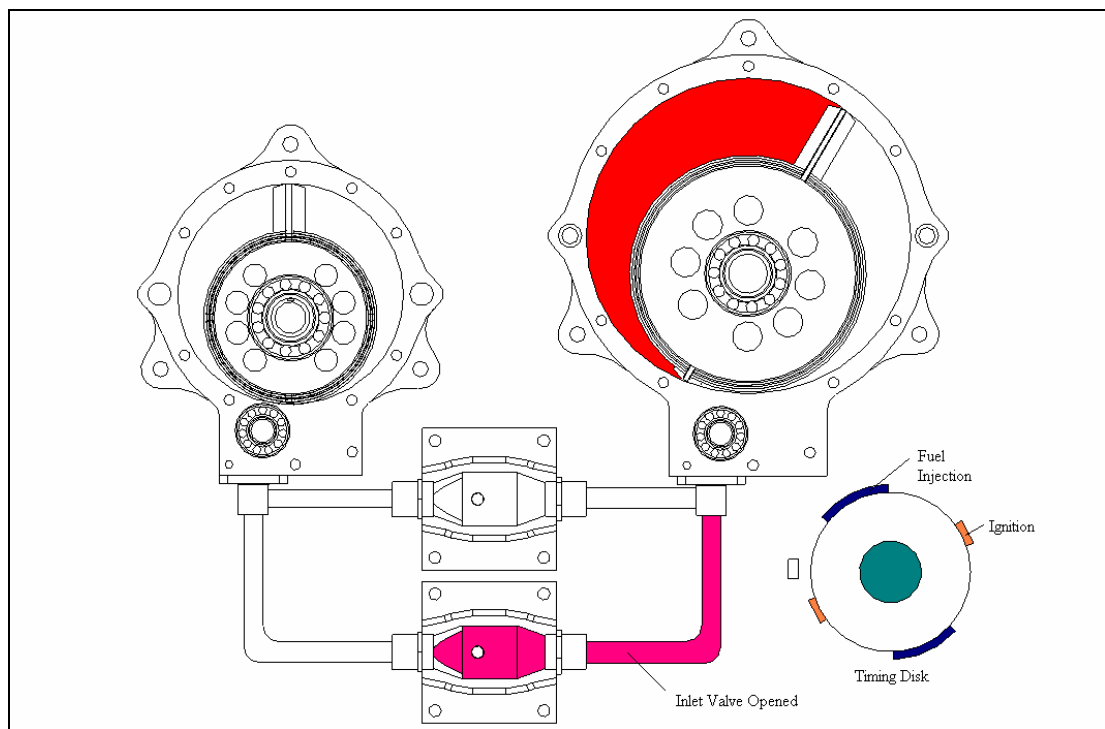
Figure 3-113   Second Combustion Gas Discharge to the Rotary Turbine

- *Exhaust of the First Combustion Gases:*

  While the second combustion gases expand in the rotary turbine, when the rotary compressor vane reaches 750 degrees, the rotary turbine vane reaches the exhaust port and the combustion gases start to be discharged out for the next 180 degrees.
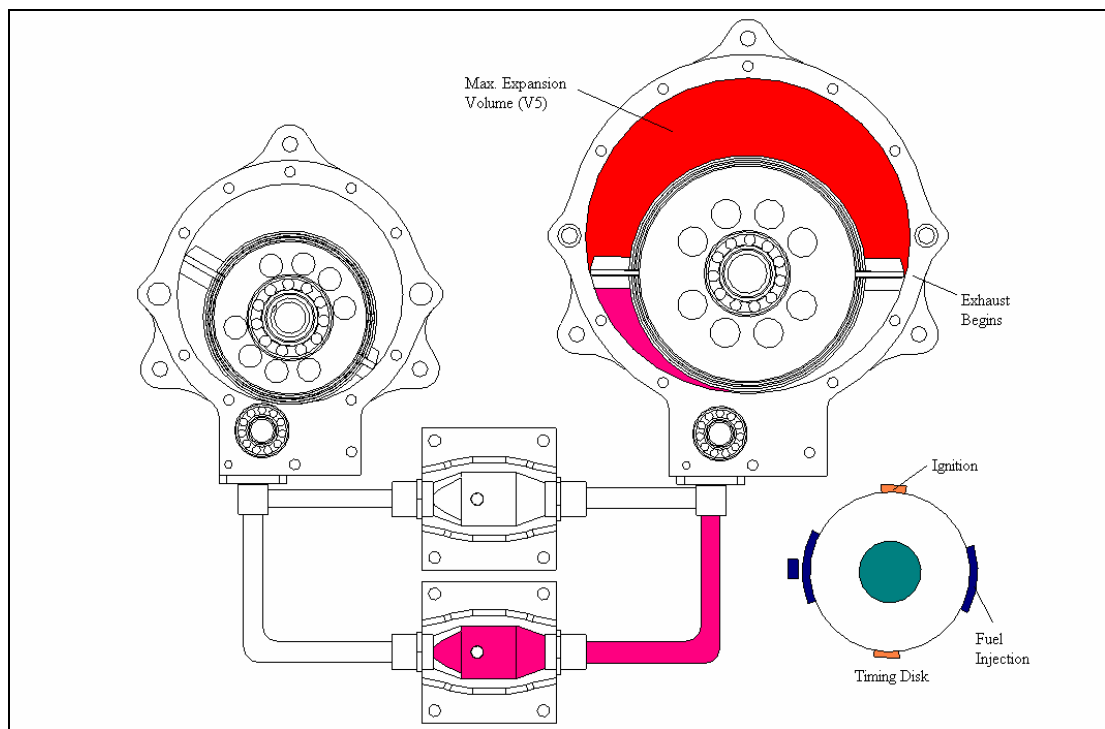
Figure 3-114   Exhaust of the First Combustion Gases

3.5 Auxiliary Systems Design

3.5.1 Fuel System [25]

Two alternative systems can be used for the fuel system in the novel rotary engine. One is the carburetion system where the fuel is mixed with air by a carburetor at the inlet of the compressor and the fuel / air mixture is compressed before ignition. (Figure 3-115)

The other one is the direct injection system, where the fuel is injected directly into the combustion chamber onto the compressed air by a fuel pump and injector. (Figure 3-117)

Carburetion System

The carburetor shown in figure 3.116 used is a standard diaphragm type. It has two fuel flow adjustment screws, one for high speed system and one for the low speed system. The carburetor is normally set for an idle speed of 2000 rpm and a maximum Wide Open Throttle (WOT) engine speed of 7500 +-100 rpm. The throttle valve is adjusted such that the designed fuel to air ratio is achieved.
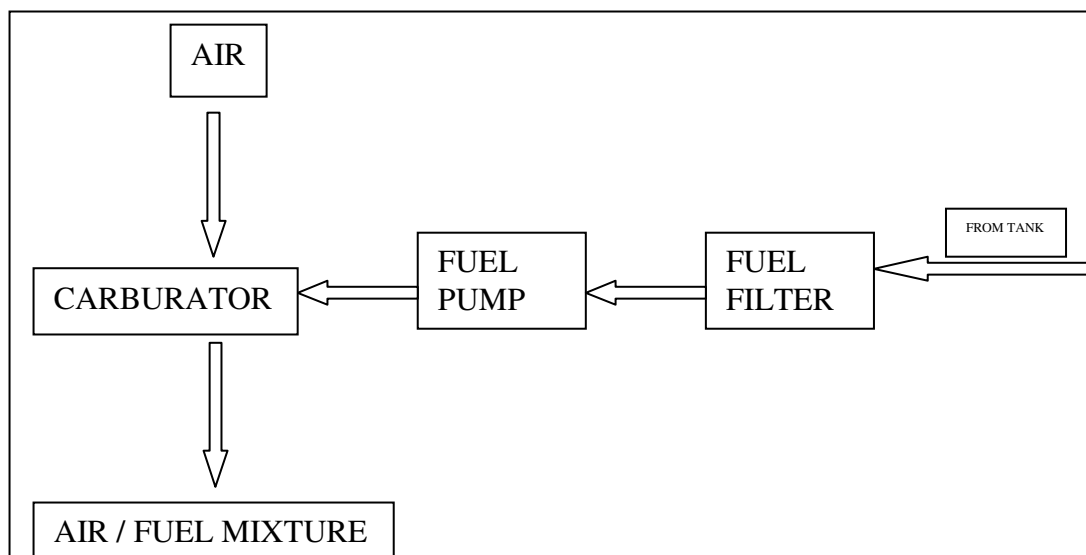
Figure 3-115   Carburetion System Schematic

163
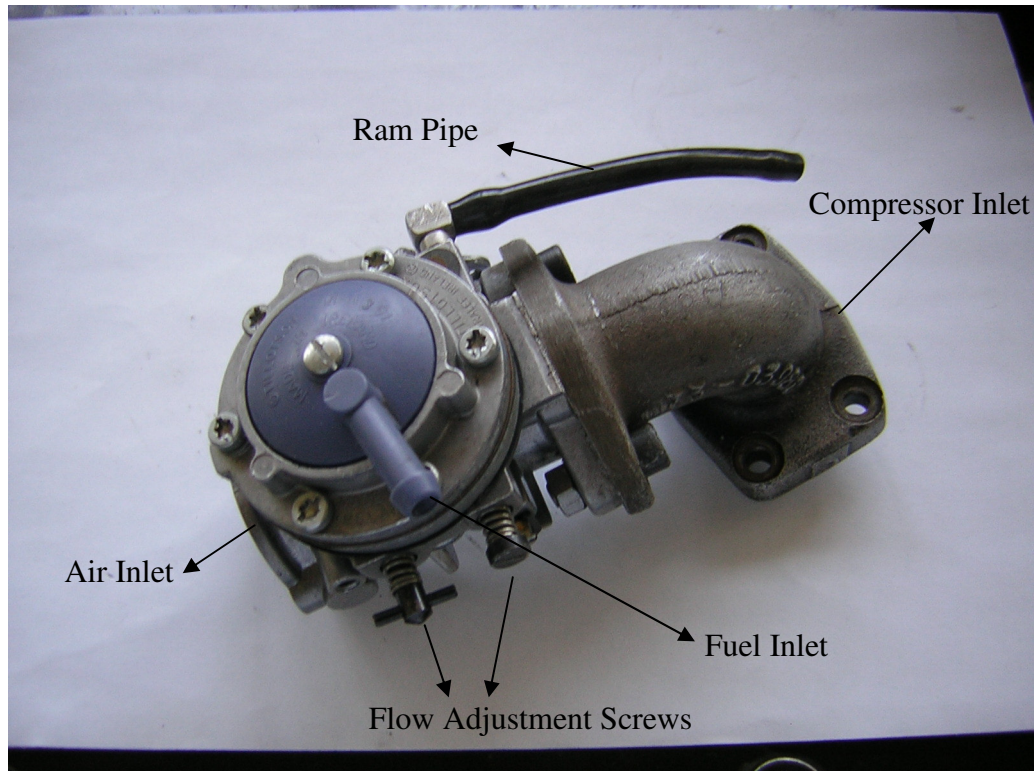
Figure 3-116   Carburetor

Direct Injection System

An injector pump shown in figure 3.118 and a multi-hole injector shown in figure 3.119 are used to spray the fuel directly into the combustion chamber onto the compressed air. The momentum and the energy of the injected fuel jets are sufficient to achieve adequate fuel distribution and rates of mixing with the air. Additional air motion is not required. The fuel is injected into the combustion chamber just after the turbine valve closes which will help to cool the chamber while vaporizing the fuel. Fuel injection can be completed in minimum 30 degrees to maximum 150 degrees which can guarantee a proper mixing before ignition. A fuel pump with a maximum pumping pressure of 10 atm is used to pump the fuel to the injector where the fuel is sprayed onto a compressed air with a pressure of min 2.5 atm to maximum10 atm.
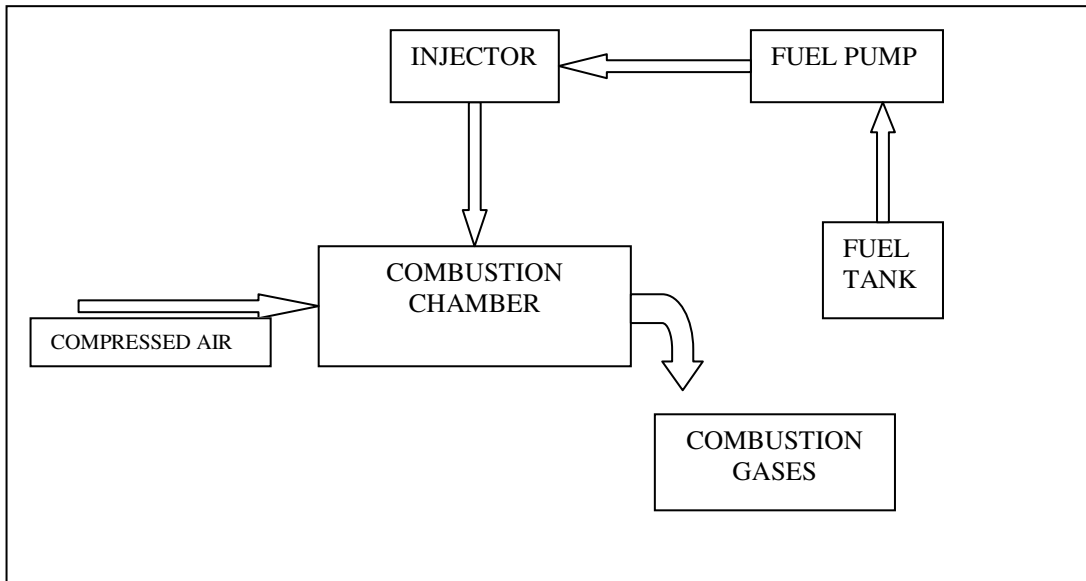
Figure 3-117   Direct Injection System Schematic

Fuel Injector

Selonoidal Valve

Injection Nozzle
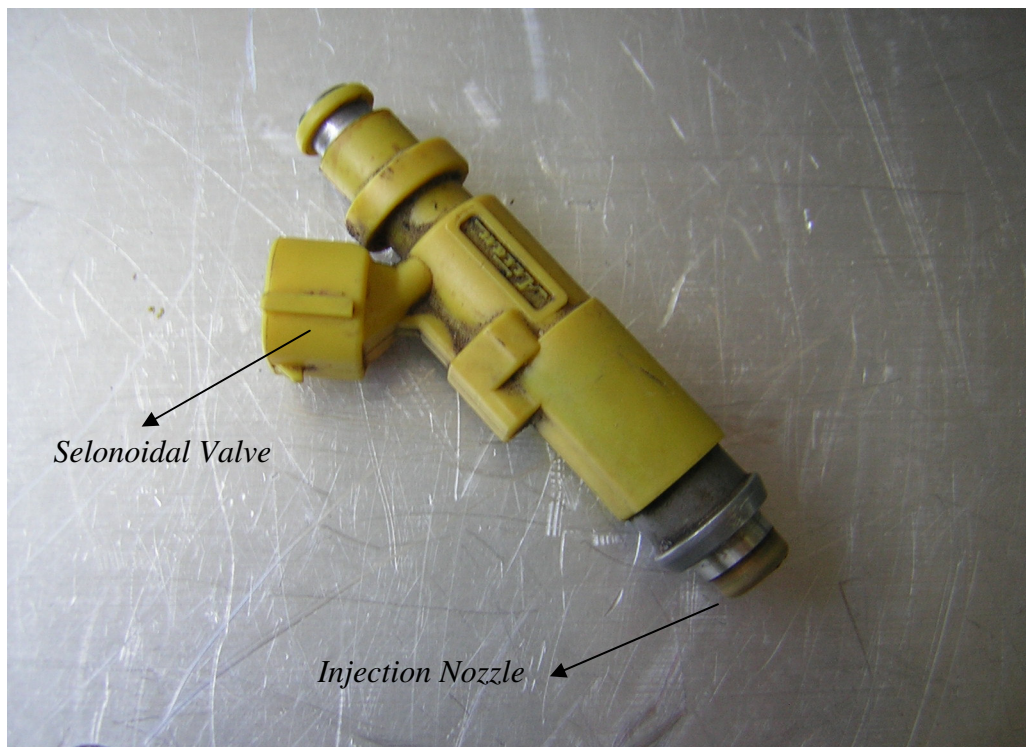
Figure 3-118   Fuel Injector

Fuel Pump
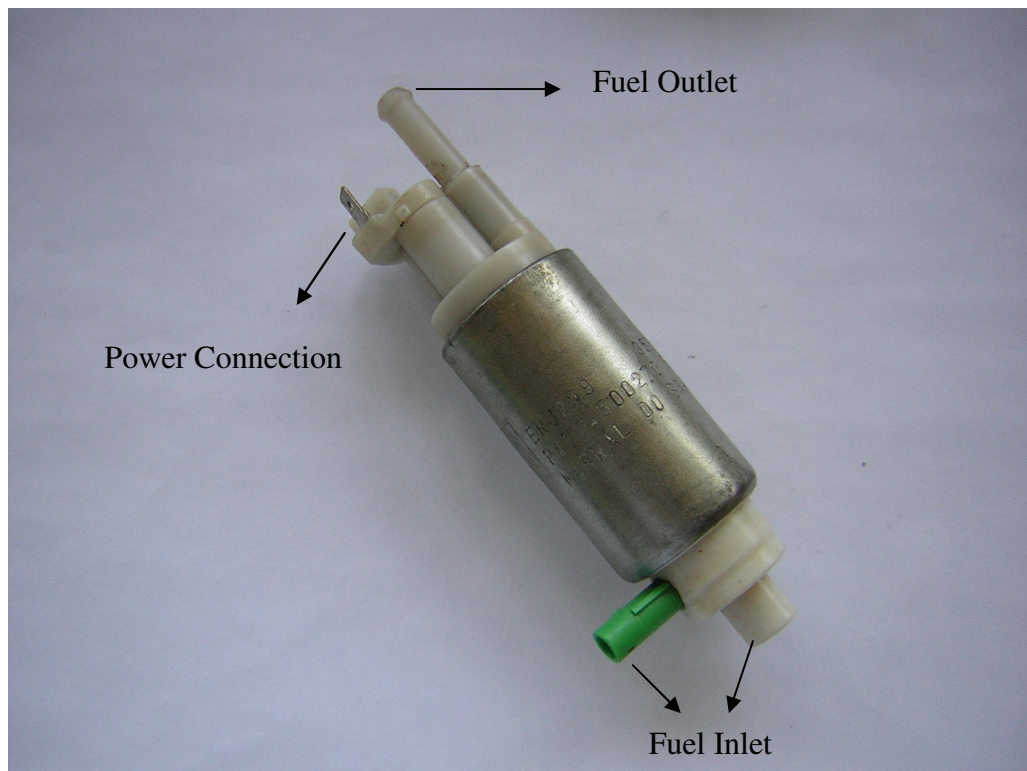
Figure 3-119   Fuel Pump

Fuel Type

The fuels most commonly used in internal combustion engines (gasoline, petrol, and diesel fuels) are blend of many different hydrocarbon compounds obtained by refining petroleum or crude oil [16]. These fuels are predominantly carbon and hydrogen (typically about 86% carbon and 14 % hydrogen by weight) though diesel fuels can contain up to 1 percent sulfur. Other fuels of interest are alcohols (which contain oxygen), gaseous fuels (natural gas and liquid petroleum gas), and single hydrocarbon compounds (e.g., methane, propane, isooctane) which are often used in engine research.

3.5.2 Lubrication System [26, 27]

The lubricant and the lubricating system perform the following functions;

- Reduce the frictional resistance of the engine to a minimum to ensure maximum mechanical efficiency.
- Protect the engine against wear.
- Contribute to cooling of the cylinder and regions of the engine where friction work is dissipated.
- Remove all injurious impurities from lubricated regions.
- Hold gas and leakage (especially between the vane and the cylinder) at an acceptable minimum level.

Lubrication of the engine is effected by four outlet metering pump shown in Figure 3-120 with two pairs of high and low outputs.

The high outputs feed oil to the compressor and turbine main bearings. Oil, coming to top main bearing passes through the rotor while lubricating the rotor top seals, and reach to the bottom main bearing.

The two low outputs feed oil directly into the cylinder from the cylinder – rotor tangent point, lubricating the apex seals and forming a thin oil film layer on the cylinder surfaces. (Figure 3-122)
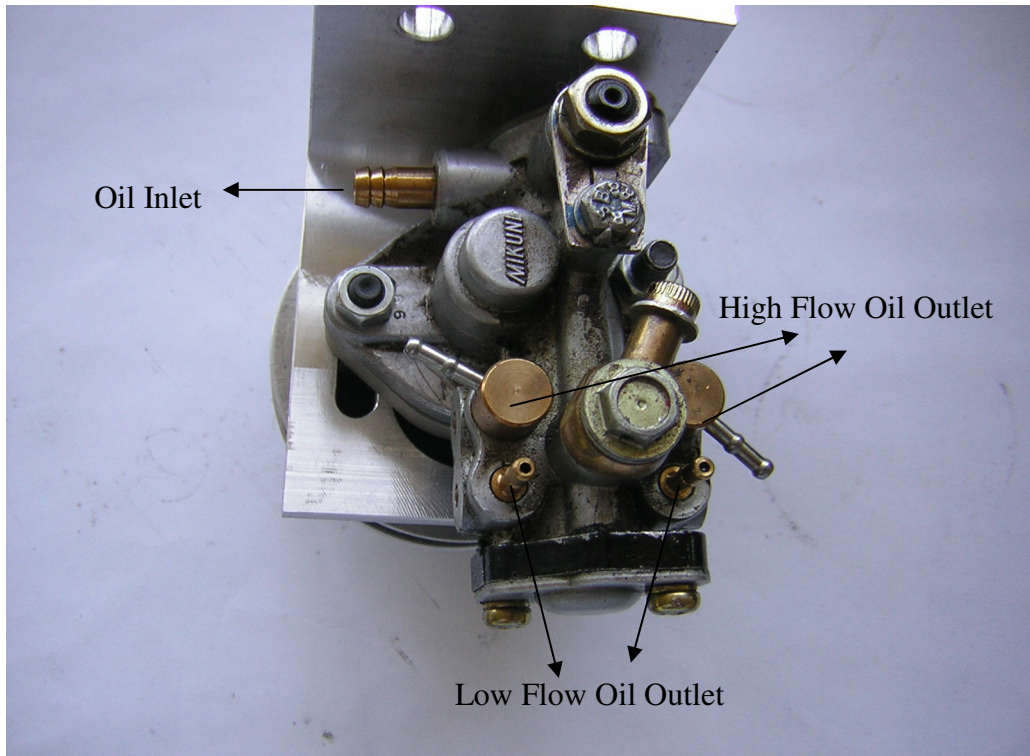
Figure 3-120   Oil Pump
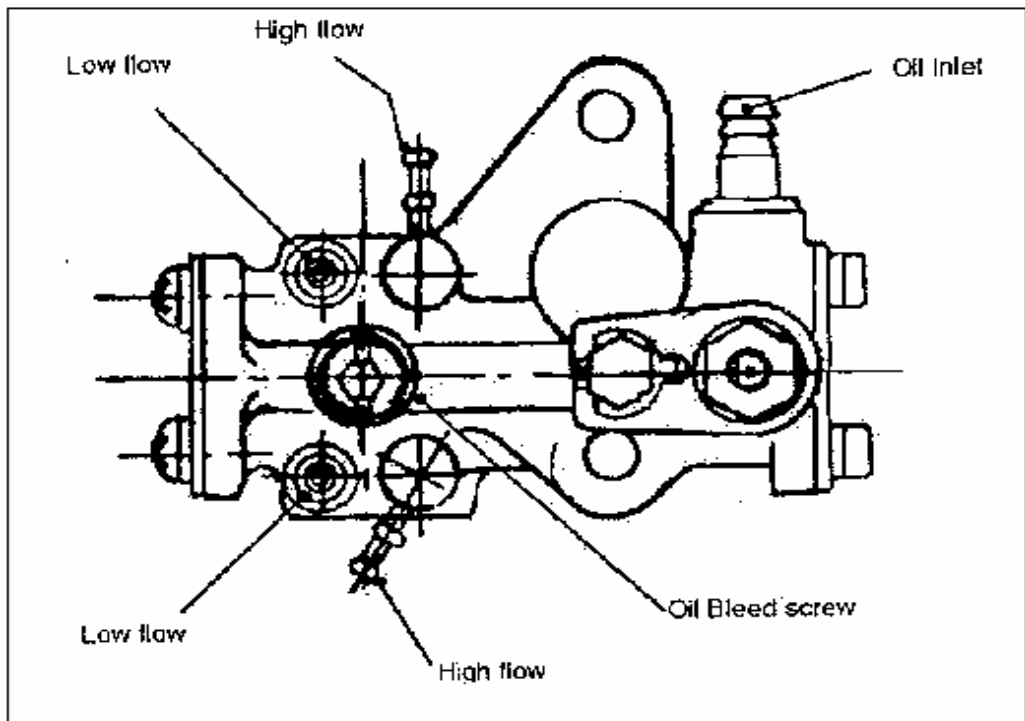
Figure 3-121   Oil Pump Drawing

Oil Type

Satisfactory oil types for lubricating the engine (depending on the ambient temperature) are given below;

- Mobil Pegasus 1

  This oil is a high grade, synthetic, low ash type and has a very low pour point of -54° C as well as other excellent characteristics.

  Viscosity @ 40° C   94cSt

  Viscosity @ 100° C   13cSt

- Mobil Pegasus 485

  Only suitable for ambient temperatures above -10° C.

- Shell Rotella SX40

  Only suitable for ambient temperatures above -10° C.

- Castrol A545

  Only suitable for ambient temperatures above -25° C.
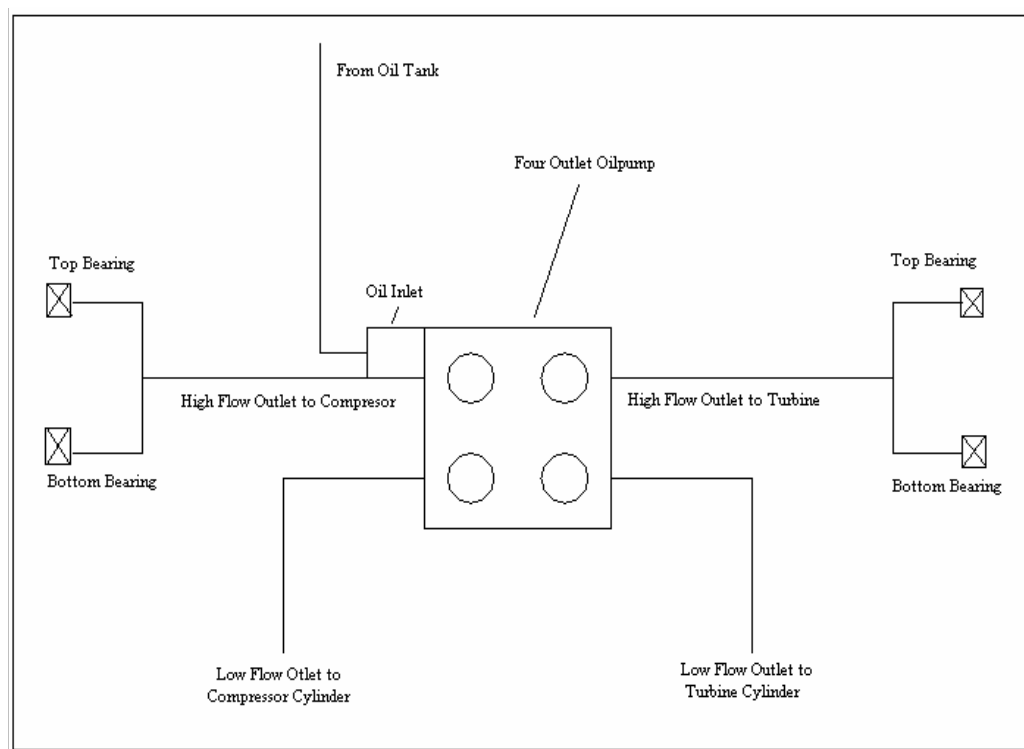
Figure 3-122   Lubrication System Schematic

3.5.3   Ignition System

In spark ignition engines, the electrical discharge produced between the spark plug electrodes by the ignition system starts the combustion process. A spark can arc from one electrode to another when sufficiently high voltage is applied. Ignition system used in this engine to provide the necessary spark is the battery system where the spark energy is stored in a capacitor and transferred as a high voltage pulse to the spark plug by means of a special transformer which is called as capacitive discharge ignition system shown in figure 3-123
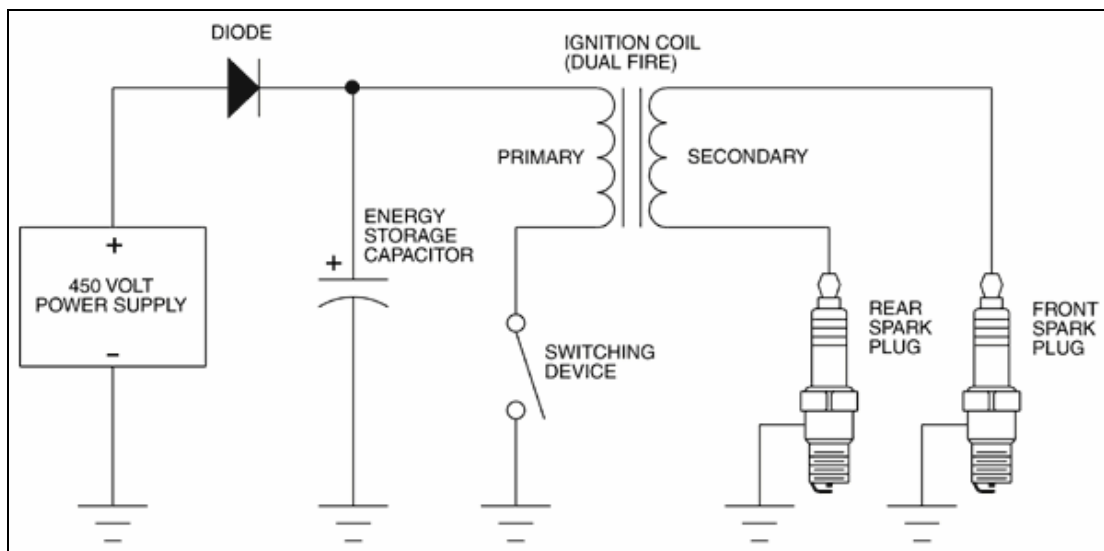
Figure 3-123   Capacitive Discharge Ignition System
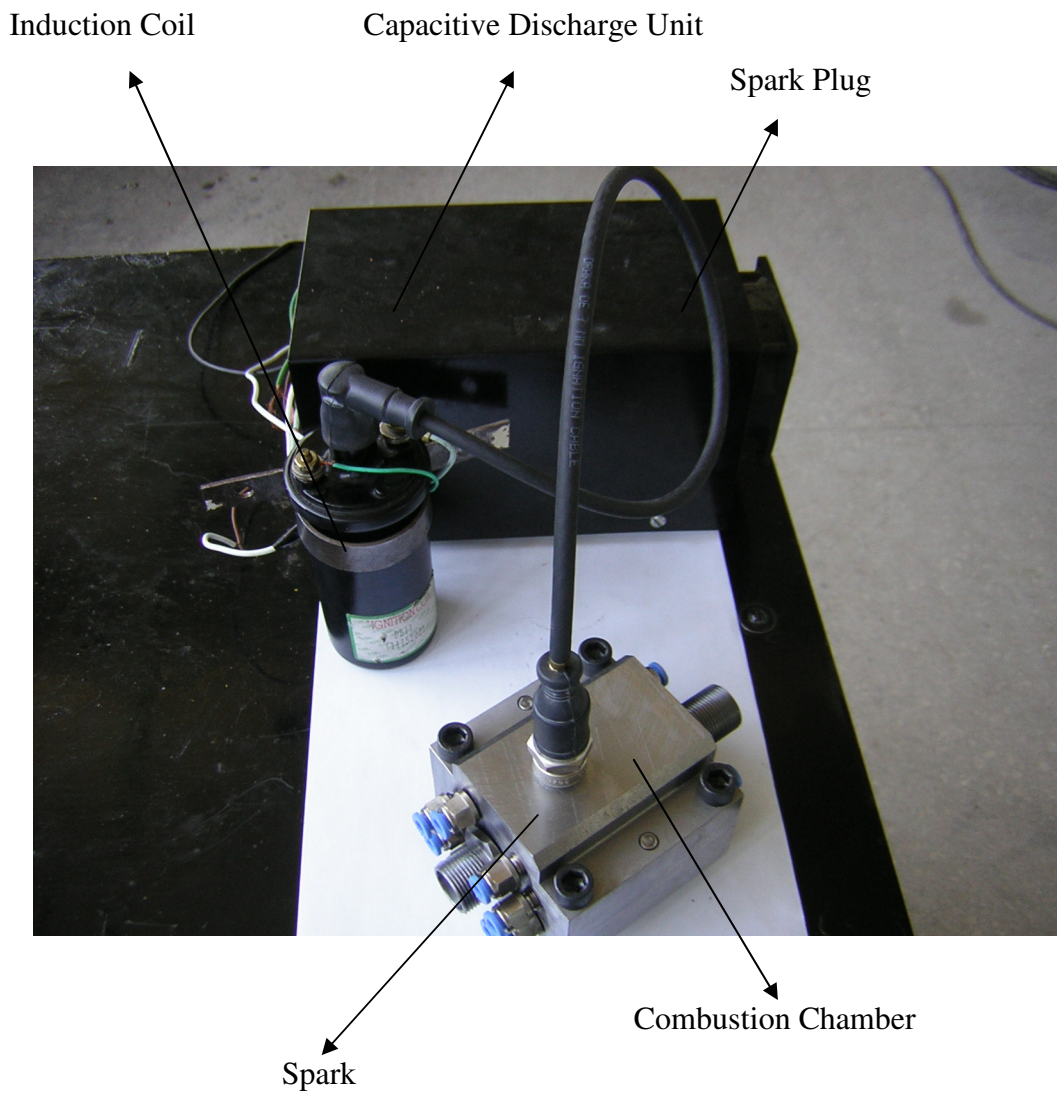
Figure 3-124   Ignition System with Combustion Chamber

3.5.4   Cooling System

The engine is designed to be ram air cooled by a substantial flow of air passing through the engine.

For ground testing, the novel engine must be provided with sufficient extra cooling to prevent overheating by arranging cooling air to be blown over the engine. This is achieved by a fan placed in front of the engine. Engine temperature should be carefully monitored to prevent the engine overheating. (Shown in Figure 3.125)

For ground testing, the combustion chamber is cooled with water passing through 8 cooling passages within the chamber body. Water at a temperature of 20° C is pumped with a water pump and passes through the channels, cooling the chamber.
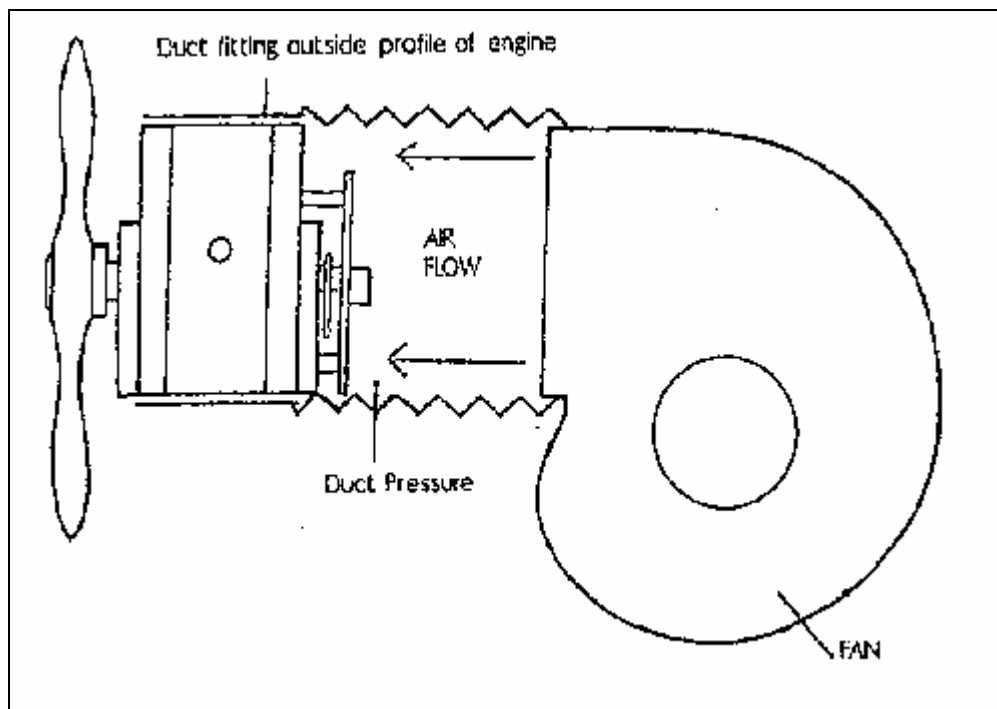
Figure 3-125   Ground Test Cooling

3.6 Overall Engine Assembly

The assembly sequence of the designed novel rotary engine is given in figure 3-126.
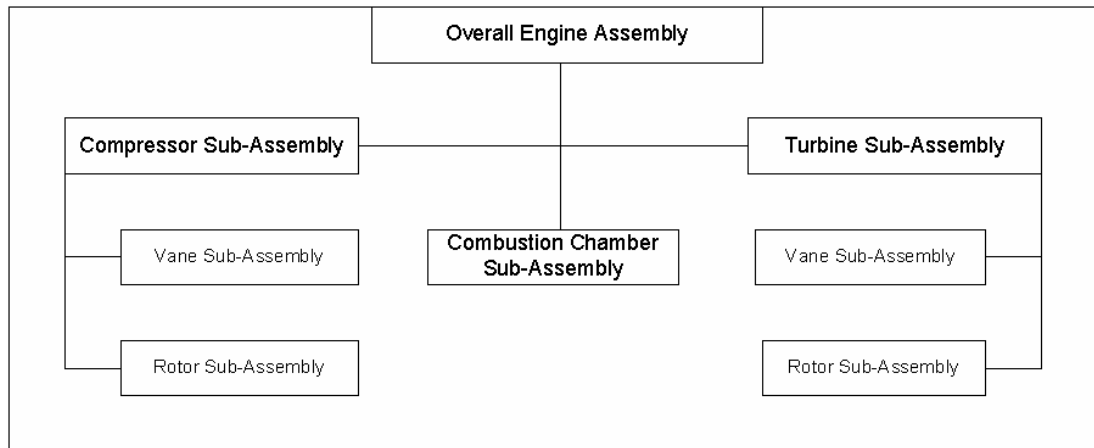
Figure 3-126   Overall Engine Assembly Scheme

- Compressor and turbine sub-assemblies are coupled with each other from their rotors with the help of a coupling.
- Two combustion chamber assemblies are mounted in between the compressor and turbine.
- The whole assembly is mounted on a test stand for ground tests.
- Compressor is coupled with a 2 kW electric motor from the drive side of the rotor for initial starting of the engine.
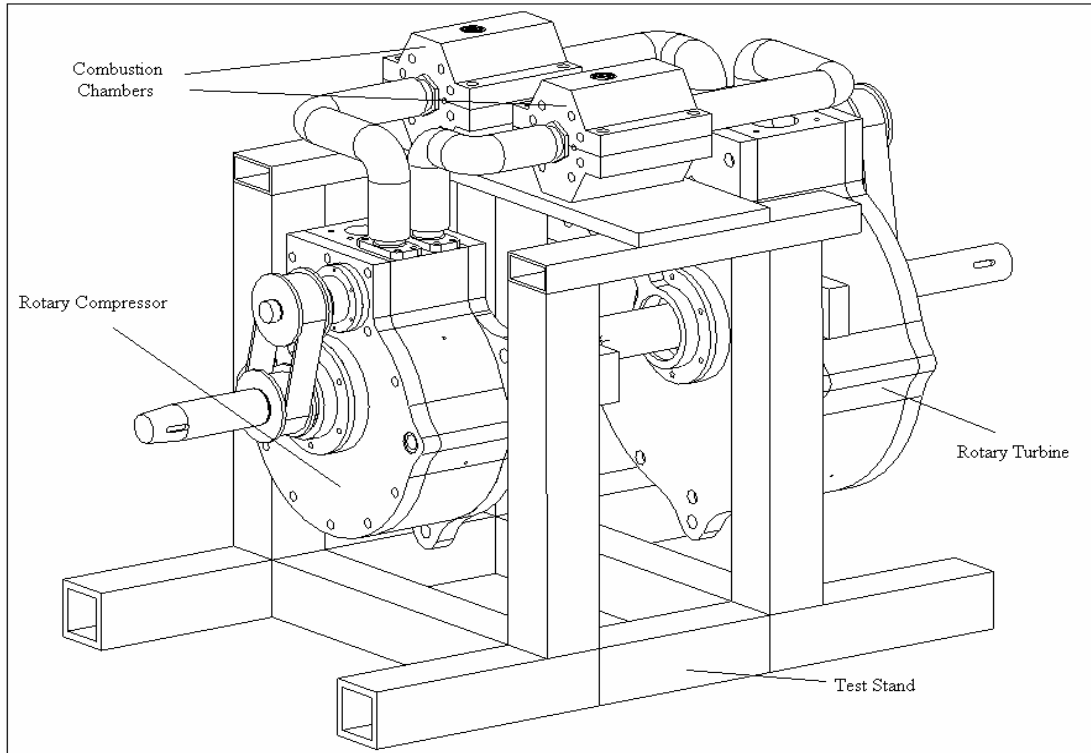
Figure 3-127   3-D   Wire-Frame Drawing of Overall Engine Assembly
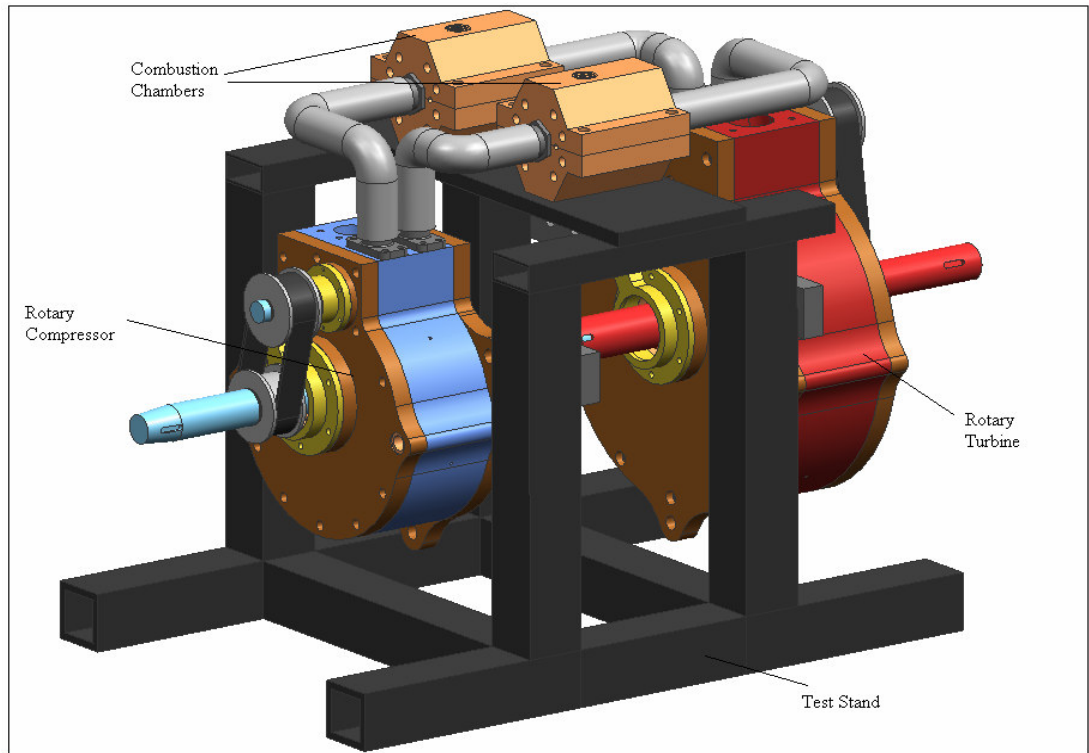
Figure 3-128   3-D CAD Model of Overall Engine Assembly

174
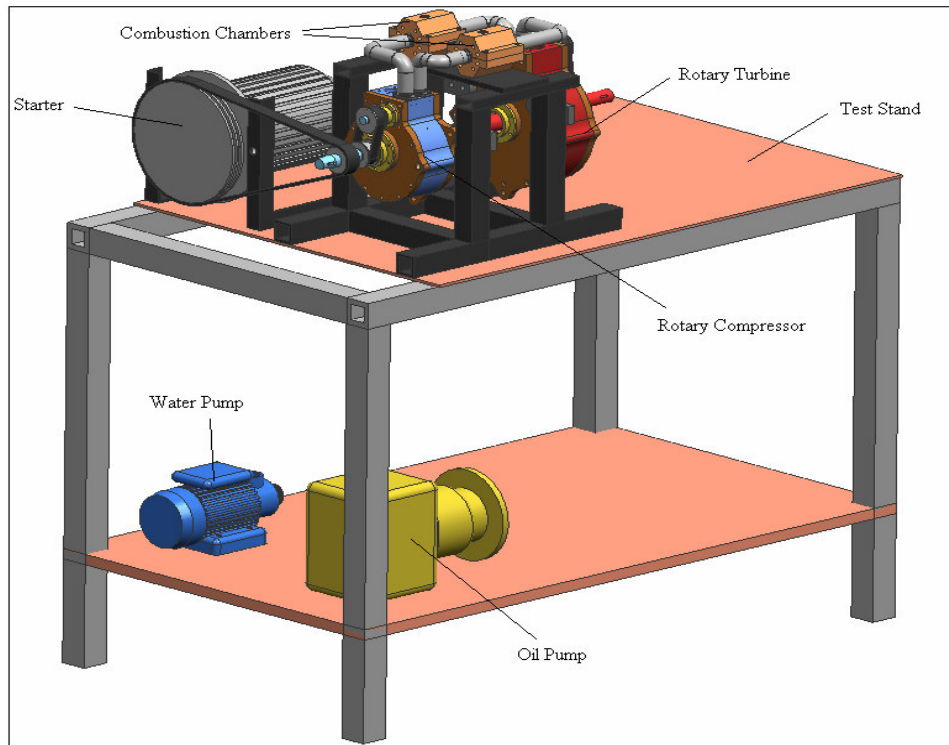
Figure 3-129   3-D CAD Model of Test Stand

Figure 3-130   Photograph of Test Stand

CHAPTER 4

TEST OF THE NOVEL ROTARY ENGINE

4.1 Compressor Tests

Test # 1:

Date : 09.03.2005	Place: TAI Tooling Facility	
- First manual rotation test after finishing assembly of the compressor group. - Compressor is fixed on table. - Bearings were all slip fit in order to ease assembly. - Tests are done without any seals. - Marker paint was sprayed inside the housing to identify the friction places. - Valve timing was not set. - One of the exits was closed with scheme. - Housing was filled with oil to prevent unwanted friction. - Aluminum housing and taps were tested with steel rotor, vane and valve.		
Rpm	**Time**	**Notes**
25	5 min.	Manual rotation with hand.
General Test Notes:		
- Valve was stuck at first assembly; bushing ends diameters were decreased to release the valve. - Timing belt was not too tight. - Factory air (6 bar) was given from the inlet; no rotation due to lack of seals and inappropriate valve timing. 6 bar pressurized air was given to the housing while valve was closed and leakage between housing and taps, housing and exit ports, taps and bearing taps were observed. Pressurized air released from exit port as it is opened by manual rotor rotation. - Excess oil was removed from housing before giving pressurized air in order to prevent pressurized oil evacuation from exit port. - All the parts were cleaned with viscous #3 solvent and inside of the housing was sprayed with marker paint before next assembly.		

Test # 2:

Date : 10.03.2005	Place: TAI Machining Facility	
- First rotary test after finishing assembly of the compressor group. - Compressor is fixed on the test tool and mounted on a horizontal machining center with a spindle of max 1200 rpm. - Tests are done without any seals. - Marker paint was sprayed inside the housing to identify the friction places. - Valve timing was set with timing pulleys and belt. - Housing was filled with oil to prevent unwanted friction. - Aluminum housing and taps were tested with steel rotor, vane and valve.		

Rpm	Time	Notes
25	1 min.	Normal working.
150	1 min.	Normal working.
325	1 min.	Normal working.
570	1 min.	Slight vibration started. Bolts attaching test tool and table were tightened. Vibration diminished.
730	1 min.	Color of the oil coming out of the housing was changed. Oil became darker and tiny aluminum pieces were observed with the oil.
940	1 min.	Normal working.
1200	1 min.	Slight temperature rise on the bottom half of the housing were friction is max. No temperature rise on the upper half of the housing.
General Test Notes:		
- Vibration and noise were normal although it was tested without seals. - Valve timing seemed to be accurate. - Pressure at both exits seemed to be same. - Balloons were attached to the exits and were filled with compressed air-oil mixture till they explode. - Compressor assembly was demounted at the end of the test. It was observed that at the bottom half of the housing, all the paint was removed. Also the paint on the tangent point between rotor and housing was completely removed. Aluminum pieces were observed inside the housing and some were stick on the vane. Inside the housing, distance between the two bushings was measured at 3 different heights with bore-gage. - Thicker oil seemed to be more appropriate for tests then the used one. - All the parts were cleaned with viscous #3 solvent and inside of the housing was sprayed with marker paint before assembly.		

Test # 3:

Date : 11.03.2005	Place: TAI Machining Facility	
<td colspan="3"> - Second rotary test after finishing assembly of the compressor group. - R&D Manager Eray Gökalp, Chief Süleyman Yangınlar, Machining Chief Recep Akçay and Prof. Sinan Akmandor were present during test. - Compressor is fixed on the test tool and mounted on a horizontal machining center with a spindle of max 1200 rpm. - Tests are done without any seals. - Marker paint was sprayed inside the housing to identify the friction places. - Valve timing was set with timing pulleys and belt. - Housing was filled with oil to prevent unwanted friction. - A micrometer was put on the housing to observe the vibration. - Aluminum housing and taps were tested with steel rotor, vane and valve. </td>		
Rpm	**Time**	**Notes**
25	1 min.	Normal working.
150	1 min.	Normal working.
325	1 min.	Normal working. 1% vibration.
570	1 min.	Normal working. 1.5% vibration.
730	1 min.	Normal working. 3% vibration.
940	1 min.	Normal working. 3.5% vibration.
1200	1 min.	Normal working. 2% vibration. Vibration decreased. Slight temperature rise on the bottom half of the housing were friction is max. No temperature rise on the upper half of the housing.
General Test Notes:		
<td colspan="3"> - Vibration and noise were normal although it was tested without seals. - Valve timing seemed to be accurate. - Pressure at both exits seemed to be same. - Compressor assembly was demounted at the end of the test. It was observed that at the bottom half of the housing all the paint was removed. Also the paint on the tangent point between rotor and housing was completely removed. Aluminum pieces were observed inside the housing and some were stick on the vane. Inside the housing, distance between the two bushings was measured at 3 different heights with bore-gage. 0.003 in. distance increase was measured manually. - Thicker oil seemed to be more appropriate for tests then the used one. </td>		

Test # 4:

Date : 24.03.2005	Place: METU Hydraulic Laboratory	
• Structure test.		
• First test in propulsion laboratory.		
• Compressor is fixed on the test tool and mounted on test table and coupled with a 200 kW electric motor.		
• Tests are done without any seals.		
• Valve timing was set with timing pulleys and belt.		
• Housing was filled with oil (20-50W) to prevent unwanted friction.		
• A micrometer was put on the housing to observe the vibration.		
• Aluminum housing and taps were tested with steel rotor, vane and valve.		

Rpm	Time	Notes
18	1 min.	Normal working.
60	1 min.	Normal working.
100	1 min.	Normal working.
150	1 min.	Normal working.
200	1 min.	Normal working.
300	1 min.	Normal working. No temp. rise

General Test Notes:

- Vibration and noise were more then the TAI tests.
- An impact with vane and housing was obvious and can be easily recognized from impact noise. (Probably because of clearance between housing and vane as no seals were mounted)
- Compressor and electric motor are not seemed to be precisely centered.
- Valve timing seemed to be accurate.
- Pressure at far exit valve seemed to be more then the other exit.
- Thicker oil used in this test. (20-50W)
- Vibration of the test table was small and seemed ok.
- Oil coming out of both exits (more from the far exit) were observed with 150 and bigger rpm values.
- Check valves were tested but because of leakage from housing taps, and other connections (as no precaution was taken), no air exit through check valves were observed. Instead, air from inlet was coming out.
- Oil leakage from housing taps, and combustion housing connections were observed.
- Pressure gage was installed at one exit but no pressure could be read.

Test # 5:

Date : 25.03.2005	Place: METU Hydraulic Laboratory	
- Structure test. - Second test in propulsion laboratory. - Compressor is fixed on the test tool and mounted on test table and coupled with a 200 kW electric motor. - Last day's setup was used as the compressor was not demounted after the test. - Tests are done without any seals. - Nazmi Ersöz (patent partner) was also participating to the tests. - Electric motor and compressor were re-centered before the test. 1st Prototype (manufactured in 1st DLMM in Eskişehir) was also tested.		
Rpm	**Time**	**Notes**
18	1 min.	Normal working.
60	1 min.	Normal working.
100	1 min.	Normal working.
General Test Notes:		
- Valve timing seemed to be accurate. - Thicker oil used in this test. (20-50W) - Vibration of the test table was small and seemed ok. - Compressor assembly was demounted at the end of the test. - While inspecting the vane seals, it was found out that they were false manufactured. They were 1.5 mm short in height. (57.80mm instead of 59.3 mm) and it was decided that they were to be re-made. - Springs were examined and they were seemed to be a bit stiffer. - Also top rotor seals seemed to be tight fit. - Compressed air (10 bars) was given to the turbine of 1st prototype and it started rotating at an approximate of 50 – 75 rpm.		

Test # 6:

Date : 25.04.2005	Place: METU Hydraulic Laboratory	
<td colspan="3"> - Structure test. - Compressor is fixed on the test tool and mounted on test table and coupled with a 200 kW electric motor. - Aluminum housing and taps were assembled. - Steel front vane seals were re-manufactured and mounted. - Electric motor and compressor were re-centered before the test. </td>		
Rpm	**Time**	**Notes**
20	1 min.	Normal working.
100	1 min.	Normal working.
200	1 min.	Normal working.
General Test Notes:		
<td colspan="3"> - Valve timing seemed to be accurate. - Vibration of the test table was small and seemed ok. - Compressor assembly was demounted at the end of the test. - Springs were examined and they were seemed to be a bit stiffer. - Vane was too tight because of the front vane seal springs. - Also there was little tolerance between the seals and their casing inside the rotor. - Inside the housing, deformation due to friction of steel seals could be easily observed. - Also the friction surfaces of the steel seals were deformed. - It is concluded that the steel seal is not a good choice. </td>		

Test # 7:

Date : 02.05.2005	Place: METU Hydraulic Laboratory

- Structure test.
- Compressor is fixed on the test tool and mounted on test table and coupled with a 200 kW electric motor.
- Aluminum housing and taps were assembled.
- Steel front vane seals were mounted.
- Gray cast iron rotor top seals were mounted.
- Electric motor and compressor were re-centered before the test.

Rpm	Time	Notes
20	1 min.	Normal working.
100	1 min.	Normal working.
200	1 min.	Normal working.
400	1 min.	Normal working. Slight temp rise.

General Test Notes:

- Valve timing seemed to be accurate.
- Vibration of the test table was small and seemed ok.
- Compressor assembly was demounted at the end of the test.
- Vane was too tight because of the front vane seal springs.
- Also there was little tolerance between the seals and their casing inside the rotor.
- Inside the housing, deformation due to friction of steel seals could be easily observed.
- Also the friction surfaces of the steel seals were deformed.
- Top rotor seals were tight fit in their casings inside the rotor. Also because of their springs stiffness they were exerting too much force on the taps.
- But the good news is that there were no deformation between the taps and seals on the friction surfaces. The seal material (gray cast iron) seemed to be well performing.

Test # 8:

Date : 09.05.2005	Place: METU Hydraulic Laboratory	
- Structure test. - Compressor is fixed on the test tool and mounted on test table and coupled with a 200 kW electric motor. - Steel housing and taps were assembled. - Steel front vane seals were mounted. - Electric motor and compressor were re-centered before the test.		
Rpm	**Time**	**Notes**
20	1 min.	Normal working.
100	1 min.	Normal working.
200	1 min.	Normal working.
400	1 min.	Normal working. Slight temp rise.
General Test Notes:		
- Valve timing seemed to be accurate. - Vibration of the test table was small and seemed ok. - Compressor assembly was demounted at the end of the test. - Vane was too tight because of the front vane seal springs. - Also there was little tolerance between the seals and their casing inside the rotor. - Inside the housing, deformation due to friction of steel seals could be easily observed. This time the deformation was a bit less compared to aluminum housing. - Also the friction surfaces of the steel seals were deformed. This time the deformation was more as steel housing was used.		

Test # 9:

Date : 12.05.2005	Place: METU Hydraulic Laboratory

- Structure test.
- Compressor is fixed on the test tool and mounted on test table and coupled with a 200 kW electric motor.
- Steel housing and taps were assembled.
- Steel front vane seals were mounted.
- Gray cast iron rotor top seals were mounted.
- Electric motor and compressor were re-centered before the test.

Rpm	Time	Notes
20	1 min.	Normal working.
100	1 min.	Normal working.
200	1 min.	Normal working.
400	3 min.	Normal working. Slight temp rise.
600	3 min.	Normal working. Slight temp rise.

General Test Notes:

- Valve timing seemed to be accurate.
- Vibration of the test table was small and seemed ok.
- Compressor assembly was demounted at the end of the test.
- Vane was too tight because of the front vane seal springs.
- Also there was little tolerance between the seals and their casing inside the rotor.
- Inside the housing, deformation due to friction of steel seals could be easily observed. This time the deformation was a bit less compared to aluminum housing.
- Also the friction surfaces of the steel seals were deformed. This time the deformation was more as steel housing was used.
- Top rotor seals were tight fit in their casings inside the rotor. Also because of their springs stiffness they were exerting too much force on the taps.
- But the good news is that there were no deformation between the taps and seals on the friction surfaces. The seal material (gray cast iron) seemed to be well performing.

Test # 10:

Date : 17.05.2005	Place: METU Hydraulic Laboratory	
<td colspan="3"> - Structure test. - Compressor is fixed on the test tool and mounted on test table and coupled with a 200 kW electric motor. - Steel housing and taps were assembled. - Steel front vane seals were mounted. - Gray cast iron rotor top seals were mounted. - Electric motor and compressor were re-centered before the test. - Aim was to reach higher rpm values. </td>		

Rpm	Time	Notes
20	1 min.	Normal working.
100	1 min.	Normal working.
200	1 min.	Normal working.
400	3 min.	Normal working. Slight temp rise.
600	3 min.	Normal working. Slight temp rise.
800	1 min.	Unusual noise came from the timing belt and test was stopped immediately.
General Test Notes:		

- Valve timing seemed to be accurate.
- Vibration of the test table was small and seemed ok.
- Compressor assembly was demounted at the end of the test.
- It was observed that a piece of material (probably from the vane seals) protruded between the valve and its casing and stack the valve. At that moment the timing pulley of the valve stopped with the valve itself but as the rotor and its pulley continued to revolve there was great friction between the timing belt and valve pulley which formed an unusual noise.
- It was observed that there was a severe deformation on the valve casing and the valve.
- Valve casing will be reworked and a new valve will be used for the next test setup.
- Also severe deformation on the contact surfaces of the vane seals was observed.
- The damaged vane seals will be grinded to get smooth contact surfaces.
- The front vane seals will be made from fiber and epoxy to avoid unwanted deformation on the housing.

Test # 11:

Date : 11.07.2005	Place: METU Hydraulic Laboratory	
- Compressor pressure test. - Compressor is fixed on the test tool and mounted on test table and coupled with a 200 kW electric motor. - Electric motor and compressor were re-centered before the test. - Tests are done with fiber front vane seals and gray cast iron rotor seals. - A compression tank was assembled to one of the exits of the compression housing to see how much it compresses. - Valve timing was set with timing pulleys and belt. - A micrometer was put on the housing to observe the vibration. - Steel housing and taps were tested with steel rotor, vane and valve.		
Rpm	**Time**	**Notes**
25	1 min.	Normal working.
150	1 min.	Normal working.
300	1 min.	Normal working. 1% vibration.
600	1 min.	Normal working. 1.5% vibration.
		Test was stopped because of oil and air leakage from the bottom tap. (Oil seal and oil tap was not mounted)
General Test Notes:		
- Vibration and noise were normal - Valve timing seemed to be accurate. - Pressure at the tank reached to 3 atm when test stopped. - Fiber seals seemed well performing. - Oil together with pressurized air was coming from the bottom bearing as there were no oil seal and tap. - Both oil seal and tap were mounted before the new test.		

Test # 12:

Date : 11.07.2005	Place: METU Hydraulic Laboratory	
• Compressor pressure test. • Compressor is fixed on the test tool and mounted on test table and coupled with a 200 kW electric motor. (Same setup as previous) • Tests are done with fiber front vane seals and gray cast iron rotor seals. • A compression tank was assembled to one of the exits of the compression housing to see how much it compresses. • Valve timing was set with timing pulleys and belt. • A micrometer was put on the housing to observe the vibration. • Steel housing and taps were tested with steel rotor, vane and valve.		
Rpm	**Time**	**Notes**
25	1 min.	Normal working.
150	1 min.	Normal working.
325	1 min.	Normal working. 1% vibration.
570	1 min.	Normal working. 1.5% vibration.
730	1 min.	Normal working. 3% vibration.
1200	1 min.	Normal working. 2% vibration. Vibration decreased. Temperature rise on the bottom half of the housing were friction is max.
		Compressor stopped immediately after 1 min of working.
General Test Notes:		
• Vibration and noise were normal • Valve timing seemed to be accurate. • There was no leakage from housing taps or valve taps. • Pressure at the tank reached to 7.5 atm. • No motion in the valve and rotor was observed after the stop. • First suspect was that the valve was stack due to over-expansion because of rising temperature. Also vane could have been stack inside the rotor as there is a little gap tolerance in between. • Fiber seals seemed well performing. • Cooling is needed to prevent unwanted over-expansions. • Compressor was disassembled and parts were inspected. It was seen that the vane stacked inside the rotor which caused immediate stop during the test. Also some scraps were present on the valve surface. • Final decision; vane over expansion (more then the gap tolerance) due to thermal effects caused it to stack inside the rotor.		

Test # 13:

Date : 27.07.2005	Place: METU Hydraulic Laboratory	
• Compressor pressure test.		
• Compressor is fixed on the test tool and mounted on test table and coupled with a 200 kW electric motor. (Same setup as previous)		
• Tests are done with fiber front vane seals and gray cast iron rotor seals.		
• A compression tank was assembled to one of the exits of the compression housing to see how much it compresses.		
• Valve timing was set with timing pulleys and belt.		
• A micrometer was put on the housing to observe the vibration.		
• Steel housing and taps were tested with steel rotor, vane and valve.		
• Deformed surfaces on the vane and inside the rotor were re-machined (hand finish) and the gap tolerance was made larger.		
• Also the vane surface was re-machined (hand finish) and the gap tolerance was made larger.		
• Continues cooling with a blower (1800 m3/h air) was achieved by blowing ambient temperature air on to the compressor surfaces.		

Rpm	Time	Notes
270	12 min.	Normal working.
600	4 min.	Normal working. Slight temp rise.
		Valve bearing gone out of is casing.
		Test was stopped.
General Test Notes:		

- Vibration and noise were normal
- Valve timing seemed to be accurate.
- There was no leakage from housing taps or valve taps.
- Pressure at the tank reached to 2 atm.
- Fiber seals seemed well performing.
- Valve tap has to be put on to the compressor in order to prevent the valve bearing to leave its casing.
- Because of the larger gap tolerance between the rotor and the vane and between the valve and its casing there was slight pressure rise.
- Compressor has to work with higher rpm values and longer periods so that the temperature will rise to the correct value which will cause the valve and the vane to expand to the optimum value.

Test # 14:

Date : 28.07.2005	Place: METU Hydraulic Laboratory		
<td colspan="4">• Compressor pressure test. • Compressor is fixed on the test tool and mounted on test table and coupled with a 200 kW electric motor. (Same setup as previous) • Tests are done with fiber front vane seals and gray cast iron rotor seals. • An orifice was assembled to one on the exits to measure the mass flow. • Valve timing was set with timing pulleys and belt. • A micrometer was put on the housing to observe the vibration. • Steel housing and taps were tested with steel rotor, vane and valve. • Continues cooling with a blower (1800 m3/h air) was achieved by blowing ambient temperature air on to the compressor surfaces. • Valve tap was mounted to prevent valve to come out of its casing.</td>			
Rpm	**Time**	**Notes**	**Mass Flow(g/s)**
90	1 min.	Normal working.	0.9
180	1 min.	Normal working.	1.8
270	1 min.	Normal working.	2.7
360	1 min.	Normal working.	3.6
450	1 min.	Normal working.	4.5
540	1 min.	Normal working.	5.4
630	1 min.	Normal working.	6.3
720	1 min.	Normal working.	7.2
810	30 sec	Irregular noise.	8.1
		Test stopped.	
General Test Notes:			
<td colspan="4">• Valve timing seemed to be accurate. • There was no leakage from housing taps or valve taps. • Fiber seals seemed well performing. • Valve was stacked inside the housing. Timing belt slipped over the timing pulley which caused an irregular noise due to friction between belt and pulley. • Rotor and vane motion was normal. • Compressor was demounted and it was observed that a foreign object (possibly a metal piece) had protruded between the valve and the casing and caused it to stop while deforming both parts.</td>			

Test # 15:

Date : 28.07.2005	Place: METU Hydraulic Laboratory		
• Compressor high rpm endurance test. • Compressor was fixed on the test tool and mounted on test table and coupled with a 200kW electric motor. (Same setup as previous) • Tests were done with fiber front vane seals and gray cast iron rotor seals. • Valve timing was set with timing pulleys and belt. • A micrometer was put on the housing to observe the vibration. • Steel housing and taps were tested with steel rotor, vane and valve. • Continues cooling with a blower (1800 m3/h air) was achieved by blowing ambient temperature air on to the compressor surfaces.			
Rpm	**Time**	**Notes**	
100	30 sec	Normal working.	
200	30 sec	Normal working.	
300	30 sec	Normal working.	
500	1 min	Normal working.	
750	1 min.	Normal working.	
1000	1 min.	Normal working.	
1200	1 min.	Normal working.	
1500	1 min.	Normal working.	
1950	30 sec	Immediate stop	
		Test stopped.	
General Test Notes:			
• Vibration and noise were normal during test. • Temperature increased slightly during the test. (Not more then 60° C) • Compressor was demounted and it was observed that vane was stacked inside the rotor. Also slight deformation on the vane tips was observed showing that the tips were touching the housing surface. • Bolts joining the electric motor and the speed increaser gear box were ruptured as the vane stacked and flew off around.			

Test # 16:

Date : 28.07.2005	Place: METU Hydraulic Laboratory		
<td colspan="4"> - Compressor high rpm endurance test. - Compressor was fixed on the test tool and mounted on test table and coupled with a 200kW electric motor. (Same setup as previous) - Tests were done with fiber front vane seals and gray cast iron rotor seals. - Valve timing was set with timing pulleys and belt. - A micrometer was put on the housing to observe the vibration. - Steel housing and taps were tested with steel rotor, vane and valve. - The gap tolerance between the rotor and the vane is made larger to avoid stacking of vane. - Continues cooling with a blower (1800 m3/h air) was achieved by blowing ambient temperature air on to the compressor surfaces. </td>			
Rpm	**Time**	**Notes**	
250	30 sec	Normal working.	
500	30 sec	Normal working.	
750	30 sec	Normal working.	
1000	1 min	Normal working.	
1250	1 min.	Normal working.	
1500	1 min.	Normal working.	
2000	1 min.	Normal working.	
2500	1 min.	Normal working.	
3100	30 sec	Immediate stop	
		Test stopped.	
General Test Notes:			
<td colspan="4"> - Max rpm reached with this prototype. - Vibration and noise were normal during test. - Temperature increased too much during the test. - Compressor was demounted and it was observed that vane was stacked inside the rotor. - Bolts joining the electric motor and the speed increaser gear box were ruptured as the vane stacked and flew off around. - It is concluded that the cooling is insufficient for the ground tests. Due to large temperature rise, unwanted over expansions could not be avoided. </td>			
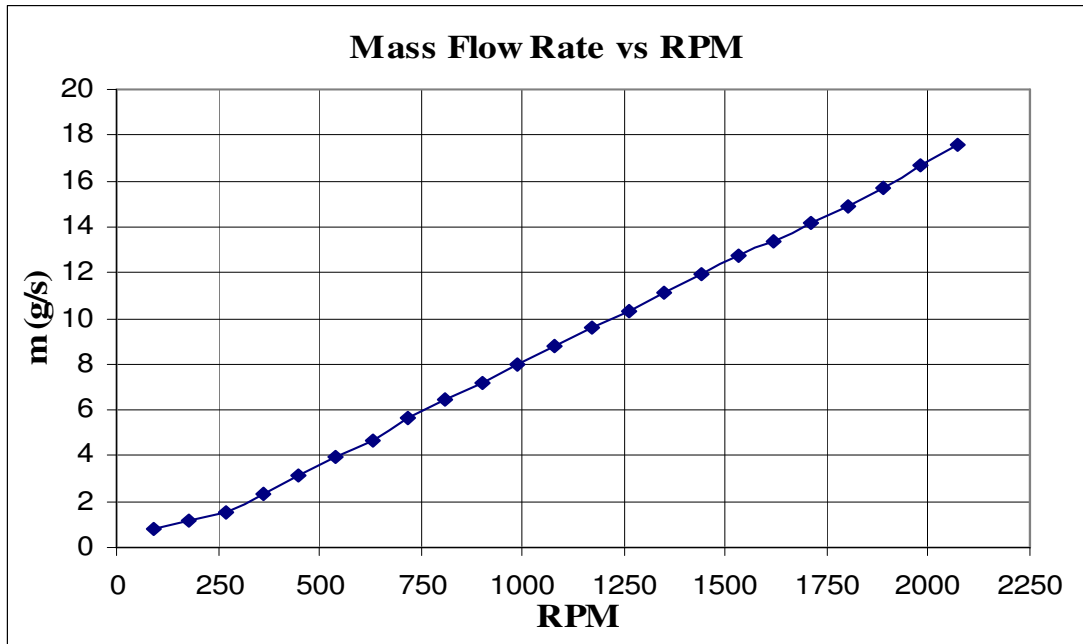
Figure 4-1 Compressor Mass Flow Rate versus Rpm Chart
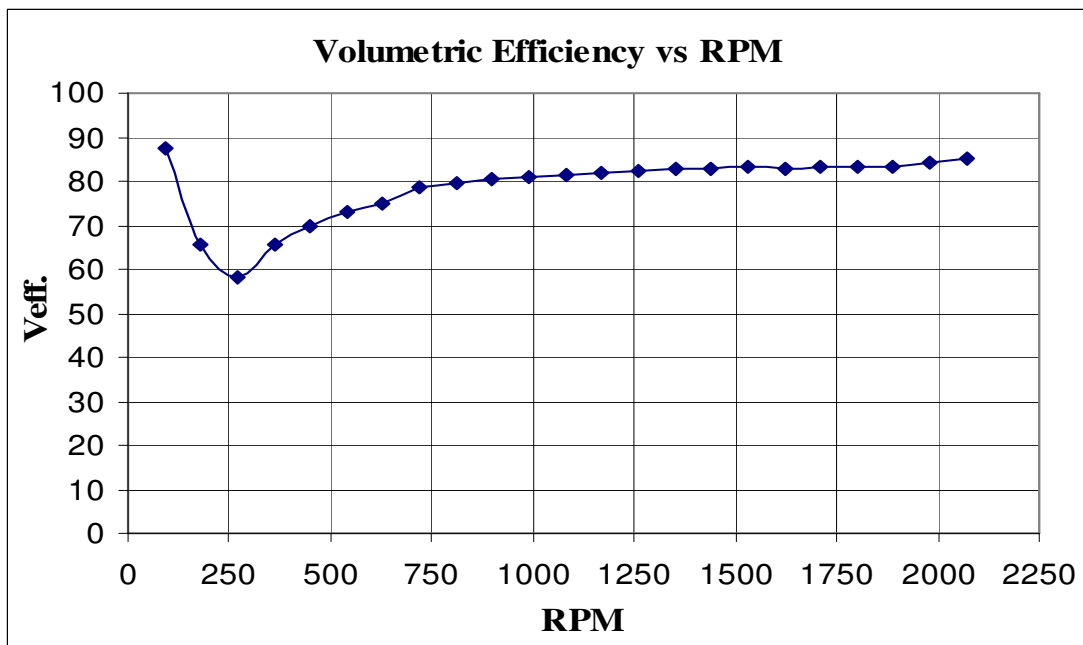
Figure 4-2   Compressor Volumetric Eff. versus Rpm Chart
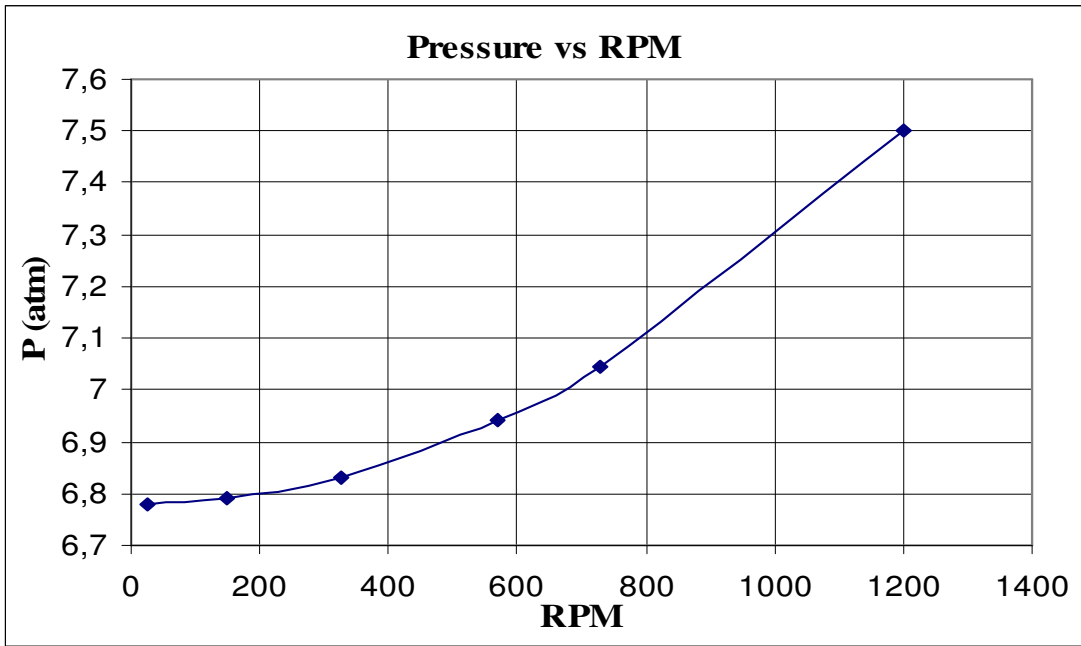
Figure 4-3   Compressor Pressure versus Rpm Chart
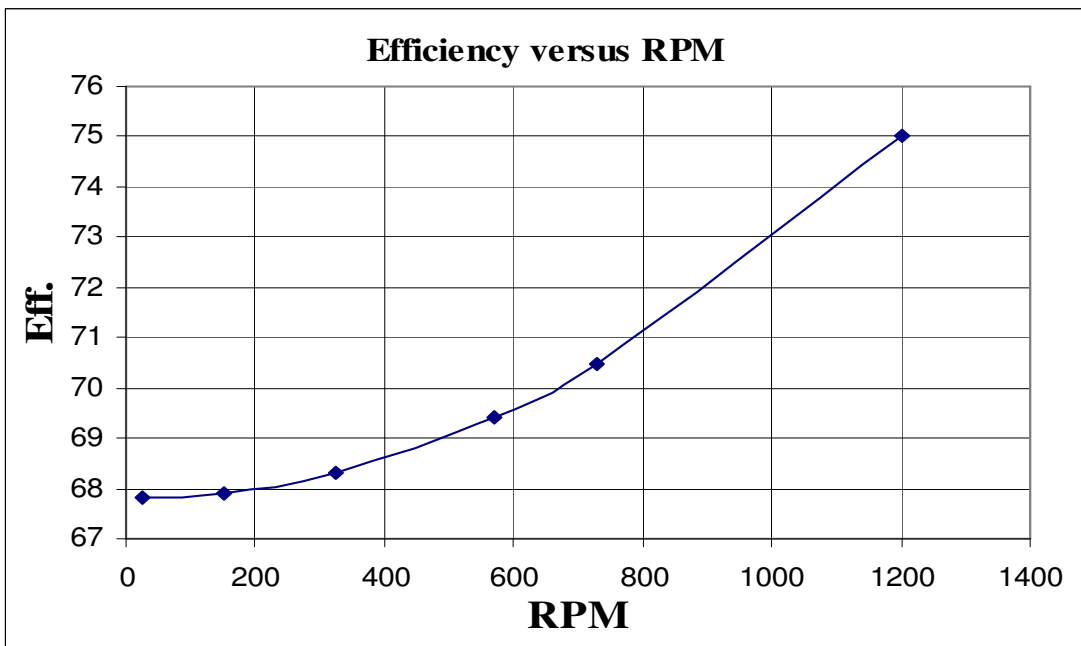
Figure 4-4   Compressor Efficiency versus Rpm Chart

4.2 Combustion Tests

Test # 1:

Date : 07.07.2005	Place: METU Hydraulic Laboratory		
- Combustion chamber test. - Combustion chamber was fixed on the test table. - Pressurized air was being given from a compressor to the chamber inlet. - Lpg tank was used as fuel supply and lpg was given into the inlet pipe of the chamber. - Continuous ignition was used. - No valves were used at the inlet and exit of the housing. - No cooling was used.			
Rpm	**Time**	**Notes**	
General Test Notes:			
- Discontinuous combustion was achieved. - Both pressurized air flow and fuel flow were regulated separately which changed combustion timing.			

Test # 2:

Date : 11.07.2005	Place: METU Hydraulic Laboratory		
<td colspan="4">• Combustion chamber test. • Combustion chamber was fixed on the test table. • Pressurized air was being given from a compressor to the housing inlet. • Lpg tank was used as fuel supply and lpg was given directly into the chamber. • Continuous ignition was used. • No valves were used at the inlet and the exit of the chamber. • No cooling was used.</td>
Rpm	**Time**	**Notes**	
General Test Notes:			
<td colspan="4">• Continuous combustion was achieved. • Both pressurized air flow and fuel flow were regulated separately which changed combustion timing. • At a proper mixing of air and fuel continuous combustion was achieved. • Combustion chamber was teared off during the test due to over heating.</td>

4.3 Turbine Tests

<u>**Test # 1:**</u>

Date : 24.05.2005	Place: METU Hydraulic Laboratory		
• Turbine structure test. • Turbine is fixed on the test tool and mounted on test table and coupled with a 200kW electric motor. • Steel housing and taps were assembled. • Steel front vane seals were mounted. • Gray cast iron rotor top seals were mounted. • Electric motor and turbine were re-centered before the test. • Aim was to revolve the turbine by giving pressurized air from the exit.			
Air Pres.	**Time**	**Notes**	
2 atm	1 min.	No motion.	
3 atm	1 min.	No motion.	
4 atm	1 min.	No motion.	
5 atm	3 min.	No motion.	
General Test Notes:			
• It was seen that the front vane seals and top rotor seals were too tight in their casings and their springs are stiffer then needed. Because of this the turbine could not revolve with pressurized air. • The front vane seals will be made from epoxy and fiber with a bigger tolerance with their casings. • The springs behind the vane seals will be made less stiff. • The rotor top seals will be grinded on their top surfaces so that together with their spring they won't exert too much force on the taps. • The springs under the top rotor seals will be made less stiff. • Used steel vane seals will be grinded to smooth their deformed surfaces with a bigger tolerance wrt their casing.			

Test # 2:

Date : 03.08.2005	Place: METU Hydraulic Laboratory		
- Turbine cold structure test. - Turbine was fixed on the test tool and mounted on test table - Tests were done with fiber front vane seals and gray cast iron rotor seals. - Valve timing was set with timing pulleys and belt. - Steel housing and taps were tested with steel rotor, vane and valve. - A 20 atm compressor was mounted to give pressurized air to the turbine from its inlet.			
Rpm	**Time**	**Notes**	
General Test Notes:			
- Turbine rotor could not complete one revolution. - It turned about 330 degrees freely but could not pass the last 30 degrees. - It was concluded that as the pressurized air was given from the exhaust, rotor could not pass the last 30 degrees where the both valves are closed (during constant volume combustion) and the air could not leave the turbine from the valve exits, therefore the air which is stacked between the rotor and the valves stop the rotor. - For the mechanism to work pressurized air must be given from the two valve inlets as it is designed so.			

Test # 3:

Date : 04.08.2005	Place: METU Hydraulic Laboratory		
• Turbine cold structure test.			
• Turbine was fixed on the test tool and mounted on test table			
• Tests were done with fiber front vane seals and gray cast iron rotor seals.			
• Valve timing was set with timing pulleys and belt.			
• Steel housing and taps were tested with steel rotor, vane and valve.			
• A 20 atm and a 10 atm compressor were mounted to give pressurized air to the turbine from its inlet.			
Pressure	**Rpm**	**Mass Flow**	
2.0 atm	300		
2.5 atm	400		
General Test Notes:			
• Turbine rotated easily as the air valve is opened.			
• Two different compressors were feeding the two turbine valves with 2.5 atm pressurized air. Each of them can be adjusted separately.			
• To give the same amount of pressurized air to both valves, they must be fed with one single compressor so that it could reflect the true engine operating condition.			

Test # 4:

Date : 04.08.2005	Place: METU Hydraulic Laboratory		
<td colspan="4"> - Turbine cold structure test. - Turbine was fixed on the test tool and mounted on test table - Tests were done with fiber front vane seals and gray cast iron rotor seals. - Valve timing was set with timing pulleys and belt. - Steel housing and taps were tested with steel rotor, vane and valve. - A 10 atm was mounted to give pressurized air to the turbine from its inlet. </td>			
Pressure (atm)	**Rpm**	**Mass Flow(g/s)**	
2.5	200	3.0	
3.0	300	3.4	
3.5	400	3.8	
4.0	450	4.2	
4.5	480	4.6	
5.0	500	5.0	
5.5	550	5.4	
6.0	600	5.8	
6.5	650	6.2	
7.0	700	6.6	
7.5	750	7.0	
General Test Notes:			
<td colspan="4"> - Turbine rotated easily as the air valve is opened. - Both turbine valves were being fed with single compressor with max 7.5 atm pressurized air. As mass flow of the compressor was separated into two the rpm of the turbine was lower then the first test case where the inlets were being fed with two separate compressors. </td>			
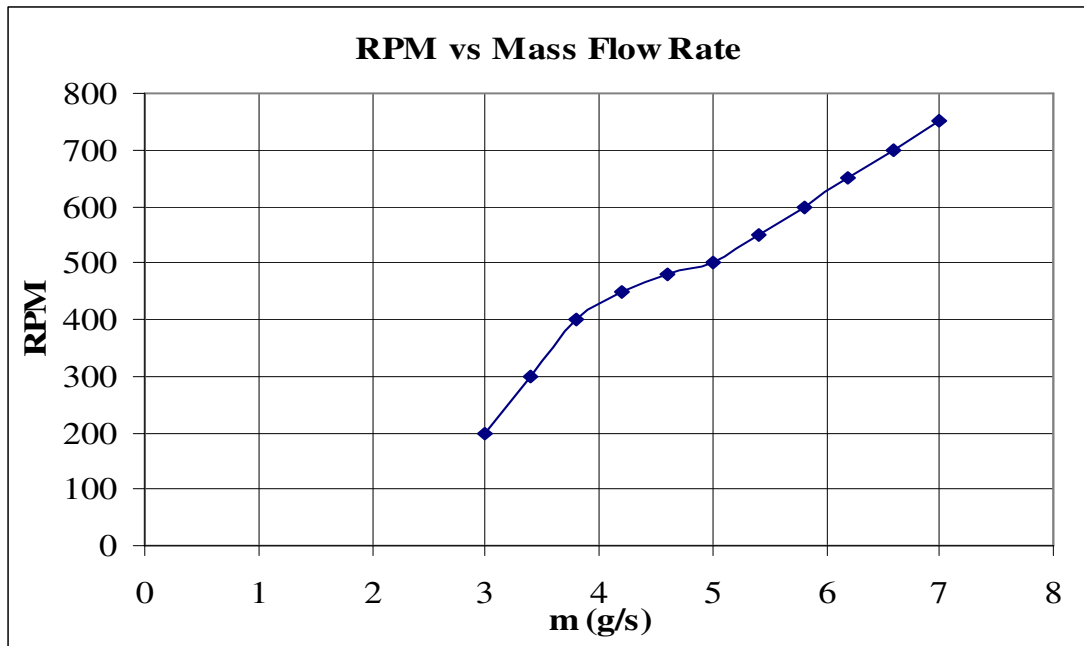
Figure 4-5   Turbine Rpm versus Mass Flow Rate Chart
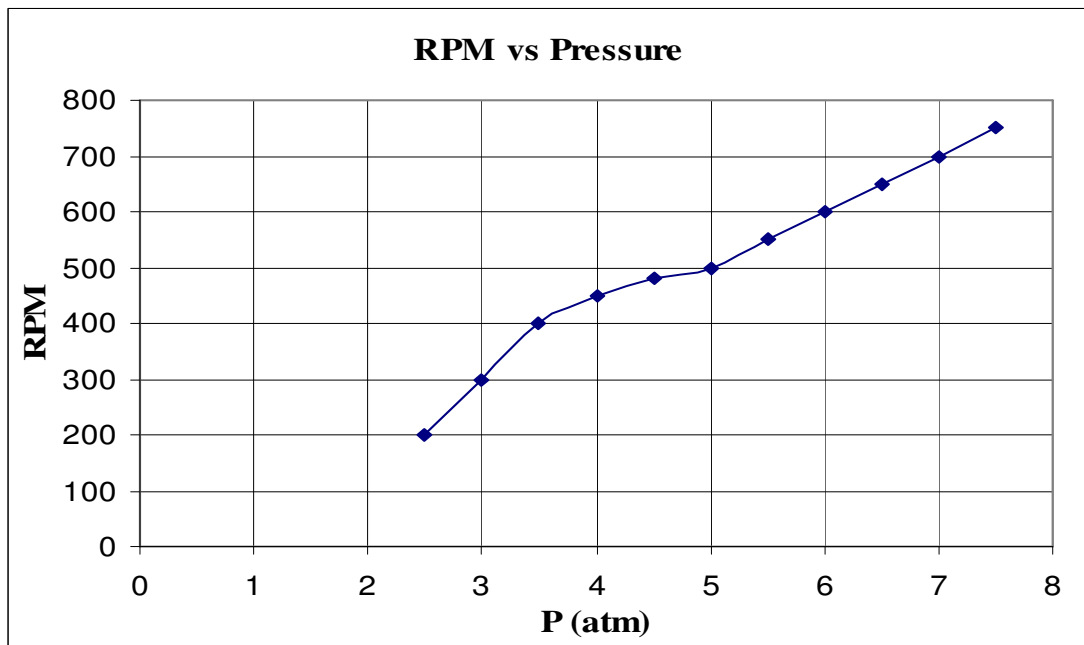
Figure 4-6   Turbine Rpm versus Pressure Chart

200
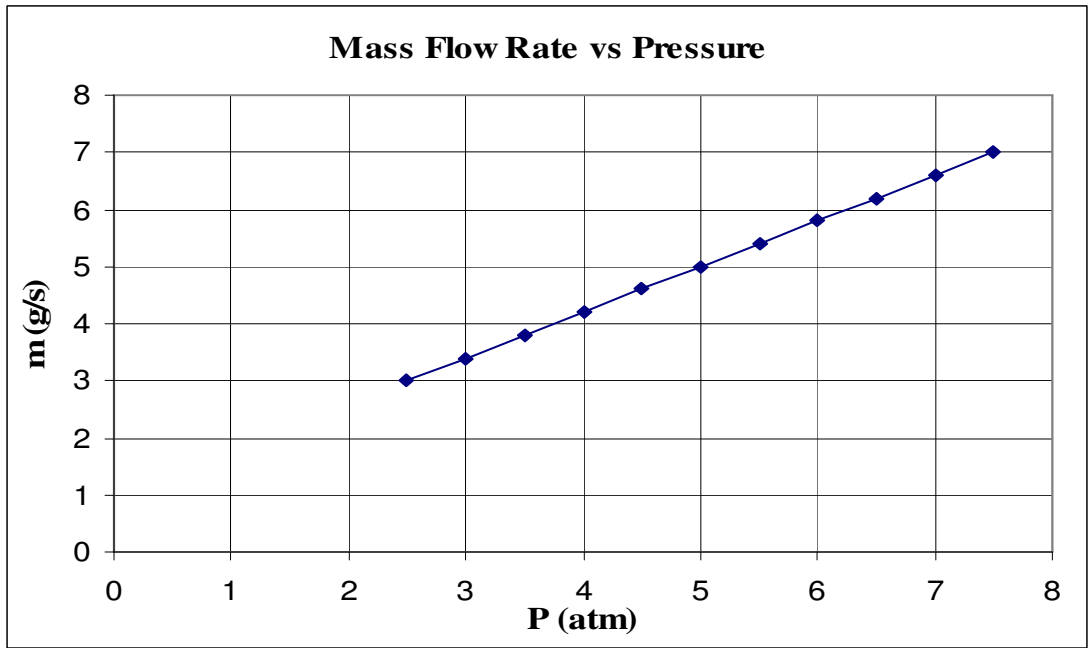
Figure 4-7   Turbine Mass Flow Rate versus Pressure Chart

Test Results

- Design rpm could not be reached during compressor tests due to structural problems. Compressor vane stacked in the rotor due to overexpansion. Efficient cooling is needed during ground tests.

- 7.5 atm is reached by the rotary compressor at 1200 rpm.
  Sealing is over safe and must be reconsidered to decrease the wear friction and the power extracted by the compressor. (That excess wear friction is also responsible for vane overexpansion)

- Over 80% of volumetric efficiency was achieved by the compressor.

- During cold turbine tests, the compressor was not capable of discharging the necessary pressurized air. Therefore, the rotary turbine speed could not exceed 1000 rpm.
  More powerful compressor is needed to discharge the necessary pressurized the air that will simulate the combustion gases.
  Sealing is over safe and must be reconsidered to decrease the wear friction and increase power delivered by the turbine.

- Vibration was not much, through out the compressor and turbine tests although, compression and turbine were unbalanced.

- Valve timing was accurate.

- Cooling system must be revised for the ground test.

- A more equipped data acquisition system must be used during the tests.

CHAPTER 5

CONCLUSION

5.1 Summary of Work

The work that has been done through out this thesis is summarized as follows;

- Thermodynamic analysis of the novel rotary engine working on a novel thermodynamic cycle has been done. A thermodynamic design code has been written to dimension the novel rotary engine. The rotary compressor and the rotary turbine of the engine have been matched and the geometric dimensions of the engine components (rotary compressor, rotary turbine, external combustion chamber) have been calculated according to the requirements of an UAV designed and manufactured by TAI on which the designed novel rotary engine is planned to be installed.

- Structural and mechanical design of the components of the novel rotary engine has been done according to the geometric data taken from the thermodynamic design code. All the components of the novel rotary engine have been modeled and assembled in CAD environment (Unigraphics NX2) and the required technical drawings of the components for the prototype manufacturing have been prepared. A structural analysis of the critical components have been carried out to define the manufacturing tolerances and to select the material of the prototype using a finite element software. (ANSYS 9.0) A prototype of the designed novel rotary engine has been manufactured in the machining facility of TAI.

- The designed components of the novel rotary engine have been manufactured in the 3-Axis NC Machining Center, 3-Axis Conventional Machining Center, Conventional Milling and Lathe Centers. The assembly of the manufactured components and the overhaul engine assembly have been done in the tooling facility of TAI.

- The component tests of the manufactured prototype of the designed novel rotary engine have been done in the Propulsion Laboratory of the Aerospace Engineering Department of METU. Rotary compressor and turbine pressure, temperature, mass flow, rpm, vibration, noise and endurance tests, combustion tests, auxiliary systems (fuel, ignition, lubrication, cooling) tests have been carried out.

- The performance parameters of the components of the designed novel rotary engine have been determined using the component test data taken through out the tests. The rotary compressor and rotary turbine maps have been plotted using the test data. Material behavior of the manufactured prototype of the designed novel rotary engine has been examined.

5.2 Recommendations for Future Work

A new prototype of the novel rotary engine should be designed, manufactured and tested taking into account the design and manufacturing experience gained through out this thesis.

The thermodynamic design code should be improved taking into account the losses due to the un-isentropic compression and expansion phases, combustion phase, mixing of compressed air with the remaining combustion gases in the combustion chamber.

Material selection of the rotary compressor, turbine and the combustion chamber should be revised. The selected rotary compressor material seemed well but care should be taken when selecting the turbine material taking into account the high temperature load on the components. Especially the seal and the spring material that will be used in the turbine should be carefully inspected. As the material of the combustion chamber is chosen to be a hot work tool steel, it seemed well but should be revised taking into account weight considerations.

Structural analysis of the critical components of the novel rotary engine should be revised using the real temperature and pressure data taken through out the tests.

The design of the prototype novel rotary engine should be changed to overcome some manufacturing difficulties. Especially the geometry of the compressor and turbine vanes and the discharge ports of the compressor are worth reconsidering.

Cooling of the engine components should be studied. Especially, the rotor, vane and valve of the rotary compressor must be cooled efficiently.

Balancing study should be done to balance the rotary compressor and turbine in order to overcome vibrations and the unwanted effects of the vibrations.

More equipped data acquisition system should be used to make the prototype engine tests so that the performance parameters of the engine could be easily monitored. Also with the help of a PLC, the engine could be controlled by processing the required engine data taken during the run.

5.3   Different Application Areas of This Novel Rotary Engine

Two different application areas whose conceptual design studies have been done are presented below;

- ***Turbo-Rotary Compound Engine.***

The present application area proposes a new turbo-rotary compound engine (TRCE) and an associated novel thermodynamic cycle. The objective is to combine the high efficiency and "no-stall" characteristics of internal combustion engines with the high mass flow, smaller size and lighter weight characteristics of the gas turbine engines. Another objective is to eliminate the long, heavy and cumbersome concentric shafts and reduction gears that are present in today's turbofan, turboprops and turbojet engines.

In this engine, shafts linking customary gas turbine engines components such as axial compressors and axial turbines are eliminated. Instead, two or multiple spools are lined up in series within the engine. In the front spool, partial admission rotary vane type turbines drive axial compressor stages. In the back spool, axial turbine stages drive partial admission rotary vane type compressors. Accordingly, the primary high mass flow through the axial compressors and turbines is mainly responsible from the generation of net engine thrust and power, where as the secondary, low mass flow through the partial admission rotary components is mainly used to generate the internal energy required to power the axial compressor stages. The energy consumed internally by the engine is minimized because less input shaft power is needed for the rotary vane compressors and higher inlet temperatures and less cooling can be tolerated by the intermittent combustion rotary vane turbines. The result is a radical improvement in both efficiency and net power output.

The conceptual design studies of this application have been done and the paper of these studies is published in ASME Turbo 2005: Power for Land, Sea and Air, June 6-9 2005, Reno – Tahoe, Nevada, USA. [28]

206

A conceptual design schematic and a 3-D model of the Turbo-Rotary Compound Engine are given in figures 5-1 and 5-2 respectively.
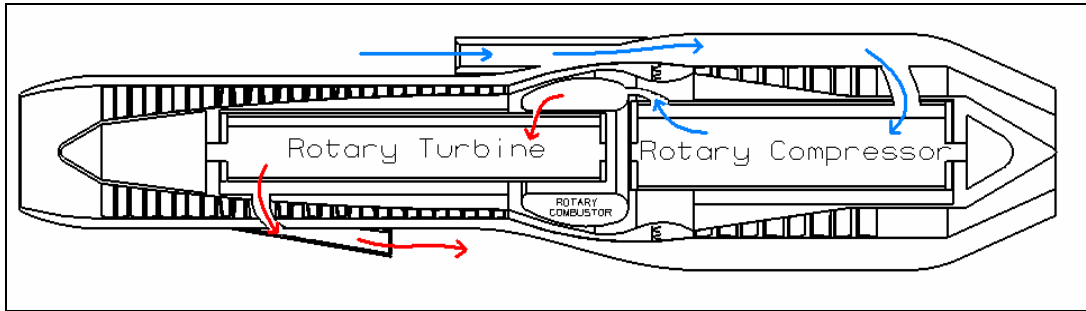
Figure 5-1   Schematic Diagram of Turbo Rotary Compound Engine
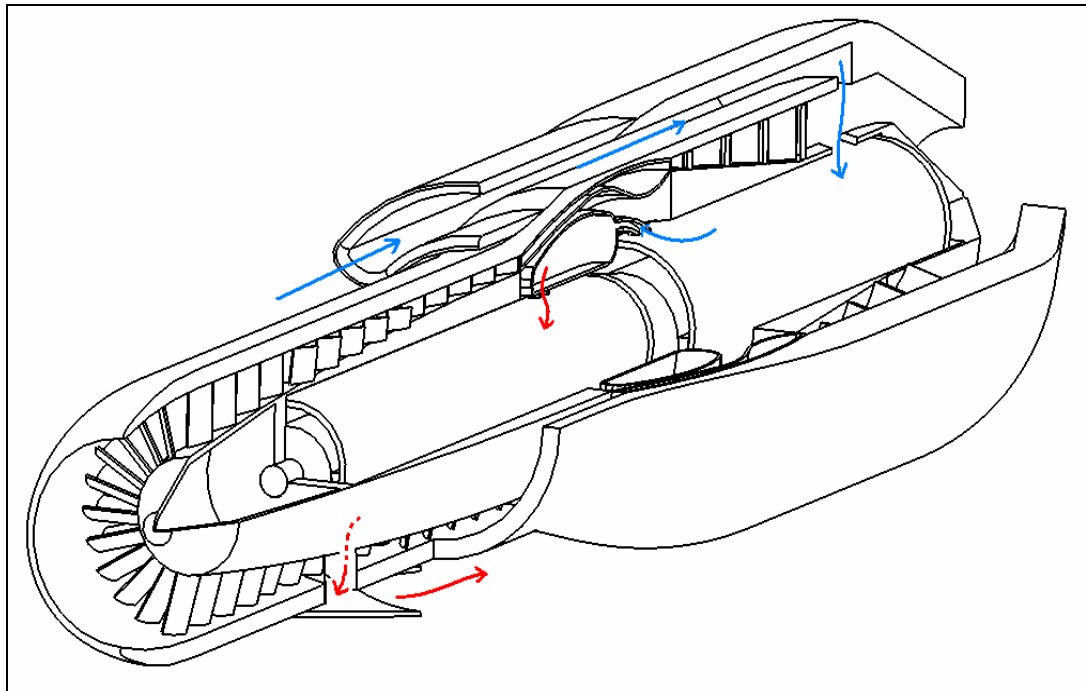
Figure 5-2   3-D Model of Turbo Rotary Compound Engine

- *Micro Vehicle Propulsion*

    Micro air vehicles are small (not larger then 20 cm) unmanned air vehicles, whose mission is surveillance without being detected. In today's Micro Air Vehicles (MAV), photovoltaic, battery, thermo-electric and internal combustion engines are being used. But today's micro internal combustion engines (0.67 hp/lb) have very low efficiency and thus 10 – 20 times more specific fuel consumption then 4 stroke ICE.

    The conceptual design study of a micro version of this novel rotary engine has been done and a presentation is done in the Tokyo University, July 2004. The geometry of the micro rotary engine is calculated using the thermodynamic design code and three micro rotary engines having 300W, 30W and 3W shaft power have been designed.

    The novel micro rotary engine, with its efficient compression done in closed volume, steady operation, large torque and good cooling capacity, and two power strokes per one rpm, is a good alternative to power the micro air vehicles. A preliminary design model of a micro rotary engine is given in figure 5-3.
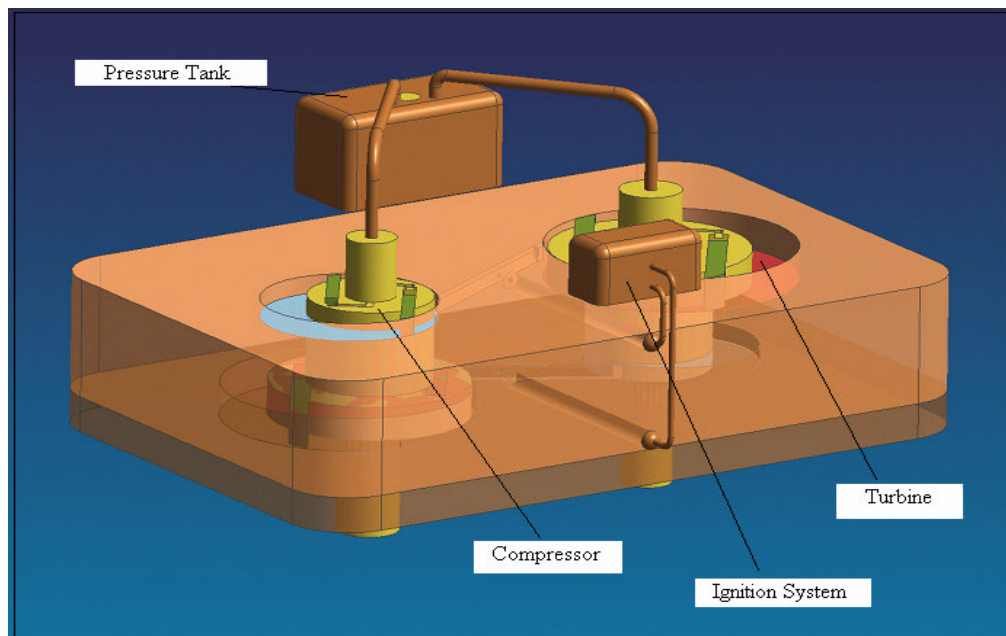
Figure 5-3 Micro Rotary Engine

REFERENCES

1. **Smith D.G.** and **Rudge, P.G.,** "Pressure-Volume Diagrams for Sliding Vane Rotary Compressors", *Proc. Instn. Mech. Engineers*, *Vol.184 Pt3R, Paper 17,* (1970), 159-166.

2. **Chou, Y.,** "Rotary Vane Engine", *USPTO 5,352,295*, (October 4th 1994).

3. **Vading, K.,** "Rotary-Piston Machine", *PCT WO 02/31318*, (April 18th 2002).

4. **Umeda, S.,** "Rotary Internal Combustion Engine", *USPTO 4,414,938,* (November 15th 1983).

5. **LAI, J.H.,** "Stage Combustion Rotary Engine", *USPTO 5,596,963*, (January 28th 1997).

6. **Jirnov, A.,** and Jirnov**, O.,** "Sliding-Blade Heat Engine with Vortex Combustion Chamber", *USPTO5, 511,525*, (April 30th 1996).

7. **Cummins, Jr., C.L.:** "Internal Fire, Carnot Press, Lake Oswego, Oreg., 1976.

8. **Cummins, Jr**.,**C.L.:** "Early IC and Automotive Engines" SAE paper 760604 in A History of the Automotive Internal Combustion Engine, SP-409, SAE Trans., vol.85, 1976.

9. **Hempson, J.G.G.:** "The Automobile Engine 1920 – 1950," SAE paper 760605 in A History of the Automotive Internal Combustion Engine, SP-409, SAE, 1976.

10. **Agnew, W**.**G.:** "Fifty Years of Combustion Research at General Motors," Progress in Energy and Combustion Science, vol 4, pp. 115-156, 1978.

11. **Wankel, F.:** Rotary Piston Machines, Iliffe Books, London, 1965.

12. **Ansade,R**.**F.:** The Wankel RC Engine Design and Performance, Iliffe Books, London, 1968.

13. **Yamamoto, K**.: Rotary Engine, Toyo Kogyo Co. Ltd., Hiroshima, 1969.

14. **Obert, E. F.:** Internal Combustion Engine, 1950.

15. **Taylor C. F. and Taylor E. S.:** The Internal Combustion Engine 1984.

16. **Heywood,J. B.:** Internal Combustion Engine Fundamentals, 1988.

17. **Akmandor, İ.S., Ersöz, N.:** Novel Thermodynamic Cycle, PTC / WO / 2004 / 022919 AI. (March 18th 2004)

18. **Chou, Y.,** "Rotary Vane Engine", *USPTO 5,352,295, (October 4th 1994).*

19. **Vading, K.,** "Rotary-Piston Machine", PCT WO 02/31318, (April 18th 2002).

20. **Umeda, S.,** "Rotary Internal Combustion Engine", *USPTO 4,414,938,* (November 15th 1983).

21. **LAI, J.H.,** "Stage Combustion Rotary Engine", USPTO 5,596,963, (January 28th 1997).

22. **Jirnov, A.,** and **Jirnov, O.,** "Sliding-Blade Heat Engine with Vortex Combustion Chamber", USPTO5, 511,525, (April 30th 1996).

23. **Akmandor, İ.S., Ercan T., Karaca M., Aran G.,** "New Engine and Thermodynamic Cycle of Tusas Aerospace Industries (TAI) Unmanned Air Vehicle", International Symposium on Innovative Aerial/Space Flyer Systems, Tokyo – Japan, December 10-11 2004

24. **Zabanski J.S. and Voevodin A.A.,** "Advanced Hard Coatings and Wear Resistant Materials for Aerospace", AGARD-CP-589, May 6-7 1996

25. **Clouser S.D. and Kamin R.A.,** "Combustion Technology Needs For Advanced High Pressure Cycle Engines", AGARD-CP-536, May 10th 1993

26. **Jacobson Bo,** "Thin Film Lubrication of Non-Smooth Surfaces", AGARD-CP-589, May 6-7 1996

27. **Woydt M.,** "Tribological Assessments and Concepts for an Oilfree Internal Combustion Engine", AGARD-CP-589, May 6-7 1996

28. **Akmandor, İ.S., Ercan T., Karaca M.,** "Turbo-Rotary Compound Engine and Novel Thermodynamic Cycle", GT2005-68234, Paper accepted for ASME Turbo-Expo 2005, Nevada USA, June 6-9 2005

APPENDIX A

DIFFERENT CONFIGURATIONS OF THE NOVEL ROTARY ENGINE

1st Side By Side Configuration (Without External Combustion Chamber)

- In this configuration, the compressor and the turbine assemblies are placed side by side.
- The compressor and the turbine assemblies are coupled with each other by the help of a gear box, in which three gears are beared.
- There is no external combustion chamber in between the compressor and the turbine. The compressed air passes directly to the turbine and combustion takes place within the turbine. (Internal combustion engine)
- Passing of compressed air from compressor to turbine is achieved by a rotary valve placed in between.
- Valve is directly coupled with the compressor rotor and timing is achieved by valve timing coupling.
- A water jacket surrounds the compressor and turbine assembly for cooling purposes.
- Cold water is also circulated on the upper and lower taps of the turbine assembly.
- A 3-D Cad model of the whole configuration and a 2-D Cad model of the compressor and the turbine are given in figures A-1 and A-2 respectively.
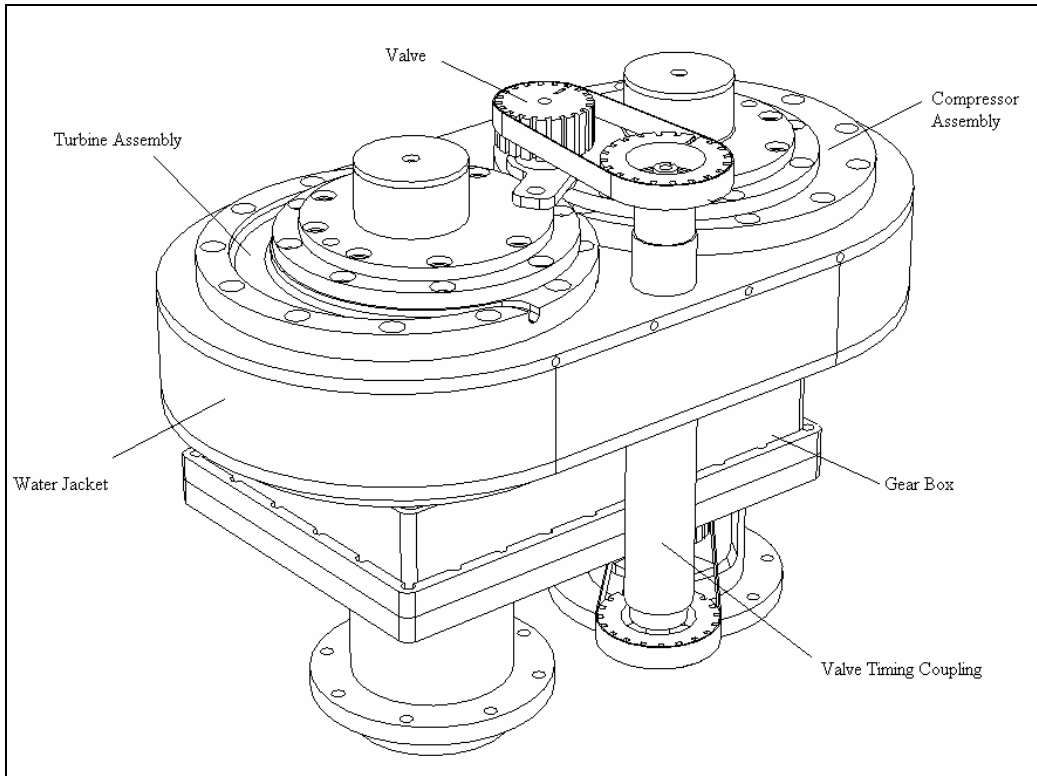
Figure A-1   3-D CAD Model of 1st Side by Side Configuration
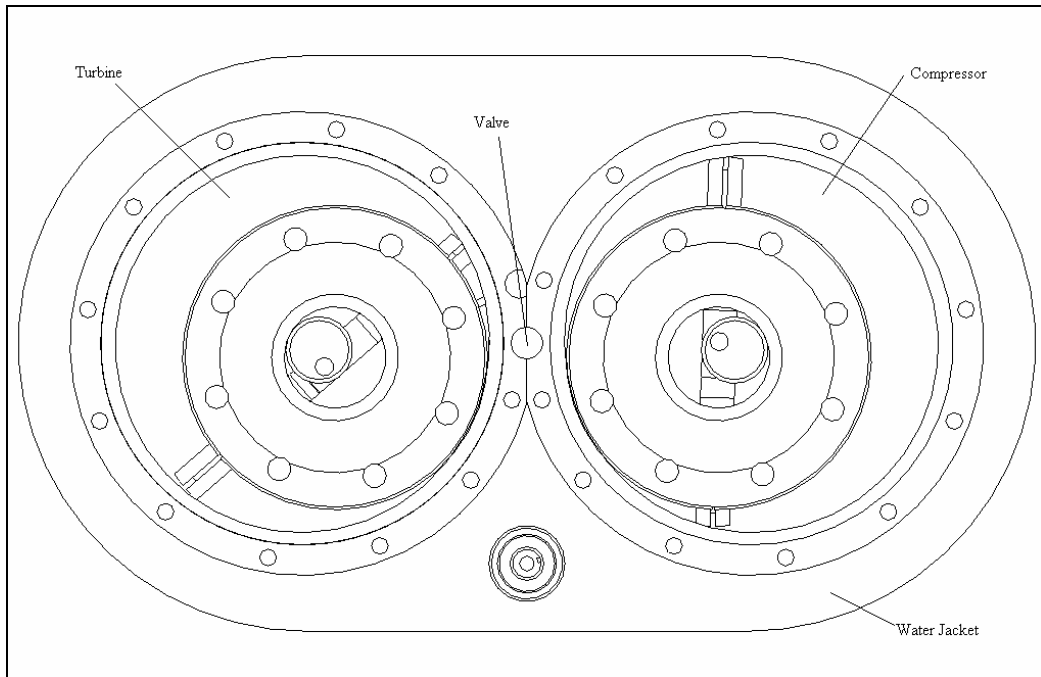
Figure A-2   2-D CAD Model of 1st Side by Side Configuration

2nd Side By Side Configuration (With External Combustion Chamber)

- In this configuration, the compressor and the turbine assemblies are placed side by side.

- The compressor and the turbine assemblies are coupled with each other by the help of a gear box, in which three gears are beared.

- There is an external combustion chamber in between the compressor and the turbine. The compressed air passes to the combustion chamber where it is mixed with fuel and combustion takes place within the chamber. (External combustion engine)

- After combustion, the combustion gases pass through the turbine where they expand.

- There is a rotating vane placed within the combustion chamber two divide the chamber into two to achieve two ignitions per one revolution.

- Vane of the combustion chamber is directly coupled with the compressor rotor and timing is achieved by vave timing coupling.

- A water jacket surrounds the compressor and turbine assembly for cooling purposes.

- Cold water is also circulated on the upper and lower taps of the turbine assembly.

- A 3-D Cad model of the whole configuration and a 2-D Cad model of the compressor and the turbine are given in figures A-3 and A-4 respectively.
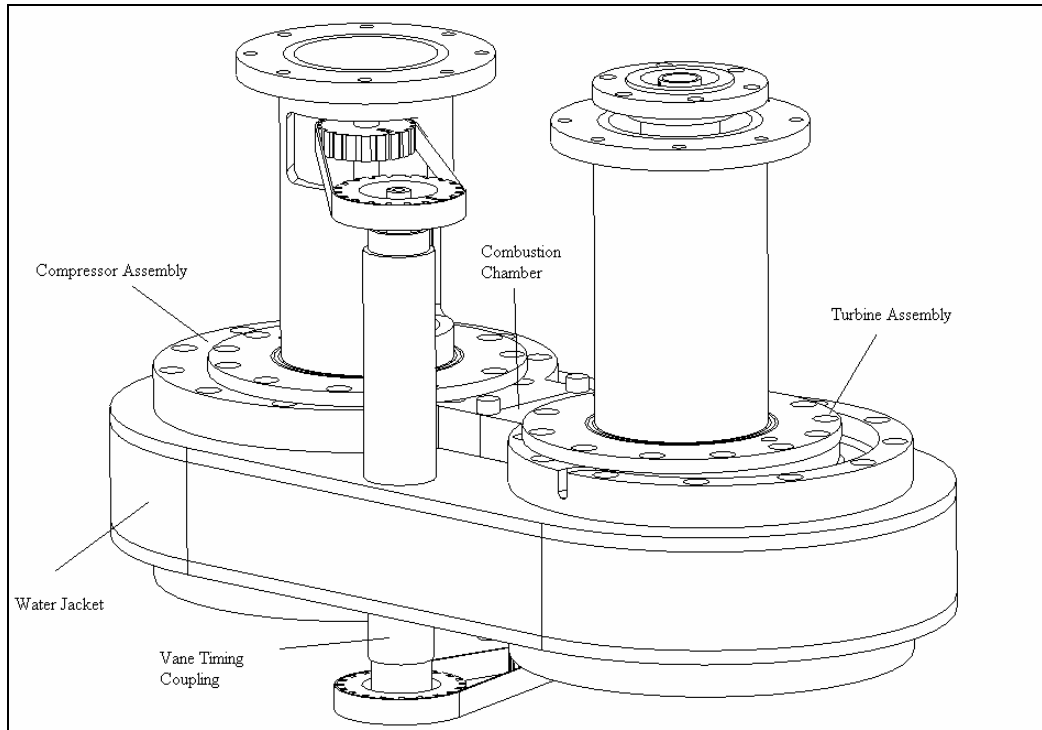
Figure A-3   3-D CAD Model of 2nd Side by Side Configuration
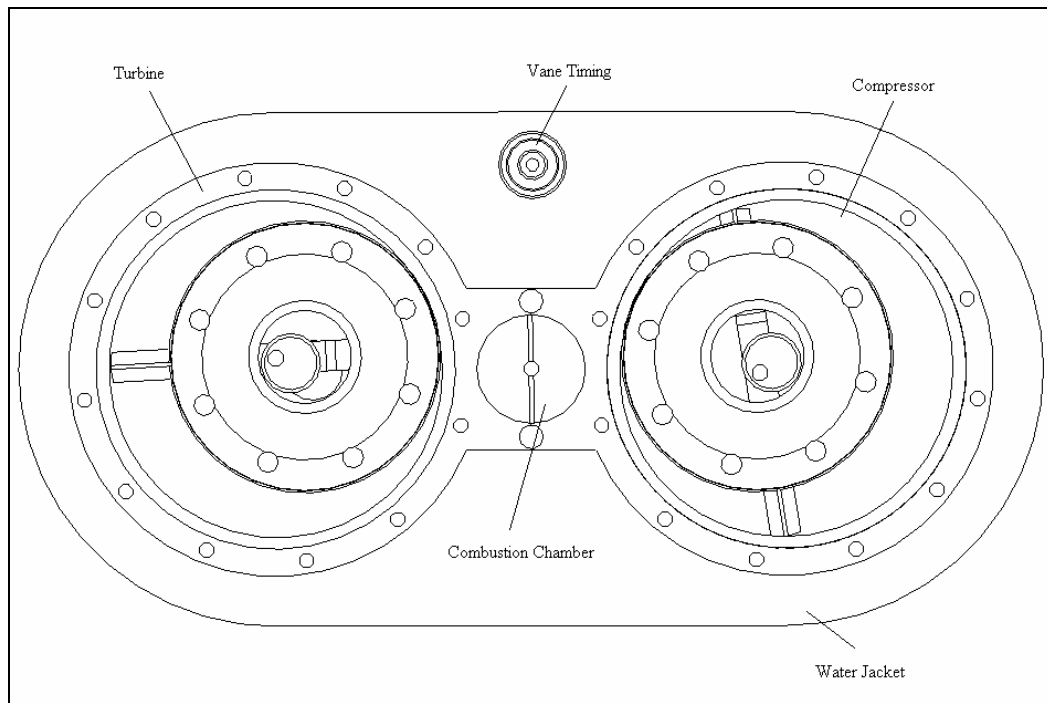
Figure A-4   2-D CAD Model of 2nd Side by Side Configuration

214

APPENDIX B

VANE TIP ANALYSIS

Objective of the vane tip analysis is;

- To analyze the interaction of the vane tip with the housing inner surface.
- To define tip clearances.
- To define vane tip geometry

The analytical geometry of the vane is given below;
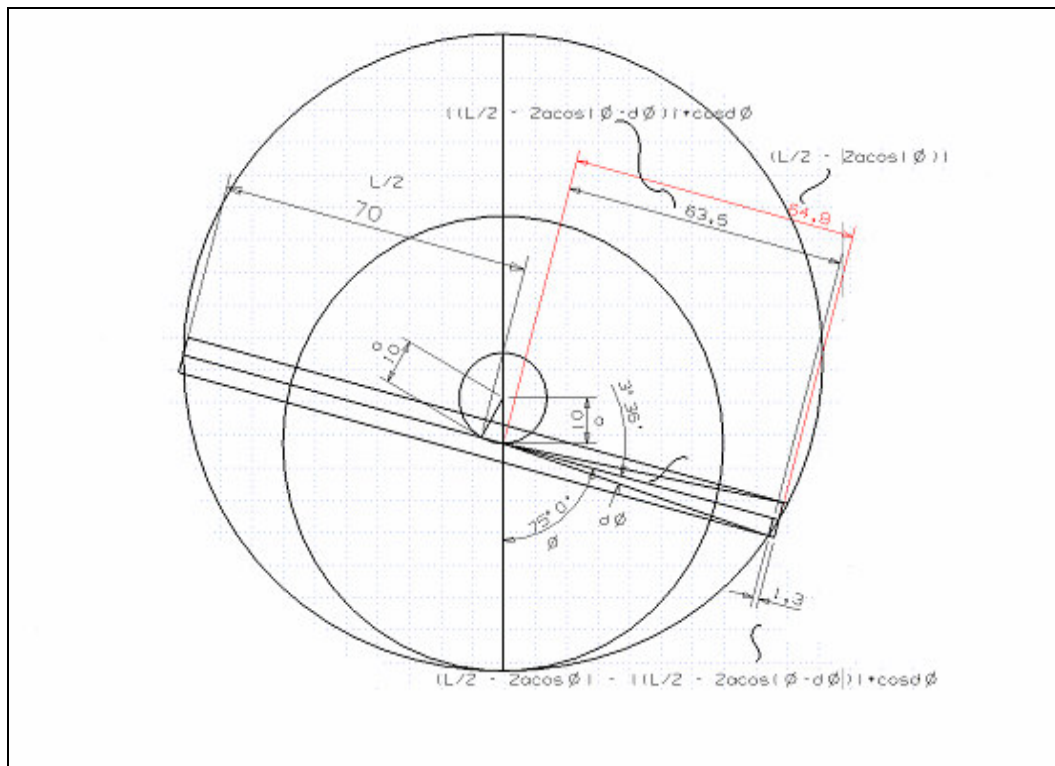
Figure B-1   Analytical Vane Tip Geometry

The vane tip clearance (T_{CL}) formulation is given below;

$$T_{CL}=1/2-(2a.\cos(\theta.2.\tfrac{\pi}{360}))-\cos\left[a\tan\left[\frac{h}{\frac{1}{2}-(2a.\cos\theta.2\frac{\pi}{360})}\right]\right]\left[\frac{1}{2}-\left[2a.\cos\left[\theta.2.\frac{\pi}{360}-a\tan\left[\frac{h}{\frac{1}{2}-(2a.\cos\theta.2\frac{\pi}{360})}\right]\right]\right]\right]$$

(B.1)

where,

θ (vane angle)	0 – 360 degrees
h (vane halfthickness)	6 mm
a (eccentricity)	15 mm
l (vane length)	140 mm

By changing θ (vane angle) from 0 degrees to 360 degress, the max contact tolerance between the vane tip and the housing inner surface due to the thickness of the vane is calculated using the vane tip clearance formulation. The maximum in contact distance is calculated as 1.301 mm where the vane angle (θ) is 75 degrees. At that angle, the vane and the housing are modeled and the vane tip geometry is determined.

After modeling the tip geometry, the kinematical motion assembly of the rotary compressor is done and the tip clearances are checked at different vane angles. Results showed that the designed vane tip geometry fits the housing inner surface at every vane angle. The vane tip contact analysis of the compressor is given in the following figure B-2.
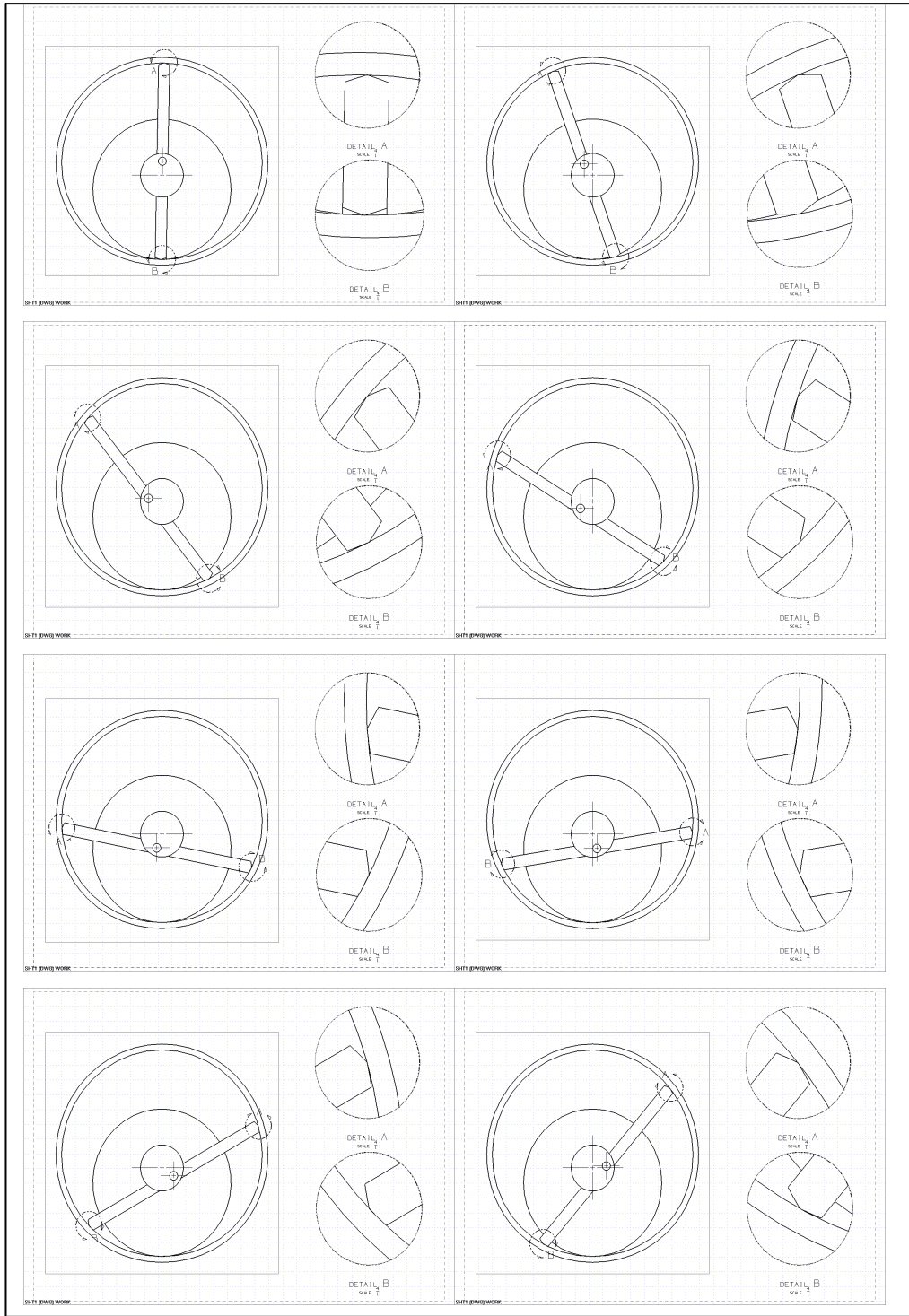
Figure B-2   Vane Tip Contact Analysis

217

APPENDIX C

PIVOT AXLE VANE RETENTION MECHANISM FOR WEAR PREVENTION

One reason for the lack of industrial attention to past rotary vane engines is that many of these engines have been faced by serious wear and sealing deficiencies. The main cause of the wear is the centrifugal force generated during high speed rotation that forces the vanes to scrap the inner peripheral of the working chamber. This has been recently addressed by using hinged vane central retention mechanisms [18, 19]. In such configurations, the sliding vane is articulated through a cylindrical sliding guidance placed between the rotor and the vane. While correcting the wear problem, the number of moving parts has increased and hence, the system became more complex. Instead of having hinged vanes, some of the prior designs do use sliding vanes slicing through the rotor [20, 21]. In these patents, a plurality of spring-loaded vanes is used and these designs do not have any central vane retention mechanism that would prevent wear. Another heat engine with 'all-through solid' vane [22] uses at least two mutually perpendicular vanes with radially extending guide. The plural use of vane within one compressor housing substantially reduces the pressure ratio per vane passage and increases the system complexity. In the present thesis, wear contacts generated by the sliding vane tips against the housing inner peripheral are eliminated by a pivot axle vane retention mechanism, centrally placed within the rotor (Figure C-1).
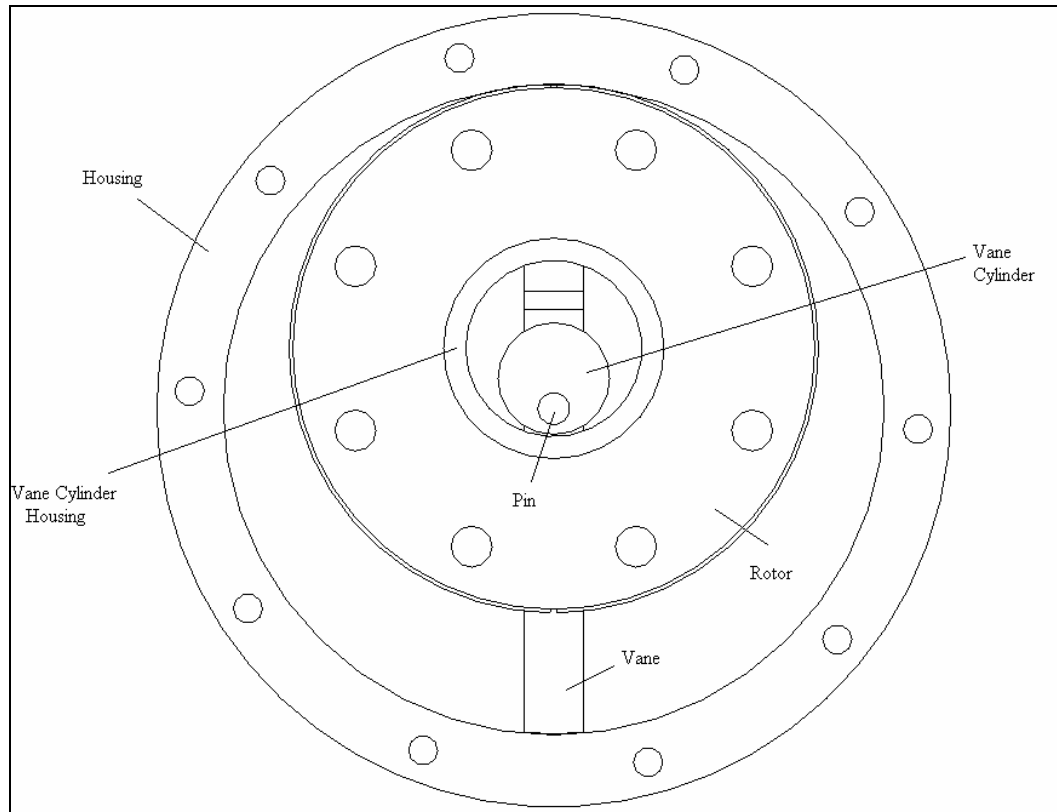
Figure C-1   Sliding Vane and Centrally Placed Vane Retention Mechanism

In this configuration, there is a vane cylinder mounted at the top of the vane by the help of a pin. This vane cylinder rotates eccentrically within its housing in the rotor and prevents the vane from touching the inner surfaces of the housing.

By arranging the eccentricity and the diameter of the vane cylinder, it forces the vane tips to follow the inner surfaces of the housing without touching.

By the help of this vane retention mechanism, the contact between the vane tips and the housing inner surfaces are avoided and thus the wear is minimized.

APPENDIX D

NOVEL ROTARY ENGINE MATERIAL

Properties of H13 Hot Work Tool Steel

Table D.1   Chemical Composition of H13

Chemical Composition (Weight %)					
C	Cr	Fe	Mo	Si	V
0.32 – 0.4	5.13 -	Min 90.95	1.33 – 1.4	1	1

Physical Properties

Density   7.8 g/cc

Mechanical Properties

Hardness	52-54 Rockwell
Ultimate Tensile Strength	1990 MPA
Yield Tensile Strength	1650 MPa
Elongation at Break	9 %
Modulus of Elasticity	210 GPa
Bulk Modulus	140 GPa
Poisson's Ratio	0.3
Machinability	50 %
Shear Modulus	81 GPa

Thermal Properties

CTE, Linear 20°C	11 μm / m-^{o}C
CTE, Linear 250°C	11.5 μm / m-^{o}C
CTE, Linear 500°C	12.4 μm / m-^{o}C
Heat Capacity	0.46 J / g-^{o}C
Thermal Conductivity	24.3 W / m-K

Properties of Aluminum 7075

Table D.2   Chemical Composition of 7075

Chemical Composition (Weight %)					
Mg	Co	Fe	Mn	S	Zn
2.1 – 2.9	1.2 – 2.0	Min 90.95	Max. 0.35	Max. 0.40	5.1 – 6.1

Mechanical Properties

Hardness	53.5 Rockwell
Ultimate Tensile Strength	572 MPA
Yield Tensile Strength	503 MPa
Elongation at Break	11 %
Modulus of Elasticity	71.7 GPa
Poisson's Ratio	0.33
Machinability	70 %
Shear Modulus	26.9 GPa

Thermal Properties

CTE, Linear 20°C	23.6 μm / m-^{o}C
CTE, Linear 250°C	25.2 μm / m-^{o}C
Heat Capacity	0.96 J / g-^{o}C
Thermal Conductivity	130 W / m-K

Properties of Gray Cast Iron

Table D.3   Chemical Composition of Gray Cast Iron

Chemical Composition (Weight %)					
C	Cr	Fe	Ni	Si	Mn
Max 0.06	5.5 -	74.4 - 81	3.5 – 5.5	Max 1	Max. 1

Mechanical Properties

Ultimate Tensile Strength	655 MPA
Yield Tensile Strength	480 MPa
Elongation at Break	16%
Modulus of Elasticity	69 GPa
CTE, Linear 20°C	12.1 μm / m-^{o}C

Properties of Elgiloy

Table D.4   Chemical Composition of Elgiloy

Chemical Composition (Weight %)					
Co	Cr	Fe	Mo	Mn	Ni
39 - 41	19 - 21	16	6 - 8	1.5 – 2.5	14 - 16

Physical Properties

Density	8.3 g/cc

Mechanical Properties

Hardness	56 Rockwell
Ultimate Tensile Strength	1930 MPA
Yield Tensile Strength	1790 MPa

Elongation at Break   2 %

Modulus of Elasticity   186.6 GPa

Poisson's Ratio   0.226

Shear Modulus   77.4 GPa

Thermal Properties

CTE, Linear 20°C   15.17 μm / m-^{o}C

CTE, Linear 250°C   15.17 μm / m-^{o}C

CTE, Linear 500°C   15.17 μm / m-^{o}C

Heat Capacity   0.43 J / g-^{o}C

Thermal Conductivity   12.5 W / m-K

Melting Point   1427 ^{o}C

<u>Properties of Inconel 718</u>

Table D.5   Chemical Composition of Inconel 718

Chemical Composition (Weight %)					
Nb	Cr	Fe	Mo	Ti	Ni
4.75 -	17 - 21	17	2.8 – 3.3	0.65 -	50 - 55

Physical Properties

Density   8.19/cc

Mechanical Properties

Ultimate Tensile Strength   1375 MPa

Yield Tensile Strength   1100 MPa

Elongation at Break   25 %

Thermal Properties

CTE, Linear 20°C   13 μm / m-^{o}C

Heat Capacity   0.435 J / g-^{o}C

Thermal Conductivity   11.4 W / m-K

Properties of Pyrowear Alloy 53 Tool Steel

Table D.6   Chemical Composition of Pyrowear Alloy 53

Chemical Composition (Weight %)					
C	Cr	Fe	Ni	Si	Mo
0.1	1	90	2	1	3.25

Physical Properties

Density   7.8 g/cc

Mechanical Properties

Ultimate Tensile Strength   1207 MPA

Yield Tensile Strength   896 MPa

Elongation at Break   12%

Thermal Properties

CTE, Linear 20°C   11.26 μm / m-^{o}C

CTE, Linear 250°C   12.06 μm / m-^{o}C

CTE, Linear 500°C   13.05 μm / m-^{o}C

CURRICULUM VITAE

GSM Tel: +90 532 7122149
Tel: +90 312 2413226
E-mail: tercan76@yahoo.com

Address: 606.Sokak, İdareciler Sitesi, 11.Blok,
Daire:7, 06530 Konutkent/ANKARA

Taylan ERCAN

Professional Experience	2004 - TUSAŞ Aircraft Industries Inc. Ankara **Structural Design Engineer**

- Working as a design engineer, responsible for the structural design and test of a 30kW noval rotary engine being designed for an UAV.
- Working as a system installation engineer, responsible for the installation of mechanic and fluid systems (fuel, oxygen, hydrolic, air condition, pneumatic systems) to the aircraft structure, in the A400M (Future Large Aircraft) project.

Publications

"*New Engine and Thermodynamic Cycle of Tusas Aerospace Industries Unmanned Air Vehicle*", I. Sinan Akmandor, Taylan Ercan, Mehmet Karaca, Gokhan Aran, International Symposium on Innovative Aerial/Space Flyer Systems, International Symposium Series on Mechanical System Innovation, The 21st Century, Center of Excellence Program of the University of Tokyo, December 10-11, 2004, Tokyo – Japan

"*Turbo-Rotary Compound Engine (TRCE) and Novel Thermodynamic Cycle*", I.Sinan Akmandor, Taylan Ercan, Mehmet Karaca, GT2005-68234, Paper accepted for ASME Turbo-Expo 2005, Reno-Tahoe, Nevada, USA June 6-9, 2005

2002 - 2003   TUSAŞ Engine Industries Inc.   Eskişehir
Product Development Engineer

- Took ANSYS Introduction 1-2 & Advanced (Material Nonlinearities, Contact, Transient Analyses) Training, November ~ December 2002 (6 Weeks).
- Took FLUENT Introduction and Advanced Training, January 2003   (3 Weeks).
- Worked as a design engineer, responsible for the structural design and analyze of a novel turbo engine.

2000 - 2001   Bosporus Software Inc.   Ankara
Cad – Cam – Cae Consultant

- Gave Basic and Advanced Cad education to the Product Development Department of Bosch, Manisa. Consulted in the water heater optimisation project.
- Gave Advanced Cad education to the Product Development Department of ARÇELİK, Bolu. Consulted in the oven front panel design, printer and plotter management.
- Gave Basic Cad education to Cad – Cam Center of BİLTİR, METU.
- Gave Basic Cad–Cam education to the Design Department of Erkunt Casting Inc., Ankara.
- Consulted in Valysis (CMM software developed by Technomatics, USA) education and installation to the CMM Department of TAI (Tusaş Aircraft Industries Inc.). Also participated in the Information Management System upgrade process using IMAN software.
- Gave Cae education to the Analysis Department of 2. Air Supply and Maintenance Centre, Kayseri. Consulted in Finite Element Methodology for the analysis of wings and fuselage.
- Consulted in the different Cad–Cam projects of the customers such as PI Machinery Inc., Ankara, HAS-IZ Mold, Ankara, 1. Air Supply and Maintenance Centre, Eskişehir.

Summer Practice   Summer, 1997   Koruma A.Ş.   Kocaeli
- Management practice for 6 weeks.

Summer, 1996   2. Air Supply and Maintenance Centre   Kayseri
- Manufacturing practice for 6 weeks.

Education	2002 - 2005	Middle East Technical University	Ankara

▪ M.Sc., Aeronautical Engineering.

Thesis Title: Thermodynamic and Structural Design and
Analysis of a Novel Turbo Rotary Engine.

	1994–2001	Middle East Technical University	Ankara

▪ B.Sc., Aeronautical Engineering.

	1987-1994	F.M.V. Işık College	İstanbul

Computer Knowledge

Cad-Cam programs : Unigraphics, CATIA, I-DEAS, AutoCAD.

CAE programs : Ansys 9.0, Fluent 7.0, Gambit, TGrid

Programming Language : Fortran77, Visual Basic 6.0

Other : MathCAD 8.0, Win NT, 2000, MS – Office.

Language

English: Very good command both written and spoken.

German: Good command both written and spoken.

Certificates

ANSYS Basic and Advanced Training (FIGES), FLUENT Basic and Advanced Training (FIGES), Sales and Marketing Techniques (Yapı Kredi Yaşam A.Ş.,Ankara), English Translation (National Education Ministry), Valysis (3-D measurement device software, Technomatics, USA), FAI Micro-light Marshalling and Model Aircraft (THK) Certificates.

Community Activities

Izmit Yachting Club and METU Aeronautical Club membership, making model aircraft and walking in nature, swimming and diving.

References

Available on request.